UNIVERSITAT ROVIRA I VIRGILI

DESIGN, FABRICATION AND CHARACTERISATION OF GAS SENSORS BASED ON NANOHYBRID MATERIALS

Radouane Leghrib

ISBN: 978-84-694-0326-6
Dipòsit Legal: T-207-2011

UNIVERSITAT ROVIRA I VIRGILI
DESIGN, FABRICATION AND CHARACTERISATION OF GAS SENSORS BASED ON NANOHYBRID MATERIALS
Radouane Leghrib
ISBN:978-84-694-0326-6/DL:T-207-2011

Radouane LEGHRIB

Design, fabrication and characterisation of gas sensors based on nanohybrid materials

DOCTORAL THESIS

Supervised by **Prof. Eduard Llobet Valero**

Department of Electronic, Electrical & Automatic Control Engineering

UNIVERSITAT ROVIRA I VIRGILI

Tarragona 2010

UNIVERSITAT ROVIRA I VIRGILI
DESIGN, FABRICATION AND CHARACTERISATION OF GAS SENSORS BASED ON NANOHYBRID MATERIALS
Radouane Leghrib
ISBN:978-84-694-0326-6/DL:T-207-2011

UNIVERSITAT ROVIRA I VIRGILI
DESIGN, FABRICATION AND CHARACTERISATION OF GAS SENSORS BASED ON NANOHYBRID MATERIALS
Radouane Leghrib
ISBN:978-84-694-0326-6/DL:T-207-2011

UNIVERSITAT
ROVIRA I VIRGILI

ESCOLA TÈCNICA SUPERIOR D'ENGINYERIA
DEPARTAMENT D'ENGINYERIA ELECTRONICA, ELÈCTRICA I AUTOMÀTICA

Avinguda dels Països Catalans, 26
Campus sescelades
43007 Tarragona
Tel. (977) 55 96 10
Fax (977) 55 96 05
e-mail: secelec@etse.urv.es
http://www.etse.urv.es/DEEEA/

I hereby confirm that this thesis entitled 'Design, fabrication and characterization of gas sensors based on nanohybrid materials' presented by Radouane Leghrib for being awarded the Doctorate Degree has been conducted under my supervision at the Department of Electronic, Electrical and Automation Engineering of this University and meets the requirements for opting to the European Mention.

Tarragona, the 2010.

Prof. Eduard Llobet

Thesis Supervisor

UNIVERSITAT ROVIRA I VIRGILI
DESIGN, FABRICATION AND CHARACTERISATION OF GAS SENSORS BASED ON NANOHYBRID MATERIALS
Radouane Leghrib
ISBN:978-84-694-0326-6/DL:T-207-2011

UNIVERSITAT ROVIRA I VIRGILI
DESIGN, FABRICATION AND CHARACTERISATION OF GAS SENSORS BASED ON NANOHYBRID MATERIALS
Radouane Leghrib
ISBN:978-84-694-0326-6/DL:T-207-2011

Acknowledgement

First of all, I would like to express my sincere gratitude to my supervisor, Professor Eduard Llobet Valero for his valuable guidance and advice, for helping me to broaden my view and knowledge, and who was always open for discussing with me all the details of my work.

I also thank the doctoral program of the University Rovira i Virgili for giving me the opportunity to elaborate this thesis.

I would like to thank the Nano2hybrid project for the financial support, and all the partners from all research laboratories working within it, without forgetting VEGA and SENSOTRAN companies.

I gratefully acknowledge Professor Christopher Paul Ewels from the “institute des materiaux Jean Rouxel in Nantes” for receiving me in his laboratory and supervising my work concerning the theoretical part of this thesis.

I would like to thank Dr. Carla Bittencourt for her help, relevant comments and suggestions during the revision of my thesis.

My deepest appreciation to all teachers and colleagues working within the MiNoS group for motivating me and ensuring me to work in a very pleasant and comfortable ambient, for all their hospitality and their help, with a special thanks to Raul Calavia for his technical support.

Many thanks to Professor Xavier Rius and Professor Francesc Diez from the faculty of chemistry for their advices and helping me in interpreting some results.

My sincere gratitude and appreciation to my Professor Benachir Bouchikhi from University Moulay Ismail of Meknes for his support and collaboration.

UNIVERSITAT ROVIRA I VIRGILI
DESIGN, FABRICATION AND CHARACTERISATION OF GAS SENSORS BASED ON NANOHYBRID MATERIALS
Radouane Leghrib
ISBN:978-84-694-0326-6/DL:T-207-2011

My heartiest gratitude to my parents, my brothers and my wife Lahlou Houda and her family for supporting me.

Finally, an honorable mention goes to all my family and friends for their understandings and supports in completing this thesis.

Without the help of the particular mentioned above, I would have faced many difficulties while doing this thesis.

UNIVERSITAT ROVIRA I VIRGILI
DESIGN, FABRICATION AND CHARACTERISATION OF GAS SENSORS BASED ON NANOHYBRID MATERIALS
Radouane Leghrib
ISBN:978-84-694-0326-6/DL:T-207-2011

Dedicated to

My dear parents

Abdelkader Leghrib
&
Lalla Hachoum Tahiri Alaoui

My dear Brothers
Fouzia & Badr

My dear wife Houda and her family

UNIVERSITAT ROVIRA I VIRGILI
DESIGN, FABRICATION AND CHARACTERISATION OF GAS SENSORS BASED ON NANOHYBRID MATERIALS
Radouane Leghrib
ISBN:978-84-694-0326-6/DL:T-207-2011

UNIVERSITAT ROVIRA I VIRGILI
DESIGN, FABRICATION AND CHARACTERISATION OF GAS SENSORS BASED ON NANOHYBRID MATERIALS
Radouane Leghrib
ISBN:978-84-694-0326-6/DL:T-207-2011

Abstract

In the last few years, there has been a growing demand for monitoring the environment, especially with the increasing concern by the release of toxic gases emitted by manmade activities. The development of nanotechnology has created a huge potential for building highly sensitive, selective, low cost, and portable gas sensors with low power consumption.

Nowadays, carbon nanotubes are receiving an intense interest from the scientific community, due to their unique geometry, morphology, electronic, mechanical, thermal and optical properties, which make them a promising candidate for many industrial applications including new gas sensors for the detection of toxic species. In this context, in this thesis a deep study is devoted to explore the sensing properties of different hybrid nanomaterials based on carbon nanotubes for an efficient detection of toxic gases. The design, fabrication, characterization, and optimization of gas sensors using hybrid materials have been carried out.

This thesis was financially supported by the European project "Nano2hybrids", which exploits the interface design of metal nanocluster-carbon nanotube hybrids via control of structural and chemical defects in a plasma discharge, for designing gas sensors with superior performance. Benzene was chosen as the principal target gas due to its serious toxic effects at low ppb levels and the fact that there are no reliable, low cost and selective benzene detectors in the market. In fact, no gas sensor able to selectively detect this gas at ppb levels and operating at ambient temperature has been reported up to now in the literature. So, the challenge of the project was to fabricate sensitive, highly selective, stable, portable, and low cost benzene gas sensor employing hybrid nanomaterials.

Herein, functionalized MWCNTs, metal decorated MWCNTs, and metal oxide decorated MWCNTs or metal oxide and MWCNT mixtures were deeply investigated in terms of their gas sensing performances (e.g, sensitivity, selectivity, stability, detection mechanism,. etc) towards the detection of different gases (benzene (C_6H_6), carbon monoxide (CO), nitrogen dioxide (NO_2), ethylene (C_2H_4), hydrogen sulfide (H_2S), ammonia (NH_3), and water (H_2O)). Our tasks were to investigate experimentally and

ISBN:978-84-694-0326-6/DL:T-207-2011

theoretically the effects of material preparation conditions (e.g., plasma treatment, nanocluster precursor and size), sensor fabrication (e.g., deposition technique, electrodes sensor metal), and sensor characterization conditions (e.g., operating temperature, gas flow) on the gas sensing properties of our devices, and to acquire knowledge in order to develop a selective benzene detector. Based on experimental and theoretical results, different mechanisms for the interaction between gases and the hybrid materials tested have been proposed.

We found that hybrid materials consisting of oxygen plasma treated multiwalled carbon nanotubes decorated with different metal nanoparticles showed room temperature sensing capability. Responsiveness to gases of these hybrid materials was higher than that of pristine or plasma functionalized carbon nanotubes. Metal decoated CNTs can be tailored for the recognition of different gases and vapors with different reactivities, which offers enormous flexibility for tuning the interfacial properties of the resulting hybrid materials and thus, of their sensing properties. When combined in a microsensor array operating at room temperature, the use of benzene-sensitive and benzene-insensitive metal-decorated multiwalled carbon nanotubes, allowed for the first time the implementation of a low cost detector prototype, which can selectively detect benzene when present at trace levels (below 50 ppb) in a gas mixture. Sensors present response and recovery times of 60 s and 10 min respectively, good stability and reproducibility. This type of sensors are protected by a patent, and licensed to a company for industrial commercialization.

UNIVERSITAT ROVIRA I VIRGILI
DESIGN, FABRICATION AND CHARACTERISATION OF GAS SENSORS BASED ON NANOHYBRID MATERIALS
Radouane Leghrib
ISBN:978-84-694-0326-6/DL:T-207-2011

Resumen

Hoy en día, la necesidad de monitorizar y controlar el medio ambiente es a cada vez más importante debido al creciente nivel de gases tóxicos que provienen de la expansión de las actividades industriales, amenazando así el medio ambiente y la salud humana. El desarrollo de la nano-tecnología ha permitido fabricar sensores de gases portables, altamente sensibles, selectivos, de bajo coste y de bajo consumo de potencia.

Los nanotubos de carbono (NTC) están ganando un interés a cada vez más considerable por parte de la comunidad científica debido a su geometría y morfología únicas y sus excelentes propiedades electrónicas, mecánicas, térmicas i ópticas. Esto hace de ellos unos candidatos prometedores para un amplio rango de aplicaciones como por ejemplo nuevos sensores de gases con propiedades mejoradas. En este contexto, mediante la presente tesis, se ha realizado un profundo estudio para explorar las propiedades de diferentes sensores basados en nano-materiales híbridos constituidos por nanotubos de carbono junto a otros materiales con el fin de detectar gases tóxicos de manera eficiente. El trabajo realizado consistió en el diseño, la fabricación, la caracterización, y la optimización de nanosensores híbridos.

Esta tesis fue financiada en el marco del proyecto Europeo “Nano2hybrids”, cuyo objetivo era de diseñar la interfaz de las nano-partículas del metal con los nanotubos de carbono a través del control de los defectos estructurales y químicos producidos por la descarga de un plasma de radiofrecuencia y aplicarlo a la detección de gases. El benceno fue elegido como gas principal, debido a sus graves efectos tóxicos a niveles de pocas ppb y también debido a la no existencia en el mercado de un detector de bajo coste para benceno. De hecho, no hay en el estado de la técnica, un sensor de gas que puede detectar de forma selectiva este gas a nivel operativo de ppb y trabajando a temperatura ambiente. Así, el reto de esta tesis era obtener un sensor altamente sensible, selectivo y estable, portátil y de bajo coste para la detección de benceno.

En este sentido, se estudiaron exhaustivamente diferentes materiales basados en nanotubos de carbono funcionalizados, decorados con nanopartículas de metal o bien decorados o mezclados con óxidos metálicos, en términos de su adecuación para la detección de gases (por ejemplo, sus sensibilidad, selectividad, estabilidad, y el

ISBN:978-84-694-0326-6/DL:T-207-2011

mecanismo de detección, etc.). En particular se estudió la detección de diferentes gases como (benceno (C_6H_6), monóxido de carbono (CO), dióxido de nitrógeno (NO_2), el etileno (C_2H_4), el sulfuro de hidrógeno (H_2S), amoníaco (NH_3) y agua (H_2O)). Nuestras tareas consistieron en investigar experimentalmente y teóricamente el efecto de las condiciones de preparación de los materiales (p.e. el tratamiento con plasma, la naturaleza del precursor y tamaño de las nanoparticulas de metales), fabricación del sensor (p.e., técnica de deposición, el efecto del tipo de metal del los electrodos del sensor), y de las condiciones de caracterización del sensor (p.e., temperatura de operación, flujo de gas,) sobre las propiedades sensoras de los mismos. Todo ello ha permitido adquirir conocimientos, explicar los mecanismos de funcionamiento en el sensado de gases de los diferentes materiales investigados y con ello desarrollar un sensor de gases adecuado para la detección de benceno.

Hemos encontrado que los materiales híbridos que consisten en nanotubos tratados con plasma de oxígeno y decorados con diferentes nanopartículas de metal, muestran una mayor capacitad de detección a temperatura ambiente respecto a los nanotubos de carbono en bruto o los funcionalizados sólo con plasma. Las propiedades interfaciales de los materiales híbridos resultantes pueden ser adaptadas, lo que ofrece una enorme flexibilidad para el ajuste de sus propiedades sensoras. Cuando se combinaron en una matriz de micro-sensores que opera a temperatura ambiente, nanotubos decorados con diferentes metales, de forma que unos resulten sensibles al benceno y otros insensibles, esto permitió por primera vez la realización de un prototipo de bajo coste capaz de detectar selectivamente y a temperatura ambiente el benceno presente a nivel de trazas (por debajo de 50 ppbs) en una mezcla de gases. El prototipo realizado presenta unos tiempos de respuesta y de recuperación de 60 s y 10 minutos respectivamente además de una buena estabilidad y reproducibilidad. Este prototipo se encuentra protegido por una patente que ha sido licenciada a una compañía que se encargará de la comercialización industrial del producto.

UNIVERSITAT ROVIRA I VIRGILI
DESIGN, FABRICATION AND CHARACTERISATION OF GAS SENSORS BASED ON NANOHYBRID MATERIALS
Radouane Leghrib
ISBN:978-84-694-0326-6/DL:T-207-2011

UNIVERSITAT ROVIRA I VIRGILI
DESIGN, FABRICATION AND CHARACTERISATION OF GAS SENSORS BASED ON NANOHYBRID MATERIALS
Radouane Leghrib
ISBN:978-84-694-0326-6/DL:T-207-2011

Resum

Recentment, hi ha una forta demanda per a la vigilància i el control del nostre medi ambient, especialment amb la creixent preocupació causada pels gasos tòxics que emeten les activitats industrials, posant en perill el medi ambient i la vida humana.

El desenvolupament de la nanotecnologia ha creat un enorme potencial per construir sensors de gasos altament sensibles, selectius i de baix cost, i sobretot portàtils amb baix consum d'energia.

Avui en dia, els nanotubs de carboni (NTC) estan rebent un gran interès de la comunitat científica, per les seves geometria i morfologia úniques, i per les seves propietats mecàniques, tèrmiques, òptiques, i electròniques que fan d'ells un candidat prometedor per a moltes aplicacions industrials (com ara, els sensors de gasos). En aquest sentit, a través d'aquesta tesi, s'ha fet un profund estudi per explorar les propietats de detecció de diferents nanomaterials hibrids basats en nanotubs de carboni per a una eficaç detecció de gasos tòxics. Això inclou el disseny, la fabricació, caracterització i optimització dels sensors de gasos a base de materials híbrids.

Aquesta tesi va ser recolzada financerament pel projecte europeu "nano2hybrids", que explota el disseny de la interfície híbrida de les nano-particles de metall/nanotubs de carboni a través del control dels defectes estructurals i químics en una descàrrega de plasma de radiofreqüència amb aplicació a l'obtenció de sensor de gasos amb propietats millorades. El benzè va ser escollit com a gas principal, a causa dels seus greus efectes tòxics a baix nivell de ppb i de la manca de solucions en el mercat per fer-ne la detecció. De fet, no hi ha fins ara a la literatura, cap sensor de gas que pugui detectar de forma selectiva i a temperatura ambient el benzè a nivell operatiu de ppb. Així, el repte de la tesi era fabricar un sensor de gas sensible, altament selectiu i estable, portàtil i de baix cost per la detecció del benzè.

En això, els nanotubes de carboni funcionalitzats, decorats amb diferents metalls o decorats (o barrejats) amb òxid de metall, van ser profundament investigats en termes del seu funcionament (per exemple, la sensibilitat, la selectivitat, l'estabilitat, el mecanisme de detecció,. etc) en la detecció de diferents gasos (benzè (C_6H_6), monòxid de carboni (CO), diòxid de nitrogen (NO_2), l'etilè (C_2H_4), el sulfur d'hidrogen (H_2S), amoníac (NH_3) i aigua (H_2O)). Les nostres tasques han consistit en investigar experimentalment i teòricament l'efecte de les condicions de preparació dels materials (tractament de plasma, precursor i mida de les nanoparticles metàl·liques), de la

ISBN:978-84-694-0326-6/DL:T-207-2011

fabricació dels sensors (tècnica de deposició, el metall dels elèctrodes del sensor), i de les condicions de caracterització del sensor (temperatura d'operació, flux de gas) sobre les seves propietats de detecció de gasos, per adquirir coneixements i amb això afinar un sensor de gasos adequat per a la detecció de benzè, així com proposar mecanismes de detecció.

Hem trobat que els materials híbrids que consisteixen en nanotubes de carboni multi-paret, tractats amb plasma d'oxigen i decorats amb diferents nanoparticules de metall, mostren major capacitat de detecció a temperatura ambient, ja sigui per els nanotubs de carboni funcionalitzats amb plasma o els no tractats. Aquests poden veure adaptades amb enorme flexibilitat les seves propietats interficials, i per tant la seva reactivitat, el que els fa molt interessants per al reconeixement dels diferents gasos i vapors. Quan es combinen en una matriu de microsensors que operen a temperatura ambient, l'ús de nanotubs de carboni decorats amb diferents metalls, sensibles al benzè i d'altres que hi son insensibles, va permetre per primera vegada la realització d'un prototip de baix cost que pot detectar selectivament benzè quan aquest està present a nivell de traces (per sota de 50 ppb) en una barreja de gasos a temperatura ambient. Aquest prototip presenta a la vegada uns temps de resposta i de recuperació de 60 s i 10 minuts respectivament, bona estabilitat i reproductibilitat i es troba actualment protegit per una patent científica registrada, i llicenciada a una companyia per la seva comercialització industrial.

UNIVERSITAT ROVIRA I VIRGILI
DESIGN, FABRICATION AND CHARACTERISATION OF GAS SENSORS BASED ON NANOHYBRID MATERIALS
Radouane Leghrib
ISBN:978-84-694-0326-6/DL:T-207-2011

Résumé

Depuis de nombreuses années, les problèmes liés à la pollution sont très étudiés et on réalise que même à l'état de traces, les polluants atmosphériques peuvent avoir des effets néfastes à la fois sur l'humain et sur l'environnement. Le développement des activités industrielles de par le monde engendre une croissance non négligeable de pollutions sous diverses formes.

Depuis quelques années seulement, l'analyse environnementale a connu un essor remarquable lié aux progrès réalisés dans le domaine de la nanotechnologie. Celle-ci-a créé un énorme potentiel pour élaborer des capteurs de gaz miniaturisés, sensibles, sélectifs, à faible coût, et surtout portables avec une faible consommation électrique.

On distingue en particulier, un matériel qui attire l'attention de nombreuses équipes scientifiques de par le monde « les nanotubes de carbone (NTCs) ». Ceux-ci ont fait l'objet de plusieurs études touchant divers domaines, en raison de leur géométrie unique, leur morphologie et leurs excellentes propriétés électroniques, mécaniques, thermiques et optiques, qui en font un candidat prometteur pour de nombreuses applications industrielles, en particulier, les capteurs de gaz, offrant ainsi une alternative intéressante aux capteurs de gaz conventionnels.

Le sujet du travail de recherche présenté ici est consacré à l'exploration des propriétés de détection de différents nanomatériaux hybrides à base de nanotubes de carbone en vue d'une détection efficace des gaz toxiques. Ceci impliquera la conception, la fabrication, la caractérisation et l'optimisation de ces capteurs.

Cette thèse a été soutenue financièrement dans le cadre du projet Européen "nano2hybrids", qui exploite la conception de l'interface hybride des nanoparticules métalliques/nanotubes de carbone à travers le contrôle des défauts structurels et chimiques produits par la décharge de plasma", pour l'application de détection de gaz.

Le benzène a été choisi comme gaz cible principal en raison de ses graves effets toxiques à des niveaux en ppb faibles et de l'inexistence de détecteurs de gaz commerciaux sélectifs et à faible coût. En fait, aucun capteur de gaz, pouvant détecter le benzène de manière sélective au niveau du ppb à température ambiente n'a été signalé jusqu'à présent dans la littérature. Ainsi, le défi du projet consiste à fabriquer des capteurs de benzène sensibles, très sélectifs, stables, portables et de faible coût.

Ici, différents NTC fonctionnalisés, décorés avec différents métaux, et décorés et ou/ mélangés avec différents oxydes métalliques, ont été profondément étudiés en fonction

ISBN:978-84-694-0326-6/DL:T-207-2011

de leurs performances (par exemple, la sensibilité, la sélectivité, la stabilité et le mécanisme de détection, etc.) en matière de détection de différents gaz (le benzène (C_6H_6), le monoxyde de carbone (CO), dioxyde d'azote (NO_2), l'éthylène (C_2H_4), l'hydrogène sulfuré (H_2S), l'ammoniac (NH_3), et de l'eau (H_2O)). Plus concrètement, une étude expérimentale et théorique est dédiée à examiner l'effet des conditions de préparation des matériaux (traitement par plasma, précurseur et taille des nanoparticules métalliques), la fabrication des capteurs (technique de dépôt, électrodes métalliques de détection), et les conditions de caractérisation (température de fonctionnement, débit de gaz) sur les propriétés de détection du capteur de gaz, d'acquérir des connaissances pour enfin réaliser un capteur de gaz approprié, ainsi qu'expliquer les mécanismes de son fonctionnement.

Nous avons constaté que les matériaux hybrides constitués de nanotubes de carbone multi-parois traités par plasma d'oxygène et décorés avec différentes nanoparticules métalliques, montrent une haute capacité de détection, notamment à température ambiente, plus élevée que celle des nanotubes de carbone vierges ou fonctionnalisés avec le plasma. Ceux-ci peuvent avoir des propriétés interfaciales adaptées, ce qui offre une grande flexibilité pour adapter leurs réactivités pour la reconnaissance des différents gaz et vapeurs cibles. Lorsqu'ils étaient inclus dans une matrice de micro-capteurs fonctionnant à température ambiente, la combinaison des nanotubes de carbone décorés avec des métaux, sensibles et insensibles au benzène, a permis pour la première fois la mise en œuvre d'un prototype à faible coût capable de détecter de manière sélective le benzène à température ambiente lorsque celui-ci est présent sous formes de traces (en dessous de 50 ppb) dans un mélange gazeux. Ce dispositif présente à la fois un temps de réponse et de récupération de 60 s et 10 min respectivement, une bonne stabilité et reproductibilité. Ce prototype fut protégé par un brevet scientifique enregistré et licencié à une société qui prend en charge la commercialisation industrielle du produit.

UNIVERSITAT ROVIRA I VIRGILI
DESIGN, FABRICATION AND CHARACTERISATION OF GAS SENSORS BASED ON NANOHYBRID MATERIALS
Radouane Leghrib
ISBN:978-84-694-0326-6/DL:T-207-2011

Thesis publications

UNIVERSITAT ROVIRA I VIRGILI
DESIGN, FABRICATION AND CHARACTERISATION OF GAS SENSORS BASED ON NANOHYBRID MATERIALS
Radouane Leghrib
ISBN:978-84-694-0326-6/DL:T-207-2011

ISBN:978-84-694-0326-6/DL:T-207-2011

Publications in international Journals

1. Ionescu, R.; Espinosa, E.H.; **Leghrib, R.**; Felten, A.; Pireaux, J.J.; Erni, R.; Van Tendeloo, G.; Bittencourt, C.; Cañellas, N.; Llobet, E, Novel hybrid materials for gas sensing applications made of metal-decorated MWCNTs dispersed on nano-particle metal oxides, Sensors and Actuators B-Chemical, 131, 174-182 (2008).

2. Charlier, J.C.; Arnaud, L.; Avilov, I.V.; Delgado, M.; Demoisson, F.; Espinosa, E.H.; Ewels, C.P.; Felten, A.; Guillot, J.; Ionescu, R.; **Leghrib, R.**; Llobet, E.; Mansour, A.; Migeon, H.N.; Pireaux, J.J.; Reniers, F.; Suarez-Martinez, I.; Watson, G.E.; Zanolli, Z, Carbon nanotubes randomly decorated with gold clusters: from nano2hybrid atomic structures to gas sensing prototypes, Nanotechnology, 20 (37), 375501-375511 (2009).

3. Espinosa, E.; Ionescu, R.; Zampolli, S.; Elmib, I.; Cardinali, G.C.; Abadc, E.; **Leghrib, R**.; Ramírez, J.L.; Vilanova, X.; Llobet, E, Drop-coated sensing layers on ultra low power hotplates for an RFID flexible tag microlab, Sensors and Actuators B-Chemical, 144 (10), 462-466 (2009).

4. **Leghrib, R.**; Pavelko, R.; Felten, A.; Vasiliev, A.; Cané, C.; Gràcia, I.; Pireaux, J.J.; Llobet, E, Gas sensing properties of MWCNTs decorated with tin oxide nanoclusters, Sensors and Actuators B-Chemical, 145, 411-416 (2010).

5. **R. Leghrib**, E. Llobet, A. Felten, J. J. Pireaux, Z. Zanolli, J.C. Charlier, I. Suarez, C. Ewels, NO_2 and CO interaction with plasma treated Au-decorated MWCNTs: detection pathways, Sensors and Actuators B-Chemical, 2010, Submitted,

6. **R. Leghrib**, A. Felten, F. Demoisson, F. Renier, J-J Pireaux and E. Llobet, Room-Temperature, selective detection of benzene at trace levels based on plasma-Treated Metal decorated Multiwalled Carbon nanotubes, Carbon, 48, 2010, 3477-3484.

7. **Leghrib, R.**; Suarez-Martinez, I.; Grobert, N.; Llobet, E.; Ewels, C, Nitrogen and boron doped carbon nanotubes for gas detection, Sensors and Actuators B-Chemical**:** 2010, in preparation.

8. **R. Leghrib**, A Feleten, J. J. Pireaux, E. Llobet, gas sensors based on doped-CNTs/SnO2 composites for NO2 detection at room temperature, Thin film, 2010, Submitted

9. **R. Leghrib**, T. Dufour, F. Demoisson, N. Claessens, F. Reniers, E. Llobet, Effect of carbon nanotubes treatment on their sensing properties, Sensors and Actuators: B-chemical, 2010, In preparation

10. Z.Zanolli, **R. Leghrib**, E. Llobet, A. Felten, J.J. Pireaux, J. C. Charlier, reactivity of gold nanoclusters into Au/CNTs based gas sensor, Nanoletters, 2010, In preparation

ISBN:978-84-694-0326-6/DL:T-207-2011

Other Publications: "Patent"

Inventor/s : Eduard Llobet, **Radouane Leghrib**, Alex, JJ, Piraux, F. Renier, F. Demoisson, J.Guillot, Ali Mansour, Marc Delagado
Title: Dispositivo para la detección selectiva de gas benceno, procedimiento para su obtención y detección del gas con el mismo
Application number: P200930969 **First priority country:** SPAIN **Date of priority:** 2009
Main institution: URV - Universitat Rovira i Virgili

ISBN:978-84-694-0326-6/DL:T-207-2011

Contributions in international conferences

1. **R. Leghrib**, E. Llobet, Enhancement of sensitivity in gas chemiresistors based on carbon nanotubes surface functionalized and decorated with nobele metal (Au or Pd) nanoclusters, conferance red IBERNAM, 2008, Tarragona (SPAIN), Poster, Abstract Book.

2. **R. Leghrib**, R. Ionescu, E.H. Espinosa, E. Sotter, A. Felten, C. Bittencourt, J-J. Pireaux, R. Erni, G. Vantendeloo and E. Llobet, Gas sensors based on Metal decorated carbon nanotubes: evaluation of different deposition methods for avoiding clusters release, International conference on carbon nanoscience and nanotechnology; NanoteC07, 2007, Brighton (UNITED KINGDOM), Oral presentation, Abstract Book.

3. **R. Leghrib**, R. Ionescu, E.H. Espinosa, E. Sotter, A. Felten, C. Bittencourt, J-J. Pireaux, R. Erni, G. Vantendeloo and E. Llobet, Novel hybrid materials for gas sensing applications made of metal decorated MWCNT dispersed on nano-particularmetal oxide, European materials research society E-MRS 2007, Spring Meeting, 2007, Strasbourg (FRANCE), Oral presentation, Abstracts Book, pp.

4. **R. Leghrib**, R. Ionescu, E.H. Espinosa, E. Sotter, A. Felten, C. Bittencourt, J-J. Pireaux, R. Erni, G. Vantendeloo and E. Llobet, Nanohybrid materials for gas sensing, Trans-Pyrenees meeting on Micro and Nanosystem-2007, 2007, Zaragoza (SPAIN), Oral presentation, Abstracts Book, pp.

5. **R. Leghrib**, R. Ionescu, E.H. Espinosa, E. Sotter, A. Felten, C. Bittencourt, J-J. Pireaux, R. Erni, G. Vantendeloo and E. Llobet, Sensitivity enhanccement in gas chemoresistors based on surfece functionalized carbon nanotubes decorated with metal nanoclusters, International conferance on carbon nanoscience and nanotechnology, 2008, Brighton (UNITED KINGDOM), Oral presentation, Abstracts Book.

6. **R. Leghrib**, R. Ionescu, E.H. Espinosa, E. Sotter, A. Felten, C. Bittencourt, J-J. Pireaux, R. Erni, G. Vantendeloo and E. Llobet, Enhancement of the sensitivity in gas chemiresistors based on carbon nanotubes surface functionalized and decorated with noble metal Au nanoclusters, 5th International workshop Semiconductor Gas Sensors (SGS'2008), 2008, Zakopane (POLAND), Invited conference, Poster, Abstracts Book, pp.

7. **R. Leghrib**, R. Ionescu, E.H. Espinosa, E. Sotter, A. Felten, C. Bittencourt, J-J. Pireaux, R. Erni, G. Vantendeloo and E. Llobet, Enhancement of the sensitivity in gas chemiresistors based on carbon nanotubes surface functionalized and decorated with noble metal Au nanoclusters, 5th International workshop Semiconductor Gas Sensors (SGS'2008), 2008, Zakopane (POLAND), Invited conference, Oral presentation, Abstracts Book, pp.

8. **R. Leghrib**, R. Ionescu, E.H. Espinosa, E. Sotter, A. Felten, C. Bittencourt, J-J. Pireaux, R. Erni, G. Vantendeloo and E. Llobet, Integrated microarrays of metal decorated carbon nanotube gas sensors, Eurosensors XXII (2008), 2008, Dresden (GERMANY), Oral presentation, Abstracts Book, pp.

ISBN:978-84-694-0326-6/DL:T-207-2011

9. **R. Leghrib**, R. Ionescu, E.H. Espinosa, E. Sotter, A. Felten, C. Bittencourt, J-J. Pireaux, R. Erni, G. Vantendeloo and E. Llobet, Responsiveness of nanoclusters decorated MWCNTs, International conferance on carbon nanoscience and nanotechnology; NanoteC09, 2009, Brussels (BELGIUM), Poster, Abstracts Book, pp.

10. **R. Leghrib**; Ionescu, R.; Espinosa, E.H.; Sotter, E.; Felten, A.; Bittencourt, C.; Pireaux, J.J.; Erni, R.; Vantendeloo, G.; Llobet, E, Gas sensing properties of MWCNTs decorated with gold or tin oxide nanoparticles, Eurosensors 2009, 2009, Lausanne (SWITZERLAND), Poster, Technical Digest of the Eurosensors 2009 conference

11. **R. Leghrib**, R. Ionescu, E.H. Espinosa, E. Sotter, A. Felten, C. Bittencourt, J-J. Pireaux, R. Erni, G. Vantendeloo and E. Llobet, NO_2 and CO interaction with plasma treated Au-decorated MWCNTs: Detection pathways, Eurosensors 2009, 2009, Lausanne (SWITZERLAND), Poster, Technical Digest of the Eurosensors 2009 conference.

12. **R. Leghrib**, A. Felten, J-J. Pireaux and E. Llobet, Gas sensing properties towards traces of toxic gases using Nano2hybrids materials, E-MRS 2009 full meeting, 2009, Warsaw University of Technology (POLAND), Invited conference, Abstracts Book, pp.

13. **R. Leghrib**, R. Pavelko, A. Felten, A. Vasiliev, C. Cané, I. Garcia, J-J. Pireaux,and E. Llobet, Metal oxide-CNTs hybrids for room temperature gas sensing, International workshop on solid state lasers: solid state lasers. 50 years after'; 17-20/03/2010, 2010, Tarragona (SPAIN), Poster, Abstracts Book, pp. P-37.

14. **R. Leghrib**, A. Felten, F. Demoisson, F. Reniers, J. J. Pireaux, and E. Llobet, Selective detection of benzene traces at room temperature using metal decorated carbon nanotubes, Eurosensors 2010, Linz (Austria), 2010, Oral communication, Abstracts Book, pp.

15. **R. Leghrib**, E. Llobet, Gas sensors based on doped-CNT/SnO_2 composites, 6th International workshop Semiconductor Gas Sensors (SGS'2010), 2010, Kraków (POLAND), Invited conference, Poster, Abstracts Book, pp.

ISBN:978-84-694-0326-6/DL:T-207-2011

Contributions in national conferences

1. **R. Leghrib**, R. Ionescu, E.H. Espinosa, E. Sotter, A. Felten, C. Bittencourt, J-J. Pireaux, R. Erni, G. Vantendeloo and E. Llobet, Enhancement of the sensitivity of gas sensors to toxic gases by using a novel hybrid material (Metal decorated MWCNTs/Metal oxide), Graduated Student Meeting on Electronic Engineering, 2007, Tarragona (SPAIN), Poster, Abstracts Book, pp. 67-68

2. E.H. Espinosa, **R. Leghrib**, E. Sotter, R. Ionescu, C. Bittencourt, A. Felten, J-J. Pireaux and E. Llobet, New TiO2 and carbon nanotube hybrid microsensors for detecting traces of O2 in beverage grade CO2, Graduated Student Meeting on Electronic Engineering, 2007, Tarragona (SPAIN), Poster, Abstracts Book, pp. 61-63

3. **Leghrib, R.**; Ionescu, R.; Espinosa, E.H.; Bittencourt, C.; Felten, A.; Pireaux, J.J.; Correig, X.; Llobet, E, MWCNT with gold and silver nanoclusters for room temperature gas sensing, NANOARACAT Scientific Workshop, 2007, Barcelona (SPAIN), Poster, Abstract book

4. **R. Leghrib**, Felten, J-J. Pireaux and E. Llobet, Enhancement of sensitivity in gas chemiresistors based on carbon nanotubes surface functionalized and decorated with nobele metal nanoclusters, Graduated Student Meeting on Electronic Engineering, 2008, Tarragona (SPAIN), Poster, Abstracts Book, pp. 53-54

5. **R. Leghrib**, R. Ionescu, E.H. Espinosa, E. Sotter, A. Felten, C. Bittencourt, J-J. Pireaux, R. Erni, G. Vantendeloo and E. Llobet, Enhancement of the sensitivity in gas chemiresistors based on carbon nanotubes surface functionalized and decorated with noble metal (Au or Pd) nanoclusters, Gas and Radiation sensors: Properties; characterisation. Thin films based sensors, 2008, Salamanca (SPAIN), Poster, Abstracts Book, pp.

6. **R. Leghrib**, R. Ionescu, E.H. Espinosa, E. Sotter, A. Felten, C. Bittencourt, J-J. Pireaux, R. Erni, G. Vantendeloo and E. Llobet, Enhancement of the sensitivity in gas chemiresistors based on carbon nanotubes surface functionalized and decorated with noble metal (Au or Pd) nanoclusters, Gas and Radiation sensors: Properties; characterisation. Thin films based sensors, 2008, Salamanca (SPAIN), Oral presentation, Abstracts Book, pp.

7. **R. Leghrib**, E. Llobet, R. Pavelko, A.A. Vasiliev, A. Felten, J.J Pireaux, Increasing surface reactivity of MWCNTs at room temperature, Graduated Student Meeting on Electronic Engineering, 2009, Tarragona (SPAIN), Oral presentation, Abstracts Book, pp. 53-54

8. **R. Leghrib**, A. Felten, F. Demoisson, F. Reniers, J-J. Pireaux, E. Llobet, Metal decorated carbon nanotubes sensor array for toxic gas discrimination, Graduated Student Meeting on Electronic Engineering, 2010, Tarragona (SPAIN), Oral presentation, Abstracts Book, pp. 43-44.

UNIVERSITAT ROVIRA I VIRGILI
DESIGN, FABRICATION AND CHARACTERISATION OF GAS SENSORS BASED ON NANOHYBRID MATERIALS
Radouane Leghrib
ISBN:978-84-694-0326-6/DL:T-207-2011

UNIVERSITAT ROVIRA I VIRGILI
DESIGN, FABRICATION AND CHARACTERISATION OF GAS SENSORS BASED ON NANOHYBRID MATERIALS
Radouane Leghrib
ISBN:978-84-694-0326-6/DL:T-207-2011

INDEX

ISBN:978-84-694-0326-6/DL:T-207-2011

UNIVERSITAT ROVIRA I VIRGILI
DESIGN, FABRICATION AND CHARACTERISATION OF GAS SENSORS BASED ON NANOHYBRID MATERIALS
Radouane Leghrib
ISBN:978-84-694-0326-6/DL:T-207-2011

UNIVERSITAT ROVIRA I VIRGILI
DESIGN, FABRICATION AND CHARACTERISATION OF GAS SENSORS BASED ON NANOHYBRID MATERIALS
Radouane Leghrib
ISBN:978-84-694-0326-6/DL:T-207-2011

UNIVERSITAT ROVIRA I VIRGILI
DESIGN, FABRICATION AND CHARACTERISATION OF GAS SENSORS BASED ON NANOHYBRID MATERIALS
Radouane Leghrib
ISBN:978-84-694-0326-6/DL:T-207-2011

1. GENERAL INTRODUCTION

UNIVERSITAT ROVIRA I VIRGILI
DESIGN, FABRICATION AND CHARACTERISATION OF GAS SENSORS BASED ON NANOHYBRID MATERIALS
Radouane Leghrib
ISBN:978-84-694-0326-6/DL:T-207-2011

ISBN:978-84-694-0326-6/DL:T-207-2011

The need for air pollutant monitoring

During the last century, the global development of industrial, chemical activities has been very strong, which has caused a radical change into human life. Some manmade activities like petrochemical industry, transport (e.g. automobile exhausts), intensive agriculture with use of pesticides, release poisonous substances the toxicity of which can seriously affect the environment and human health in different ways depending on their nature, their concentration and exposure duration [1-6].

As an example of the effects of air pollutants on the environment is acid rain [7, 8], a form of precipitation that contains high levels of sulphuric or nitric acids which can contaminate drinking water, cause harm to vegetation and aquatic life, and erode buildings. Other effects caused by pollutants are the depletion of the ozone layer, the greenhouse effect, etc [9-13].

Concerning humans, toxic gases can get into the human body through breathing, ingestion or skin absorption [14]. Once inside the body, they can stay in lungs, be exhaled or move into the blood (from the lungs, the digestive system or skin) (Figure 1).

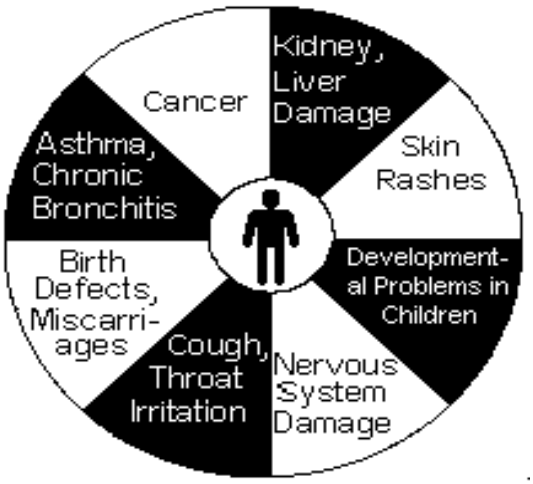

Figure 1: Toxic gases impact on human health

They most commonly change chemical reactions within individual cells, resulting in different health problems (Figure 1). For example, inhaling benzene fumes that are given off when pumping gas into the car can increase the chances of experiencing health effects that have been associated with exposure to benzene, such as “leukaemia”. Nitrogen dioxide (NO_2) is a common pollutant in the atmosphere and is difficult to decompose at room temperature. It produces acid rain and destroys ozone. Nitrogen

ISBN:978-84-694-0326-6/DL:T-207-2011

oxides (NO_x) can cause lung irritation and weaken the body's defences against respiratory infections such as pneumonia and influenza. Carbon monoxide (CO) can also be formed by the combustion of gasoline. When inhaled, it blocks the transport of oxygen to the brain, heart, and other vital organs in human body, etc [5, 6 and 14].

Thus, the awareness of the need to protect the global environment has significantly increased since the first United Nations (UN) Conference on the Environment in Stokholm in June 1972 [15]. Since the 1990's, attitudes within the industry have been changing very quickly and are getting closer to the public perception that there is a need for promoting the protection of the environment protection and the health and security of workers.

Worldwide, environment safety commissions keep lowering the exposure limits to toxic gases in order to protect human health from the threats that can be caused by those hazardous gases. This is especially true for employees working in critical areas (e.g. in refineries). This has suggested investigating effective techniques in order to measure the level of contaminants in air. We should notice that there are two types of detection systems used for monitoring toxic gases: analytical instruments and solid state gas sensors:

Conventional analytical instruments

Nowadays, some classical analytical techniques are being used efficiently to monitor the environment contaminant level. For example:

- **Fourier transform infrared (FTIR) instruments** [16]
- **Gas chromatograph** [17]
- **Mass spectrometer** [18]

These instruments provide fairly accurate and selective gas readings. However, they require skilled and knowledgeable operators, are generally very expensive and designed for laboratory tabletops or specific on-line applications for in-plant installations. Many of them suffer from limitations such as high cost, high maintenance, slow response time, and large size, making them impractical monitors for area air quality and safety [19].

On the other hand, solid state gas sensors can be integrated in another kind of detection systems that can be used for gas identification and control. These systems rely on a

ISBN:978-84-694-0326-6/DL:T-207-2011

sensing layer that allows to recognize the gas with which it interacts and a system allowing to transform that chemical interaction into an electrical signal.

Solid state semiconductor gas sensors

Chronological development

The idea of solid state semiconductor gas sensors is not a recent one. In fact, the first-generation of such gas sensors appeared in 1968 with a metal oxide-based gas sensor which was accidently discovered. In fact, it was observed that the semi-conductor properties of metal oxides are affected by the change in the partial pressure of oxygen in air. This attracted the scientists' attention and finally Naoyoshi Tagushi demonstrated that SnO_2 can be used as gas sensitive material [20]. This finding has opened new challenges for the use of gas sensors and since then many metal oxides have been explored as gas sensitive materials (SnO_2, WO_3, ZnO, Fe_2O_3, etc). More recently other semiconductor materials have been explored as candidate materials for detecting gases such as graphene or carbon nanotubes.

Today, a wide spectrum of solid state semiconductor gas sensors is available, which can detect wide range of toxic gases at sub-ppm levels.

Detection systems based on such sensors have demonstrated their practical and simpler use than conventional gas monitoring techniques because they are [21]:

- ✓ Rugged and corrosion-resistant
- ✓ Weather- and dust-proof
- ✓ Capable of being installed in hazardous areas
- ✓ Durable and long-term
- ✓ Operationally stable
- ✓ Easy to maintain
- ✓ Operated by a minimally skilled person

A lot of efforts have been oriented to the enhancement of their above promising characteristics more especially to their miniaturization. Nowadays, silicon micro-technology has allowed fabricating low cost, portable-small size and mechanically robust gas sensors [22-24].

The operating mechanism of most solid state semiconductor sensors is the change of their conductivity upon adsorption of gases. Unfortunately, up to now, no semiconductor gas sensors exist that are 100 % intrinsically selective to a target gas.

ISBN:978-84-694-0326-6/DL:T-207-2011

Achieving such selectivity requires the use of chemical or physical filters or sensor arrays with overlapping sensitivities [25].

A new trend: Carbon nanotube materials

In the last few years, different studies have shown the excellent potential of carbon nanotubes (CNTs) as sensitive material for detecting biological and chemical molecules [26-27]. Via a functionalisation of CNT sidewalls, a better chemical bonding between a specific functional group and the nanotube can be reached and the selectivity of the adsorption process can be enhanced [26-27]. Some properties of CNTs make them very attractive to produce small, wearable sensors for industrial and transport environments [28]:

- Their intrinsic strength makes them suited for miniaturised sensors and usable on flexible substrates [19].
- They respond even operated at room temperature, which is optimal for ultra-low power, wearable, battery-operated devices. Such devices could easily meet the requirements of intrinsically safe operation, needed in industrial environments where the occurrence of flammable/explosive atmospheres is possible.
- Once functionalised, the adsorption of a small quantity of chemical species can result in a dramatic change of the CNT conductivity. Therefore, CNT are suited to detect species at low concentrations (e.g. low ppb level).
- A sensor can be built using a simple transducer (comb electrodes) to monitor the electrical resistance of a CNT-based film.

Application to benzene monitoring

Among the most harmful substances that are usually found in the environment, volatile organic compounds, particularly benzene, deserve special attention. Benzene is a flammable and toxic gas from the family of aromatic hydrocarbons, recognized as human carcinogen by European Union [29].

Benzene is an aromatic hydrocarbon organic chemical compound with the molecular formula C_6H_6 (figure 2). It is a non polar molecule. Benzene is a colorless or light yellow liquid at room temperature. It has a sweet odor and is highly flammable. Benzene evaporates into the air very quickly. Its vapor is heavier than air and may sink

ISBN:978-84-694-0326-6/DL:T-207-2011

into low-lying areas. Benzene dissolves only slightly in water and will float on top of water.

Benzene is formed from both natural processes and human activities. Natural sources of benzene include volcanoes and forest fires. Benzene is also a natural part of crude oil, gasoline, and cigarette smoke. Some industries use benzene to make other chemicals that are used to make plastics, resins, and nylon and synthetic fibers. Benzene is also used to make some types of lubricants, rubbers, dyes, detergents, drugs, and pesticides.

Outdoor air contains benzene coming from tobacco smoke, gas stations, motor vehicle exhaust, and industrial emissions. Indoor air generally contains levels of benzene higher than those in outdoor air. The benzene in indoor air comes from products that contain benzene such as glues, paints, furniture wax, and detergents. The air around hazardous waste sites or gas stations can contain higher levels of benzene than in other areas. Benzene leaks from underground storage tanks or from hazardous waste sites containing benzene can contaminate well water. People working in industries that make or use benzene may be exposed to the highest levels of it. A major source of benzene exposure is tobacco smoke. Benzene works by causing cells not to work correctly. For example, it can cause bone marrow not to produce enough red blood cells, which can lead to anemia. Also, it can damage the immune system by changing blood levels of antibodies and causing the loss of white blood cells [2-5, 30]. The seriousness of poisoning caused by benzene depends on the amount, route, and time exposure, as well as the age and preexisting medical condition of the exposed person.

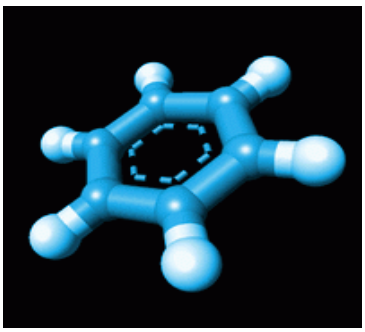

Figure 2: planar structure of benzene molecule

This is why the permissible exposure limit has been lowered from 10 ppm to 100 ppb in the last 10 years. And this limit could be further reduced because there may be no safe exposure level for benzene. Occupational exposure to benzene occurs in the petrochemical industry (i.e Benzene is one of the constituents of the complex mixtures

ISBN:978-84-694-0326-6/DL:T-207-2011

coming from the cracking and catalytic reforming of petroleum hydrocarbures), land reclamation, coke/oven operators, petrol stations, motor vehicle repair and roadside works [2-5, 30].

An effective and accurate monitoring of benzene needs the use of simple, affordable and widespread sensing systems. Two paramount features of such sensing systems should be their sensitivity, since the concentration of benzene must be detected in the ppb range (1 to 100 ppb) [31], and their selectivity. The reference methods for the analysis of benzene imply pumped sampling and subsequent analysis for chromatographic determination, the use of colorimetric detector tubes and PID detectors (which are not selective for benzene and give, in fact, a total reading for volatile organic compounds) [32]. Therefore, a very sensitive, selective and affordable benzene sensor/monitor that can be used in industrial, and transport environments is still to be developed. In parallel, during the past decade, several studies have been reported on modifying thin and thick film semiconductor metal oxide (SMO) sensors for atmospheric gaseous pollutants like VOCs [33-36]. Several sensors have been fabricated during the last decade to selectively detect various VOC components such as ethanol, acetone, and aromatic hydrocarbons (Benzene) [37]. However, these materials require high power consumption due to their high operating temperature (250-500 ºC).

Recent development of nanotechnology has created huge potential to build highly sensitive, low cost, portable sensors with low power consumption. The extremely high surface to- volume ratio and hollow structure of nanomaterials is ideal for gas molecules adsorption and storage. Furthermore, nanotubes exhibit interesting electrical conduction properties. Therefore, gas sensors based on nanomaterials, such as carbon nanotubes (CNTs), nanowires, nanofibers, and nanoparticles, have been investigated widely [38].

Carbon nanotubes, since been firstly discovered by Iijima in 1991 [39], have drawn high research interests because of their unique geometry, morphology, and properties. For example, CNTs-based gas sensing systems and the theoretical analysis of gas adsorption and collision effects on the nanotubes have been the subject of intense research [40- 42].

Carbon nanotubes are known to interact with molecular benzene. The physisorption of benzene is an example of non-covalent functionalisation involving π-stacking interactions and corresponding to a weak binding energy. Despite these and the aforementioned interesting properties, no benzene sensors based on CNT films have been reported until now. In fact, *ab initio* calculations have shown that the electronic properties of CNTs remain unchanged upon benzene adsorption [43].

UNIVERSITAT ROVIRA I VIRGILI
DESIGN, FABRICATION AND CHARACTERISATION OF GAS SENSORS BASED ON NANOHYBRID MATERIALS
Radouane Leghrib
ISBN:978-84-694-0326-6/DL:T-207-2011

This thesis is a fruit of the Nano2hybrids project. Its aim was the design and fabricate semiconductor gas sensors based on CNT-metal cluster hybrids with superior performance (highly selective and sensitive towards benzene), able to work at room temperature. Although a detector for molecular benzene was the main application to be developed, the detection of other pollutants/toxic species such as ammonia, nitrogen dioxide, carbon monoxide is also addressed.

The whole work within the project was shared between eight partners. Our group (**URV**[1]) was in charge of the design, fabrication, characterization, and optimization of gas sensor.

LISE[2], **CHANI**[3], and **SAM**[4] teams, worked on the preparation (functionalization and metal decoration), structural characterization (SEM, TEM, XPS, etc) and optimization (grain size, dispersion and homogeneity of nanocluster, etc) of the nano2hybrid materials. Two others teams (**IMN**[5], and **PCPM**[6]) carried out the modelling and simulation of the electronic structure of the nano2hybrid materials including their interaction with gases. **Sensotran**[7] **Company** was in charge of the validation of the industrial application. Finally, **VEGA**[8] **Company** provided science outreach.

Gas sensitive materials used

In addition to the metal-decorated materials provided by the three partners of the Nano2hybrids project, other nano-hybrid materials were also investigated during this thesis.

[1] Microsystems and Nanotechnology for Chemical Analysis group, Rovira i Virgili University, Spain

[2] Laboratoire Interdisciplinaire de Spectroscopie Electronique, Namur University, Belgium

[3] Service de Chimie Analytique et Chimie des Interfaces, Brussels University, Belgium.

[4] Service d'Analyse des Matériaux, Institut Gabriel Lippmann, Luxembourg.

[5] Institut des Matériaux de Nantes, CNRS-IMN, France

[6] Unité de physico-chimie et de physique des matériaux, Louvain University, Belgium

[7] Sensotran S.L, Spain

[8] VEGA Science Trust, United Kingdom

ISBN:978-84-694-0326-6/DL:T-207-2011

In fact, metal-oxide doped carbon nanotubes are a new trend in the fabrication of gas sensors. These materials either home synthesized or commercial were mixed with oxygen functionalized carbon nanotubes or with different metal decorated carbon nanotubes.

Finally, nitrogen and boron doped carbon nanotubes were also employed. These materials were provided by the Department of Materials from Oxford University, UK.

All those materials were compared in terms of their sensing performance towards gases such as ammonia (NH_3), nitrogen dioxide (NO_2), carbon monoxide (CO), ethylene (C_2H_4), hydrogen sulphide (H_2S) and benzene (C_6H_6). The aim is to build a detector able to selectively detect toxic gases in ambient air.

The experimental characterization of those sensors was supported by ab-initio calculations in order to predict or explain the behaviour of those materials towards gases.

Structure of the thesis

The second chapter of this thesis will be dedicated to review the state of art of carbon nanotubes based gas sensors. In this section, the fabrication and functionalization procedures of carbon nanotubes reported in the literature will be reviewed, and then the use of carbon nanotubes as gas sensors will be presented for the detection of toxic gases in general and with a special emphasis on benzene. In the case of benzene, carbon nanotubes based sensors will be compared to other conventional gas detectors.

In the third chapter, we will explain the experimental work performed during this thesis concerning the fabrication and characterization of the different active materials. The technological steps involved in the fabrication of the gas sensor including the gas sensor membrane and the deposition techniques used to deposit the active layer over the membrane will be described. At the end, the characterization procedure of the sensing properties of those sensors towards different gases will be shown.

The fourth chapter will focus on the procedure used to perform the ab-initio calculations and some theoretical results obtained with nitrogen and boron doped carbon nanotubes during a stay in the “Institut des Matériaux Jean Rouxel de Nantes” in France.

Within the fifth chapter, we will explain the characterization results of all the hybrid active layers towards the different gases. We will focus mainly on the study of metal decorated carbon nanotubes for the selective detection of the toxic gases tested.

ISBN:978-84-694-0326-6/DL:T-207-2011

The selective detection of benzene will be reported in depth in the sixth chapter of this thesis. This allowed the development of the first prototype of benzene detector based on a four sensor array. This was patented as new invention and licensed to Sensotran company [44].

Finally, the general conclusions derived from this work will be presented.

ISBN:978-84-694-0326-6/DL:T-207-2011

References

[1] (a) S. F. Watts, The mass budgets of carbonyl sulfide, dimethyl sulfide, carbon disulfide and hydrogen sulfide, Atmospheric Environment, 34, 761–779 (2000).

(b) D. Gabriel and M.A. Deshusses, Retrofitting existing chemical scrubbers to biotrickling filters for H_2S emission control, PNAS 100, 6308–6312 (2003).

[2] R.E. Hester, R.M. Harrison, Volatile organic compounds in the atmosphere, Issues in Environmental Science and Technology, The Royal Society of Chemistry, Cambridge, UK, 4, 140 (1995).

[3] D. Dougherty, S. Garte, A. Barchowsky, J. Zmuda, E. Taioli, NQO1, MPO, CYP2E1, GSTT1 and GSTM1 polymorphisms and biological effects of benzene exposure- a literature review, Toxicology Letters, 182, 7-17 (2008).

[4] A.P. DeCaprio, The toxicology of hydroquinone- Relevance to occupational and environmental exposure, Critical Reviews in Toxicology, 29, 283-330 (1999).

[5] H.G. Abadin, C.-H.S.J. Chou, F.T. Llados, Health effects classification and its role in the derivation of minimal risk levels: Immunological effects, Regulatory Toxicology and Pharmacology, 47, 249-256 (2007).

[6] R. Duarte-Davidson, C. Courage, L. Rushton, L. Levy, Benzene in the environment: an assessment of the potential risks to the health of the population, Occupational and Environmental Medicine, 58, 2-13 (2001).

[7] G. E Likens, W. C. Keene, J. M. Miller and J. N. Galloway. 1987, Chemistry of precipitation from a remote, terrestrial site in Australia, Journal of geophysical research, 92, 13299-13314 (1987)

[8] K. C. Weathers, G. E. Likens, T. J. Butler, and A. Elliott, Acid rain, 1549-1561. In: W. Rom (ed.). Environmental and Occupational Medicine, 4th edition. Lippincott-Raven Publishers, Philadelphia (2006)

[9] Part III. The Science of the Ozone Hole, http: //www.atm.ch.cam.ac.uk/tour/part3.html. Retrieved 2007-03-05

[10] "Chlorofluorocarbons (CFCs) are heavier than air, so how do scientists suppose that these chemicals reach the altitude of the ozone layer to adversely affect it?". http://www.sciam.com/article.cfm?id=chlorofluorocarbons-cfcs. Retrieved 2009-03-08.

[11] R. Dobson, Ozone depletion will bring big rise in number of cataracts". BMJ 331 7528, 1292. doi:10.1136/bmj.331.7528.1292-d. PMID 16322012. (2005)

[12] (a) P. A Newman, "Chapter 5: Stratospheric Photochemistry Section 4.2.8 ClX catalytic reactions". in Todaro,

(b) Richard M. Stratospheric ozone: an electronic textbook. NASA Goddard Space Flight Center Atmospheric Chemistry and Dynamics Branch.

http://www.ccpo.odu.edu/SEES/ozone/class/Chap_5/index.htm.

[13] Stratospheric Ozone Depletion by Chlorofluorocarbons (Nobel Lecture) Encyclopedia of Earth

[14] http://www.eoearth.org/article/Absorption_of_toxicants

[15]http://www.unep.org/Documents.Multilingual/Default.asp?documentid=97&articleid=1503

ISBN:978-84-694-0326-6/DL:T-207-2011

[16] J. Heland, R. Haus, K. Schafer, Remote sensing and analysis of trace gases from hot aircraft engine plumes using FTIR-emission-spectroscopy, Science of The Total Environment, 158, 85-91 (1994).

[17] K.M. Van Geem, S.P. Pyl, M-F Reyniers, J. Vercammen, J. Beens, G. B. Marin, On-line analysis of complex hydrocarbon mixtures using comprehensive two-dimensional gas chromatography, Journal of Chromatography A, Article in Press, Corrected Proof doi:10.1016/j.chroma.2010.04.006 (2010)

[18] A. J. Taylor, R.S.T. Linforth, Direct mass spectrometry of complex volatile and non-volatile flavour mixtures, International Journal of Mass Spectrometry, 223, 179-191 (2003)

[19] http://www.gotgas.com/pdf/Intro_Chap01.pdf

[20] N. Tagushi, Japan Patent 45-38200, (applied in 1962)

[21] S. M. Kanan, O. M. El-Kadri, I. A. Abu-Yousef and M. C. Kanan, Semiconducting Metal Oxide Based Sensors for Selective Gas Pollutant Detection, Sensors, 9, 8158-8196 (2009).

[22] W. Lang, Silicon microstructuring technology, Materials Science and Engineering, 17, 1-55 (1996)

[23] V. Demarne, A. Grisel, R. Sanjines, F. Lévy, Integrated semiconductor gas sensors evaluation with an automatic test system, Sensors and Actuators B: Chemical, 1, 87-92 (1990).

[24] Q. Wu, K.M. Lee, C.C. Liu, Development of chemical sensors using microfabrication and micromachining techniques, Sensors and Actuators B, 13/14, 1-6 (1993)

[25] A. Star, V. Joshi, S. Skarupo, D. Thomas, and J-C P. Gabriel, Gas Sensor Array Based on Metal-Decorated Carbon Nanotubes, **Journal of Physical Chemistry B**, 110, 21014-21020 (2006)

[26] P. Bondavalli, P. Legagneux, D. Pribat, Carbon nanotubes based transistors as gas sensors: State of the art and critical review, Sensors and Actuators B Chemical, 140, 304-318 (2009).

[27] C. Li, E.T. Thostenson, T.W. Chou, Sensors and actuators based on carbon nanotubes and their composites: A review, Composites Science and Technology, 68, 1227-1249 (2008).

[28] W-D. Zhang and W-H. Zhang, Carbon Nanotubes as Active Components for Gas Sensors, Journal of Sensors Volume 2009, Article ID 160698, 16 pages doi:10.1155/2009/160698

[29] http://www.sciencelab.com/xMSDS-Benzene-9927339

[30] R. Duarte-Davidson, C. Courage, L. Rushton, L. Levy, Benzene in the environment: an assessment of the potential risks to the health of the population, Occupational and Environmental Medicine, 58, 2-13(2001)

[31] Directive 2008/50/EC of the European Parliament and of the Council of 21 May 2008 on ambient air quality and cleaner air for Europe, Official Journal of the European Union, L 152/1 (2008)

ISBN:978-84-694-0326-6/DL:T-207-2011

[32] W.R. Haag, Effective benzene monitoring saves lives, compliance magazine, pp. 20-21, May 2006

[33] I. Elmi, S. Zampollia, E. Cozzania, F. Mancarella and G.C. Cardinali, Development of ultralowpower consumption MOX sensors with ppb level VOC detection capabilities for emerging applications, Sensors and Actuators B 135 342–351 (2008)

[34] P. Ivanov, F. Blanco, I. Gracia, N. Sabate, X. Vilanova, X. Correig, L. Fonseca, E. Figueras, J. Santander, R. Rubio, C. Cane, ASDAM06. International Conference on Advanced Semiconductor Devices and Microsystems, 2006, 185 – 188 (2006)

[35] J. Hubálek, K. Malysz, J. Prášek, X. Vilanova, P. Ivanov, E. Llobet, J. Brezmes, X. Correig, Z. Svěrák, Pt-loaded Al_2O_3 catalytic filters for screen-printed WO_3 sensors highly selective to benzene, Sensors and Actuators B: Chemical, 101, Issue 3, Pages 277-283 (2004)

[36] P. Ivanov, M. Vilaseca, E. Llobet, X. Vilanova, J. Hubalek, J. Coronas, J. Santamaria, X. Correig, Selective detection of ammonia and benzene via zeolite films deposited on SnO_2/Pt-SnO_2 thick film gas sensors, 2005 Spanish Conference on Electron Devices, Proceedings, 597-601 (2005)

[37] J. Getino, M.C Horrillo, J. Gutierrez, L. Ares, J.I. Robla, C. Garcia, I. Sayago Analysis of VOCs with a tin oxide sensor array, Sensors and Actuators B: Chemical, 43, , Issues 1-3, 200-205 (1997)

[38] G. Jimenez-Cadena, J. Riu, F.X. Rius, Gas sensor based on nanostructured materials, ANALYST, 132, 1083-1099 (2007)

[39] S. Iijima, Helical microtubules of graphitic carbon, Nature, 345, 56, (1991

[40] J-C Charlier, X. Blase, S. Roche, electronic and transport properties of nanotubes, reviews of modern physics, 79, 677–732 (2007)

[41] N. Koratkar, A. Modi, E. Lass and P. M. Ajayan, Temperature effects on resistance of aligned multiwalled carbon nanotube films, Journal of Nanoscience and Nanotechnology, 4, 744 (2004).

[42] G. U. Sumanasekera, C. K. W. Adu, S. Fang, and P. C. Eklund, Effects of Gas Adsorption and Collisions on Electrical Transport in Single-Walled Carbon Nanotubes, Physical Review Letters, 85, 1096–1099 (2000)

[43] F. Tournus, and J.-C. Charlier, ab initio study of benzene adsorption on carbon nanotubes, physical review B 71, 165421 (2005)

[44] E. Llobet, R. Leghrib, A. Felten, J.J, Pireaux, F. Renier, F. Demoisson, J.Guillot, A. Mansour, M. Delagado, Dispositivo para la detección selectiva de gas benceno, procedimiento para su obtención y detección del gas con el mismo, P200930969, (2009)

UNIVERSITAT ROVIRA I VIRGILI
DESIGN, FABRICATION AND CHARACTERISATION OF GAS SENSORS BASED ON NANOHYBRID MATERIALS
Radouane Leghrib
ISBN:978-84-694-0326-6/DL:T-207-2011

2. STATE OF THE ART OF CARBON NANOTUBES BASED GAS SENSORS

UNIVERSITAT ROVIRA I VIRGILI
DESIGN, FABRICATION AND CHARACTERISATION OF GAS SENSORS BASED ON NANOHYBRID MATERIALS
Radouane Leghrib
ISBN:978-84-694-0326-6/DL:T-207-2011

ISBN:978-84-694-0326-6/DL:T-207-2011

In this chapter, the structure, fabrication, modification of CNTs with functional groups, metals, metal oxides and polymers for developing gas sensors will be explained. Finally, the gas sensing characteristics of CNTs based materials will be reviewed. We will focus on the detection of benzene, first by conventional detection methods and then by carbon nanotubes based gas sensors.

2.1. Review of CNTs properties

2.1.1. Fabrication and purification of pristine carbon nanotubes

Carbon nanotubes belong to the family of fullerene structures. There are two types of nanotubes: single-walled carbon nanotubes (SWCNTs) and multiwalled carbon nanotubes (MWCNTs) [1]. A SWCNT can be considered as a one-atom thick layer of graphite rolled up into a seamless cylinder with a diameter of several nanometers, and length on the order of 1–100 microns. MWCNTs consist of multiple layers of graphite wrapped up together to form a tube shape, sharing the same central axis (Figure 1).

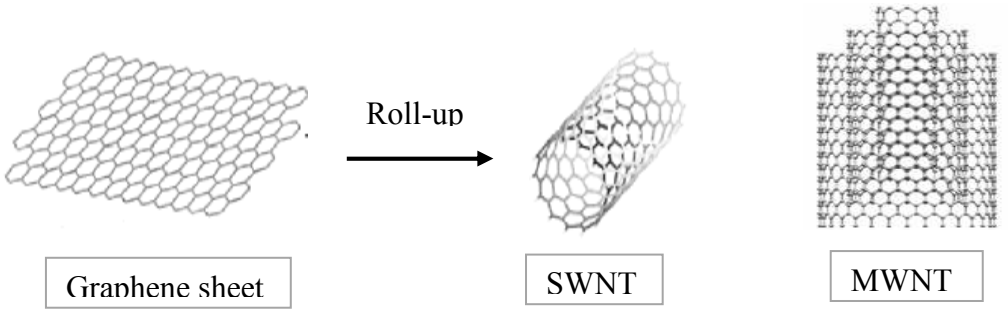

Figure 1: Different structures of CNTs: SWCNTs and MWCNTs

Mechanically, CNTs are the strongest and stiffest fibers that are known currently due to the C–C bond. Thermally, CNTs have high thermal stability. In terms of electrical properties, CNTs can be either metallic or semiconducting, depending upon the tube diameter and the direction in which the graphite sheet is rolled to form the tube [2].
Their potential applications include field emitters [3], gas storage and separation [4] nanoprobes [5], chemical sensors [6], high strength composites [7] and fuel cells [8-10].

Different techniques have been reported for the fabrication of MWCNTs. The most widely used methods to produce high-quality MWCNTs are laser ablation [11], electric arc discharge [12] and chemical vapor deposition (CVD) [13-14]. The laser ablation and

ISBN:978-84-694-0326-6/DL:T-207-2011

arc discharge methods are difficult to scale-up nanotube production to industrial levels. The CVD method presents better results to obtain MWCNTs with less impurities and using relatively low temperature and can be scaled-up to meet industry needs. The spray-pyrolysis is a modification of the CVD method, enabling large-scale production of MWCNTs, which can be obtained at a lower cost.

- **The carbon arc-discharge** method is the first technique that was used to grow CNTs. The process is carried out in a vacuum chamber with two carbon electrodes as carbon source. Inert gas is supplied to increase the speed of carbon deposition. When high dc voltage is applied between the carbon anode and cathode, plasma of the inert gas is generated and carbon atoms evaporate from the anode. The ejected carbon atoms are then deposited on the negative electrode to form CNTs. Both SWNTs and MWNTs can be grown by this method, but the growth of SWNTs requires the use of metal catalysts. It is the principal method to produce high quality CNTs with nearly perfect structures [15].
- In **the laser ablation** technique, a carbon target is ablated by intense laser pulses in a furnace in the presence of an inert gas and a catalyst. CNTs are formed and collected on a cold substrate. Both the arc-discharge and laser-ablation methods require high growth temperature, which is about 3000–4000 ºC for the evaporation of carbon atoms from solid carbon source [15].
- In a **CVD** system, a gas hydrocarbon source (usually methane, acetylene or ethylene) flows into the reaction chamber. The hydrocarbon molecules are broken into reactive species at the temperature range of 550–1000◦C. The reactive species react in the presence of catalysts (metal particles such as Ni, Fe or Co) that are pre-deposited on the substrate, leading to the formation of CNTs. Compared with the first two techniques. CNTs can be synthesized at relatively low temperature using the CVD method. By modification and calculated control of the growth parameters, the growth of vertically aligned MWCNTs can be achieved by the CVD technique. High-quality SWCNTs can also be obtained by the optimization of the catalysts. However, one of the main disadvantages of the CVD technique is the relatively high defect densities in MWCNTs, which can be attributed to the lack of sufficient thermal energy.

ISBN:978-84-694-0326-6/DL:T-207-2011

In all of these three growth methods, CNTs come with a number of impurities (e.g.presence of metal nanoparticles and amorphous carbon), which may have negative effects on CNTs' inherent properties [15].

In order to make CNT-based devices more efficient and consistent, purification is an important process to obtain high-purity nanotubes. Generally, the most commonly observed impurities are carbonaceous impurities and metallic impurities. The carbonaceous components are the byproducts of the reaction process while the metallic impurities are residual catalysts. To eliminate the carbonaceous impurities, the main method is oxidation.

There are different steps in purification of nanotubes [16-17]:

- **Air Oxidation:**

Air oxidation is useful in reducing the amount of amorphous carbon and metal catalyst particles (Ni, etc.). This can be performed by heating the CNTs to high temperatures around 400 ºC.

- **Acid Refluxing**

Refluxing the sample in strong acid is effective in reducing the amount of metal particles and amorphous carbon. Different acids can be used such as hydrochloric acid (HCl), nitric acid (HNO_3) and sulphuric acid (H_2SO_4), but HCl was identified to be the ideal refluxing acid.

- **Surfactant aided sonication, filtration and annealing**

After acid refluxing, the CNTs become purer but, tubes can be entangled together, trapping most of the impurities, such as carbon particles and catalyst particles, which are difficult to remove with filtration. So, surfactant-aided sonication can be carried out, followed by an ultra filtration and an annealing at temperatures as high as 1000 ºC in nitrogen ambient for several hours (Typically 4 h). Annealing is effective in optimizing the CNT structures. It was proved [17] that the surfactant-aided sonication is effective to untangle CNTs, thus to free the particulate impurities embedded in the entanglement.

After nanotube purification, their surface can be modified by adding new dopants that can act as active sites for the adsorption of gas molecules.

Extrinsic doping of nanotube surfaces can lead to localized electronic states. This disrupts the smooth, largely chemically inert, nanotube π-cloud, making the tubes chemically active. For this reason extrinsically doped tubes should make excellent starting candidates for a new generation of controlled chemically functionalized

ISBN:978-84-694-0326-6/DL:T-207-2011

nanotube materials. In the case of non-homogenously distributed dopants within the tube wall, doping provides a way to 'activate' regions along the tube wall. For single walled nanotubes (SWNTs), and for the outer layer of multi-walled nanotubes (MWNTs), this will lead to increased surface reactivity. These regions can be utilized for chemical functionalisation with molecules. Notably many applications like gas sensing, require chemical functionalisation or chemically active nanotube surfaces, those needing high electron densities near the Fermi level.

Here we will review the different dopants and doping techniques reported in the literature, we will focus more especially on oxygen functionalized carbon nanotubes and metal decorated, metal oxide doped and nitrogen or boron doped carbon nanotubes.

2.1.2. Surface modification: Use of defects in CNTs

Due to their strong sp^2 bonding in a near perfect hexagonal network, pristine carbon nanotubes are rather chemically inactive and this prevents the formation of chemical bonds with most molecules [18]. Carbon nanotube reactivity can be improved by functionalising their sidewalls with chemical groups, which act as reactive sites for the grafting of functional groups [19-24]. In the recent years, many efforts have led to the development of versatile methods to modify CNTs to obtain derivatives with more attractive features. To this end, a wide range of others materials, such as inorganic solids, small organic molecules, polymers and biomolecules have been introduced onto CNTs. Among these hybrid structures, an interesting class of CNT derivatives is obtained by the deposition of inorganic materials, such as metallic nanoparticles (NPs) and semiconductor nanoparticles, on the surface of CNTs. The combination of two classes of materials (CNTs and NPs) may lead to new hybrid materials with properties useful for catalysis, nanotechnology, and other applications [25-26].

a. Surface functionalization

Prior to the decoration of carbon nanotubes with metals or metal oxides, these are previously treated, either chemically or physically, in order to produce oxygen functional groups. The outermost walls functionalization is an important step to the direct synthesis of metal oxide nanoparticles on the MWCNTs surface, since the oxygen-containing groups act as sites for nucleation of nanoparticles.

Carbon nanotubes can be chemically oxidized using strong acids or oxidizing agents such as H_2SO_4, H_2NO_3, $KMnO_4$ and O_3, to produce oxygen functional groups such as

ISBN:978-84-694-0326-6/DL:T-207-2011

hydroxyl (-OH), carbonyl (-C=O) and carboxylic (-COOH) groups that serve as active sites for the nucleation of nanoparticles [27]. Hsu et al [28], reported that –COOH group grafted on MWCNTs provides reactive sites via esterification or elimination [29].

Carbon nanotubes can be also functionalized with oxygen species using an oxygen plasma [30]. This method allows to control the amount of functional groups that can be attached to the surface by adjusting the plasma reactor power and deposition time, also this method offers the possibility to homogeneously create oxygenated defects on the surface of CNTs, which is very interesting for obtaining a more well dispersed decoration with nanoparticles. This physical method has some advantages over chemical treatments, which will be discussed in annex.1.

b. Surface decoration

Physical metal deposition processes have also been successfully applied for CNTs decoration. The main methods used so far were thermal evaporation (including electron-beam evaporation), and sputtering. Electron beam evaporation was used to decorate CNTs with Pd [31], Pt, Sn, Rh [32]. Using sputtering [33, 34], SWCNTs were decorated with Pd and MWCNTs were decorated with Ti [35], Pt and Au [36]. The differences in chemical reactivities of metal nanoparticles resulted in selective detection of gases like H_2, CH_4, CO, H_2S, NO_2 and O_2.

Generally, the deposition of NPs onto CNTs can be achieved in two principal ways that differ in how the NPs are generated. NPs can either be grown onto CNTs directly or can be synthesized previously and then grafted to CNTs using covalent or noncovalent linkages.

The reduction of noble metal salts is commonly used to generate NPs. If the reduction process is carried out in the presence of CNTs, the NPs are attached to the CNTs through Van Der Waals or other weak interactions. Various methods, including the application of heat, light, and reducing agents, have been applied to perform the reduction process [37]. Commonly used metals are Pt, Au, Pd, Ru, and Ag. These metals often are active as heterogeneous catalysts and their performance can be enhanced when CNTs are used as support materials. They are also used as gas sensors, biosensors and hydrogen storage materials. To improve coverage, the surface of CNTs can be modified and organic molecules anchored onto the surface. Noncovalent wrapping by polymers has also been used to bind NPs formed in solution through electrostatic interactions or specific affinity [38]. Dai et al reported that Au and Pt NPs

ISBN:978-84-694-0326-6/DL:T-207-2011

could be formed in the presence of CNTs from metal precursors, without adding any reducing agent. This electroless process can be effectively used to deposit CNTs with Au and Pt NPs. Other metal cations such as Ag^{+}, Ni^{+}, and Cu^{+} could not be reduced to metal NPs because of their low redox potential [39]. However, two years later, Chen et al employed a substrate enhanced electroless deposition process, which can be used to coat CNTs with Ni and Cu NPs [40]. Microemulsion, supercritical fluids, and polyol solutions have also been used to form NPs on the surface of CNTs. Recently, Mitani et al reported a single-atom-to-cluster (SAC) approach to finely control the size of NPs on the surface of CNTs [41-42].

NPs can also be introduced onto the surface of CNTs through covalent binding or weak interactions. In these approaches, the NPs are prepared and modified with suitable functional groups to enable the connection to the CNT surface. The linkers can be categorized into two types: functional groups that form covalent bonds with functional groups present on the CNTs [43]; and linkers that bind to the CNT surface through weak interactions such as π-π interactions, hydrophobic, or electrostatic interactions. The most important requirement for the future development of NP-CNT hybrid materials for technology applications is to develop powerful synthetic methods to produce materials with reproducible properties and performance.

c. Doping with other nanomaterials

There have been numerous ways of fabricating carbon nanotube nanocomposites. For example, the conventional impregnation method, sol-gel technique, chemical vapor deposition, electrochemical reduction, and solution growth, including microemulsion technique, have been employed for the preparation of nanocomposites, especially for introducing active inorganic components such as noble metals, transition metals, and their oxides and sulfides [44].

The electronic, chemical and mechanical properties of CNTs can be tailored by replacing some of the carbon (C) atoms with either boron (B) or nitrogen (N). If B (has one electron less compared with C) or N (one electron more than C) replaces some C atoms, a *p* or *n* type semiconductor can be formed, respectively. From the chemical point of view, these doped structures would be more likely to react with donor or acceptor-type molecules depending on the doping. The B or N doped CNTs can be obtained during the growth process of carbon nanotubes using several techniques such

ISBN:978-84-694-0326-6/DL:T-207-2011

as the arc method by arching either B- or N-graphite electrodes in an inert atmosphere. Laser [45] and CVD [46] methods have been also used for their production.

Aside from nitrogen incorporation during their growth, it is also possible to nitrogen-dope nanotubes through post treating pristine carbon nanotubes. Chemical substitution has been used to nitrogen-dope SWNTs through partial substitution reactions of undoped tubes, using B_2O_3 vapor and N_2 gas at 1500-1700K [47]. This results in irregularly damaged nanotube walls with less than 1% N substitution, comparable with arc-discharge techniques.

D.C. magnetron sputtering has successfully been applied by Suenaga et al, achieving high nitrogen concentrations of 15-30% though not in CNTs but mainly in carbon nanoturbolites [48]. It has also been used for the production of heavily nitrogen doped carbon onions, centered on the azofullerene C48N12 [49].

Other interesting materials for gas sensing applications are polymer/CNT nanocomposites. Various processing methods were reported for producing these nanocomposites [50], in particular melt mixing [51], solution processing and in-situ polymerization [52].

Among the organic polymers, conducting polymers are promising materials for gas sensing as they have delocalized bonds that make them semiconducting or even highly conductive. Several conducting polymers, for example, polyaniline, polypyrrole, polythiophene have been demonstrated to be good sensing materials to function at room temperature [29].

In the next section, the state of the art of gas sensors based on CNTs will be presented an discussed.

2.2. Sensing properties of CNT composites for gas detection

CNT gas sensors have been attracting intensive research interest due to the demand of sensitive, fast response, and stable sensors for industry, environmental monitoring, biomedicine, and so forth [53].

- *Types of gas sensors based on carbon nanotubes*

We must remark that there is a wide range of sensors which used CNTs as active layer: Chemiresistor gas sensors (“semiconducting CNTs Field Effect Transitor (FET)” gas sensors [6,54-57] or CNTs based “two terminal resistor” gas sensors [58-59], CNTs

ISBN:978-84-694-0326-6/DL:T-207-2011

enhanced "ionization chamber" gas sensors [60-66], CNTs based gas sensing "capacitors" [67-68] and finally "resonance frequency shift" gas sensors [69-71]. Details about the different configurations and the working principle of the above gas sensors can be found elsewhere [53]. In this section, we will focus on chemoresistive gas sensors, which measure the resistance or conductivity change of the active layer upon adsorption of gas molecules.

The Field Effect Transitor (FET) devices are mainly based on metal-insulator-semiconductor (MIS) capacitors. They act as capacitive voltage divider. In contrast to a conventional metal-insulator-metal (MIM) capacitor, the depletion capacitance C_D in the semiconductor is not negligible. However, above the threshold voltage V_T, which is defined for the onset of strong inversion of charge carriers at the insulator–semiconductor interface, C_D is almost constant [72]. Hence, a change of the potential drop between the Fermi level W_F of the semiconductor and the conduction band energy W_C of the metal, expressed as the sum of the applied gate voltage V_G and the internal potential V_{int}, will act only across the insulator capacitance C_i. This yields a change in the free carrier concentration within the inversion layer of the semiconductor, which, in turn, can be measured easily [73].

In the "Two terminal resistor" gas sensors, the resistance of the active material under exposure to a gas can also be detected by two terminal resistors with DC voltage. Interdigited electrodes are generally applied in this kind of sensors to provide larger sensing areas and sufficient contacts between the electrodes and the coated sensing layer [58]. In this case, the material is deposited or grown above the patterned electrodes, or the material is deposited and then the electrodes are suspended above the sensing material.

- *Fabrication techniques of gas sensor based on CNTs*

Deposition of CNTs in a desired position and formation of reliable electrical contacts are among the biggest challenges on the way to mass production of CNTs-based devices. In fact, the electrical transport properties of a CNT-based device are dependent on the metal-CNT contact properties. For metal electrodes, a junction with semiconductor SWCNT may result in a Schottky barrier (SB) and a junction with metallic CNT may produce an ohmic contact. To develop and design CNT-based devices, low values of contact resistances are required, because high resistances result in higher noise, especially at elevated working temperatures.

ISBN:978-84-694-0326-6/DL:T-207-2011

Many techniques of deposition or controlled growth have been developed in the last years. The carbon nanotubes samples can be deposited over the gas sensor support by many ways:

Carbon nanotubes can be directly grown over the surface of the sensor substrate using the conventional synthesis methods of carbon nanotubes already presented in the section 2.1.1, or deposited above the sensor using different deposition techniques (Drop coating, etc).

When directly grown over the surface of the sensor, depending on the synthesis conditions, the as-grown CNTs can be vertically aligned [74-76], laterally aligned [77] or grown in bundles over the electrodes area [78].

When deposited over the sensor substrate, the previously prepared carbon nanotube powders can be dispersed in suitable organic solvents (Dimethylformamide, acetone, ethanol, etc) or water mixed with surfactants, and the resulting suspension is drop-coated [79], spin coated [80] or airbrushed over the electrodes area[34], etc. After the evaporation of the solvent, a network of nanotubes is subsequently formed over the support. Another simple method is screen printing of a CNT paste onto patterned electrodes [81]. The paste is prepared by mixing CNTs with a matrix containing for example terpineol, ethylcellulose, and glass frit as organic binder. The organic binder is then removed by annealing in N_2 ambient. However, when using these methods, the amout of nanotubes is not well controlled and their orientation is random.

Finally, fabrication of carbon nanotube sensors can also be achieved by the dielectrophoresis (DEP) method. DEP is the electrokinetic motion of dielectrically polarized materials in a nonuniform electrical field and has been used to manipulate CNTs for separation, and for orientation and positioning of CNTs [82-88]. With this technique, the amount of trapped CNTs over the sensor electrodes can be controlled by monitoring electrical impedance of the sensor [75]. This method was demonstrated to establish a good electrical connection between CNTs and the electrodes [89].

To summarize, direct growth of CNTs over the sensor provides a good control of the sensing properties of the material. Especially, Self aligned CNTs were proved to be better for gas sensing applications regarding the possibility to avoid the CNT/CNT junctions, which affect the current transport across the sensing layer. This method allows also establishing a good electrical contact between CNTs and the electrodes.

ISBN:978-84-694-0326-6/DL:T-207-2011

In contrast, post growth deposition methods are a simpler fabrication alternative. However, the materials are deposited in bundles which disturb the contact between the target gas and the active sites of the CNTs. Dielectrophoresis can be used to align the CNTs and separate the bundles.

After the CNTs have been deposited using previous techniques (Drop coating, airbushing, screen printing, etc) under the metal electrodes, the resistance of the device is generally high. One way to reduce the contact resistance is to perform a thermal treatment. In fact, Sayago et al. demonstrated that by performing a thermal heating on SWCNT based sensor from 25 to 300 ºC, the sensor contact resistance diminished resulting in a high response to H_2. The non treated samples were not able to detect H_2 [34]. In [90], the electrical characterization before the thermal treatment of MWCNTs based gas sensors has shown a typical rectifying behavior for metal-MWCNT junctions. It was suggested that the observed effect can be attributed to the presence of water, surfactants and oxide layers in the interface between the nanotubes and electrodes.

2.2.1. Gas sensors based on pristine CNTs

Experimental reports have shown that upon exposure to toxic gases such as NO_2, NH_3 , CO, benzene or ethanol, the electrical conductance of semiconducting CNT changes, even when they are operated at low temperatures [59, 91-100], thus considerably reducing the power consumption of the sensing device.

In general, SWCNTs exhibit a higher gas response than MWCNTs. Suehiro et al. [30] demonstrated that the normalized response of a SWCNT sensor was higher than the one of MWCNT based sensor. It was suggested that probably SWCNTs contained more semiconducting tubes. From the practical point of view, it is difficult to obtain only semiconducting tubes during the synthesis of SWCNTs. Those are usually a mixture of both metallic and semiconducting SWCNTs [101]. In general, MWCNTs show predominantly a conducting (metallic) behavior at room temperature. However, they could contain some semiconducting tubes among the metallic ones which are responsible for the low response obtained in their case. Compared with SWCNTs, the mechanism of MWCNTs response to gas adsorption is more complicated due to the multilayer tube structure. However, they also show sensitivity to specific gases [30, 55]. The main advantage of MWCNTs is their low cost compared to SWCNTs. For that reason, it is a challenge to investigate the possibility to improve their sensing properties.

ISBN:978-84-694-0326-6/DL:T-207-2011

❖ *Adsorption mechanism of pristine CNTs*

Using the interaction of NO_2 as example, Chung and co-workers reported in [56] that clean SWCNTs practically behave like graphite and, at room temperature, adsorb gases through physisorption. On the other hand, Larciprete in [102] and Goldoni in [103] reported the formation of many chemisorbed species at the surface of carbon nanotubes. It was found that gas adsorption within single wall carbon nanotubes can occur in four distinct sites (Figure 2): (1) the external surface of the bundle, (2) the groove formed at the contact between adjacent tubes on the outside of the bundle, (3) the interior pore of individual tubes and (4) interstitial channel formed between adjacent tubes within the bundle [104-105].The gas adsorption on these sites is decided by the binding energy (E_b) of the gas molecule as well as the site availability. Some of these sites will not be available for certain gases because of gas molecule dimensions and site diameter.

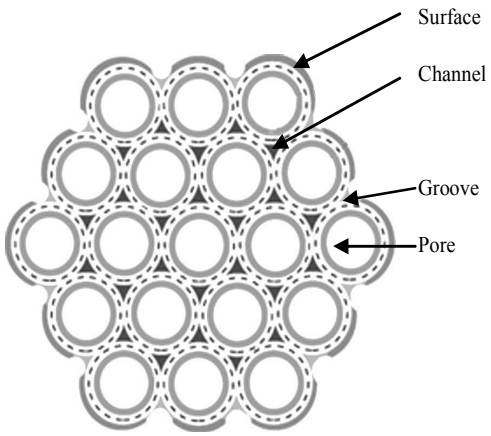

Figure 2: Schematic structure of a SWCNT bundle showing available sites for gas adsorption [104-b].

Considering that at room temperature, the presence of chemisorbed species is quite unusual (in graphite-like surfaces), it can be derived that the sensitivity of CNTs is, therefore, due to the presence of contaminants or defects on the surface of CNTs, which are responsible for chemisorption. These defects can be produced during the purification process of carbon nanotubes through acid treatments or washing. To confirm this observation, Valentini et al. [106] compared defective carbon nanotubes (i.e. subjected to high temperature exposure to reactive plasma) and non defective nanotube structures. They found that defective CNTs achieved higher sensitivity to NO_2 than non defective CNTs. This was in accordance with theoretical calculations, which attribute chemisorption of some gas molecules to defects in carbon nanotubes.

Other works attributed the high sensitivity of carbon nanotubes towards NO_2 to the changes at the interface between the nanotubes and the metallic electrodes and not to

ISBN:978-84-694-0326-6/DL:T-207-2011

molecules adsorbed on the CNT surface [107]. Other studies [107-108] observed that the sensitivity to NO_2 depended on the electrode material used (Au, Pd, Pt,..etc).

This suggests the possibility to create new defects (vacancies or atom substitutions) and /or the decoration of the carbon nanotubes surface with metal or metal oxide nanoparticles for increasing their reactivity to gases at ambient temperature.

Even if the response time of pristine carbon nanotubes is quite small [55], an important drawback is the slow recovery of their baseline resistance at ambient temperature. CNTs can take between several hours [84] to several days [55] to reach their baseline. In this case external energy can be supplied to the material for quickening the desorption of chemisorbed speciees from the CNTs. By either heating the sensors at temperatures up to 400 ºC [104] or illuminating them with ultraviolet light [84], the desorption process can be speeded up, so it takes from some seconds to several minutes.

On the other hand, the agglomeration of CNT into bundles during their synthesis appears as a drawback for forming well-dispersed active layers. To overcome this inconvenience, a plasma functionalization process applied to the CNT has proved to be efficient [109].

2.2.2. Plasma functionalized carbon nanotubes based gas sensors

This treatment, in addition to the better dispersion sought, gives rise to functional groups attached to the surface of the nanotubes, which modifies the CNT-surface reactivity and can further improve gas detection.

Most of the previous reports are based on utilization of carboxylic acid (–COOH) groups grafted on the surface of CNTs, which provide reactive sites for interacting with different compounds. Hsu et al. [28] reported that the –COOH group grafted on MWCNTs provides reactive sites via esterification or elimination, and the MWCNTs retain the graphitic structure.

So far, sensors fabricated with multiwall CNT (MWCNT) functionalized with oxygen have proved to give good results when operated at ambient temperature, above all showing good responsiveness to low concentrations of NO_2 [30]. Sin et al. [110] studied the response of chemically functionalized MWCNTs to alcohol vapors. –COOH groups were grafted along the sidewall and the tube ends of the nanotubes. The functionalized carbon nanotubes increased the sensitivity from 0.9 to 9.6 % compared to non treated carbon nanotubes. It is believed that with the polar COOH groups attached onto the nanotube surface, the sensors will give stronger responses towards alcohol vapors, as

ISBN:978-84-694-0326-6/DL:T-207-2011

their adsorption efficiency with these volatile organic molecules will be increased due to the dipole-dipole interactions (mainly hydrogen bonding) between the COOH and the polar organic molecules. Figure 3 shows the schematic diagram of how ethanol molecules interact with the COOH groups through hydrogen bonds.

R. Ionescu et al. used plasma functionalized MWCNTs for the detection of NO_2 and NH_3. They were able to detect them at 500 ppb and 200 ppm respectively with good sensitivities. By increasing the oxygen plasma treatment time, the amount of –COOH groups on the surface of the nanotubes increased, resulting in an increased sensitivity to the tested gases [30].

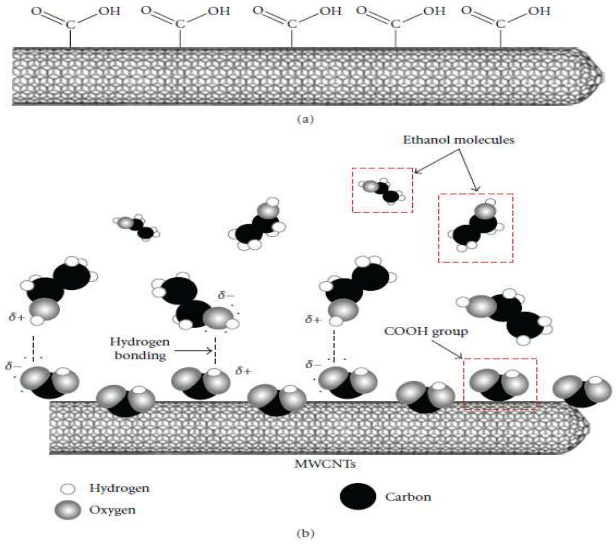

Figure 3: Schematic diagram of the interaction between COOH groups attached along the sidewall of MWCNTs and alcohol [110]

In spite of the observed potential of either untreated or functionalized MWCNT to detect gases, they show quite low sensitivities to the hazardous species detected, that cannot be improved even if the sensor operating temperature is increased. In order to overcome this drawback, it is considered worthy to investigate the approach of decorating carbon nanotubes with metal nanoclusters, and we recently reported a significant improvement of sensitivity to NO_2 when employing MWCNT decorated with Au or Ag nanoclusters as compared with the response obtained by un-doped MWCNT [111]. Moreover, a previous functionalization process of the carbon nanotubes in an oxygen plasma provided a more homogeneous distribution of the metal nanoclusters on the CNT surface as compared with cluster dispersion on non-treated CNT [112].

ISBN:978-84-694-0326-6/DL:T-207-2011

2.2.3. Metal-decorated carbon nanotubes

As an extension of the usual functionalisation techniques, CNT can be decorated with metal nanoparticles. Since metal nanoclusters show a wide range of advanced physico-chemical properties (e.g. high catalytic activity, adsorption capacity, efficient charge transfer, etc.), they can provide a full range of reactivity towards different gases [113]. In such a case, nanoclusters play a principal role in the gas detection pathway in which sensitivity and selectivity can be tuned based on the reactivity of the nanoclusters surfaces and on the nature of the charge transfer between carbon nanotubes and nanoclusters induced by gas adsorption [114, 115]. For this approach to be successful, it is important to achieve highly pure nanoclusters with well defined and thermally stable size. Very low content of impurities and narrow size distribution are important to reach controlled and reproducible adsorption and catalytic properties. Additionally, a good control of interfacial properties determined by the presence of structural and chemical defects on carbon nanotube walls is important to control the diffusion and stabilisation of nanoclusters. For example, Pd-coated CNTs become sensitive to H_2 [31]. Metal clusters have a broad range of diverse structures and can provide a wide range of reactivity with different species.

The concept of using CNT-metal cluster hybrids as the sensitive material of a device where the metal cluster surfaces act as reactive sites for the adsorption of the target molecules has been introduced recently in a theoretical study. In this study CNT-Al clusters are considered and it is shown that such a system displays initial specificity towards ammonia [116]. The adsorption of ammonia produces a substantial polarisation and accumulation of charge in the region between the Al cluster and the nanotube. This charge transfer between the Al cluster and the nanotube provides important information regarding the system's electronic response. It affects the ionic component of the bonding, alters the position of the Fermi level and the band alignment. Therefore, the variations in the electrical conductance of the CNT-Al system are a measure of the sensitivity of chemical sensors based on this material [116]. According to these preliminary theoretical results, CNT-metal cluster hybrids could be tailored for the recognition of chemical species with high sensitivity and selectivity. The key concept is to use nano-clusters (small size is essential to maximise the effect of adsorbates on metal clusters) that donate or accept a significant amount of charge upon adsorption of a target molecule, so that electron transport in the nanotube is affected. However, this

ISBN:978-84-694-0326-6/DL:T-207-2011

concept is still to be applied in chemical sensors. This approach constitutes one of the most important aspects of this thesis

Several groups demonstrated room-temperature detection of H_2 when carbon nanotubes were functionalized by Pt or Pd nanoparticles [31, 117]. Those metals act as catalysts for the adsorption of H_2. In this way, Pd- or Pt-CNTs became very sensitive to H_2, while pristine ones did not show any response to that gas. In fact, hydrogen molecules dissociate into atomic hydrogen on Pt surfaces and form PtH, which will lower the work function of Pt and cause the electron transfer from Pt to MWCNTs [118-120].

Y. Sun et al. [121] proposed a mechanism for the detection of hydrogen using Pd/SWCNTs. They suggested that when the Pd-decorated semiconducting SWNTs are exposed to hydrogen, the Pd atoms are converted to palladium hydride (PdH*x*), which possesses a lower work function than that of pure Pd. As a result, the formation of PdH*x* is beneficial to the accumulation of more electrons around the carbon atoms of the SWNTs (the right side of Figure 4). The higher level of accumulation of electrons around the carbon atoms further decreases the valence band energy level, leading to a sensitive decrease of the conductance of the SWNTs. This mechanism provides the basis for sensing hydrogen molecules with the use of *p*-type semiconducting SWNTs decorated with Pd nanoparticles. The sensing process is dominated by three reactions when the SWNTs decorated with Pd nanoparticles are exposed to hydrogen molecules in air. The reactions include:

$$\frac{1}{2}H_2 + Pd_{active} \underset{k2}{\overset{k1}{\rightleftharpoons}} Pd_{active}/H \qquad \textbf{(1)}$$

$$\frac{1}{2}O_2 + Pd_{active} \underset{k_{-2}}{\overset{k2}{\rightleftharpoons}} Pd_{active}/O \qquad \textbf{(2)}$$

$$\frac{1}{4}O_2 + Pd_{active}/H \xrightarrow{k3} Pd_{active} + \frac{1}{2}H_2O \qquad \textbf{(3)}$$

$$Pd_{active}/O + H_2 \rightarrow Pd_{active} + H_2O \qquad \textbf{(4)}$$

Where Pd $_{active}$ represents the active Pd site for reaction with either hydrogen or oxygen. Pd_{active}/H and Pd_{active}/O denote the active Pd site occupied with an H and O atom, respectively. Reaction (1) corresponds to the sensing step toward hydrogen. The involvement of reaction (2) is confirmed by the fact that the sensitivity of a sensor made of SWNTs/Pd in pure argon is much higher than that in air. Reaction (3) is reflected by the enhanced recovery speed in air compared to that in Ar. In addition, the Pd active/O species can also react with H_2 to regenerate Pd_{active} and water (H_2O) through the reaction (4).

ISBN:978-84-694-0326-6/DL:T-207-2011

Pd-functionalized CNTs were shown to be highly sensitive towards H_2 with a response time of 5-10 s, and a recovery time between 30 and 400 s. Both the response time and sensitivity decreased with increasing temperature. The Pd-CNTs are also sensitive to CH_4, with enhanced sensitivity, reduced size and power consumption compared to conventional metal oxide gas sensors [33]. Li et al. reported a composite of MWCNTs/Pd prepared by a facile method of chemical reduction. It exhibited a reversible and reproducible response magnitude of 4.5% toward 2% CH_4 at room temperature [122]. The response and recovery times were estimated to be 310 seconds and 176 seconds, respectively. The inert CH_4 does not undergo a charge transfer reaction with the MWCNTs to initiate a change in the electrical properties of CNTs, so MWCNTs alone are insensitive to methane. In the composite, the palladium nanoparticles undergo a weak interaction with the CH_4 molecules adsorbed on the composite to form a long-range weakly-bound complex $Pd\delta+(CH4)\delta-$ at room temperature. The MWCNTs donate electrons to Pd_0 to promote the formation of the complex where CH_4 is electronegative. The hole density in the MWCNTs is thus increased, resulting in a higher current in the composite.

In [33], the sensing mechanism of SWCNTs based FET sensor was shown (Figure 5).

Carbon nanotubes have also been modified with other metals for designing gas sensors. Kamarchuk et al. demonstrated the effect of point hetero-contact between SWCNTs and a gold microwire on the gas response [123]. Au- SWCNTs heterocontact sensors exhibit high response to NH_3 and NO_2 with fast response and relaxation and these two gases can be distinguished based on the direction of charge transfer between the analyte and the SWCNTs. The response time to 200 ppb NH_3 was 150 seconds, and the recovery time was 200 seconds. The mechanism of sensing is associated with formation of a thin conductive channel between Au and SWCNTs but the sign of the resistance change is controlled by the SWCNTs.

ISBN:978-84-694-0326-6/DL:T-207-2011

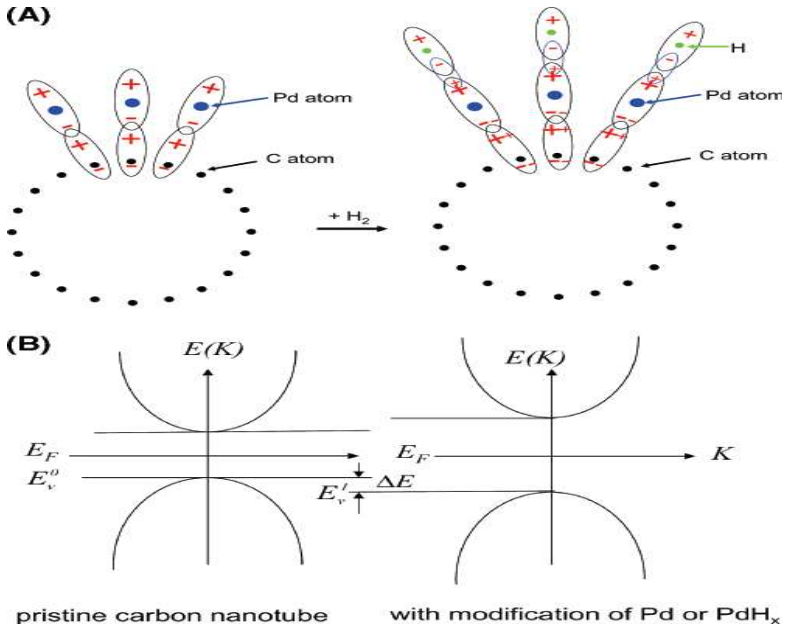

Figure 4: (A) Schematic illustration of dipoles induced by modification of a SWNT with Pd atoms and palladium hydrides. More electrons accumulate around the C atoms when Pd atoms are converted into palladium hydrides. (B) Sketch of the energy level of a pristine SWNT (left) and a SWNT decorated with Pd nanoparticles or palladium hydride (right). EF represents the Fermi energy [121].

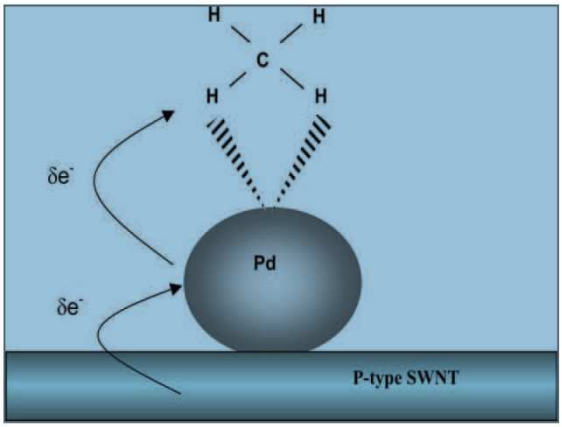

Figure 5: Interaction mechanism of Pd/SWCNTs with methane [33]

Penza et al. presented Au and Pt nanocluster functionalized MWCNTs chemiresistive sensors for detecting NO_2 and NH_3 working at a temperature range of 100–250◦C [36]. Au and Pt nanoclusters were sputtered on the surface of MWCNTs. The gas response of Pt- and Au-functionalized MWCNT gas sensors was significantly improved by a factor up to an order of magnitude for NH_3 and NO_2 detection, respectively. The enhancement of the gas response of the metal-modified MWCNT sensors could be caused by a combination of two additional effects of (1) direct charge injection and (2) catalytically induced charge into functionalized MWCNTs. Espinosa et al. coated MWCNTs with

ISBN:978-84-694-0326-6/DL:T-207-2011

Au or Ag nanoclusters deposited by electron beam evaporation [111]. The decorated MWCNT sensors were able to detect NO_2 in the range of 500 ppb–6.5 ppm at room temperature and were significantly more selective than sensors based on MWCNTs without metal nanoclusters attached to their surface. The response of Au-MWCNTs sensors to NO_2 was higher than the one of Ag-MWCNTs. Both materials showed a reversible behavior after NO_2 exposure, provided that their operating temperature was raised to 150℃ in a flow of dry air.

The importance of the size of metal nanocluster in the reactivity of the hybrid materials towards gases has been studied. In fact, it is known that small size clusters lead to a stronger interaction with gases [124]. However, Penza et al. [125], studied the effect of three different Au nanocluster sizes on the performance of Au/MWCNTs towards H_2S, NH_3 and NO_2. He found the existence of a critical size in which the interaction is maximum. He suggested that small size particles around 2.5 nm showed a tendency to agglomerate leading to sensitivities close to those obtained for bigger nanocluster sizes of about 10 nm. In contrast, 5 nm nanoparticles gave the best results. These particles remained isolated on the external wall of nanotubes, which explains the improved sensitivity to gases shown by this material.

Metal nanoparticle functionalized CNT sensor arrays have also been reported. Star et al. fabricated gas sensor arrays by site-selective electroplating of Au, Pt, Pd, and Rh metals on isolated SWCNTs networks located on a single chip [32]. The difference in catalytic activities of the metal nanoparticles tuned the sensitivity for the detection of H_2, CH_4, CO, H_2S, NH_3, and NO_2. The output of the sensor array was analyzed using principal component analysis (PCA) and partial least squares regression (PLS) in order to identify the above-mentioned gases. Lu et al. demonstrated a gas sensor array composed of 32 sensing elements with pristine, metal-decorated (Pd, Au), and polymer-decorated SWCNTs for discriminating gases such as NO_2, HCN, HCl, Cl_2, acetone, and benzene at ppm levels [92]. CNTs-based technology holds the potential to excel in the design of arrays because the inherently small size of CNTs devices will allow for the integration of large numbers of functionalized CNTs sensor elements that would show a unique response to numerous species.

ISBN:978-84-694-0326-6/DL:T-207-2011

2.2.4. Metal oxide doped carbon nanotubes

Metal oxides are well-known materials suitable for detecting a wide spectrum of gases with enough sensitivity. Among these materials, SnO_2, WO_3 and TiO_2 have proved to be very suitable candidates for gas sensing, but when the detection of toxic species is devised, they typically need to be operated at temperatures ranging between 200 and 800 ºC [126-127]. It is generally known that, in practice, the sensitivity of metal oxide gas sensors can be enhanced by using bulk dopants or by the addition of metal clusters to the sensing material [128]. When metal oxide sensors are operated at high temperatures, changes in the microstructure of the gas-sensitive film are likely to occur (i.e. structural changes or coalescence [129]). At higher temperatures, the mobility of oxygen vacancies becomes appreciable and the mechanism of conduction becomes mixed ionic–electronic. The diffusion of oxygen vacancies is known to be a mechanism responsible for long-term drift in metal oxide gas sensors [130-131]. Therefore, a strategy to avoid long-term changes in their response could consist in operating the sensors at temperatures low enough so that appreciable structural variation never occurs, provided that gas reactions occur at a reasonable rate.

Recently, hybrid films based on tin or tungsten oxide and carbon nanotubes have been introduced as new gas-sensitive materials with improved sensitivity [111,132-135]. These works indicated that the detection at ambient temperature of toxic gases such as nitrogen dioxide, carbon monoxide and ammonia or ethanol vapors can be improved by dispersing an adequate quantity of carbon nanotubes into a metal oxide matrix.

A model was presented to relate potential barriers to electronic conduction in the hybrid material. This model suggested that the high response is associated with the stretching of the depletion layers at the grain boundaries of SnO_2 and the SWCNTs interfaces when detected gases are adsorbed [132]. Hoa et al. fabricated a NH_3 sensor with a composite of SWCNTs and SnO_2 [136]. The sensor could detect the concentration of NH_3 down to 10 ppm at room temperature, and exhibited a fast response time of 100 seconds and recovery time of about 3.2 minutes. The SWCNTs in the matrix of SnO_2 provide the main conducting channel that effectively varies in its conductance upon adsorption of NH_3. The recovery time depends on the bonding force of NH_3 molecules to the SWCNT surface with respect to desorption under a nitrogen flow. Thus, it can vary with the nitrogen flow rate. In [137], the MWCNTs/SnO_2 sensor exhibited good sensing responses to liquefied petroleum gas (LPG) and ethanol (C_2H_5OH) vapor with fast response and recovery within seconds at temperature of 335℃. Furthermore, the

ISBN:978-84-694-0326-6/DL:T-207-2011

gas sensor response increased linearly with the increment of gas concentration of LPG and ethanol. The high response and low resistance may be attributed to the particular electrical transport mechanism. The resistance of the sensor is dominated by the barriers among the SnO_2 grains on the MWCNTs. Electrons travel through the SnO_2 grains into the MWCNTs, and then conduct in the MWCNTs with low resistance. In [138], the response of the MWCNTs/SnO_2 sensor to NH_3 increases with increasing MWCNTs content and the composites using MWCNTs with the larger diameter show higher response because larger diameter MWCNTs would increase the number of gas molecules adsorbed on the material.

The effect of hybrid SnO_2/CNT annealing temperature on the response to gases was studied [139]. It was found that the resistance of the composite decreases with increasing annealing temperature from 200 to 500 ºC. One possible explanation is that with increasing annealing temperature, the crystal structure of the SnO_2 nanoparticles becomes more and more perfect, and the SnO_2 nanoparticles attach to MWNT-COOHs more closely, which leads to the improvement of the conductivity of the composite. However, the resistance of the unannealed composite is much lower than that annealed at 200 ºC. Although the sample is dried under vacuum before calcination, there is still some water in the composite. After being annealed at a temperature as high as 200 ºC, the residual water is fully removed so that contact resistance between SnO_2 nanoparticles is increased. Therefore, the high conductivity of the composite without heat treatment may be caused by the existence of the residual water.

In [134], oxygen plasma functionalized/MWCNTs were added toWO_3 by drop-coating deposition method. The adsorption at the surface of CNTs modifies the depletion layer at the n-WO_3/p- MWCNTs hetero-junctions and this results in the modulation of the depletion layer at the surface of WO_3 grains. This change in the depletion layer at the n/p junction that induces change in the WO_3 matrix may explain the improvement in response shown by hybrid sensors. The detection of acetone and NH_3 was found to be possible at ambient temperature with TiO_2/MWCNTs gas sensors fabricated by sol-gel method [140]. Increasing the annealing temperature may result in the improvement of the contact between metal oxide nanoparticles and CNTs but employing high calcination temperatures may also result in burning of CNTs by residual oxygen or damaging of CNTs structure. An increase in the thickness of the thin film composite results in a decrease in the response due to the increase of the diffusion length of gases.

ISBN:978-84-694-0326-6/DL:T-207-2011

In [141], hybrid sensors containing MWCNTs respond at significantly lower operating temperature than their non-hybrid counterparts. These new hybrid sensors show a strong potential for monitoring traces of oxygen (i.e., <10 ppm) in a flow of CO_2. The hetero-structure n-TiO_2/p-MWCNTs can be formed at the interface between titania and carbon nanotubes. Hybrid sensors are significantly more responsive to oxygen than pure or Nb-doped titania sensors because a slight change in the concentration of adsorbed oxygen at its surface can result in a significant change in the depletion layer at the n-TiO_2/p-MWCNT hetero-structure.

A ZnO/MWCNT sensor was implemented recently. It showed better sensing performance when compared to bare MWCNTs. The former allows for the discrimination of low CO concentrations (20, 50 and 200 ppm) which is important for several practical applications [142].

Finally, electrical and sensing properties of gas sensors based on hybrid vanadium oxide-coated carbon nanotubes (V_2O_4-CNTs) were studied by Willinger et al [143] for the detection of NO_2. The strict contact between V_2O_4 coating and CNTs contribute to the improvement of sensing performance.

New multi-hybrid structures based on metal oxide and carbon nanotubes have been prepared recently by mixing those structures with metal nanoparticles, further enhancement in the sensitivity towards gases was achieved. Systems such as Au/CNT/SnO_2, Nb-Pt co doped/CNT/TiO_2 and Sb/CNT/SnO_2, etc were applied to the identification of CO, NH_3, ethanol, formaldehyde, toluene, NO_2, C_6H_6 and O_2. The hybrid material sensors improved the gas sensing performance by factors of 2-5 compared to that of the sensor without CNT inclusion. Moreover, all hybrid sensors can operate with high sensitivity and stability at a relatively low operating temperatures (<335 ºC) [141].

A CNT/Au/SnO_2 hybrid synthesized via layer-by-layer assembly has been applied in a room-temperature CO gas sensor. It exhibited better performance compared with Au/SnO_2 nanocrystals and CNT/SnO_2 hybrids because of the doping of Au nanocrystals, the higher surface-to-volume ratio and nanotubular structure [144].

2.2.5. Nitrogen or Boron doped carbon nanotubes

The incorporation of nitrogen or boron atoms into the honeycomb lattice leads to chemical activation of the rather passive surface of a carbon nanotube and adds additional electronic states around the Fermi level. Nitrogen or boron introduction to

ISBN:978-84-694-0326-6/DL:T-207-2011

nanotubes significantly modifies their physical and chemical properties, notably changing their solubilities and increasing surface reactivity [145].

Although pristine carbon nanotubes show good sensitivity to oxygen [146], they often show little response to pollutant gases such as NO_2 [30,147], as supported by theoretical modelling showing only weak surface-gas interaction [30]. The modification of states in N- or B-doped tubes suggests that their interaction with absorbing gas species and resultant transport properties should also be modified, and thus doped nanotubes appear in principle as promising candidates for gas sensing purposes.

N- or B-CNTs should show significant advantages over undoped nanotubes for gas sensor applications, both due to their reactive tube surfaces, and the sensitivity of their transport characteristics to the presence, distribution and chemistry of nitrogen and boron. Peng and Cho first performed calculations suggesting that N-CNT may be useful in gas sensing for CO_2 and H_2O, due to the ability of nitrogen dopants to bind to incoming gas species [108].

Villalpando-Páez et al. [148] proved the concept introduced by Peng and Cho by investigating the conductivity of both aligned N-CNT films and N-CNT compressed pellets with various gases (NH_3) and solvent vapors (ethanol, acetone, chloroform, gasoline, pyridine, benzene). Both chemisorption (permanent conductance change) and physisorption (transient conductance change) was observed, depending on the species. The films showed moderate sensitivities (i.e. the gases were tested at very high concentrations ranging from 1% up to 16%). Despite their moderate sensitivity towards the species tested, N-CNT films were found to be more efficient than un-doped CNT films for detecting toxic gases. This was attributed to the presence of highly reactive pyridine-like sites on the surface of N-CNTs. Using ab initio calculations, they confirmed that pyridine-type regions on the tube surface bind strongly to ammonia, acetone and hydroxyl groups, thus altering the tube density of states.

Bai and Zhou demonstrated that NH_3 and NO_2 are physisorbed in (10, 0) pristine SWCNTs with weak binding and little charge transfer. The N-doping does not change NH_3 adsorption in SWCNTs, but the B-doping makes NH_3 chemisorption in SWCNTs feasible with an adsorption energy of -0.70 eV and a charge transfer of 0.31 e V (from the adsorbed molecule into the tube). The conductance change of B-doped SWCNTs due to charge transfer can be used to detect NH_3. NO_2 can be chemisorbed on the B- or N-doped SWCNTs. However, the very strong binding of NO_2 in B-doped SWCNTs makes desorption difficult, which precludes its applications to NO_2 sensors. N-doped

ISBN:978-84-694-0326-6/DL:T-207-2011

SWCNTs should be good NO_2 sensors with quick response and short recovery time [149]. Wang et al studied intrinsic and B atom, N atom and BN atoms doped single-walled carbon nanotubes (SWCNTs), as sensors to detect hydrogen sulfide, using density functional theory (DFT). The calculated results show that the B-doped SWCNTs present high sensitivity to the gaseous hydrogen sulfide molecule, and their geometric structures and electronic properties present dramatic changes after the adsorption of H_2S molecule, compared with the intrinsic SWCNTs. While N-doped SWCNTs and BN-doped SWCNTs cannot improve the sensing performance of the SWCNTs to H_2S molecule. So it is suggested that B-doped SWCNTs would be promising candidates for serving as effective sensors to detect the presence of H_2S molecules [150].

2.2.6. Polymer coated carbon nanotubes

Among the organic polymers, conducting polymers are promising materials for gas sensing as they have delocalized bonds that make them semiconducting or even highly conductive. Several conducting polymers, for example, polyaniline, polypyrrole, polythiophene have been demonstrated to be good sensing materials to function at room temperature. They have been applied as conductometric, potentiometric, amperometric and voltammetric transducers for the detection of a wide variety of gas or vapors such as NH_3, NO_2, CO and VOCs [29]. However, their selectivity and the environmental stability are poor. Recently, enhanced gas sensing by combining SWCNTs with organic polymers has been demonstrated. Qi et al. showed that noncovalently drop coating of polyethyleneimine (PEI) and Nafion (a polymeric perfluorinated sulfonic acid ionomer) onto SWCNTs FETs resulted in gas sensors with improved response and selectivity for NO_2 and NH_3 [151]. The PEI functionalization changed the SWCNTs from p-type to n-type semiconductors. Chemical functionalization of SWCNTs with covalently attached poly-(m-aminobenzene sulfonic acid) (PABS) has been demonstrated to result in better sensing performance toward NH_3 and NO_2 than simply carboxylated SWCNTs. Sulfonic acid groups as dopants play an important role in balancing the charge distribution within the polymer, and they are especially attractive for introducing acid-base response. CNTs have also been incorporated into polymers to form nanocomposites, which are usually casted to thin films and serve as sensing elements. Modification of CNTs with polymers also improves their sensing properties toward vapors of organic compounds (VOCs). Abraham et al. developed a compact wireless

ISBN:978-84-694-0326-6/DL:T-207-2011

gas sensor based on an MWCNTs/PMMA composite chemiresistor [152]. The composite film was made by ultrasonication of MWCNTs and PMMA (1:4 by weight) for 2 hours in dichloromethane, and the chemiresistors were fabricated by dip-coating. The sensor showed fast response (2–5 seconds) and 102-103 order increase in resistance upon exposure to dichloromethane, chloroform and acetone vapors. It returned to the initial level immediately after removing the gas. The sensing mechanism was explained by swelling of the polymer due to absorption of organic vapors into the PMMA and the charge transfer when polar organic vapors adsorb on the CNT surface. Solvents such as methanol, ethyl acetate and toluene, in which PMMA is insoluble or less soluble, also showed response. Sorption of organic vapors into the polymeric phase of the composites leads to swelling of the matrix, expands the interparticulates' intervals and partially destroys the conductive networks. As a result, a drastic rise in resistivity of the materials is perceived. When the amount of MWCNT in the composites is low, tunneling effect contributes to conduction of the composites to a great extent besides the direct interfiller contacts. In the case of high MWCNT content, the excessive fillers inevitably resulted in aggregation of MWCNTs and broke the conducting paths. Only at certain optimized filler content, the conducting paths are mainly constructed by the bridged MWCNTs, which are easy to be broken down by the swelling of the matrix, and the vapor response reaches the maximum.

Niu et al. constructed a highly selective gas sensor by chemical modification of MWCNTs containing carboxyl groups (MWCNT-COOH) with poly(ethylene glycol) (PEG) in the presence of N,N-dicyclohexylcarbodiimide (DCC) [153]. The MWCNTs grafted PEG sensor displayed high chemical selectivity, fast response and good reproducibility/ high stability to chloroform vapor at room temperature.

Vertically aligned carbon nanotubes have also been modified with polymers for gas sensors. Valentini et al. fabricated a gas sensor by selective growth of aligned CNTs on Si_3N_4/Si substrates patterned by metallic platinum [154]. The sensor was presented for inorganic vapor detection at room temperature. Poly(o-anisidine) (POAS) deposition onto the CNTs device was shown to impart higher response to the sensor.

Wei et al. developed novel multifunctional chemical sensors based on vertically aligned MWCNTs and polymer composites [155]. The sensors were fabricated by partially coating perpendicularly aligned MWCNTs with polymers, such as poly(vinyl acetate), polyisoprene, and then sputtering with gold electrodes. Rapid and reversible sensing of high concentrations of a variety of volatile organic solvents was demonstrated. The

ISBN:978-84-694-0326-6/DL:T-207-2011

sensing mechanism was attributed to the charge transfer interaction with gas molecules and/or the intertube distance change induced by polymer swelling during gas adsorption.

2.2.7. Summary

A recent review about gas sensors based on CNTs proposed a good summary about the sensing performances of pristine, metal functionalized, metal oxide doped CNTs sensors reported up to 2009. This summary is re-elaborated in Table 1 [20].

From this table, we can observe that carbon nanotubes have been extensively studied as gas sensors. Pristine carbon nanotubes based gas sensors were able to detect some gases at room temperature. This detection, such in the case of NO_2 is mainly due to chemisorption. Since carbon nanotubes behave like graphite at room temperature, the chemisorptions must be attributed to the defects formed in the carbon nanotubes during their post fabrication or post purification step. This has lead scientists to work in the idea of functionalizing the CNTs via creating oxygenated defects or decorating them with metals and metal oxides, polymers, etc.

From the table, we can see that thanks to functionalization, the range of detectable gases either using SWCNTs or MWCNTs was increased, the detection limit was decreased down to ppb levels, response time was decreased to some seconds and recovery time to some minutes thanks to heating, illumination or using higher carrier gas flows. Up to now, new sensors arrays are being built for the selective detection of toxic gases but generally, very few works were reported on benzene detection using gas sensors based on carbon nanotubes. The next section will be devoted to the review of the state of benzene gas sensors from common detectors to carbon nanotubes based gas sensors.

ISBN:978-84-694-0326-6/DL:T-207-2011

Table 1: Summary of carbon nanotubes based gas sensor performance [20]

CNT type	*Sensor configuration*	*Targeted analytes*	*Detection limit*	*Response time*	*Receovery time*	*Reference*
Pristine CNTs						
S-SWCNT	FET	NO_2, NH_3	2 ppm NO_2, 0.1 % NH_3	< 10 min	~ 1 h (200 ºC)	[13]
SWCNTs	Resistor	NO_2, Nitrotoluene	44 ppb NO_2, 262 ppb nitrotoluene	10 min	10 min (UV)	[79]
SWCNTs	Resistor	NH_3	5 ppm	~10 min	~20 min (80 ºC)	[156]
MWCNTs	Capacitor and Resistor	NH_3	10 ppm	2-3 min	Several days (100 ºC in vaccum)	[157]
MWCNTs	Resistor	NH_3	2500 ppm	N/S	N/S	[158]
MWCNTs	FET	NO_2	50 ppm	~500 s	~10 min (10 V bias potential)	[159]
MWCNTs	Resistor	SO_2, HF	10 ppm SO_2 4 ppm HF	N/S	N/S	[160]
MWCNTs	Electrochemical gas sensor	Cl_2	100 ppm	~150 s	~ 150 s	[161]
ACNTs	Resistor	NO_2	10 ppb	~60 min	~60 min (165 ºC)	[59]
ACNTs	Resistor	NO_2	10 ppm	N/S	N/S	[162]
ACNTs	Resistor	NO, NO_2	2 ppm NO, 2 ppm NO_2	N/S	~20 min (150 ºC and UV)	[163]
ACNTs	Resistor	NH_3	~0.1 %	N/S	N/S	[164]
ACNTs	FET	N_2	50 mTorr	N/S	N/S	[74]

UNIVERSITAT ROVIRA I VIRGILI
DESIGN, FABRICATION AND CHARACTERISATION OF GAS SENSORS BASED ON NANOHYBRID MATERIALS
Radouane Leghrib
ISBN:978-84-694-0326-6/DL:T-207-2011

Metal functionalized CNTs						
Pd- S-SWCNTs	FET	H_2	< 40 ppm	5- 10 s (For half resistance change)	400 s	[31]
Pd- SWCNTs	Resistor	H_2	1000 ppm	N/S	N/S	[34]
Pd- SWCNTs	Resistor	H_2	100 ppm	10 min	20 min	[165]
Pd- SWCNTs	Resistor	H_2	100 ppm	3-60 s (Foor half 36.8 % resistance change)	~5 min	[166]
Pd- SWCNTs	Resistor	H_2	~10 ppm	< 10 min	< 30 s	[57]
Pd- ACNTs	Resistor	H_2	100 ppm	< 7 min	~N/S	[75]
Pd- SWCNTs	Resistor	CH_4	6 ppm	2-4 min	N/S	[33]
Pd- MWCNTs	Resistor	CH_4	2 %	~310 s	~176 s	[122]
Pt- MWCNTs	Resistor	H_2	N/S	10 min	15 min	[167]
Pd- MWCNTs	Resistor	H_2	N/S	7 min	7 min	[80]
Pt- MWCNTs	Resistor	H_2, NO_2, H_2O	N/S	~10 min	~14 min	[168]
Au- SWCNTs	Resistor	NH_3, NO_2	< 120 ppb NH_3	150 s	200 s	[123]
Au, Pt- MWCNTs	Resistor	NO_2, NH_3	100 ppb NO_2, 5 ppm NH_3	N/S	N/S	[36]
Au, Ag- MWCNTs	Resistor	NO_2	500 ppbs NO_2	~20 min	N/S	[111]
Pt, Pd, Sn, Rh- SWCNTs	FET	H_2, CH_4, CO, H_2S, NO_2, HCN, HCl	N/S	~5 min	N/S	[32]

UNIVERSITAT ROVIRA I VIRGILI
DESIGN, FABRICATION AND CHARACTERISATION OF GAS SENSORS BASED ON NANOHYBRID MATERIALS
Radouane Leghrib
ISBN:978-84-694-0326-6/DL:T-207-2011

Pd, Au- SWCNTs	Resistor	Cl_2, acetone, benzene	5 ppm	N/S	N/S	[92]
Metal oxide functionalized CNTs						
SnO_2- SWCNTs	Resistor	NO_2	N/S	9 min	1.5 min	[132]
SnO_2- SWCNTs	Resistor	H_2	300 ppm	2-5 s (200- 250 ºC)	3-5 s (200-250 ºC)	[169]
SnO_2- SWCNTs	Resistor	NH_3	10 ppm	~100 s	~3.2 min	[136]
SnO_2- MWCNTs	Resistor	LPG,	10 ppm	N/S	N/S	[137]
SnO_2- MWCNTs	Resistor	C_2H_5OH	10 ppm	~1 s (300 ºC)	~10 s (300 ºC)	[133]
SnO_2- MWCNTs	Resistor	NO_2	100 ppb	N/S	20 min (150 ºC)	[170]
SnO_2- MWCNTs	Resistor	NH_3	60 ppm	< 5 min	< 5 min	[138]
SnO_2- MWCNTs	Resistor	Formaldehyde	0.03 ppm	100 s (250 ºC)	90 s (250 ºC)	[171]
WO_3- MWCNTs	Resistor	NO_2, CO, NH_3	500 ppb NO2, 10 ppm CO, 10 ppm NH3	N/S	N/S	[134]
TiO_2- MWCNTs	Resistor	Acetone, NH_3	N/S	10-40 s (acetone)	10-300 s (acetone)	[140]
TiO_2- CNTs	Resistor	O_2	10 ppm	5-8 min (350-550 ºC)	~20 min (350 s)	[141]
SnO_2, TiO_2 MWCNTs, SWCNTs	Resistor	C_2H_5OH	100 ppm	< 10 s (210-400 ºC)	< 10 s (210-400 ºC)	[172]

ISBN:978-84-694-0326-6/DL:T-207-2011

2.3. State of the art of benzene detection

2.3.1. Detection of benzene by conventional gas detectors

Several kinds of benzene portable detectors exist now at the industrial market scale [173]. Among the existing detectors, infrared detectors are fast and have good selectivity, they have detection limit over 1 ppm for benzene and are relatively expensive and heavy. Portable gas chromatographs offer an accuracy for benzene of 0.1 ppm. However, they can often measure other aromatics such as toluene and xylene, and they tend to be heavy, complicated to operate, and more expensive. Photoionization detectors (eg. UltraRAE 3000 c/w 9.8 eV lamp, ToxiRAE plus PID) are commercially available as portable devices for the monitoring of benzene in the range of 0.05-200 ppm (Figure 6). They are the most accurate portable instrument with an accuracy of 0.1 ppm for benzene. Furthermore, these instruments are lightweight, the analysis are fast requiring about 1 or 2 min. However, their main drawback is their reactivity with a wide range of VOCs, which does not enable the selective detection of benzene and their cost can overpass 4000 euros.

To achieve a selective analysis, retention tubes can be placed as filters prior to analysis. These tubes act as filters by trapping different gases exception made of benzene. However, these filter devices are disposable, and thus must be replaced after each measurement (the cost of a single measurement is over 3 €).

Figure 6: Commercial benzene detectors

Other type of detectors based on optical analysis have been reported [174]. Colorimetric devices contain channels which are filled with a substance whose color specifically changes with the analyte to be measured. Those reactive substances change their color

ISBN:978-84-694-0326-6/DL:T-207-2011

in the presence of the analyte to be detected. The concentration of the analyte can be known by measuring the intensity of the change of the substance color. Nevertheless, these devices are very expensive regarding the high cost of the reactive substances they use and their response is credible only when benzene concentration is higher than 200 ppb. Other types of detectors have been used but their high cost and their lack of selectivity make them impractical for the detection of benzene at the ppb level [173].

Metal oxide gas sensors have been used also as commercial gas sensors (eg. Tagushi gas sensors) (Figure 6). Especially, tin oxide and tungsten oxide gas sensors have been used widely for the detection of toxic gases [175]. Their main problem is their non intrinsic selectivity towards benzene, as they can strongly interact with other gases such as alcohols and nitrogen oxides, ammonia, sulfur compounds, etc [176]. As a solution for the lack of selectivity experienced with metal oxides, several options can be envisaged. Metal oxide gas sensors were used as detectors for micro-GC-systems. In fact, by coupling them to GC microcolumns, a temporal separation of different gases in a complex mixture, including benzene, was achieved [177-178]. These sensors were also doped with different noble metals metals such as Au or Pt, to enhance their selectivity towards some ppb of benzene [179-180]. Another option consists of using a catalytic filters such as porous Al_2O_3 [181] or zeolites [182]. In this approach, different metal oxide based gas sensors were combined in an array of different sensors for the discrimination of toxic gases in a mixture including benzene [183-185]. However, their high operating temperature (>300 ºC) causes drift in their response due mainly to the change of the structure of the active layer [129] and also to the degradation of the electrodes at such high temperatures [186]. The diffusion of oxygen vacancies is known to be a mechanism responsible for long-term drift in metal oxide gas sensors as well [130-131]. This remains an inconvenient for the long term use of those sensors.

Low cost, low power consumption, long lifetime and selective gas sensors are required for practical benzene detection. Nowadays, scientists are focusing on the investigation of carbon nanotubes as a solution for common gas sensor problems.

As can be seen from section 2.2.3, those sensors have been used widely for the sensing of different toxic gases. However, very few works have been devoted to benzene detection. We will present here a discussion on what has been reported about the detection of benzene with CNT based sensors.

ISBN:978-84-694-0326-6/DL:T-207-2011

2.3.2. Detection of benzene by gas sensors based on CNT composites

The interaction of benzene with pristine CNTs is known as to be a physisorption through π-π interaction within carbon-carbon atoms [187]. This interaction is known to be very weak leading to a very small charge transfer between benzene and CNTs.

J. Li [188] reported a gas sensor fabricated by the simple casting of single-walled carbon nanotubes (SWNTs) for gas and organic vapor detection. These sensors were exposed to nitrogen dioxide, acetone, benzene, nitrotoluene, chlorine, and ammonia in the concentration range of ppb to ppm at room temperature. However, for benzene, only a small sensor response to 20 ppm benzene was observed. The response time was about some seconds and the recovery time about some minutes.

Y.W. Chang and co-workers [189] obtained refreshable sensors inversing the polarity of the gate voltage after NO_2 and NH_3 gas exposure. Indeed, they observed that the rate of desorption of the gas molecules was dependent on their nature. They observed that after exposure to 30 and 300 ppm of NH_3 and after refreshing the CNT/FET based sensor applying a gate voltage of 10V (to accelerate gas desorption), the slope of the decay rate as a function of time was the same in both cases (−0.1 nA s−1) and was not due to the concentration but only to the gas type. After having exposed the same device to ethanol (1000 ppm) and benzene (15 ppm), they obtained, after refreshing at the same voltage, different decay rates: −0.07 nA s−1 for ethanol and −0.04 nA s−1 for benzene. These results suggest that the decay rate could be used to perform selective measurements of the gas species considering that this time interval is univocally related to the binding energy of the adsorbed molecules.

More recently, Silva [190] reported the development of a NTFET detector coupled to a gas chromatograph (GC) for the detection of benzene, toluene, ethylbenzene, *m*-xylene, *p*-xylene and *o*-xylene (BTEX). The response of the NTFET device to the different analytes occurs due to a charge transfer between the nanotube conducting channel and the aromatic molecules adsorbed onto the CNT. Aromatic compounds are known to interact with SWCNTs through a π-π electron–donor–acceptor mechanism, responsible for the uptake of BTEX by CNTs. The analytical signal and sensitivity obtained for BTEX determination with the developed NTFET detector, increases in the following order: benzene < toluene < ethylbenzene < xylene. The developed analytical system based on GC–NTFET showed a linearity of the analytical signal between 5.00 and

ISBN:978-84-694-0326-6/DL:T-207-2011

95.00 mg/L, allowing the separation and determination of aromatic compounds with a detection limit ranging from 1.8 mg/L for *o*-xylene to 3.7mg/L for benzene.

In [191], the response at 165 ºC of as deposited and air oxidized CNTs were compared. The films have been exposed to mixtures of dry air and one of the following gases: NO_2 (100 ppb), NH_3 (500 ppm), C_6H_6 (100 ppm), H_2O (RH 80%) and CH_3CH_2OH (Ethanol) (500 ppm). Comparing the results obtained with both films, it turns out a smaller change of the electrical sensitivity of the air oxidized CNTs with respect to the as deposited ones.

Despite the important efforts made for enhancing the sensitivity of carbon nanotubes based gas sensors to benzene, the detection limits are still very high and the sensitivity very low compared to other gases. Other authors have worked on modified carbon nanotubes in order to enhance the interaction with benzene through the use of metal decorated and polymer doped CNT based sensors.

Titanium and ruthenium [192-194] have been found to play an important role in the catalytic oxidation or hydrogenation of this chemical species. The decoration of carbon nanotubes with ruthenium nano-clusters and its high catalytic activity (at room temperature) in the hydrogenation of benzene has been reported in [194].

Guo and co-workers oxidized nanotubes in nitrosulfuric acid and decorated them with Pd by a reduction method for detecting benzene [195]. However, the concentration of benzene detected were three orders of magnitude higher than the required detection threshold for ambient safety applications.

In [92], a new kind of conductive polymer composites was fabricated by in situ polymerization of styrene (PS) in the presence of multi-walled carbon nanotubes (MWCNTs) and solution mixing of polystyrene with MWCNTs, respectively. The experimental results showed that the in situ polymerization method has more advantages to improve the dispersion of MWCNTs in PS matrix, and produces composites with high sensitivity and rate of response for the vapors of good solvents of PS at filler range from 5 to 15 wt.%. A rise in testing temperature raised the rate of response but lowered the maximum responsiveness of the composites. Good responsiveness was shown for benzene. In [196], a gas sensor based on SWCNTs/Ethtyl Cellulose composite was tested towards benzene in the range of [1000-5000] ppm with a sensitivity of 9 % for 5000 ppm of benzene. However these concentrations are very high for the requirements of benzene monitoring.

ISBN:978-84-694-0326-6/DL:T-207-2011

The selective detection of benzene in the presence of other species has been envisaged in very few works.

Lu and co-workers [197] fabricated an array of 32 sensors based on three different categories: (1) pristine single walled carbon nanotubes, (2) carbon nanotubes coated with different polymers (chlorosulfonated polyethylene and hydroxypropyl cellulose), (3) carbon nanotubes loaded with Pd nanoparticles and monolayer protected clusters of gold nanoparticles for discriminating NO_2, HN, HCl, Cl_2, acetone and benzene. However, the sensors showed small sensitivity to gases and the concentrations tested were in the range of 5-45 ppm.

J. Wang et al fabricated a formaldehyde gas sensor based on tin oxide doped with hydroxyl-functionalized multiwall carbon nanotubes (MWCNTs) [171]. The sensor response of the MWCNTs doped SnO_2 tested towards 50 ppm of formaldehyde, acetone, methanol, toluene, benzene and ammonia exhibited a response much higher than that of an undoped SnO_2 sensor. For benzene, the sensitivity of the hybrid sample was about 1 % for a concentration of 50 ppm.

The performance of another hybrid sensor based on Sb/SnO_2/CNT was tested and compared in terms of sensitivity to SnO_2 and Sb/SnO_2 [198] towards formaldehyde, ammonia, benzene, and toluene for concentrations ranging from 100 to 1000 ppm. The ternary hybrid sensors showed higher responses than SnO_2 and Sb/SnO_2 sensors. However, for benzene, the response of the hybrid materials was similar with sensitivity between 2 and 4 % but higher than for SnO_2 pure material. The recovery and response times were about some seconds for all materials. Furthermore, on the surface of Sb-CNT-SnO_2 thin film with array-like protrusions, the existence of an electric field is proposed as the explanation for high-speed response to formaldehyde, ammonia, and toluene as polar molecules and ordinary performance to benzene, which is non polar.

As can be noticed, despite the efforts devoted to increase the performance of carbon nanotube based sensors, the detection limits are still high and the sensitivity very small compared to conventional metal oxide gas sensors. However, the possibility to achieve the detection of that gas at ambient temperature is a very good advantage that encourages further investigating the detection of this gas on CNT based gas sensors.

ISBN:978-84-694-0326-6/DL:T-207-2011

References

[1] R. Hirlekar, M. Yamagar, H. Garse, M. Vij, V. Kadam, Carbon nanotubes and its applications: A review, Asian Journal of Pharmaceutical and Clinical Research, 2, 4, 17-27 (2009)

[2] (a) R. Saito, M. Fujita, G. Dresselhaus, and M. S. Dresselhaus, Electronic structure of chiral graphene tubules, Applied Physics Letters, 60, 2204-2206 (1992).,

(b) R.H. Baughman, A.A. Zakhido v, and W.A.de Heer, Carbon nanotubes –the route toward applications, Science 297,787 (2002).

[3] Y. Satio, K. Hamanguchi, T. Hata, K. Tohji, A. Kasuya, Y. Nishina, Field emission patterns from single-walled carbon nanotubes. Japanese Journal of Applied Physics part 2-letters, 36 (10A) L1340-L1342 **(**1997)

[4] H. Cheng, Q. Yang, C. Liu, Hydrogen storage 3.257 in carbon nanotubes, Carbon 39, 1447-1454 (2001).

[5] S.P. Jarvis, T. Uchihashi, T. Ishida, H. Tokumoto and Y. Nakayama, Local solvation shell measurement in water using a carbon nanotube probe, Journal of. Physical Chemistry, B 104, 6091–6094 (2000).

[6] J. Kong, N. R. Franklin, C. Zhou, M. G. Chapline, S. Peng, K. Cho, H. Dai, Nanotube molecular wires as chemical sensors, Science, 287, 5453, 622– 625 (2000).

[7] P.M. Ajayan, L.S. Schadler, C. Giannaris, A. Rubio, Single-walled carbon nanotube-polymer composites: Strength and weakness, Advanced Materials. 12, 750-753 (2000)

[8] C. Wang, M. Waje, X. Wang, J. M. Tang, R. C. Haddon, and Y. Yan, Proton Exchange Membrane Fuel Cells with Carbon Nanotube Based Electrodes, Nano Letters, 4, 2, 345–348.(2004)

[9] Z. Liu, X. Lin, J. Y. Lee,, W. Zhang,, M. Han and L. M. Gan, Preparation and Characterization of Platinum-Based Electrocatalysts on Multiwalled Carbon Nanotubes for Proton Exchange Membrane Fuel Cells, Langmuir, 18, 10, 4054–4060 (2002).

[10] W. Li, Ch. Liang, W. Zhou, J. Qiu, H. Li, G. Sun, Q. Xin, Homogeneous and controllable Pt particles deposited on multi-wall carbon nanotubes as cathode catalyst for direct methanol fuel cells, Carbon 42 (2) 436-439 (2004).

[11] A. Thess, R. Lee, P. Nikolaev, H.J. Dai, P. Petit, J. Robert, C.H. Xu, Y.H. Lee, S.G. Kim, A.G. Rinzler, D.T. Colbert, G.E. Scuseria, D. Tomanek, J.E. Fischer, R.E. Smalley, Crystalline ropes of metallic carbon nanotubes, Science 273, 5274, 483–487. (1996)

[12] C. Journet, W.K. Maser, P. Bernier, A. Loiseau, M. Lamy de la Chapelle, S. Lefrant, P. Deniard, R. Lee, J.E. Fischer, Large-scale production of single-walled carbon nanotubes by the electric-arc technique, Nature 388, 756-758 (1997)

[13] M. Su, B. Zheng, J. Liu, A scalable CVD method for the synthesis of single walled carbon nanotubes with high catalyst productivity, Chemical Physics Letters, 322, 321-326 (2000)

[14] B. Kitiyanan, W.E. Alvarez, J.H. Harwell, D.E. Resasco, Controlled production of single-wall carbon nanotubes by catalytic decomposition of CO on bimetallic Co-Mo catalysts, Chemical Physics Letters, 317, 497-503 (2000).

ISBN:978-84-694-0326-6/DL:T-207-2011

[15] N. Sinha, J. Ma, and J. T.W. Yeow, Carbon Nanotube Based Sensors, Journal of Nanoscience and Nanotechnology, 6, 573–590 (2006).

[16] P.X. Hou, S. Bai, G.H. Yang, C. Liu, H.M. Cheng, Multi-step purification of carbon nanotubes, Carbon, 40, 81-85 (2002).

[17] D. Akiladevi, Sachinandan Basak, Carbon Nanotubes (CNTs) Production, Characterisation and Its Applications, International Journal of Advances in Pharmaceutical Sciences, 1 (2010) 187-195

[18] V.N. Popov, Carbon nanotubes: properties and application, Materials Science and Engineering R 43 (2004) 61–102.

[19] G. Jiménez Cadena, J. Riu, F.X. Rius, Gas sensors based on nanostructured materials, Analyst 132 (2007) 1083–1099.

[20] Wei-De Zhang and Wen-Hui Zhang, Carbon nanotubes as active components for gas sensors, journal of sensors, 2009, Article ID 160698, 16 pages, Doi: 10.1155/2009/160698

[21] A Goldoni, L Petaccia, S Lizzit, and R Larciprete, Sensing gases with carbon nanotubes: a review of the actual situation, J. Phys.: Condens. Matter 22 (2010) 01 3001

[22] J.A. Robinson, E.S. Snow, S.C. Badescu, T.L. Reinecke, F.K. Perkins, Role of defects in singlewalled carbon nanotube chemical sensors, Nano Letters 6 (2006) 1747–1751.

[23] C.G. Hu, B. Feng, Y. Xi, Z.W. Zhang, N. Wang, Modification of carbon nanotubes and their electrochemical detection, Diamond and Related Materials 16 (2007) 1988–1991.

[24] J. Kong, M.G. Chapline, H. Dai, Functionalized carbon nanotubes for molecular hydrogen sensors, Advanced Materials 13 (2001) 1384–1386.

[25] G. G. Wildgoose, C. E.Banks, R. G. Compton, Metal Nanoparticles and Related materials Supported on Carbon Nanotubes: Methods and applications, Small, 2, 182-193 (2006)

[26] V. Georgakilas, D. Gournis,, V. Tzitzios, L.Pasquato, D. M. Guldi, M. Prato, Decorating Carbon Nanotubes with Metal or Semiconductor Nanoparticles, Journal of Materials Chemistry,17, 2679-2694 (2007).

[27] F.P. Rouxinol, R. V. Gelamo and S. A. Moshkalev, gas sensors based on decorated carbon nanotubes. *sciyo.com/download/pdf/pdfs_id/10008*

[28] H.-L. Hsu, J.-M. Jehng, Y. Sung, L.-C. Wang, and S.-R. Yang, The synthesis, characterization of oxidized multi-walled carbon nanotubes, and application to surface acoustic wave quartz crystal gas sensor, Materials Chemistry and Physics, 109, 1, 148–155 (2008).

[29] W-D Zhang and W. H. Zhang, Carbon Nanotubes as Active Components for Gas Sensors, Journal of Sensors Volume 2009, Article ID 160698, 16 pages doi:10.1155/2009/160698 (2009)

[30] R. Ionescu, E.H. Espinosa, E. Sotter, E. Llobet, X. Vilanova, X. Correig, A. Felten, C. Bittencourt, G. Van Lier, J.-C. Charlier and J.J. Pireaux, Oxygen functionalisation of MWNT and their use as gas sensitive thick-film layers, Sensors and Actuators B, 113, 36–46 (2006)

ISBN:978-84-694-0326-6/DL:T-207-2011

[31] J. Kong, M. G. Chapline, and H. J. Dai, Functionalized carbon nanotubes for molecular hydrogen sensors, Advanced Materials, 13, 18, 1384–1386 (2001).

[32] A. Star, V. Joshi, S. Skarupo, D. Thomas, and J.-C. P. Gabriel, Gas sensor array based on metal-decorated carbon nanotubes, Journal of Physical Chemistry B, 110, 42, 21014–21020 (2006).

[33] Y. Lu, J. Li, J. Han, H.-T. Ng, C. Binder, C. Partridge and M. Meyyappan, Room temperature methane detection using palladium loaded single-walled carbon nanotubes sensors, Chemical Physics Letters, 391, 4–6, 344–348 (2004).

[34] I. Sayago, , E. Terrado, M. Aleixandre, M.C. Horrillo, M.J. Fernández, J. Lozano, E. Lafuente, W.K. Maser, A.M. Benito, M.T. Martinez, J. Gutiérrez and E. Muñoz, Novel selective sensors based on carbon nanotube films for hydrogen detection, Sensors and Actuators B, 122, 1, 75–80 (2007).

[35] R. V. Gelamo, F. P. Rouxinol, C. Verissimo, A. R. Vaz, M. A. B. de Moraes & S. A. Moshkalev, Low-temperature gas and pressure sensor based on multi-wall carbon nanotubes decorated with Ti nanoparticles, Chemical Physics Letters, 482, 302-306 (2009)

[36] M. Penza, G. Cassano, R. Rossi, M. Alvisi, A. Rizzo, M. A. Signore, Th. Dikonimos, E. Serra, and R. Giorgi, Enhancement of sensitivity in gas chemiresistors based on carbon nanotubes surface functionalized with noble metal (Au, Pt) nanoclusters, Applied Physics Letters, 90, 17, 171231– 171233 (2007).

[37] H. Xu , Decorating Carbon Nanotubes with Nanoparticles, Literature Seminar, 2007

[38] D. Wang, Z. C. Li, L. Chen, Templated synthesis of single-walled carbon nanotubes and metal nanoparticles assemblies in solution, Journal of the American.Chemical Society, 128, 15078-15079 (2006)

[39] H.C. Choi, M. Shim, S. Bangsaruntip, and H. Dai, Spontaneous reduction of metal ions on the Sidewalls of Carbon Nanotubes, Journal of the American.Chemical Society, 124, 9058-9059 (2002)

[40] L. Qu, L. Dai, Substrate-enhanced electroless deposition of metal nanoparticles on Carbon Nanotubes, Journal of the American Chemical Society, 127, 10806-10807 (2005)

[41] Y. T. Kim,, K. Ohshima , K. Higashimine, T. Uruga, M. Takata, H. Suematsu, T. Mitani, Fine Size Control of Platinum on Carbon Nanotubes: From Single Atoms to Clusters, Angewandte Chemie International Edition, 45, 407-411 (2006).

[42] Y.T. Kim, T. Uruga, T. Mitani, Formation of Single Pt atoms on thiolated carbon nanotubes using a moderate and large-scale chemical approach, Advanced Materials, 18, 2634-2638 (2006).

[43] K.S. Coleman, S. R. Bailey, S. Fogden, and M. L. H. Green, Functionalization of single-Walled Carbon Nanotubes via the Bingel Reaction, Journal of the American Chemical Society,125, 8722-8723 (2003)

[44] J. Li, S. Tang, L. Lu, and H. C. Zeng, Preparation of Nanocomposites of Metals, Metal Oxides, and Carbon Nanotubes via Self-Assembly, Journal of the American Chemical Society, 129, 30, 9401–9409 (2007)

ISBN:978-84-694-0326-6/DL:T-207-2011

[45] Y. Zhang, H. Gu, K. Suenaga, S. Iijima, Heterogeneous growth of B---C---N nanotubes by laser ablation, Chemical Physics Letters 279, 264 (1997)

[46] M. Terrones, N. Grobert, J. Olivares, J. P. Zhang, H. Terrones, K. Kordatos, W.K. Hsu, J. P. Hare, P. D. Townsend, K. Prassides, A. K. Cheetham, H. W. Kroto, R. M. D Walton Controlled production of aligned-nanotube bundles, Nature 388, 52-55 (1997)

[47] D. Goldberg, Y. Bando, L. Bourgeois, K. Kurashima, T. Sato, Large-scale synthesis and HRTEM analysis of single-walled B- and N-doped carbon nanotube bundles, Carbon, 38 (14), 2017-2017 (2000)

[48] K. Suenaga, M. P. Johansson, N. Hellgren, E. Broitman, L. R. Wallenberg, C. Colliex, J. –E. Sundgren, L. Hultman, Carbon nitride nanotubulite – densely-packed and well-aligned tubular nanostructures, Chem. Phys. Lett., 300, 695-700 (1999).

[49] L. Hultman, S. Stafstrom, Z. Czigany, J. Neidhardt, N. Hellgren, I. F. Brunell, K. Suenaga, C. Colliex, Cross-Linked Nano-onions of Carbon Nitride in the Solid Phase: Existence of a Novel C48N12 Aza-Fullerene, Phys. Rev. Lett., 87, 225503-225507 (2001)

[50] O. Breuer, U. Sundararaj, Big returns from small fibers: A review of polymer/carbon nanotube composites, Polymer Composites, 25, 6, 630–645 (2004)

[51] P. Pötschke, A. R. Bhattacharyya and A. Janke, Melt mixing of polycarbonate with multiwalled carbon nanotubes: microscopic studies on the state of dispersion, European Polymer Journal, Volume 40, 1, 137-148 (2004)

[52] B. Zhang, R. W. Fu, M. Q. Zhang, X. M. Dong, P. L. Lan, and J. S. Qiu, Preparation and characterization of gas-sensitive composites from multi-walled carbon nanotubes/ polystyrene, Sensors and Actuators B, 109, 2, 323–328 (2005).

[53] Y. Wang, J. T. W. Yeow, A Review of Carbon Nanotubes-Based Gas Sensors, Journal of Sensors, Volume 2009, Article ID 493904, 24 pages doi:10.1155/2009/493904 (2009).

[54] T. Someya, J. Small, P. Kim, C. Nuckolls, and J. T. Yardley, Alcohol vapor sensors based on single-walled carbon nanotubes field effect transistors, Nano Letters, 3, 7, 877–881 (2003).

[55] O. K. Varghese, P. D. Kichambre, D. Gong, K. G. Ong, E. C. Dickey, and C. A. Grimes, Gas sensing characteristics of multi-wall carbon nanotubes, Sensors and Actuators B, 81, 1, 32–41 (2001).

[56] J. Chung, K.-H. Lee, J. Lee, D. Troya, and G. C. Schatz, Multiwalled carbon nanotubes experiencing electrical breakdown as gas sensors, Nanotechnology, 15, 11, 1596–1602 (2004).

[57] J. Sippel-Oakley, H. T. Wang, B. S. Kang, Z. Wu, F. Ren, A. G Rinzler and S. J. Pearton, Carbon nanotube films for room temperature hydrogen sensing, Nanotechnology, 16, 2218–2221 (2005).

[58] T. Ueda, S. Katsuki, K. Takahashi, H. A. Narges, T. Ikegami, and F. Mitsugi, Fabrication and characterization of carbon nanotube based high sensitive gas sensors operable at room temperature, Diamond and Related Materials, 17, 7– 10, 1586–1589 (2008).

ISBN:978-84-694-0326-6/DL:T-207-2011

[59] L. Valentini, C. Cantalini, I. Armentano, J. M. Kenny, L. Lozzi, and S. Santucci, Highly sensitive and selective sensors based on carbon nanotubes thin films for molecular detection, Diamond and Related Materials, 13, 4–8, 1301– 1305 (2004).

[60] A. Modi, N. Koratkar, E. Lass, B. Wei, and P. M. Ajayan, Miniaturized gas ionization sensors using carbon nanotubes, Nature, 424, 6945, 171–174 (2003).

[61] W. A. De Heer, A. Chatelain, and D. Ugarte, A carbon nanotube field-emission electron source, Science, 270, 5239, 1179–1180 (1995).

[62] N. de Jonge, Y. Lamy, K. Schoots, and T. H. Oosterkamp, High brightness electron beam from a multi-walled carbon nanotube, Nature, 420, 6914, 393–395 (2002).

[63] S. J. Kim, Gas sensors based on Paschen's law using carbon nanotubes as electron emitters, Journal of Physics D, 39, 14, 3026–3029 (2006).

[64] J. Wu, H. Liu, D. Xu, et al., in Proceedings of the 3rd IEEE International Conference on Nano/Micro Engineering and Molecular System, Sanya, China, January 2008.

[65] A. Wadhawan, R. E. Stallcup II, K. F. Stephens II, J. M. Perez, and I. A. Akwani, Effects of O_2, Ar, and H_2 gases on the fieldemission properties of single-walled and multiwalled carbon nanotubes, Applied Physics Letters, 79, 12, 1867– 1869 (2001).

[66] Z. Yong, L. Junhua, and L. Xin, The structure optimization of the carbon nanotube film cathode in the application of gas sensor, Sensors and Actuators A, 128, 278–289 (2006).

[67] J. T. W. Yeow and J. P. M. She, Carbon nanotube-enhanced capillary condensation for a capacitive humidity sensor, Nanotechnology, 17, 21, 5441–5448 (2006.)

[68] E. S. Snow, F. K. Perkins, E. J. Houser, S. C. Badescu, and T. L. Reinecke, Chemical detection with a single-walled carbon nanotube capacitor, Science, 307, 5717, 1942– 1945 (2005).

[69] S. Chopra, A. Pham, J. Gaillard, A. Parker, and A. M. Rao, Carbon-nanotube-based resonant-circuit sensor for ammonia, Applied Physics Letters, 80, 24, 4632– 4636 (2002).

[70] S. Chopra, K. McGuire, N. Gothard, A. M. Rao, and A. Pham, Selective gas detection using a carbon nanotube sensor, Applied Physics Letters, 83, 11, 2280–2282 (2003).

[71] M. Penza, F. Antolini, and M. Vittori Antisari, Carbon nanotubes as SAW chemical sensors materials, Sensors and Actuators B, 100, 1-2, 47–59 (2004).

[72] 11. S.M. Sze, K. K. Ng, Physics of Semiconductor Devices, New York (1981).

[73] I. Eisele, T. Doll and M. Burgmair, Low power gas detection with FET sensors, Sensors and Actuators B: Chemical, 78, 1-3, 19-25 (2001),

[74] C. S. Huang, B. R. Huang, Y. H. Jang, M. S. Tsai, and C. Y. Yeh, Three-terminal CNTs gas sensor for N_2 detection, Diamond and Related Materials, 14, 11-12, 1872–1875 (2005).

[75] M. Tabib-Azar and Y. Xie, Sensitive NH_3OH and HCl gas sensors using self-aligned and self-welded multiwalled carbon nanotubes, IEEE Sensors Journal, 7, 10, 1435– 1439 (2007).

ISBN:978-84-694-0326-6/DL:T-207-2011

[76] D. Ding, Z. Chen, S. Rajaputra, and V. Singh, Hydrogen sensors based on aligned carbon nanotubes in an anodic aluminum oxide template with palladium as a top electrode," Sensors and Actuators B, 124, 1, 12–17 (2007).

[77] Y.-T. Jang, S.-I. Moon, J.-H. Ahn, Y.-H. Lee, and B.-K. Ju, A simple approach in fabricating chemical sensor using laterally grown multi-walled carbon nanotubes, Sensors and Actuators B, 99, 1, p118–122 (2004).

[78] J. Li, Y. Lu, Q. Ye, L. Delzeit, and M. Meyyappan, A Gas Sensor Array Using Carbon Nanotubes and Microfabrication Technology, Electrochemical and Solid-State Letters, 8-11 H100-H102 (2005)

[79] J. Li, Y. Lu, Q. Ye, Q. Ye, M. Cinke, J. Han, and M. Meyyappan, Carbon nanotubes sensors for gas and organic vapour detection, Nano Letters, 3, 7, 929–933 (2003).

[80] M. K. Kumar, S. Ramaprabhu**,** Palladium dispersed multiwalled carbon nanotube based hydrogen sensor for fuel cell applications, International Journal of Hydrogen Energy, 32, 13 , 2518-2526 (2007).

[81] Y. D. Lee, W.-S. Cho,S.-I. Moon, Y-H Lee, J. KKim, S. Nahm and B-K Ju, Gas sensing properties of printed multiwalled carbon nanotubes using the field emission effect, Chemical Physics Letters, 433, 1–3, 105–109 (2006).

[82] K. Yamamoto, S. Akita, and Y. Nakayama, Orientation and purification of carbon nanotubes using ac electrophoresis, Journal of Physics D, 31, 8, L34–L36 (1998).

[83] K. Bubke, H. Gnewuch, M. Hempstead, J. Hammer, and M. L. H. Green, Optical anisotropy of dispersed carbon nanotubes induced by an electric field, Applied Physics Letters, 71, 14, 1906–1908 (1997).

[84] T. Prasse, J.-Y. Cavaille, and W. Bauhofer, Electric anisotropy of carbon nanofibre/epoxy resin composites due to electric field induced alignment, Composites Science and Technology, 63, 13, 1835–1841 (2003).

[85] X. Q. Chen, T. Saito, H. Yamada, and K. Matsushige, Aligning single-wall carbon nanotubes with an alternating-current electric field, Applied Physics Letters, 78, 23, 3714– 3716 (2001).

[86] X. Liu, J. L. Spencer, A. B. Kaiser, and W. M. Arnold, Electricfield oriented carbon nanotubes in different dielectric solvents, Current Applied Physics, 4, 2–4, 125–128 (2004).

[87] F. Wakaya, T. Nagai, and K. Gamo, Position control of carbon nanotube using patterned electrode and electric field, Microelectronic Engineering, 63, 1–3, 27–31 (2002).

[88] R. Krupke, F. Hennrich, H. B. Weber, D.Beckmann, O. Hampe, S. Malik, M. M Kappes, H. v Löhneysen, Contacting single bundles of carbon nanotubes with alternating electric fields, Applied Physics A, 76, 3, 397–400 (2003).

[89] J. Suehiro, G. Zhou, and M. Hara, Fabrication of a carbon nanotube-based gas sensor using dielectrophoresis and its application for ammonia detection by impedance spectroscopy, Journal of Physics D, 36, 21, L109– L114 (2003).

[90] Y. Zhang, T. Ichihashi, E. Landree, F. Nihey and S. Iijima, Heterostructures of

Single-Walled Carbon Nanotubes and Carbide Nanorods,Science, 285, 1719-1722 (1999)

ISBN:978-84-694-0326-6/DL:T-207-2011

[91] C. Cantalini, L. Valentini, I. Armentano, L. Lozzi, J.M. Kenny, S. Santucci, Sensitivity to NO_2 and cross-sensitivity analysis to NH3, ethanol and humidity of carbon nanotubes thin film prepared by PECVD, Sensors and Actuators B, 95 195–202 (2003)

[92] Y. Lu, C. Partridge, M. Meyyappan, J. Li, A carbon nanotube sensor array for sensitive gas discrimination using principal component analysis, Journal of Electroanalytical Chemistry, 593, 105–110 (2006)

[93] S-H. Jhi, S. G. Louie and M. L. Cohen, Electronic Properties of Oxidized Carbon Nanotubes, Physical Review Letters 85, 1710-1713 (2000).

[94] X. Y. Zhu, S. M. Lee, Y. H. Lee and T. Frauenheim, Adsorption and Desorption of an O_2 Molecule on Carbon Nanotubes, Physical Review Letters 85, 2757-2760 (2000).

[95] S. Peng and K. Cho, Chemical control of nanotube electronics, Nanotechnology 11, 57 (2000).

[96] H. Chang, J. D. Lee, S.M. Lee and Y. H. Lee, Adsorption of NH_3 and NO_2 molecules on carbon nanotubes, Applied Physics Letters 79, 3863 (2001).

[97] J. J. Zhao, A. Buldum, J. Han and J. P. Lu, Gas molecule adsorption in carbon nanotubes and nanotube bundles , Nanotechnology 13 (2), 195 (2002)

[98] S. Peng and K. Cho, Ab Initio Study of Doped Carbon Nanotube Sensors, Nano Lett. 3 (5), 513 (2003)

[99] P. Giannozzi, R. Car and G. Scoles, Oxygen adsorption on graphite and nanotubes journal of Chemical Physics 118, 1003 (2003).

[100] S.G. Wang, Q. Zhang, D.J. Yang, P.J. Sellin, G.F. Zhong, Multi-walled carbon nanotube-based gas sensor for NH_3 detection, Diamond and Relatated Materials, 13, 1327–1332 (2004)

[101] J. Suehiro, G. Zhou, H. Imakiire, W. Ding, and M. Hara, Controlled fabrication of carbon nanotube NO_2 gas sensor using dielectrophoretic impedance measurement, Sensors and Actuators B, 108, 1-2, 398–403 (2005).

[102] R. Larciprete, L. Petaccia, S. Lizzit and A. Goldoni, The role of metal contact in the sensitivity of single walled carbon nanotubes to NO_2, Journal of Physical Chemistry C 111, 12169 (2007)

[103] A. Goldoni, R. Larciprete, L. Petaccia and S. Lizzit, Single-Wall Carbon Nanotube Interaction with Gases: Sample Contaminants and Environmental Monitoring, Journal of American Chemical Society 125, 11329-11333 (2003).

[104] (a) A. Goldoni, L. Petaccia, L. Gregoratti, B. Kaulich, A. Barinov, S. Lizzit, A. Laurita, L. Sangaletti, R. Larciprete, Spectroscopic Characterization of Contaminants in purified Single-walled Carbon Nanotubes: Cleaning Procedure and Influence on The Interaction With Gases, Carbon 42, 2099 (2004).

(b) K. A.Williams and P. C. Eklund, Monte Carlo simulations of H_2 physisorption in finite-diameter carbon nanotube ropes, Chemical Physics Letters, 320, 3-4, 352–358 (2000).

[105] G. Stan and M.W. Cole, Hydrogen adsorption in nanotubes, Journal of Low Temperature Physics, 110, 1-2, 539– 544 (1998).

ISBN:978-84-694-0326-6/DL:T-207-2011

[106] L. Valentini, Reversible oxidation effects on carbon nanotubes thin films for gas sensing applications, Materials Science and Engineering C, 23, 523–529 (2003)

[107] J. Zhang, A. Boyd, A. Tselev, M. Paranjape and P. Barbara, Mechanism of NO_2 interaction in carbon nanotube field effect transistor chemical sensors, Applied Physics Leters 88, 123112 (2006).

[108] (a) P. Bondavalli, P. Legagneux, D. Pribat, A. Balan and S. Nazeer, Gas fingerprinting using carbon nanotubes transistor arrays, Journal of Experimental Nanoscience 3, 347-356 (2008).

(b) P. Bondavalli, P. Legagneux and D. Pribat, Carbon nanotubes based transistors as gas sensors: State of the art and critical review,Sensors and Actuators B 140, 304-318 (2009).

[109] N.O.V. Plank, R. Cheung, Functionalisation of carbon nanotubes for molecular electronics, Microelectron Engineering, 73/74, 578–582 (2004)

[110] M. L. Y. Sin, G. C. T. Chow, G. M. K. Wong, W. J. Li, P. H. W. Leong, and K. W. Wong, Ultralow-power alcohol vapor sensors using chemically functionalized multiwalled carbon nanotubes, IEEE Transactions on Nanotechnology, 6,no. 5, 571–577 (2007).

[111] E.H. Espinosa, R. Ionescu, C. Bittencourt, A. Felten, R. Erni, G. Vantendeloo, J.-J. Pireaux, E. Llobet, Metal-decorated multi-wall carbon nanotubes for low temperature gas sensing, Thin Solid Films, 515, 8322–8327 (2007)

[112] A. Felten, C. Bittencourt, J.-F. Colomer, G. Van Tendeloo, J.-J. Pireaux, Nucleation of metal clusters on plasma treated multiwall carbon nanotubes, Carbon, 45, 110–116 (2007).

[113] A. Starr, V. Joshi, S. Skarupo, D. Thomas, J.C.P. Gabriel, Gas sensor array based onMetal decorated carbon nanotubes, J. Phys. Chem. B 110 (2006) 21014–21020.

[114] A. Felten, C. Bittencourt, J.-F. Colomer, G. Van Tendeloo and J.-J. Pireaux. Nucleation of metal clusters on plasma treated multi wall carbon nanotubes. Carbon 2007; 45 (1), 110-116.

[115] G.H. Lu. L.E. Ocola, J. Chen. Room temperature gas sensing based on electron transfer between discrete tin oxide nanocrystals and multiwalled carbon nanotubes. Adv. Mater. 2009; 21: 2487-2491.

[116] Q. Zhao, M.B. Nardelli, W. Lu, J. Bernhoc, Carbon nanotubes-metal cluster composites : A new road to chemical sensors, Nano Letters 5, 847-851 (2005)

[117] I. Sayago, E. Terrado, E. Lafuente, M.C. Horrillo, W.K. Maser, A.M. Benito , R. Navarro E.P. Urriolabeitia, M.T. Martinez and J. Gutierrez, Hydrogen sensors based on carbon nanotubes thin films, Synthetic Metals, 148, 1, 15–19 (2005).

[118] A. T. Gee, B. E. Hayden, C. Mormiche, and T. S. Nunney, The role of steps in the dynamics of hydrogen dissociation on Pt(533) Journal of Chemical Physics, 112, 17, 7660–7668 (2000).

[119] R. A. Olsen, S. C. Badescu, S. C. Ying, and E. J. Baerends, Adsorption and diffusion on a stepped surface: atomic hydrogen on Pt(211), Journal of Chemical Physics, 120, 24, 11852–11863 (2004).

[120] A. Mandelis and C. Christofides, Physics, Chemistry and Technology of Solid State Gas Sensor Devices, John Wiley & Sons, New York, NY, USA (1993).

ISBN:978-84-694-0326-6/DL:T-207-2011

[121] Y. Sun, H. H. Wang, and M. Xia, Single-Walled Carbon Nanotubes Modified with Pd Nanoparticles: Unique Building Blocks for High-Performance, Flexible Hydrogen Sensors, Journal of Physical Chemistry C, 112, 1250-1259 (2008).

[122] Y. Li, H. Wang, Y. Chen, and M. Yang, A multi-walled carbon nanotube/palladium nanocomposite prepared by a facile method for the detection of methane at room temperature, Sensors and Actuators B, 132, 1, 155–158 (2008).

[123] G. V. Kamarchuk, I. G. Kolobov, A. V. Khotkevich, I. K. Yansona, A. P. Pospelovb, I. A. Levitskyc, and W. B. Euler, New chemical sensors based on point heterocontact between single wall carbon nanotubes and gold wires, Sensors and Actuators B, 134, 2, 1022–1026 (2008).

[124] B. Hvolbæk, T. V.W. Janssensb, B.S. Clausenb, H. Falsigc, Claus H. Christensenc and J. K. Nørskov, Catalytic activity of Au nanoparticles, Nanotoday, 2, 4,,14-18 (2007).

[125] M. Penza, R. Rossia, M. Alvisia, G. Cassanoa and E. Serra, Functional characterization of carbon nanotube networked films functionalized with tuned loading of Au nanoclusters for gas sensing applications, Sensors and Actuators B, 140, 176–184 (2009)

[126] I. Simon, N. Barsan, M. Bauer, U. Weimar, Micromachined metal oxide gas sensors: opportunities to improve sensor performance, Sensors and Actuators B, 73, 1–26 (2001).

[127] M. Graf, D. Barrettino, K.-U. Kirstein, A. Hierlemann, CMOS microhotplate sensor system for operating temperatures up to 500 ºC, Sensors and Actuators B, 117, 346–352 (2006)

[128] W.Göpel, Newmaterials and transducers for chemical sensors, Sensors and Actuators B, 18, 1–21 (1994)

[129] E. Comino, Metal oxide next term nano-crystals for gas sensing, Analytica Chemica Acta, 568, 28–40 (2006).

[130] P.K. Clifford, D.T. Tuma, Characteristics of semiconductor gas sensors. 1. Steady-state gas response, Sensors and Actuators, 3, 233–254 (1983)

[131] P.K. Clifford, D.T. Tuma, Characteristics of semiconductor gas sensors. 2.Transient-response to temperature-change, Sensors and Actuators, 3, 255–281 (1983)

[132] B.Y. Wei, M.C. Hsu, P.G. Su, H.M. Lin, R.J. Wu, H.J. Lai, A novel SnO_2 gas sensor doped with carbon nanotubes operating at room temperature, Sensors and Actuators B, 101, 81–89 (2004)

[133] Y. Chen, C. Zhu, T. Wang, The enhanced ethanol sensing properties of multi-walled carbon nanotubes/SnO_2 core/shell nanostructures, Nanotechnology, 17, 3012–3017 (2006)

[134] C. Bittencourt, A. Felten, E.H. Espinosa, R. Ionescu, E. Llobet, X. Correig, J.-J. Pireaux, WO_3 films modified with functionalised multi-wall carbon nanotubes: Morphological, compositional and gas response studies, Sensors and Actuators B, 115, 33–41 (2006).

[135] E.H. Espinosa, R. Ionescu, E. Llobet, A. Felten, C. Bittencourt, E. Sotter, Z. Topalian, P. Heszler, C.G. Granqvist, J.J. Pireaux, X. Correig, Highly selective NO_2 gas

ISBN:978-84-694-0326-6/DL:T-207-2011

sensors made of MWCNTs and WO_3 hybrid layers, Journal of Electrochemical Society, 154, J141–J149 (2007).

[136] N. D. Hoa, N. V. Quy, Y. S. Cho, and D. Kim, Nanocomposite of SWCNTs and SnO2 fabricated by soldering process for ammonia gas sensor application, Physical Status Solidi A, 204, 6, 1820–1824 (2007).

[137] Y.-L. Liu, H.-F. Yang, Y. Yang,Z.-M. Liu, G.-L. Shen, and R.-Q. Yu, Gas sensing properties of tin dioxide coated onto multiwalled carbon nanotubes, Thin Solid Films, 497, 1-2, 355–360 (2006).

[138] N. Van Hieu, L.T. B. Thuy, and N. D. Chien, Highly sensitive thin film NH_3 gas sensor operating at room temperature based on SnO_2/MWCNTs composite, Sensors and Actuators B, 129, 2, 888–895 (2008).

[139] S- Z. Kang, Z. Cui, J. Mu, Electrical Property of Tin Oxide Doped with Multi-Walled Carbon Nanotubes, Journal of Dispersion Science and Technology, 28, 569–571 (2007).

[140] M. Sanchez, R. Guirado, and M. E. Rinc, Multiwalled carbon nanotubes embedded in sol-gel derived TiO_2 matrices and their use as room temperature gas sensors, Journal of Materials Science: Materials in Electronics, 18, 11, 1131–1136 (2007).

[141] E. Llobet, E. H. Espinosa, E. Sotter, R. Ionescu, X. Vilanova, J. Torres, A. Felten, J. J Pireaux, X. Ke, G. Van Tendeloo, F. Renaux, Y. Paint, M. Hecq and C. Bittencourt, Carbon nanotube- TiO_2 hybrid films for detecting traces of O_2, Nanotechnology, 19, 37, Article ID 375501, 11 pages (2008).

[142] J. Khanderi, R. C. Hoffmann, A. Gurlo and J. J. Schneider, Synthesis and sensoric response of ZnO decorated carbon nanotubes, Journal of Materials Chemistry, 19, 5039–5046 (2009),

[143] M. G. Willinger, G. Neri, A. Bonavita, G. Micali, E. Rauwel, T. Herntrich and N. Pinna, The controlled deposition of metal oxides onto carbon nanotubes by atomic layer deposition: examples and a case study on the application of V_2O_4 coated nanotubes in gas sensing, Physical Chemistry Chemical Physics 11, 3615 (2009).

[144] N. Du, H. Zhang, X. Ma,, D. Yang, Homogeneous coating of Au and SnO_2 nanocrystals on carbon nanotubes via layer-by-layer assembly: a new ternary hybrid for a room-temperature CO gas sensor, Chemical Communications, 6182–6184 (2008).

[145] R. Ionescu, E.H. Espinosa, R. Leghrib, A. Felten, J.J. Pireaux, R. Erni, G. Van Tendeloo C. Bittencourt, N. Cañellas and E. Llobet, Novel hybrid materials for gas sensing applications made of metal-decorated MWCNTs dispersed on nano-particle metal oxides, Sensors and Actuators B, 131, 174–182 (2008)

[146] P. G. Collins, K. Bradley, M. Ishigami and A. Zettl, Extreme oxygen sensitivity of electronic properties of carbon nanotubes, Science 287, 1801–1804 (2000).

[147] L. Valentini, I. Armentano, J.M. Kenny, C. Cantalini, L. Lozzi, S. Santucci, Sensor for sub-ppm NO_2 gas detection based on carbon nanotubes thin films, Applied Physics Letters 82, 961–963 (2003).

[148] F. Villalpando-Páez, A. H. Romero, E. Muñoz-Sandoval, L. M. Martínez, H. Terrones, M. Terrones, Fabrication of vapor and gas sensors using films of aligned CN_x nanotubes, Chemical Physics Letters, 386, 137-143 (2004).

ISBN:978-84-694-0326-6/DL:T-207-2011

[149] L. Bai, Z. Zhou, Computational study of B and N doped single-walled carbon nanotubes as NH_3 and NO_2 sensors, Carbon 45, 2105-2110 (2007).

[150] R.X. Wang, D.J. Zhang, J. Wu, C.B. Liu, Theoretical study on the sensing properties of the boron and nitrogen doped carbon nanotubes for hydrogen sulfide, ACTA CHIMICA SINICA 65 (2), 107-110 (2007) .

[151] P. Qi, O. Vermesh, M. Grecu, A. Javey, Q. Wang, and H. Dai, Toward large arrays of multiplex functionalized carbon nanotube sensors for highly sensitive and selective molecular detection, Nano Letters, 3, 3, 347–351 (2003).

[152] J. K. Abraham, B. Philip, A. Witchurch, V. K. Varadan, and C. C. Reddy, A compact wireless gas sensor using a carbon nanotube/PMMA thin film chemiresistor, Smart Materials and Structures, 13 (5), 1045–1049 (2004).

[153] L. Niu, Y. Luo, and Z. Li, A highly selective chemical gas sensor based on functionalization of multi-walled carbon nanotubes with poly(ethylene glycol), Sensors and Actuators B, 126 (2), 361–367 (2007).

[154] L. Valentini, V. Bavastrello, E. Stura, I. Armentano, C. Nicolini, and J.M. Kenny, Sensors for inorganic vapor detection based on carbon nanotubes and poly(o-anisidine) nanocomposite material, Chemical Physics Letters, 383, 5-6, 617– 622 (2004).

[155] C. Wei, L. Dai, A. Roy, and T. B. Tolle, Multifunctional chemical vapor sensors of aligned carbon nanotube and polymer composites, Journal of the American Chemical Society, 128, 5, 1412–1413 (2006).

[156] N. H. Quang, M. Van Trinh, B.-H. Lee, and J.-S. Huh, Effect of NH_3 gas on the electrical properties of single-walled carbon nanotube bundles, Sensors and Actuators B, 113, 1, 341–346 (2006).

[157] O. K. Varghese, P. D. Kichambre, D. Gong, K. G. Ong, E. C. Dickey, and C. A. Grimes, Gas sensing characteristics of multi-wall carbon nanotubes, Sensors and Actuators B, 81, 1, 32–41 (2001).

[158] L. H. Nguyen, T. V. Phi, P.Q. Phan, H. N. Vu, C. Nguyen-Duc, and F. Fossard, Synthesis of multi-walled carbon nanotubes for NH_3 gas detection, Physica E, 37, 1-2, 54–57 (2007).

[159] S.-I. Moon, K.-K. Paek, Y.-H. Lee, H-K Park, J-K Kim, S-W Kim and B-K. Ju, Bias-heating recovery of MWCNT gas sensor, Materials Letters, 62 (16), 2422–2425 (2008).

[160] J. Suehiro, G. Zhou, and M. Hara, Detection of partial discharge in SF_6 gas using a carbon nanotube-based gas sensor, Sensors and Actuators B, 105 (2), 164–169 (2005).

[161] G. Sun, S. Liu, K. Hua, X. Lv, L. Huang, and Y.Wang, Electrochemical chlorine sensor with multi-walled carbon nanotubes as electrocatalysts, Electrochemistry Communications, 9 (9), 2436–2440 (2007).

[162] W.-S. Cho, S.-I. Moon, K.-K. Paek, Y.-H. Lee, J.-H. Park, and B.-K. Ju, Patterned multiwall carbon nanotube films as materials of NO_2 gas sensors, Sensors and Actuators B, 119, 1, 180–185 (2006).

[163] T. Ueda, M. M. H. Bhuiyan, H. Norimatsu, S. Katsuki, T. Ikegami, and F. Mitsugi, Development of carbon nanotubebased gas sensors for NO_x gas detection working at low temperature, Physica E, 40, 7, 2272–2277 (2008).

ISBN:978-84-694-0326-6/DL:T-207-2011

[164] N. D. Hoa, N. Van Quy, Y. Cho, and D. Kim, An ammonia gas sensor based on non-catalytically synthesized carbon nanotubes on an anodic aluminum oxide template, Sensors and Actuators B, 127, 2, 447–454 (2007).

[165] S. Mubeen, T. Zhang, B. Yoo, M. A. Deshusses, and N. V. Myung, Palladium nanoparticles decorated single-walled carbon nanotube hydrogen sensor, Journal of Physical Chemistry C, 111, 17, 6321–6327 (2007).

[166] Y. Sun and H. H. Wang, Electrodeposition of Pd nanoparticles on single-walled carbon nanotubes for flexible hydrogen sensors, Applied Physics Letters, 90, 21, Article ID 213107, 1–3 (2007).

[167] M. K. Kumar and S. Ramaprabhu, Nanostructured Pt functionlized multiwalled carbon nanotube based hydrogen sensor, Journal of Physical Chemistry B, 110, 23, 11291–11298 (2006).

[168] M. K. Kumar, A. L. M. Reddy, and S. Ramaprabhu, Exfoliated single-walled carbon nanotube-based hydrogen sensor, Sensors and Actuators B, 130, 2, 653–660 (2008).

[169] J. Gong, J. Sun, and Q. Chen, Micromachined sol-gel carbon nanotube/SnO_2 nanocomposite hydrogen sensor, Sensors and Actuators B, 130, 2, 829–835 (2008).

[170] E. H. Espinosa, R. Ionescu, B. Chambon, G. Bedis, E. Sotter, C. Bittencourt A. Felten, J.-J. Pireaux, X. Correig and E. Llobet, Hybrid metal oxide and multiwall carbon nanotube films for low temperature gas sensing, Sensors and Actuators B, 127, 1, 137–142 (2007).

[171] J. Wang, L. Liu, S.-Y. Cong, J.-Q. Qi, and B.-K. Xu, An enrichment method to detect low concentration formaldehyde, Sensors and Actuators B, 134, 2, 1010–1015 (2008).

[172] N. Van Duy, N. Van Hieu, P. T. Huy, N. D. Chien, M. Thamilselvan, and J. Yi, Mixed SnO_2/TiO_2 included with carbon nanotubes for gas-sensing application, Physica E: Low-dimensional Systems and Nanocstructures 41 (2), 258-263 (2008).

[173] W.R. Haag, Effective benzene monitoring saves lives, compliance magazine, 20-21 (2006).

[174] http://www.jmtest.com/Data_Sheet_RAE-Sep_Benz7_Rev_G.pdf

[175] A. Szczurek, M. Maciejewska Recognition of benzene, toluene and xylene using TGS array integrated with linear and non-linear classifier, Talanta, 64 (3), 609-617 (2004)

[176] X-L. Li, T-J. Lou, Xi-M. Sun, and Y-D. Li, Highly Sensitive WO_3 Hollow Sphere Gas Sensors, Inorganic Chemistry 43, 5442-5449 (2004).

[177] S. Zampolli, I. Elmi, F. Mancarella, P. Betti, E. Dalcanale, G.C. Cardinali and M. Severi, Realtime monitoring of sub ppb concentrations of aromatic volatiles with a MEMS enabled miniaturized gas chromatograph, Sensors and Actuators B, 141, 322–328 (2009).

[178] J-B Sanchez, F. Berger, M. Fromm and M-H. Nadal, A selective gas detection micro-device for monitoring the volatile organic compounds pollution, Sensors and Actuators B, 119, 227–233 (2006)

ISBN:978-84-694-0326-6/DL:T-207-2011

[179] I. Elmi, S. Zampolli, E. Cozzani, F. Mancarella and G.C. Cardinali, Development of ultralowpower consumption MO_X sensors with ppb level VOC detection capabilities for emerging applications, Sensors and Actuators B, 135, 342–351 (2008)

[180] P. Ivanov, F. Blanco, I. Gracia, N. Sabate, , X. Vilanova, X. Correig, , L. Fonseca, E. Figueras, J. Santander, R. Rubio, C. Cane, Influence of the doping material on the benzene detection, ASDAM '06: Sixth International Conference on Advanced Semiconductor Devices and Microsystems, Conference Proceedings, 185-188 (2006).

[181] J. Hubálek, K. Malysz, J. Prášek, X. Vilanova, P. Ivanov, E. Llobet, J. Brezmes, X. Correig and Z. Svèrák, Pt-loaded Al_2O_3 catalytic filters for screen-printed WO_3 sensors highly selective to benzene, Sensors and Actuators B: Chemical, 101, 3, 277-283 (2004)

[182] P. Ivanov, M. Vilaseca, E. Llobet, X. Vilanova, J. Hubalek, J. Coronas, J. Santamaría, X. Correig, Selective detection of ammonia and benzene via zeolite films deposited on SnO_2/Pt-SnO_2 thick film gas sensors, 2005 Spanish Conference on Electron Devices, Proceedings, 597-601 (2005).

[183] I. Elmi, S. Zampolli and G.C. Cardinali, Optimization of a wafer-level process for the fabrication of highly reproducible thin-film MO_X sensors, Sensors and Actuators B: Chemical, 131, 2, 548-555 (2008)

[184] J. Getino, M. C. Horrillo, J. Gutiérrez, L. Arés, J. I. Robla, C. García and I. Sayago, Analysis of VOCs with a tin oxide sensor array, Sensors and Actuators B: Chemical, 43, 1-3, 200-205 (1997)

[185] D. S. Lee, D-S. Lee, J-K. Jung, J.W. Lim, J-S. Huh and D-D. Lee, Recognition of volatile organic compounds using SnO_2 sensor array and pattern recognition analysis, Sensors and Actuators B: Chemical, 77, 1-2, 228-236 (2001)

[186] J. Puigcorbe, D. Vogel, B. Michel, A. Vilà, I. Gràcia, C. Cané and J. R. Morante, High temperature degradation of Pt/Ti electrodes in micro-hotplate gas sensors, Journal of Micromechanics and Microengineering, 13, 4, S119-S124 (2003)

[187] Y-h Shih, M-S. Li, Adsorption of selected volatile organic vapors on multiwall carbon nanotubes, Journal of Hazardous Materials, 154, 21–28 (2008)

[188] J. Li, Y. Lu, Carbon Nanotube Based Chemical Sensors for Space and Terrestrial Applications, Meeting Abstracts, Electrochemical Society , 901, 1514 (2009)

[189] Y.W. Chang, J.S. Oh, S.H. Yoo, H.H. Choi, K.H. Yoo, Electrically refreshable carbon nanotubes based gas sensors, Nanotechnology 18, 435504 (2007)

[190] L. I. B. Silva, F.D. Ferreira, T.A. Rocha-Santos, A.C, Duarte, Carbon nanotube field effect transistor detector associated to gas chromatography for speciation of benzene, toluene, ethylbenzene, (o, m and p) xylene, Journal of Chromatography A, 1216, 6517–6521 (2009)

[191] L. Valentini, C. Cantalini, L. Lozzi, S. Picozzi, I. Armentano, J. M. Kenny and S. Santucci, Effects of oxygen annealing on cross sensitivity of carbon nanotubes thin films for gas sensing applications, Sensors and Actuators B, 100, 33–40, (2004)

[192] C. Odenbrand, S. L. T. Anderson, Hydrogenation of benzene to cyclohexene on an unsupported ruthenium catalyst-an esca study of titanium poisoned catalysts, Journal of chemical technology and biotechnology a-chemical technology, 33, 3, 150-156, (1983)

ISBN:978-84-694-0326-6/DL:T-207-2011

[193] V.N. Romannikov, K. G. Ione, L. A. Pedersen, Transformations of hydrocarbons on zeolites of type Y: III. Hydrogenation of unsaturated hydrocarbons on Pd-, Pt-, and Ru-containing zeolites, Journal of Catalysis 66, 121-129 (1980).

[194] C. Milone, G. Neri, A. Donato, M.G. Musolino, L. Mercadante, Selective Hydrogenation of Benzene to Cyclohexene on Ru/g-Al_2O_3, Journal of catalysis 159, 253-258 (1996).

[195] M. Guo, M. Pan., J.Chen, Y. Mi, X. Zhang, Y. Chen, Palladium modified multi-walled carbon nanotubes for benzene detection at room temperature. Chinese Journal of Analytical Chemistry, 34, 1755-1758 (2006).

[196] S. M. Cho, M. C. Seong, J. K. Young, Y. S. Kim, Y. Yang, S-C. Ha, The Application of Carbon Nanotube – Polymer Composite as Gas Sensing Materials, IEEE Sensors conference, Vienna, AUTRICHE (2004).

[197] J. Wang, L. Liu, S-Y Cong, J-Q, Qi and B-K. Xu, An enrichment method to detect low concentration formaldehyde, Sensors and Actuators B, 134, 1010–1015 (2008).

[198] J. Liu, Z. Guo, F. Meng, Y. Jia, and J. Liu, A Novel Antimony-Carbon Nanotube-Tin Oxide Thin Film: Carbon Nanotubes as Growth Guider and Energy Buffer. Application for Indoor Air Pollutants Gas Sensor, Journal of Physical Chemistry C, 112, 6119-6125 (2008).

UNIVERSITAT ROVIRA I VIRGILI
DESIGN, FABRICATION AND CHARACTERISATION OF GAS SENSORS BASED ON NANOHYBRID MATERIALS
Radouane Leghrib
ISBN:978-84-694-0326-6/DL:T-207-2011

UNIVERSITAT ROVIRA I VIRGILI
DESIGN, FABRICATION AND CHARACTERISATION OF GAS SENSORS BASED ON NANOHYBRID MATERIALS
Radouane Leghrib
ISBN:978-84-694-0326-6/DL:T-207-2011

3. MATERIALS AND METHODS

UNIVERSITAT ROVIRA I VIRGILI
DESIGN, FABRICATION AND CHARACTERISATION OF GAS SENSORS BASED ON NANOHYBRID MATERIALS
Radouane Leghrib
ISBN:978-84-694-0326-6/DL:T-207-2011

ISBN:978-84-694-0326-6/DL:T-207-2011

3.1. Materials preparation and characterization

3.1.1. Nano2hybrids materials: LISE, ULB and SAM

Different samples of metal decorated CNTs were produced by three different partners of the Nano2hybrids European project.

The mean idea of the different groups is the treatment of the carbon nanotube surfaces using physical treatment methods which are reflected in the use of low temperature, low-vacuum and atmospheric reactive pressure plasmas. The carbon nanotubes were functionalized in order to increase their surface reactivity [1-6]. Details about the interest of carbon nanotubes functionalization can be found in the introduction and section 2.1.2

In annex I, we will explain in detail the fabrication of pristine carbon nanotubes and the different steps of their functionalization and decoration procedures used by the three partners. The results related to the characterization of those materials using Transmission Electron Microscopy (TEM) and X-ray Photoelectron Microscopy (XPS), carried out by the three different laboratories, will be commented.

3.1.2. Hybrid metal oxide-CNTs

The challenge to develop gas sensors with superior performance for both domestic and industrial applications opens different investigation ways when searching for desirable properties such as room temperature operation and recovery, high sensitivity or improved selectivity.

In order to further enhance the interesting gas sensing properties offered by carbon nanotubes [7,9], the idea was to combine these and metal oxides [10,11]. The plasma treated carbon nanotubes were subjected to mixing with two types of metal oxide materials. In each case, a preparation procedure is adopted either mixing the powders of both CNTs and metal oxides or decorating CNT wall by metal oxide nanoparticles [12-16].

3.1.2.1. Materials based on commercial metal oxides

Many works concerning the fabrication of gas sensors based on CNTs decorated or mixed with metal oxides have been published [10-16].

Considering the gas sensing properties of metal oxides, an improvement in their sensing properties (e.g., enhancing their sensitivity, decreasing the operating temperature or making them more selective to a given target species) has been achieved by adding

ISBN:978-84-694-0326-6/DL:T-207-2011

small amounts of noble metals to the metal oxide active layer [17]. Thus, it can be suggested that besides the presence of CNTs, the presence of noble metal clusters inside the metal oxide matrices can act improving their sensing properties.

On the basis of these studies, we prepared sensing materials using commercially available SnO_2 and WO_3 nanopowders (Sigma–Aldrich) mixed with Au and Ag decorated carbon nanotubes prepared by LISE group [18]. The Hybrid materials were obtained by adding two different amounts of metal-decorated MWCNT to 70 mg of metal oxide, thus obtaining two different proportions of MWCNT embedded into the metal oxide matrix (1/500 and 1/250 wt%, respectively) [18]. An adequate mixture of the components was obtained by dispersing them in glycerol (employed as organic vehicle), and stirring the resulting solution in an ultrasonic bath at 75 ºC for 2 h. The powder of metal oxide was added to the adequate amount of nanotubes, dispersed in glycerol previously, and was carefully mixed in a mortar in order to get a good homogeneous paste. The amount of nanotubes to be added to the metal oxide matrix was based on a previous study [19].

The pastes obtained were deposited above the sensor membrane by drop coating technique. The as-deposited sensing films were firstly dried at 140 ºC during 2 h in order to burn out the organic vehicle, using a slow temperature ramp of 2.5 ºC/min in order to avoid the occurrence of cracks in the films. We used for this process a lower temperature (140 ºC) than the boiling point of glycerol (i.e., 182 ºC [20]) in order to avoid producing cracks in the films deposited. The drying time was however sufficiently long for the complete evaporation of the organic vehicle. Finally the films were annealed in situ at 450 ºC during 3 h in ambient atmosphere (this also ensures the complete removal of the organic vehicle). During the annealing process, the temperature was raised from ambient to 450 ºC using again a ramp of 2.5 ºC/min. The mean grain size of the metal oxides particles, determined in a previous study, was near 40 nm [11].

The chemical composition of the samples surfaces was investigated by means of XPS analysis. XPS analysis were performed using an ESCA-300 (SCIENTA, Sweden) photoelectron spectrometer equipped with a monochromatized Al Kα = 1486.7 eV. The size of the metal clusters and their dispersion on the CNT walls were studied by means of high-resolution transmission electron microscopy (HRTEM) carried out using a Philips CM30 FEG instrument operated at 300 kV. The morphology of the hybrid films deposited onto the microhotplate substrates was investigated by means of scanning

ISBN:978-84-694-0326-6/DL:T-207-2011

electron microscopy (SEM). SEM measurements were performed using a Joel JSM 6400 equipment, with a resolution of 0.3 nm.

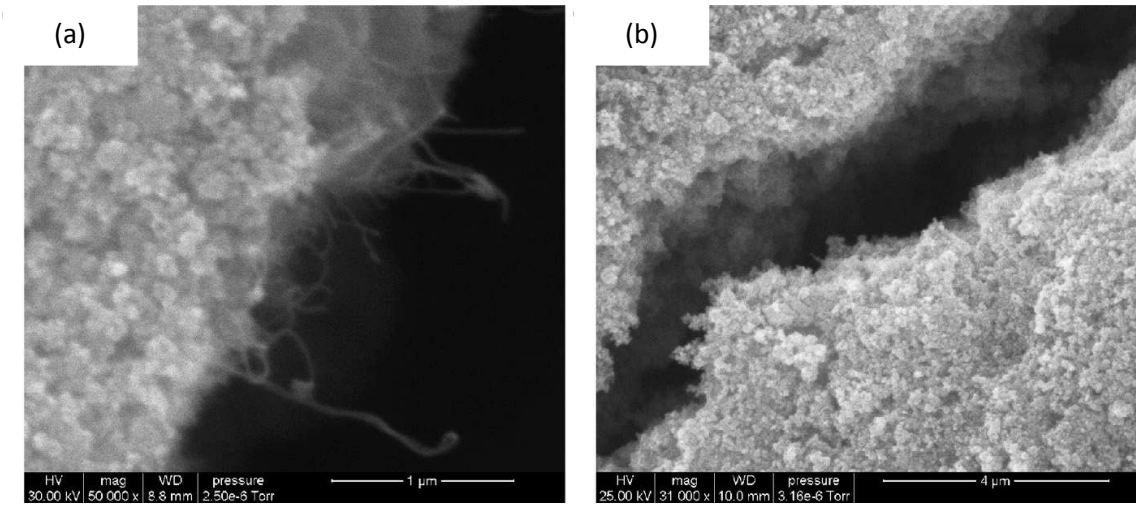

Figure 1: SEM images recorded on different hybrid films: (a) Ag-MWCNT/WO3 (1/500 wt%); (b) Ag-MWCNT/SnO2 (1/250 wt%).

Figure 1 shows SEM images recorded on the different hybrid carbon nanotubes/metal oxide sensing films deposited over the sensors substrates. The micrographs show the presence of WO_3 and SnO_2 metal oxide grains, whereas carbon nanotubes are observed only in WO_3/CNT hybrids. This can be associated to the low proportion of carbon nanotubes embedded in the metal oxide matrix (1/500 or 1/250 wt%) as well as to the difference in density between WO_3 and SnO_2 (7.16 and 6.95 g/cm3, respectively [22]). In order to obtain the desired weight proportions between the metal oxide and CNTs, a higher amount of SnO_2 than WO_3 is present in the hybrid materials.

3.1.2.2. Materials based on home-synthesized metal oxide

Oxygen functionalized carbon nanotubes provided by LISE group were mixed with a home-prepared tin oxide nanopowder [23].

As a precursor for the synthesis of tin oxide nanoclusters, tin (II) acetate solution in water free acetic acid was used. Synthesis of tin (II) acetate was performed from tin powder and glacial acetic acid according to the protocol described in [24]. Oxygen plasma functionalized MWCNTs were added to the precursor solution and dispersed by ultra-sonication at room temperature. Three solutions were prepared with different CNT to tin oxide precursor ratios: 12 mg of plasma treated nanotubes were dispersed in 10, 20 and 40 ml of the tin oxide precursor solution. Tin oxide nanoclusters were obtained by the precipitation from these solutions by “drop by drop” addition of an aqueous ammonia solution. After the precipitation, the samples were centrifuged and washed

ISBN:978-84-694-0326-6/DL:T-207-2011

several times with deionized water. This was made in order to ensure that only tin oxide decorated MWCNTs were retained for further processing. In other words, tin oxide nanoclusters not attached to CNT sidewalls were washed away. Then the powders were dried carefully at 150 ºC and annealed at 300 ºC for 72 h.

Transmission electron microscopy (TEM) was used to establish the morphology and to evaluate nanocluster size distributions (Jeol JEM 1011, operating at 100 kV) (Fig. 2).

The resulting nanomaterials were dispersed in an organic vehicle (dimethylformamide), ultrasonically stirred during 1 h at 45 ◦C and subsequently sprayed onto micromachined sensor substrates.

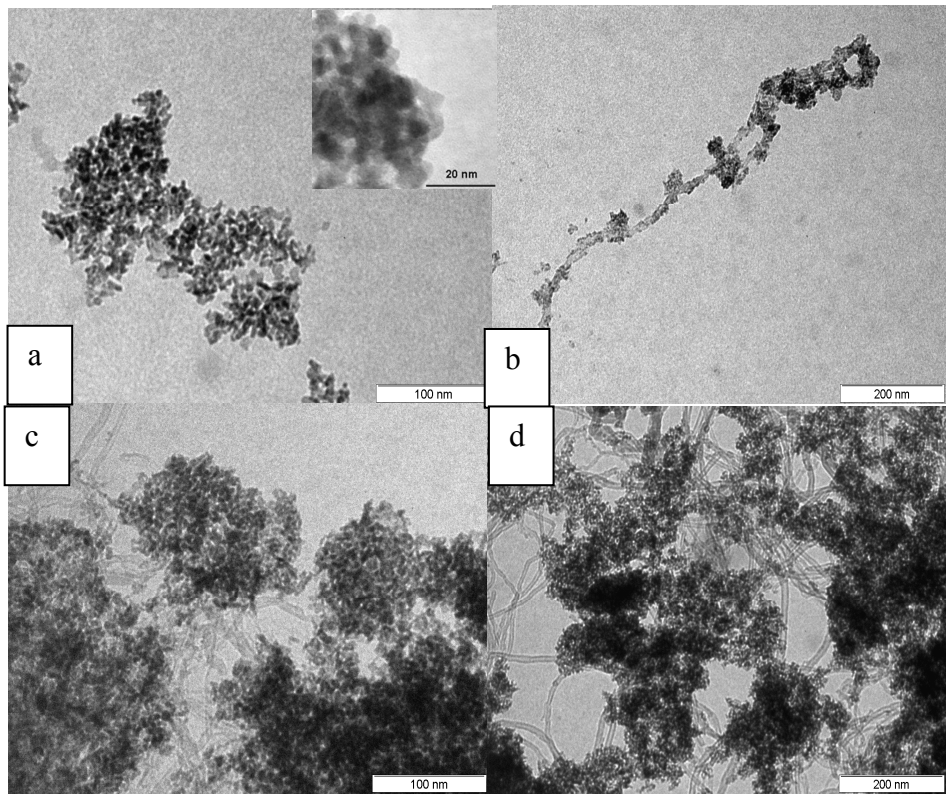

Figure 2: TEM images of tin oxide nanoparticles synthesised without the presence of carbon nanotubes (a), with 12mg of oxygen plasma treated carbon nanotubes dispersed in 10 ml (b), 20 ml (c) and 40 ml (d) of the tin oxide precursor solution.

The active films coated the membrane areas through a shadow mask. During deposition, membranes were kept at 50 ºC, which ensured the evaporation of the solvent. The films were annealed at 300 ºC during 4 h in inert atmosphere. A temperature ramp of 10 ºC/min was used for heating and cooling down the films. After encapsulation and wire bonding, the sensors were ready for characterization.

ISBN:978-84-694-0326-6/DL:T-207-2011

3.1.3. N or B-doped CNTs

The fabrication of these materials was carried out by Dr. Grobert's group from Department of Materials at Oxford University in the UK. Further details about the samples fabrication and characterization can be found in [25-26].

Herein, we will compare N- and B-doped nanotubes made in the same experimental setup at similar experimental parameters for accurate comparison of the samples.

3.2. Sensor fabrication

Once the sensing nano-materials have been fabricated, it is necessary to choose an adequate transducer to carry out the measurement of the gas sensing properties of these active materials.

The most common materials used to fabricate the gas transducers are: Silicon or alumina (Al_2O_3). Silicon is often used in nano- and micro-electronics as a support for depositing active layers [27]. This material offers many advantages [28-29]:

- ✓ It is very stable chemically
- ✓ It is easy for use and manipulation
- ✓ It has excellent mechanical properties (hard and resistant).
- ✓ It has low defects (Less than $10^{11}/cm^2$)
- ✓ It helps to solve the heating and temperature sensing problems
- ✓ It offers the possibility of miniaturization and low power consumption.

In our case, we used a gas sensor membrane based on a silicon micro-hotplate structure fabricated by the "National Center of Microelectronics" (CNM) in Barcelona. This substrate comprises 4 independent microsensors. Each one includes a heating resistor and platinum interdigitated electrodeds. In the Annex I, the main technological steps involved in the transducer fabrication are described.

3.2.1. Thermo-electrical characterization

The encapsulated silicon chip with four sensors was firstly characterized thermoelectrically, which allows knowing the variation of the heater's temperature versus the voltage applied through it. After knowing this variation, the sensors coated with an active layer can be operated at different known temperatures. So this characterization consists of applying, using a DC power supply, different values of voltage to the heater. In this case the voltage was varied in the range of [0-7 V] with a step of 0.5 V. The current values corresponding to each applied voltage through the

ISBN:978-84-694-0326-6/DL:T-207-2011

sensor heater were recorded using an Agilent multimeter (34970A) controlled by a Labview program.

In the range of the sensing temperatures that we need in our case, the resistivity can be considered as a linear function of temperature. In this case, the resistance dependence on temperature will be expressed as follows:

$$R(T) = R(T0) \times [1 + \alpha (T - T0)] \qquad \text{(eq 1)}$$

Where:

α : Temperature coefficient of resistance (1/ºC) that was already measured by the CNM staff.

T : The operating temperature (ºC)

T0 : The room temperature (ºC)

R (T0) : The initial heater resistance at room temperature (Ω)

R (T) : The heater resistance at the operating temperature (Ω)

Following the ohm law we have: $U=R\times I$ (eq 2)

So, from the recorded values of the measured current and voltage we can find the values of the resistance for each value of applied voltage using Ohm law, and finally we get the curve of temperature values versus applied voltage (Fig. 3) replacing equation (eq 1) in (eq 2). In the following table (Table 1), we have the results obtained from the thermoelectrical characterization of the sensors (a fitting was performed using the OriginPro software).

Table 1: Operating temperature versus voltage or current through the sensor heater.

Voltage (V)	Current (mA)	Temperature (ºC)
1.14	1.98	50
2.01	3.40	100
2.70	4.40	150
3.28	5.19	200
3.80	5.83	250
4.27	6.36	300
4.70	6.81	350
5.10	7.20	400
5.48	7.53	450

ISBN:978-84-694-0326-6/DL:T-207-2011

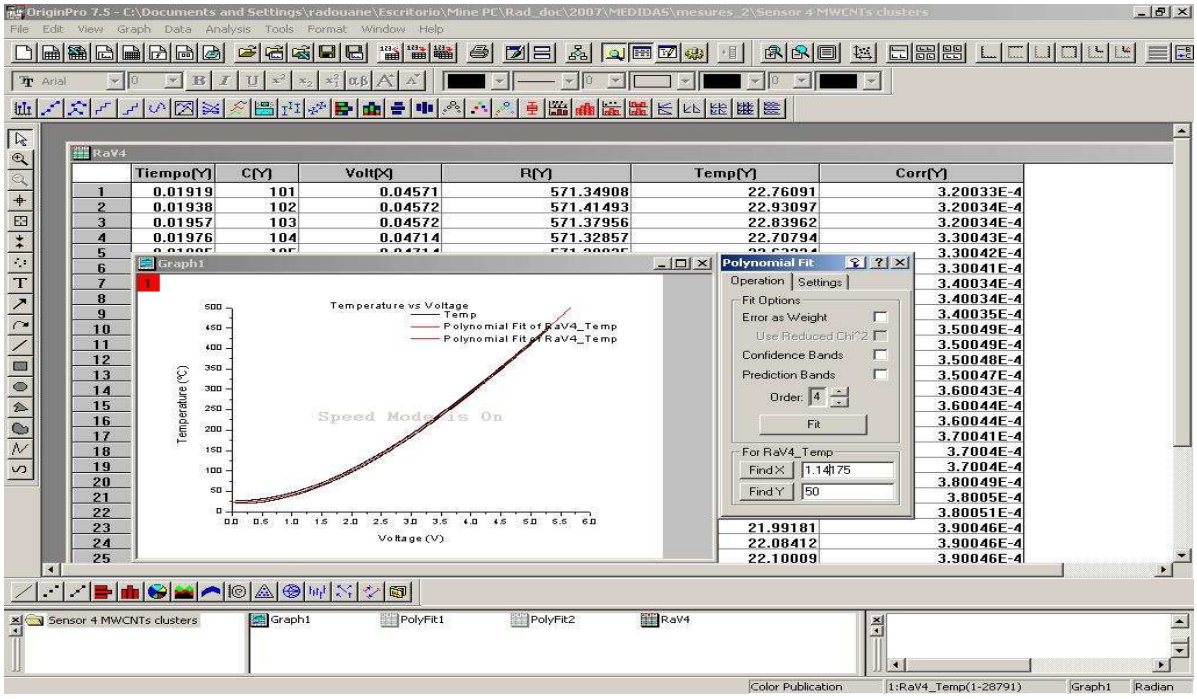

Figure 3: Image of the program originPro showing the fit performed to calculate the sensor operating temperature versus voltage applied to the heater.

3.2.2. Sensing layer deposition and characterization

The different gas sensitive based on nano-materials presented in section 3.1 were deposited onto the silicon transducers. Different organic solvents were used to disperse the nanotubes prior to their deposition using different coating techniques. The aim was to be able to get a homogeneous and a uniform layer of nanotubes well adhered over the area of the sensor electrodes.

For gas sensors, it is preferable to adjust the resistance of the active layer in the order of some kOhms for the sensors to be easily measured employing simple electronic multimeters. For that reason, it is important to be able to adjust the deposited amount of sensing material.

Consequently, it is necessary to look for a convenient deposition method that can satisfy the above mentioned requirements. So, the effect of the following parameters will be studied:

- The dispersing organic solvent
- The deposition technique itself
- The post-deposition thermal treatment

ISBN:978-84-694-0326-6/DL:T-207-2011

3.2.2.1. Suspension preparation

a. ***General procedure*:**

Whatever is the deposition technique, the carbon nanotube samples must be at first well dispersed in an organic solvent.

In order to have a good dispersion of the pristine, functionalized or/and metal decorated nanotubes, a high number of proportions between the volume of the solvent and the weight of the nanotube powder were tested. For all the solvent and materials tested, the optimized ratio was set to 0.1 milligram per milliliter of solvent.

In the second step, the vials (the containers of the suspension) were put inside an ultra-sonic bath and stirred (ULTRASONS MEDI-II (J.P. Selecta, S.A)) at 40 KHz and at a defined temperature during several minutes in order to achieve a good dispersion and homogeneity of the nanotubes in the organic solvent. The optimized parameters will be shown later.

b. ***Importance of the dispersing organic solvent***

Prior to deposition, it is important to select a suitable organic solvent for the dispersion of the carbon nanotube samples. Indeed, the solvent must be able to separate to the maximum the agglomerated carbon nanotubes of the as received powder into isolated ones, if not the deposited layer will not be very homogeneous. Layer homogeneity is in fact important for gas sensing applications; because it influences gas sensing properties (e.g. adsorption and diffusion phenomena are affected). Furthermore good homogeneity of the active layers is necessary for reaching good sensor reproducibility [30]. However, some criteria must be well considered:

- ✓ The first thing to check is the influence of the solvent on the structure of the carbon nanotube. Indeed, the solvent must not show any dissolving effect on the carbon nanotube structure. Also, the solvent must not affect the surface composition of the sample once it is evaporated.
- ✓ The polarity of the solvent must be adapted to the nature of the material to be dispersed. In our case, the deposition tests will be performed on samples of pristine carbon nanotubes and other pre-treated with oxygen plasma. In this case, polar solvents are preferred to well disperse the nanotube samples.
- ✓ It is important also that the solvent can be easily eliminated after deposition. For that reason, the solvent boiling point must be as low as possible.

ISBN:978-84-694-0326-6/DL:T-207-2011

- ✓ The viscosity of the solvent must be adapted to the deposition technique to be used.

In the next section, we will explain each deposition technique implemented, the organic solvents selected and the optimized experimental working parameters to be used in each case.

3.2.2.2. Deposition techniques

a. ***Drop coating***

The first attempt of deposition of the nanotube samples was performed using the drop coating technique. This technique relies on the deposition of drops of the sample suspension over the electrodes area of the sensor substrates.

When using the drop coating method, the first organic vehicle that was tried was glycerol, this solvent is quite viscous which permits to control the position of the suspension drop above the surface of the sensor allowing by this way to delimit the area of the deposited material. The obtained suspension was ultra-sonicated at 75 ºC during 30 min to obtain a homogeneous paste. The resulting paste was poured in a syringe and then dropped onto the substrate using a micro-injector (JBE1113 Dispenser, I&J FISNAR Inc., USA) [31]. The micro-injector dispenses fairly reproducible amounts of the material. After deposition, the film is dried and, then annealed at a higher temperature (250ºC-450ºC). The annealing temperature is chosen according to the organic vehicle employed and should be higher than the maximum sensing temperature to be used during the gas sensing tests. This annealing temperature is chosen higher than the operating temperature to ensure that the film mechanical properties remain unaltered during normal operation and thus, long-term sensor drift is minimised. Figure 4 shows the experimental set up.

Before thermally treating the deposited layers, the effect of the ultra-sonication on the nanotube samples was investigated. Following TEM analysis (Fig. 5), it was found that the ultra-sonication at 75 ºC causes the detachment of metal nanoclusters from the nanotube's wall. By performing the ultra-sonication at room temperature, a good dispersion of the nanotubes is obtained and the detachment effect is avoided.

After performing the thermal treatment on the samples ultra-sonicated at room temperature, some problems still appeared which consisted of:

- The thermal treatment at temperatures higher than 400 ºC of the as deposited

ISBN:978-84-694-0326-6/DL:T-207-2011

material affects the stability of the metal nanoclusters in the case of metal decorated nanotube samples (Fig. 6) [31].

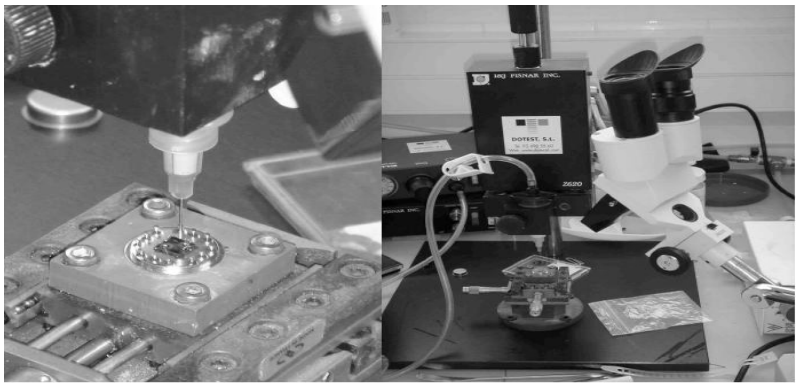

Figure 4: Micro injector employed for depositing nano2hybrids materials. The picture shows the setup when micro-machined silicon substrates are used.

To solve the problem due to the thermal treatment effect, solvents of lower boiling points had to be tested. However, the existing solvents that respond to these conditions are of low viscosity (e.g. water like). In this case, some difficulties to control the deposition area arise. However, three options are proposed:

- To change the solvent
- To change the deposition method
- To change the thermal treatment, by lowering the annealing temperature.

As first option, we preferred to change the organic solvent.

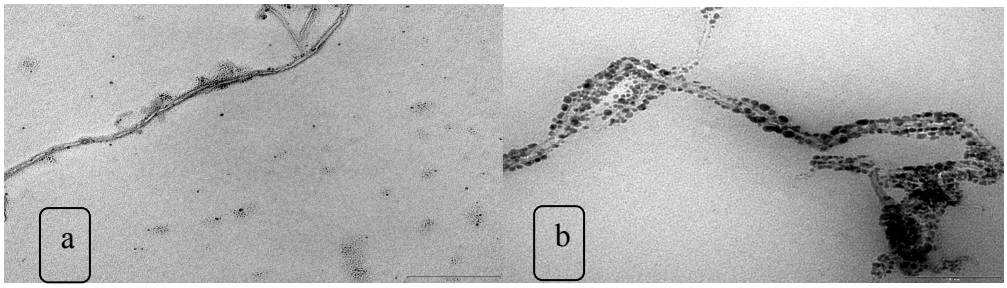

Figure 5: ultra-sonication of Au-MWCNTs/Acetone during 30 min: a) with heating at 75ºC and, b) without heating.

ISBN:978-84-694-0326-6/DL:T-207-2011

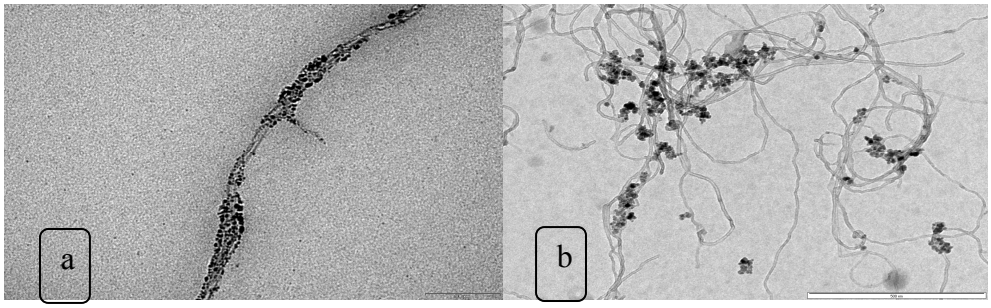

Figure 6: Au decorated MWCNTs: a) before thermal treatment, b) after thermal treatment at 450 ºC during 2 h.

b. *Organic solvent selection*

A variety of organic solvents of different polarities, viscosities and boiling points were tested. Table 2 summarizes the characteristics of each solvent.

Some of the low viscosity solvents such as ethanol and dichloromethane were mixed with the most viscous solvents like terpineol and glycerol in order to get a final solvent with higher viscosity and lower boiling point (Table 3).

The results obtained with each solvent are summarized in table 3. The dispersion and deposition quality of the nanotubes obtained with each solvent are shown. The thermal treatment conditions and any solvent residues remaining after the solvent thermal treatment are also studied.

Regarding these results (Fig. 7), glycerol and terpineol were avoided because of their high boiling point. Pentane did not allow for well dispersing the nanotubes.

When using ethanol, a good dispersion could be obtained only for a very small concentration of the nanotubes in the suspension. This will not be practical for the deposition of a uniform layer of nanotubes, especially when drop coating is used.

Dichloromethane was also discarded because it was found to destroy the nanotube structure according to [32].

Table 2: Datasheet of all the organic vehicles used in deposition of the nanotubes

Properties	Dichloro-methane	Dimethyle-formamide	Water	Glycerol	Terpineol	Acetone	Ethanol	Pentane
Molecular formula	CH_2Cl_2	C_3H_7NO	H_2O	$C_3H_5(OH)_3$	$C_{10}H_{18}O$	CH_3COCH_3	CH_3CH_2OH	C_5H_{12}
Molar mass	84.93 g/mol	73.09 g/mol	18.0153 g/mol	92.09382 g/mol	154.25 g/mol	58.08 g/mol	46.06844(232) g/mol	72.15 g/mol
Density	1.3255 g/cm³ liquid	0.944 g/cm³ liquid	0.998 g/cm³ (liquid at 20 °C, 1 atm) 0.917 g/cm³ (solid at 0 °C, 1 atm)	1.261 g/cm³	0.9338 g/cm³	0.79 g/cm³, liquid	0.789 g/cm³, liquid	0.626 g/cm³, liquid
Melting point	-96.7 °C (175.7 K)	-61 °C (212 K)	0 °C (273.15 K) (32 °F)	18 °C (64.4°F)	39 °C	–94.9 °C (178.2 K)	–114.3 °C (158.8 K)	–129.8 °C (143 K)
Boiling point	39 °C (312.8 K)	153 °C (426 K)	99.974 °C (373.124 K) (211.95 °F)	290 °C (554°F)	81-82 °C at 4.5 mmHg	56.53 °C (329.4 K)	78.4 °C (351.6 K)	(308 K)

ISBN:978-84-694-0326-6/DL:T-207-2011

Table 3: Results of the drop-coating and air brushing techniques employing different organic vehicles.

Organic vehicle	*Dispersion*	*Drop features*	*Thermal treat.*	*Traces*	*Adhesion*
Terpineol (T)	Fair	Wide drop	240ºC/ 3 h	Minimal	Poor
Glycerol (G)	Fair	Narrow	240ºC/ 3 h	Evident	Excellent
Ethanol (E)	Fair	Wide	80ºC/ 3 h	No	Fair
Dichloromethane (D)	Bad	Wide	Room	No	Poor
Pentane (P)	Bad	Wide	Room	No	Poor
Acetone (A)	good	Wide	Room	No	Good
T (50%) + E	Fair	Wide	200ºC/ 3h	Minimal	Poor
T (25%) + E	Fair	Wide	200ºC/ 3h	Minimal	Fair
T (50%) + D	Fair	Wide	200ºC/ 3h	Minimal	Poor
T(25%) + D	Fair	Wide	200ºC/ 3h	Minimal	Poor
G(50%) + E	Fair	Narrow	200ºC/ 3h	Evident	Good
G25%) + E	Fair	Wide	200ºC/ 3h	Evident	Fair
G(50%) + D	Fair	Narrow	200ºC/ 3h	Evident	Good
G25%) + D	Fair	Wide	200ºC/ 3h	Evident	Fair
Dimethylformamide	Good	Wide	150ºC/ 3h	Minimal	Good

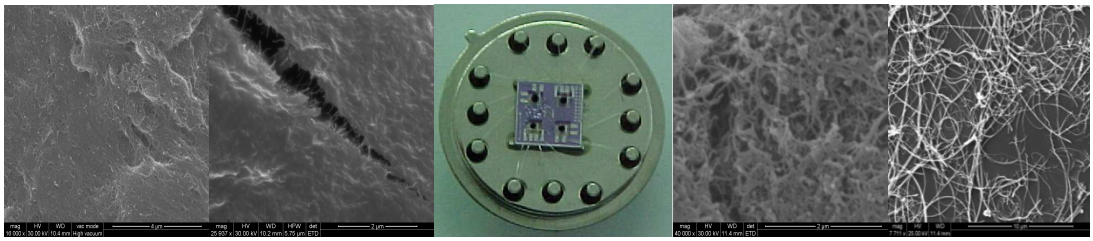

Ethanol+Glycerol ***Terpineol*** ***Glycerol*** ***DMF***

Glycerol ***Dichloromethane*** ***Water***

Figure 7: Examples ESEM images and suspensions of dispersing MWCNTs in organic solvent

Finally, the best results in terms of dispersion quality and adhesion were obtained using Acetone and N,N-dimethylformamide (DMF) [33-36]. However, some difficulties to

ISBN:978-84-694-0326-6/DL:T-207-2011

control the deposition area arise due to the low viscosity of those solvents.

The second option was then to change the deposition method.

❖ **Effect of organic solvent on CNTs**

After the selection of the suitable organic solvents for the nanotube sample dispersion, further tests were performed to check any possible chemical effect of those solvents on the carbon nanotube samples, but also to determine the optimal thermal treatment profile that could be used to completely eliminate the solvent or any of its residues from the samples. These tests were made using Thermo-gravimetric analysis (TGA) coupled to differential thermal analysis (DTA).

- **TGA measurements**

This technique is performed on our samples to determine the changes in their weight in relation to the change in their heating temperature [37]. It allows for determining the degradation temperature of the samples and the decomposition point of any solvent residues (In our case, DMF and acetone) present in it.

These TGA measurements were coupled with DTA to enable detecting any phase transition of the material that can occur during its heating.

- **DTA measurements**

In DTA, in general, the material under study and an inert reference are made to undergo identical thermal cycles, while recording any temperature difference between sample and reference [38]. This differential temperature is then plotted against time, or against temperature (DTA curve or thermo-gram). Changes in the sample, either exothermic or endothermic, can be detected relative to the inert reference. Thus, a DTA curve provides data on the transformations that have occurred, such as crystallization, melting and sublimation, etc. The area under a DTA peak is the enthalpy change and is not affected by the heat capacity of the sample.

A DTA instrument consists of a sample holder comprising thermocouples, sample containers and a ceramic or metallic block; a furnace; a temperature programmer; and a recording system [38]. The key feature is the existence of two thermocouples connected to a voltmeter. One thermocouple is placed in an inert material, in our case Al_2O_3, while the other is placed in a sample of the material under study. As the temperature is increased, there will be a brief deflection of the voltmeter if the sample is undergoing a phase transition. This occurs because the input of heat will raise the temperature of the inert substance, but be incorporated as latent heat in the material changing phase (In our case, treated and untreated carbon nanotubes samples)

ISBN:978-84-694-0326-6/DL:T-207-2011

- **Results of DTA-TGA measurements**

To check the effect of the DMF and acetone, samples of pristine carbon nanotubes were Dispersed in acetone and DMF at the same CNT weight to solvent ratio and then dried at ambient temperature. Both samples were subjected to TGA analysis and compared to the results obtained with pristine carbon nanotubes (With no previous contact with the solvents) as reference samples.

The measurements were performed using a TA Instruments equipment, model SDT 2960, which allows simultaneous DTA and TGA analysis.

Platinum pots were used as containers, and alumina was chosen as reference material for DTA analysis. In order to simulate the real conditions of the thermal treatment normally undergone by samples, analyses were performed in an air flow of 90 cm^3/min.

For studying any possible phase transition, a ramp of 10ºC/min until 600ºC was used in the case of reference pristine carbon nanotubes, while the same ramp until 750ºC in the case of solvent treated samples. For all samples, the cooling was performed at a rate of 10ºC/min until room temperature.

Regarding the results of DTA-TGA measurements of the three different samples, the difference in baseline (Fig. 8) is due only to the difference in the initial weight of each sample.

On the one hand, we can observe that the sample of lower transition temperature corresponds to the DMF treated samples. Following TGA, a decrease of this sample weight is observed starting at 450ºC (Fig. 8). This is accompanied with an increase in the temperature difference between the reference and the sample as observed in the DTA curve of this sample (Fig. 9).

On the other hand, the sample of untreated carbon nanotubes presents the intermediate transition temperature at about 490-500ºC (Fig. 8 and 9). Finally, the highest transition temperature was observed in the case of acetone-treated sample at about 510ºC (Fig. 8 and 9). For all samples, once the corresponding transition temperature is reached, the weight of the sample starts to drop drastically until 25 % approximately for the non treated samples, and from 2 to 5 % from the treated ones (With DMF and acetone).

From the results obtained from TGA and DTA analysis, in the case of untreated samples, the weight loss is due only to the carbon nanotubes burning. While when using DMF, the burning of nanotubes is a little bit delayed, in the case of acetone treated samples, the transition is more delayed. This can be explained by the existence of impurities coming from the residues that remain after the evaporation of organic

ISBN:978-84-694-0326-6/DL:T-207-2011

solvent. So, the residues burned first and then the nanotubes. The oxidation temperature of the nanotubes delay depends on the amount of residues remained in the nanotubes surface.

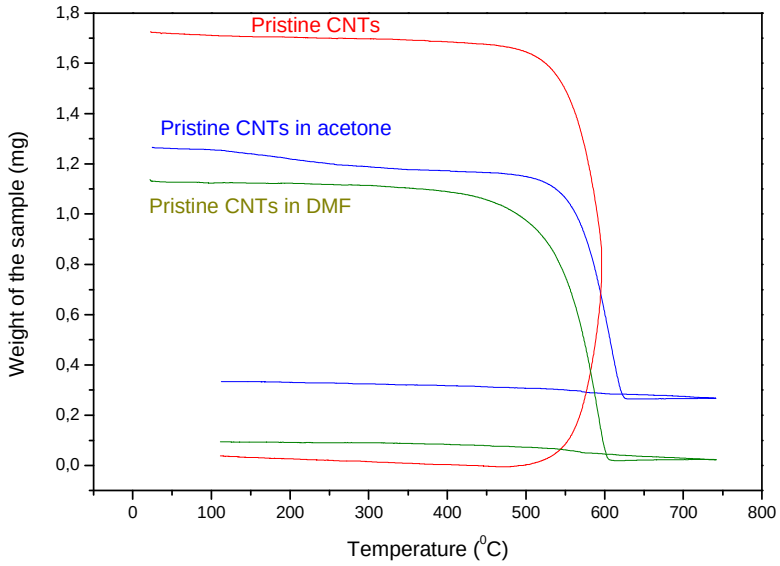

Figure 8: TGA curves of different samples of carbon nanotubes

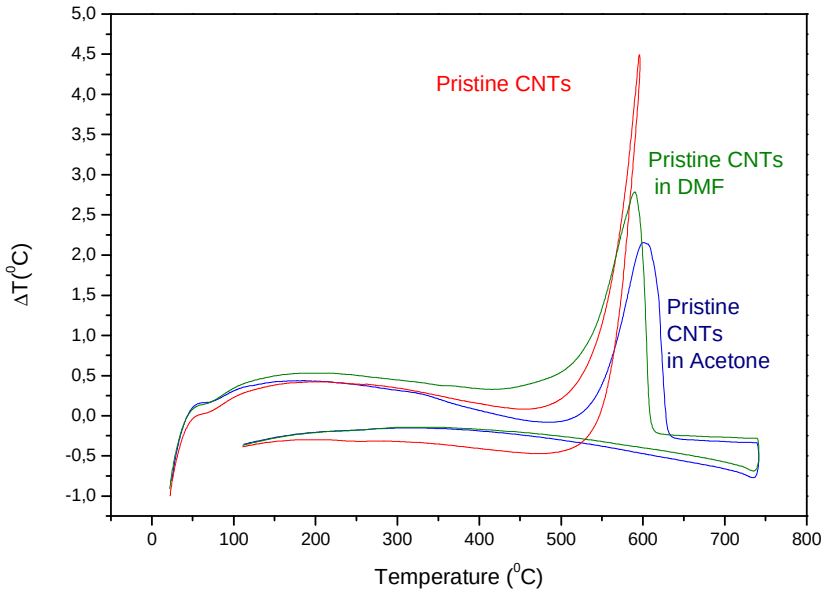

Figure 9: DTA curves of different samples of carbon nanotubes

So, to be sure that we eliminate completely these organic vehicles, the thermal treatment is performed, in both cases, at 250 ºC during 4 h.

❖ **Selection and effect of the thermal treatment**

The thermal treatment is important, first because it enables eliminating completely the solvent from the deposited layer and also to improve the adhesion to the silicon substrate.

ISBN:978-84-694-0326-6/DL:T-207-2011

However, it can sometimes be aggressive towards the active layer by affecting either the material itself or the functional groups attached to its surface. So, the thermal treatment must be carefully adapted to the sensing material characteristics.

Following previous DTA-TGA results, the thermal treatment will be performed at a rate of 4.2 ºC/min until 250 ºC, this temperature will be maintained constant for 2 hours followed by a cooling rate of 4.2 ºC/min until room temperature is reached. In this way, we ensure the complete elimination of the solvents and their residues.

c. ***Inverse drop coating***

The aim of using the inverse drop coating method was to minimize the risk of contamination and also to prevent the partial removal of the metal nanoclusters during the deposition process said above. This modified drop coating method was implemented and tested. It consists of employing the drop coating technique to deposit untreated carbon nanotubes dispersed in acetone on the silicon substrate before packaging in TO-8. Once deposited, the nanotubes undergo the functionalization in oxygen plasma followed by metal decoration [39]. In such a way, no extra steps would be required after metal decoration to obtain the sensors and this would also prevent contaminating the nano2hybrids materials or partially removing the metal nanoclusters from the surface of the nanotubes.

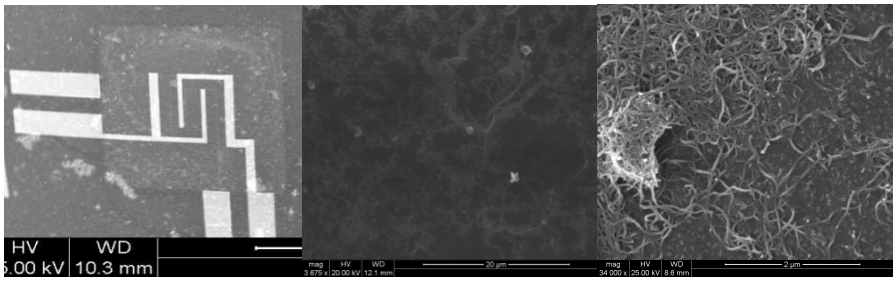

Figure 10: ESEM images of Au-decorated MWCNTs/Acetone deposited by inverse drop coating

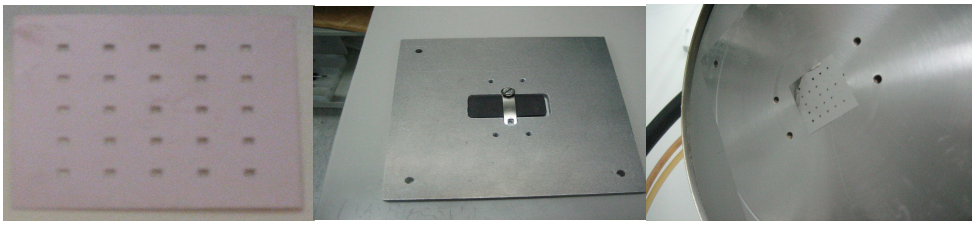

Figure 11: From left to right, shadow mask, back side of the holder showing the magnet used to set in place the shadow mask and front view of the holder with the shadow mask.

ISBN:978-84-694-0326-6/DL:T-207-2011

A holder and a shadow mask have been designed and fabricated to be used during direct thermal evaporation on the plasma treated carbon nanotubes deposited on the sensors. The use of this mask is judged necessary to avoid the short-circuit of comb electrodes during the metallization step. Figure 11 shows the shadow mask and the holder designed.

The problem when using the inverse drop coating method (as for the direct drop coating method) is the difficulty to delimit the deposition area especially when solvents such as acetone of a viscosity similar to the one of water are used (Fig. 10)**.** So**,** we were obliged to seek another deposition method.

d. ***Air-brushing***

To avoid the problems described above, we searched for another alternative method to deposit the materials onto the silicon membrane. Airbrushing seems to be an ideal one.

The first step consists of dispersing the metal decorated carbon nanotubes in DMF (0,1 mg of M-CNTs/1 ml of DMF) which was adequate to reach a good dispersion. Then, the suspension is put in an ultra sonication bath during 30 min at 30 ºC. The said conditions are the optimal ones after a high number of tests checking the dispersion of Metal-CNTs in DMF were carried out [34-37]. Following that, the suspension is introduced inside a container connected to a spraying nozzle (located at a distance of 5-10 cm from the substrate) (Fig. 12), and using a gas flow (nitrogen is preferred to overcome the contamination of the samples (oxidation), 8 L/ min), we get a spray of the suspension over the substrate. The substrate is kept heated at 180ºC to completely evaporate the solvent from the treated sample surface (Fig. 13) [40-41].

The airbrushing steps are explained as follows:

- We put the integrated micro-hotplates with arrays of 100 micro-sensors onto the hotplate which should reach a higher temperature than the boiling point of the organic solvent. Indeed, the heating helps to evaporate the solvent simultaneously with the deposition. In this way, the adhesion of the layer to the substrate is promoted.
- We put a mask on the top of the membranes, which we need to align previously with the substrates. This serves to delimit the deposited layer over the electrode area of the chips.
- To have a homogeneous solvent evaporation temperature during the deposition process, we keep the system (sensors membrane and mask) under heating

ISBN:978-84-694-0326-6/DL:T-207-2011

several minutes to reach the desired temperature. Temperature is controlled by a controller connected to the hotplate.

- When all the conditions are adequate, we start spraying the solution.

To get a good adhesion of the material to the electrodes or to the membrane, an annealing process at 250 ºC during 4h is performed [34]. This thermal treatment consists in the heating profile explained before.

Once the deposition process is finished, the sensors are sent to the "National Center of Microelectronics" (CNM) in Barcelona to be mounted on a TO-8 package.

Finally, the packaged sensors are ready to be used for the detection of our target gases.

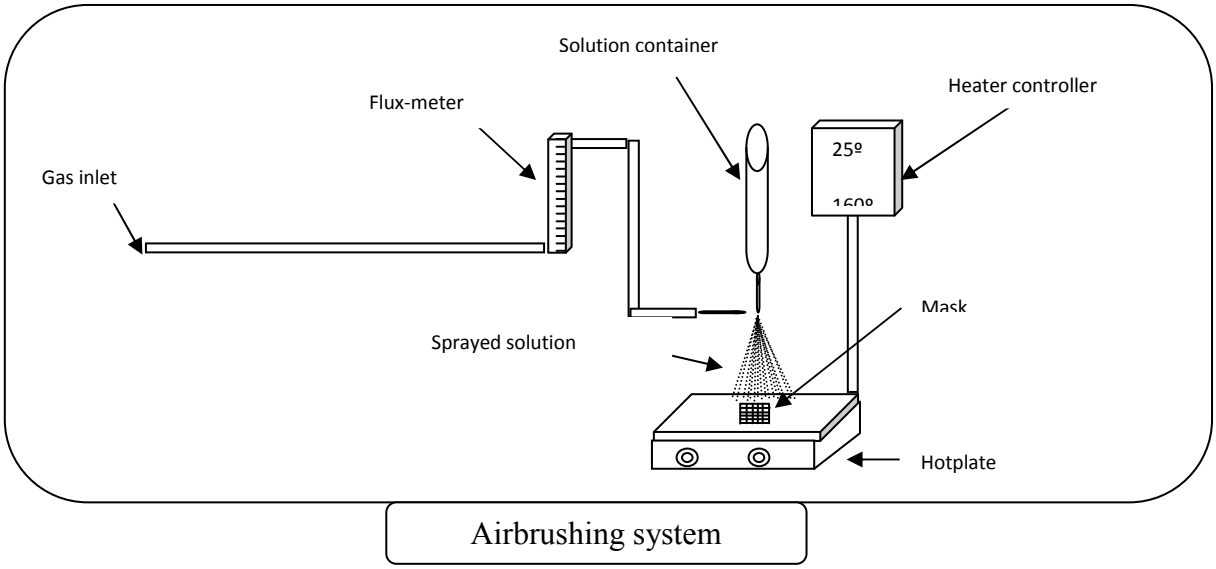

(a)

(b)

Figure 12: Air-brushing (a) system Scheme (b) system picture

ISBN:978-84-694-0326-6/DL:T-207-2011

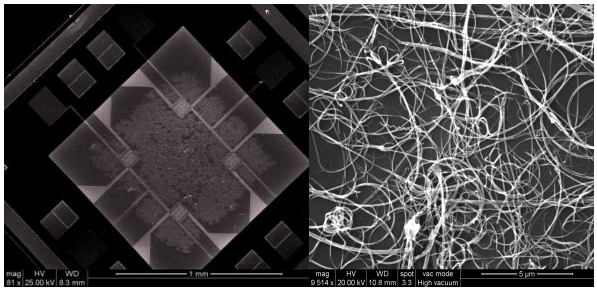

Figure 13: ESEM images of MWCNTs/Acetone deposited by airbrushing

❖ ***Summary*:**

- From the different studies conducted, we can conclude that:
  - The selection of the organic solvent was found to depend on the deposition method to be used.
  - After the deposition, the thermal treatment can vary from a solvent to another but must be selected so as not to affect the properties of the active material.
  - By comparing the advantages and drawbacks of each technique (in terms of compatible solvents, homogeneity of the resulting films, etc.) (Table 4), it is evident that the air-brushing method remains the best one for gas sensor fabrication using the nanohybird materials. Indeed, this technique matches between good uniformity of the deposited layer, good definition of deposited area, absence of impurities after the deposition, and the possibility to adjust the resistance of the active layer.
  - The optimal solvent for this technique was selected and the suitable thermal treatment to completely eliminate the solvent is determined. This method will be then adopted for the deposition of metal decorated MWCNTs.

N.B: Inverse method with air brushing

By analogy to inverse drop coating, the inverse method can be implemented also using airbrushing. In fact, it is possible to deposit the untreated carbon nanotubes dispersed in acetone on the sensor electrodes. The same thermal treatment is performed as before. The obtained sensors are then sent to LISE lab to be functionalized and metal-decorated. Finally, as before, the packaging is carried out in the CNM.

- Table 5 summarizes the deposition method used for the deposition of each hybrid sample prepared by the three different partners of the nano2hybrids project.

ISBN:978-84-694-0326-6/DL:T-207-2011

Table 4: comparison of the characteristics of the different deposition methods

Deposition method	**solvent**	**Homogeneity and continuity**	**traces**	**Delimitation of deposition area**	**Effect on Nanoparticles stability**	**Active layer Resistance**
Drop coating	Viscous (exp: Glycerol)	Depending on the solvent	evident	Good	Evident	fair
	Non-viscous (exp: Acetone)	Depending on the solvent	minimal	poor	minimal	poor
Inverse drop coating	DMF or Acetone	Good	no	Good	no	Too high
Air brushing	DMF or Acetone	Good	no	Good	minimal	Good
Inverse air brushing	DMF or Acetone	Good	no	Good	no	Good

ISBN:978-84-694-0326-6/DL:T-207-2011

Table 5: Summary of the deposition techniques used for each hybrid sample

Groups/ Material (X-CNTs)	LISE	CHANI	SAM
O_2	Inverse drop coating/Airbrushing	-	-
Au	Direct drop coating / Inverse drop coating	Airbushing	-
Ag	Direct drop coating	-	-
Pd	Inverse drop coating	-	Airbrushing
Pt	-	Airbushing	Airbushing
Ni	Ni (10 Aº) Direct drop coating/Inverse drop coating Ni (1Aº),Ni (5Aº) Airbushing	Airbushing	Airbushing
Ti	Inverse drop coating	-	-
Fe	-	Airbushing	Airbushing
Rh	Air brushing	Airbushing	-

3.3. Set-up of the methodology for gas sensor characterization

After the fabrication of gas sensors, next step is the characterization of their performance towards the detection of different hazardous species. Different species like nitrogen dioxide, carbon monoxide, ammonia, ethylene and benzene vapours were tested at different concentrations. The effect of moisture was also considered at 50 and 80 %RH. The sensors were operated at different temperatures. We will focus mainly on the evaluation of the following gas sensing properties:

ISBN:978-84-694-0326-6/DL:T-207-2011

- **Sensor response**: It is the main criterion used to evaluate the capability of a gas sensor to detect a given analyte (i.e, the exposure to the gas affects the physical of chemical properties of the sensor or not). In general, sensor response is measured as the relative conductivity or resistance change of the sensing material upon exposure to a given gas. It is calculated by the following formula:

$$S(\%) = \frac{R_g - R_a}{R_a} * 100$$

Where:

R_g: The resistance of the sensor in presence of the contaminant.

R_a: The resistance of the sensor in the presence of the carrier gas only (Ex. air, CO_2 N_2, etc), which is called also sensor baseline.

- **Response and recovery time:** The response time is calculated as the time the sensor takes to reach 90 % of the steady state resistance in the presence of a given contaminant.

  Recovery time is calculated as the time the sensor needs to completely desorb the contaminant and reach the baseline in the presence of the carrier gas.
- **Stability:** The ability of the sensor to reach the same baseline upon successive cycles of exposure to a given contaminant.
- **Reproducibility:** The ability of the sensor to give the same response upon exposure to the same contaminant concentration.
- **Detection limit:** Is the minimal concentration of the contaminant that the sensor can detect.
- **Linearity:** Evaluation of the range of concentrations in which the sensitivity of the response is linear.
- **Selectivity:** The abilitiy of the sensor to discriminate between the contaminant and other interfering species.

To determine the properties of the different sensors fabricated, a measurement system was implemented. The system comprises a gas testing chamber that hosts the sensors to be tested. An injection system composed by the contaminant gas supply, a carrier gas connected to the chamber by means of some Teflon tubes and, finally a data acquisition and measurement system which allows monitoring the electrical resistance of the sensor when subjected to gas cycling. The purity of the gases used was aas follows: C6H6

ISBN:978-84-694-0326-6/DL:T-207-2011

(99.95 %); NO2 (99.80%); CO (99.95 %); C2H4 (99.99%); H2S (99.95%); and Dry air (99.998%).

- **Data acquisition**.

During the measurement process, a digital Agilent 34970A multimeter was used for continuously monitoring the electrical resistance of the sensors. This multimeter has 20 channels which can be configured to measure resistance in the range of [0-120 M-ohms]. The data acquired was then stored in a PC for further analysis.

Two different measurement systems were implemented. In both cases, dry air was used as carrier gas for the analytes to be detected. The main difference between both systems being the analyte supply.

3.3.1. Manual measurement circuit

To perform the first measurements, the sensor was introduced in 5.3 dm^3 chamber (Fig. 14) and the desired concentrations of each contaminant under study were introduced by the direct injection method using a gas-tight chromatographic syringe. In this case a gas cylinder was filled with the content of gas coming from a calibrated bottle of the contaminant diluted in air (Fig. 15). The gas sample was then extracted by the syringe and then injected to the gas sensor chamber equipped with a fan that allows homogenizing the gas concentration. The volume of gas extracted by the syringe was adjusted depending on the required concentration of the contaminant. Dry air was used as carrier gas and was connected to the chamber to allow the purge of the sensors after the contaminant injection stage. Its flow was fixed at 100 ml/min using a flow-meter.

The sensor's chamber allowed to host five chips of sensors (Each chip contains 4 sensors) connected to the data acquisition system through a PCB card (Fig. 14).

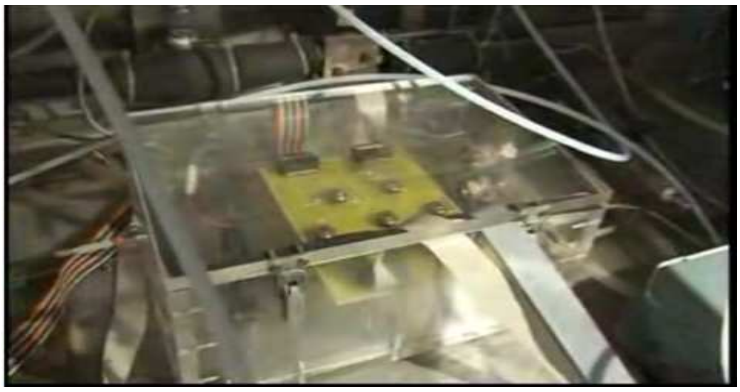

Figure 14: First gas sensor testing chamber

ISBN:978-84-694-0326-6/DL:T-207-2011

The characterization of the sensors was performed in two main steps:

- System conditioning: For the first use of the sensors, a total purge of the system is performed using dry air at 100 ml/min to remove any possible contaminants which can be adsorbed at the sensor surface. The sensors are heated in parallel and then let at ambient temperature.
- Analyte injection: Data acquisition started 10 min before injecting into the measurement chamber the required volume corresponding to the lowest concentration of the contaminant measured.

  After reaching a steady state, a new amount of the same contaminant was injected, so that the second concentration to be tested was reached. Successive injections were repeated until all desired concentrations of the gas were measured. In this case, three different sensing temperatures were tested: Ambient temperature, 150 and 250 ºC.
- Analyte desorption: After each series of successive injections, the sensor chamber was flushed using 100 ml/min of pure dry air at 250 ºC for 3 h, which ensured the cleaning of both the chamber and the sensor surface. Finally, the heating was stopped and the sensors were left to recover their baseline resistance at ambient temperature before performing a new set of measurements.

To assess the reproducibility of the results, for each experiment, the measurements were replicated 4 times.

This system suffers of some problems:

- ✓ The concentration of the sample cannot be determined in an accurate way.
- ✓ The volume of the sensor chamber is quite high, which can make longer the time needed for the analyte to reach the sensor surface. The homogeneity of the sample distribution inside the chamber is also affected.
- ✓ The injection of the sample being indirect and manual, it makes impractical the realization of many repeated experiments.

3.3.2. Automatic measurement circuit

So, to solve the above-mentioned problems, we designed another system in which some improvements were made (Fig. 16):

- The manual injection system using the syringe was replaced by a Bronkhorst mass flow controller system connected to calibrated bottles of the analytes

ISBN:978-84-694-0326-6/DL:T-207-2011

diluted in dry air. This system allows to inject and control automatically the sample concentration employing a software (LabVIEW).

- The sensor chamber was replaced by a smaller one, with much smaller dead volume for an efficient contact of the analyte with the sensors. This new one can host four sensor chips.

Using this system, two characterization procedures were used:

a. <u>Procedure 1</u>

- Analyte injection: The sensor was placed inside a (2×10^{-5} m^3) volume Teflon/Stainless steel test chamber (Fig. 17) and the baseline of the sensor was stabilized under 100 ml/min of dry air. Data acquisition started 10 min before injecting into the measurement chamber the lowest concentration of the contaminant measured.

  After reaching a steady state, a new amount of the same contaminant was injected, so that the second concentration to be tested was reached. Successive injections were repeated until all desired concentrations of the gas were measured. In this case, two different sensing temperatures were tested: Ambient temperature and 150 ºC.
- Analyte desorption: After the injection of the last concentration, the sensor is subjected to heating at 150 ºC under dry air at 100 ml/min during 3 hours and then let at ambient temperature until the sensor recovered its baseline.

Once the sensor baseline is recovered, another injection cycle was initiated.

For each experiment, the measurements were replicated 4 times to assess the reproducibility of the results.

To study the ability of the sensor to recover the baseline after each injection, another characterization procedure was used.

ISBN:978-84-694-0326-6/DL:T-207-2011

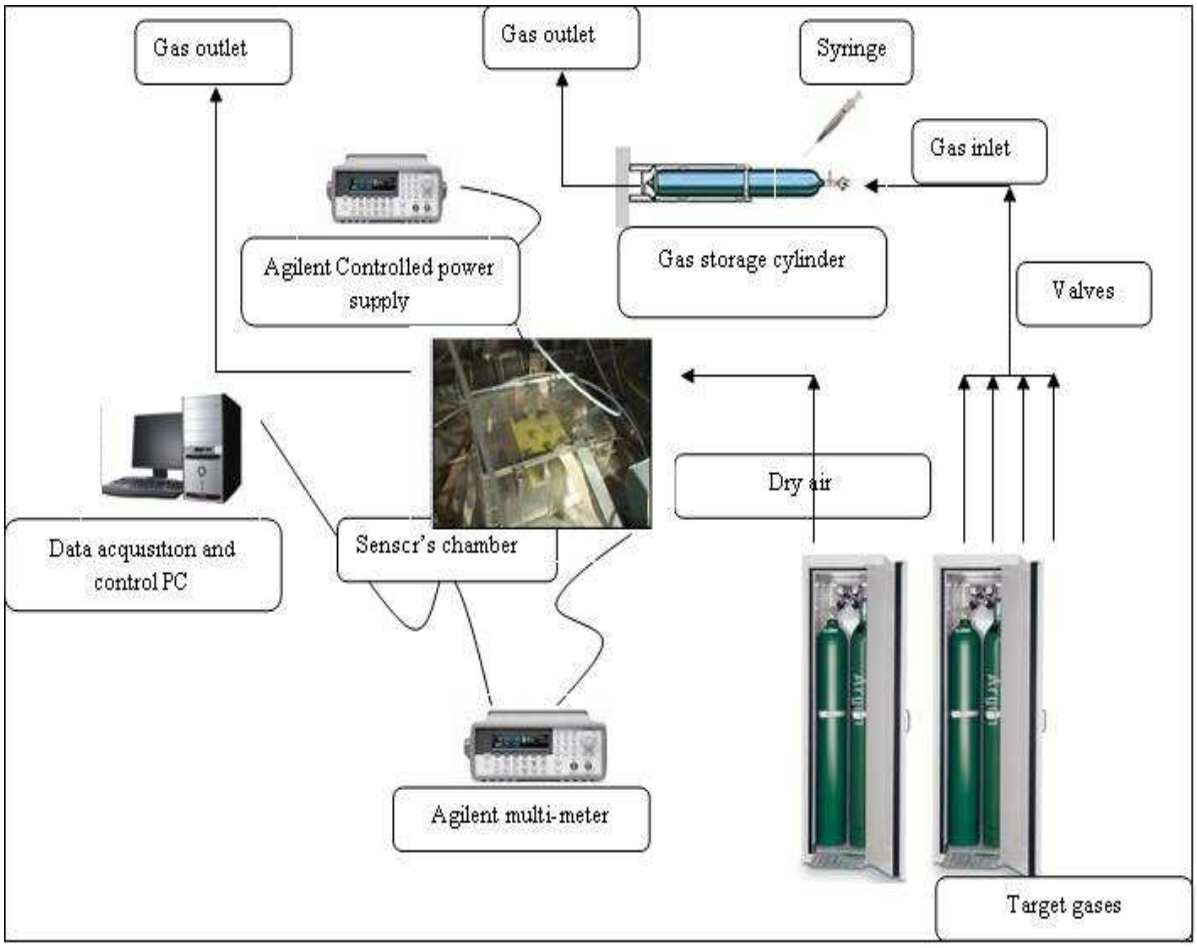

Figure 15: First sensor characterization circuit based on manual injection

b. <u>Procedure 2</u>

In contrast to the first procedure in which the sensor is heated after the injection of all concentrations, here the sensor is subjected to heating after the injection of each analyte concentration. This allowed to know whether the sensor was able to recover its baseline after the contact with the gas or not and evaluate the recovery time of the sensor under desorption at 150 ºC. This was performed in three steps:

- The sensor is maintained in air at ambient temperature during 10 min at 100 ml/min to visualize the sensor baseline.
- The contaminant is injected to the sensor at a given concentration at ambient temperature during 10 min at 100 ml/min.
- The sensor is subjected to heating at 150 ºC during 15 min at 100 ml/min for contaminant desorption.

ISBN:978-84-694-0326-6/DL:T-207-2011

- Once the sensor is recovered, another concentration of the contaminant is injected, etc.

Also here, for each experiment, measurements were replicated 4 times.

❖ **Data processing**

In both cases the data processing was made employing the Origin software, which allowed plotting the graphs of sensor resistance versus acquisition time. Other calculations like sensor response, etc were performed employing Microsoft Excel.

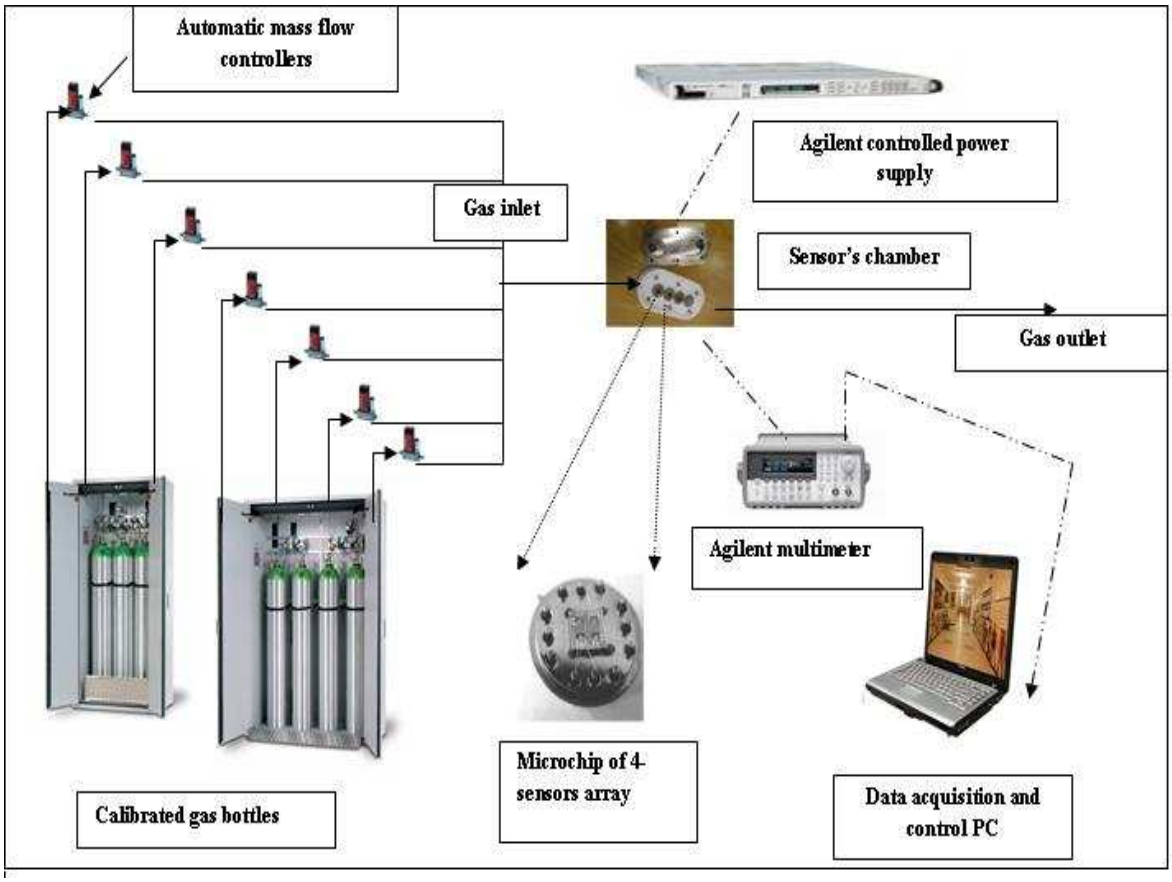

Figure 16: Second sensor characterization circuit based on automatic injection

Figure 17: Pictures of the stainless steel and Teflon sensor chamber. Closed (on the left) and with its cover open (on the right). The chamber can house up to 4 sensor array chips packaged in standard TO-8. Each chip consists of 4 micromachined gas sensors

ISBN:978-84-694-0326-6/DL:T-207-2011

References

[1] R. S. Lee, H. J. Kim, J. E. Fischer, A. Thess, and R. E. Smalley, Conductivity enhancement in single-walled carbon nanotube bundles doped withKand Br ,Nature (London) 388, 255 (1997)

[2] H. Kuzmany, A. Kukovecz , F. Simon, M. Holzweber, Ch. Kramberger, T. Pichler, Functionalization of carbon nanotubes, Synthetic Metals 141, 113–122 (2004)

[3] J. Lyskawa, A. Grondein, D. Bélanger, Chemical modifications of carbon powders with aminophenyl and cyanophenyl groups and a study of their reactivity, Carbon 48, 1271– 1278 (2010)

[4] F. Mercuri, A. Sgamellotti, Theoretical investigations on the functionalization of carbon nanotubes, Inorganica Chimica Acta 360, 785–793 (2007)

[5] A. Felten, J. Ghijsen, J-J. Pireaux, R. L. Johnson, C. M. Whelan, D. Liang, G. Van Tendeloo and C. Bittencourt, Effect of oxygen rf-plasma on electronic properties of CNTs, JOURNAL OF PHYSICS D-APPLIED PHYSICS 40, 23, 7379-7382 (2007)

[6] R. Ionescu, E.H. Espinosa, R. Leghrib, A. Felten, J.J. Pireaux, R. Erni,G. Van Tendeloo, C. Bittencourt, N. Cañellas, E. Llobet, Novel hybrid materials for gas sensing applications madeof metal-decorated MWCNTs dispersed on nano-particle metal oxides, Sensors and Actuators B 13, 174–182 (2008)

[7] L. Valentini, C. Cantalini, I. Armentano, J.M. Kenny, L. Lozzi, S. Santucci, Highly sensitive and selective sensors based on carbon nanotubes thin films for molecular detection, Diamond Relat. Mater. 13, 1301–1305 (2004).

[8] S.G. Wang, Q. Zhang, D.J. Yang, P.J. Sellin, G.F. Zhong, Multi-walled carbon nanotube-based gas sensor for NH_3 detection, Diamond Relat. Mater. 13, 1327–1332 (2004).

[9] R. Ionescu, E.H. Espinosa, E. Sotter, E. Llobet, X. Vilanova, X. Correig, A. Felten, C. Bittencourt, G. Van Lier, J.-C. Charlier, J.J. Pireaux, Oxygen functionalisation of MWNT and their use as gas sensitive thick-film layers, Sens. Actuators B 113, 36–46 (2006).

[10] I. Simon, N. Barsan, M. Bauer, U. Weimar, Micromachined metal oxide gas sensors: opportunities to improve sensor performance, Sens. Actuators B 73, 1–26 (2001).

[11] M. Graf, D. Barrettino, K.-U. Kirstein, A. Hierlemann, CMOS microhotplate sensor system for operating temperatures up to 500 ºC, Sens. Actuators B 117, 346–352 (2006).

[12] E.H. Espinosa, R. Ionescu, C. Bittencourt, A. Felten, R. Erni, G. Vantendeloo, J.-J. Pireaux, E. Llobet, Metal-decorated multi-wall carbon nanotubes for low temperature gas sensing, Thin Solid Films 515, 8322–8327 (2007).

[13] B.Y. Wei, M.C. Hsu, P.G. Su, H.M. Lin, R.J. Wu, H.J. Lai, A novel SnO_2 gas sensor doped with carbon nanotubes operating at room temperature, Sensors and Actuators B 101, 81–89 (2004).

[14] Y. Chen, C. Zhu, T. Wang, The enhanced ethanol sensing properties of multi-walled carbon nanotubes/SnO_2 core/shell nanostructures, Nanotechnology 17, 3012–3017 (2006).

ISBN:978-84-694-0326-6/DL:T-207-2011

[15] C. Bittencourt, A. Felten, E.H. Espinosa, R. Ionescu, E. Llobet, X. Correig, J.-J. Pireaux, WO_3 films modified with functionalised multi-wall carbon nanotubes: Morphological, compositional and gas response studies, Sensors and Actuators B 115, 33–41 (2006).

[16] E.H. Espinosa, R. Ionescu, E. Llobet, A. Felten, C. Bittencourt, E. Sotter, Z. Topalian, P. Heszler, C.G. Granqvist, J.J. Pireaux, X. Correig, Highly selective NO_2 gas sensors made of MWCNTs and WO_3 hybrid layers, Journal of Electrochemical Society 154, J141–J149 (2007).

[17] S. Santucci, C. Cantalini, M. Crivellari, L. Lozzi, L. Ottaviano, M. Passacantando, X-ray photoemission spectroscopy and scanning tunneling spectroscopy study on the thermal stability of WO_3 thin films, Journal of Vacuum Science and Technology A 18, 1077–1082 (2000).

[18] R. Ionescu, E.H. Espinosa, R. Leghrib, A. Felten, J.J. Pireaux, R. Erni, G. Van Tendeloo, C. Bittencourt, N. Cañellas, E. Llobet, Novel hybrid materials for gas sensing applications made of metal-decorated MWCNTs dispersed on nano-particle metal oxides, Sensors and Actuators B 131, 174–182 (2008).

[19] C. Bittencourt, A. Felten, E.H. Espinosa, R. Ionescu, E. Llobet, X. Correig, J.-J. Pireaux, WO_3 films modified with functionalised multi-wall carbon nanotubes: Morphological, compositional and gas response studies, Sensors and Actuators B 115, 33–41 (2006).

[20]http://www.sigmaaldrich.com/catalog/search/ProductDetail/FLUKA/49770?LastFive.

[21] P. Ivanov, E. Llobet, F. Blanco, A. Vergara, X. Vilanova, I. Gracia, C. Cané, X. Correig, On the effects of the materials and the noble metal doping to NO_2 detection, Sensors and Actuators B, 118, 11-317 (2006).

[22] http://www.sigmaaldrich.com.

[23] R. Leghrib, R. Pavelko, A. Felten, A. Vasiliev, C. Cané, I. Gràcia, J-J. Pireaux, E. Llobet, Gas sensors based on multiwall carbon nanotubes decorated with tin oxide nanoclusters, Sensors and Actuators B 145, 411–416 (2010).

[24] G. Kirschstein (Ed.), Gmelins Handbuch der Anorganischen Chemie, Zinn, Teil B, Das Element, Verlag Chemie GmbH, Weinheim, (1971).

[25] A. A. Koós, M. Dowling, K. Jurkschat, A. Crossley, N. Grobert, Effect of the experimental parameters on the structure of nitrogen-doped carbon nanotubes produced by aerosol chemical vapour deposition, CARBON 47, 30 – 37 (2009).

[26] A. A. Koós, F. Dillon, E. A. Obraztsova, A. Crossley and N. Grobert, Comparison of structural changes in nitrogen and borondoped multi-walled carbon nanotubes, carbon, doi: 10.1016/j.carbon.2010.04.026

[27] W. Lang, Silicon microstructuring technology, Materials Science and Enginiering, R17, 1-55 (1996)

[28] V. Demarne, A. Grisel, R. Sanjines, F. LeÂvy, Integrated semiconductor gas sensors evaluation with an automatic test system, Sens. Actuators B 1, 87±92 (1990).

[29] Q. Wu, K.M. Lee, C.C. Liu, Development of chemical sensors using microfabrication and micromachining techniques, Sensors and Actuators B 13/14 1±6 (1993).

ISBN:978-84-694-0326-6/DL:T-207-2011

[30] W. Göpel, T. A. Jones, M. Kleitz, I. Lundström, T. Seiyama, Edts, Sensors: A Comprehensive Survey, Vol. 2, Pt. I, Chemical and Biochemical Sensors, VCH, Weiheim, 1991

[31] R. Ionescu, E.H. Espinosa, R. Leghrib, A. Felten, J.J. Pireaux, R. Erni, G. Van Tendeloo, C. Bittencourt, N. Cañellas, E. Llobet, Novel hybrid materials for gas sensing applications made of metal-decorated MWCNTs dispersed on nano-particle metal oxides, Sensors and Actuators B 131, 174–182 (2008).

[32] K. R. Moonoosawmy and P. Kruse, To Dope or Not To Dope: The Effect of Sonicating Single-Wall Carbon Nanotubes in Common Laboratory Solvents on Their

Electronic Structure, Journal of American Chemical Society 130, 13417–13424 (2008).

[33] B. Trzaskowski, *Æ*. Adamowicz, Chloromethane and dichloromethane decompositions inside nanotubes as models of reactions in confined space, Theoretical Chemistry Accounts 124:95–103 (2009).

[34] J.B. Xu, T.S. Zhao, Synthesis of welldispersed Pt/carbon nanotubes catalyst using

dimethylformamide as a crosslink, Journal of Power Sources 195, 1071–1075 (2010).

[35] M. D. Clark and R. Krishnamoorti, Dispersion of Functionalized Multiwalled Carbon Nanotubes, Journal of Phyical Chemistry C, 113, 20861–20868 (2009).

[36] K. Lee, J-W. Lee, K-Y. Dong, B-K. Ju, Gas sensing properties of single-wall carbon nanotubes dispersed with dimethylformamide, Sensors and Actuators B 135, 214-218 (2008).

[37] E. Mansfield & A. Kar & S. A. Hooker, Applications of TGA in quality control of SWCNTs, Analytical and Bioanalytical Chemistry) 396:1071–1077 (2010

[38] K. Traore, Differential thermal analysis and reaction kinetics.1. generalities and equations of curves for differential thermal analysis, Journal of thermal analysis, 4 (1) 19 (1972).

[39] R Ionescu, E.H Espinosa, R. Leghrib, A. Felten. J.J. Pireaux, R. .Erni, G. Van Tendeloo, C. Bittencourt, N. Cañellas, E. Llobet, Novel hybrid materials for gas sensing applications made of metal-decorated MWCNTs dispersed on nano-particle metal oxides, - Sensors and Actuators B-Chemical, 131, 174 – 182 (2008).

[40] I. Jiméneza, A. Cirera, A. Cornet, J.R. Morante, I. Gracia, C. Cane, Pulverisation method for active layer coating on microsystems, Sensors and Actuators B 84, 78–82 (2002)

[41] H. Lahlou, X. Vilanova, V. Fierro, A. Celzard , E. Llobet , X. Correig, Fabrication and mass spectrometry characterization of a planar pre-concentrator for benzene based on different airbrushed activated carbon materials, Procedia Chemistry 1, 987-990 **(**2009)

UNIVERSITAT ROVIRA I VIRGILI
DESIGN, FABRICATION AND CHARACTERISATION OF GAS SENSORS BASED ON NANOHYBRID MATERIALS
Radouane Leghrib
ISBN:978-84-694-0326-6/DL:T-207-2011

UNIVERSITAT ROVIRA I VIRGILI
DESIGN, FABRICATION AND CHARACTERISATION OF GAS SENSORS BASED ON NANOHYBRID MATERIALS
Radouane Leghrib
ISBN:978-84-694-0326-6/DL:T-207-2011

4. THEORETICAL CALCULATIONS

UNIVERSITAT ROVIRA I VIRGILI
DESIGN, FABRICATION AND CHARACTERISATION OF GAS SENSORS BASED ON NANOHYBRID MATERIALS
Radouane Leghrib
ISBN:978-84-694-0326-6/DL:T-207-2011

ISBN:978-84-694-0326-6/DL:T-207-2011

In parallel with the experimental work related to the fabrication and characterization of the gas sensors based on doped carbon nanotubes, we decided to support this work by performing theoretical calculations which were useful for understanding the interaction mechanism of the different doped CNTs and oriented us in predicting, in some cases, the sensing behaviour of some materials. The simulations were performed using the "ab initio modelling PRO gram" (AIMPRO) code based on density functional theory (DFT) working under the local density approximation (LDA). This work was performed during my stay at the Institut des Matériaux de Nantes and comprises the study of pristine and nitrogen or boron doped carbon nanotubes.
At the beginning of this chapter, I will introduce the theoretical background of the quantum method used in "ab initio modelling PRO gram" (AIMPRO) code [1-8] with which we performed our calculations, and then we will move to the simulation part of this work.

4.1. Introduction to quantum theoretical background

The objective of theoretical studies is the explanation and /or prediction of experimental results by simulating and optimizing the electronic structure of a system of atoms. So, it is necessary to solve the non-relativistic and time independent Schrödinger equation (1.1) of the assembly of ions and electrons constituting the system that we want to simulate.

$$\hat{H}\Psi = E\Psi \quad (1.1)$$

Where:

- $\hat{H}$ is the Hamiltonian operator,
- Ψ is the total wave-function of the system
- E is the energy.

The complete formula of the Hamiltonian of a system constituted of many atoms (M nuclei and N electrons) is:

$$\hat{H} = T_{nuclear} + T_{electronic} + V_{electron\text{-}electron} + V_{nucleus\text{-}nucleus} + V_{electron\text{-}nucleus} \quad (1.2)$$

$$\hat{H} = -\frac{1}{2}\sum_{A=1}^{M}\frac{1}{M_A}\nabla_A^2 - \frac{1}{2}\sum_{i=2}^{N}\nabla_i^2 + \sum_{i=1}^{N}\sum_{j>i}^{N}\frac{1}{r_{ij}} + \sum_{A=1}^{M}\sum_{B>A}^{M}\frac{Z_A Z_B}{R_{AB}} - \sum_{i=1}^{N}\sum_{A=1}^{M}\frac{Z_A}{r_{iA}} \quad (1.3)$$

Where:

- T and V: are kinetic energy and electrostatic potential respectively.
- M_A and Z_A: are the masses and charges of the nuclei respectively.
- r_{ij} :is the distance between electrons
- R_{AB} : is the distance between the nuclei

ISBN:978-84-694-0326-6/DL:T-207-2011

- r_{iA} :is the distance between the nucleus and electrons

What is known in the literature of computational chemistry is that Schrödinger equation is only analytical solvable for a few simples cases, such as the hydrogen atom and one electron positive ions.

In this work, we are using AIMPRO code to solve this equation for many nucleus and electrons structures, which is the case of different defects on carbon nanotubes that include: vacancies, oxygen, nitrogen and boron, and /or metal nanoparticle decorated carbon nanotubes, and /or the interaction with gas molecules.

AIMPRO code is based on density functional theory (DFT) working under the local density approximation (LDA) [7], which leads to a number of approximations. In the following part, we will describe the approximations:

- The first is the Bohr-Oppenheimer approximation, in which they consider the nuclei as a frozen mass in the atomic system because of the much larger nuclei mass than of that of the electrons. So, $T_{nuclear} = 0$ and $V_{nucleus\text{-}nucleus}$= constant, thereby, the solution of the Schrödinger equation will depend only on the distance (R) of the electrons which are moving in the field of fixed nuclei.
- The second approximation is the electron-electron interaction. In this case, there are two theories: Hartree-Fock (HF) and Density functional theory (DFT) [9], in both cases they replace the electrostatic potential of the other electrons acting on an electron by a potential of a system formed by the other electrons and the nuclei which is called "exchange correlation potential". In what follows, we will see only DFT which is the one used in our calculation and because also of the complication of the HF method.

  DFT is based on electron charge density $n(\vec{r})$ [9], which uniquely characterizes the system ground state as the wavefunction does, but with less variables (for a system of N electrons, the variables are reduced from 4N variables to 4 variables). The main advantage of this method is its lower computational time.
- The third approximation is to determine an expression for the exchange correlation potential. They are many reported approximations but the most widely used are: Local functional density (LDA) [10] and generalized gradient (GGA) approximations [11-14]. In these calculations, we are using LDA which considers that the exchange-correlation energy of a system at a given point as the exchange-correlation energy associated with a homogeneous electron gas of the same density.

ISBN:978-84-694-0326-6/DL:T-207-2011

- ❖ The last approximation is the pseudo-potential which is used for the simplified description of complex systems. The pseudo-potential is constructed to replace the atomic all-electron potential such that core states are eliminated and the valence electrons are described by nodeless pseudo-wavefunctions. In this approach only the chemically active valence electrons are dealt with explicitly, while the core electrons are 'frozen', being considered together with the nuclei as rigid non-polarisable ion cores. There are three types of pseudopotential implemented in AIMPRO, but in our case we are using Hartwigsen, Goedecker and Hutter (HGH) type [15].

The wavefunctions are expanded via basis set functions, from which, we mention three commonly used function types :

- Plane waves type: Has a general form of : exp ($i\vec{G}\,\vec{r}$), $\vec{G}$ and $\vec{r}$ are respectively position and propagation vector.
- Slater type: It has an exponential radial in the form of : exp (-r)
- Gaussian type: Which is the basis set expansion used in AIMPRO, It has the following form: $\phi_i(r) = (x - R_{ix})^{n1}(y - R_{iy})^{n2}(z - R_{iz})^{n3}\, e^{-\alpha_i (r-R_i)^2}$

  Where:

  n_1, n_2, n_3: integers that determine the symmetry of the orbitals

- ❖ K-points sampling of the Brillouin zone [16]:

  Brillouin zone is a uniquely defined primitive cell in reciprocal space. Taking surfaces at the same distance from one element of the lattice and its neighbours, the volume included is the first Brillouin zone. Another definition is as the set of points in k-space that can be reached from the origin without crossing any Bragg plane. For a smaller primitive cell, it requires a larger number of k-points to achieve a good accuracy of calculations.

4.2. Set-up of DFT calculations

DFT calculations within the local density approximation are carried out on an 8 · 8 supercell of graphene, i.e. a monolayer of 128 carbon atoms. Graphene was chosen as a reasonable approximation for a large diameter MWNT surface. Fully spin polarized single k-point calculations were geometrically optimized from multiple possible starting
structures. Hartwigsen, Goedecker, and Hutter (HGH) relativistic pseudopotentials were used for all atoms. Atom-centered Gaussian basis functions are used to construct the many-electron

ISBN:978-84-694-0326-6/DL:T-207-2011

wave function with angular momenta up to l = 2. Electronic level occupation was obtained using a Fermi occupation function with kT = 0.04 eV. In the energetic analysis that follows, binding energies are defined as the difference in energy between the relaxed combined system (final state) and the isolated perfect graphite sheet plus a single isolated gas molecule (initial-state), unless otherwise stated.

The energy of the localized charge pair is estimated from the Mulliken formula, based on the values of the molecular ionization potential and electron affinity [17].

The charge state on individual atoms within our system is calculated using Mulliken population analysis. This is a way of taking a system wave function and projecting it onto local atomic-like orbitals on each atom. By summing these orbitals we can say what fraction of the system wavefunction is located on each atom within the system. By summing these electron fractions over all occupied states, the resultant total gives the amount of charge located on that atom. By comparing this with the expected total valence charge on the atom we can thus determine its charge state.

4.3. Study of the interaction of defective CNTs towards gases

In this work we report a first-principles simulation of the interactions between several molecules (NO_2, C_2H_2, CO, C_2H_4, NH_3, and H_2O) and different types of doped CNTs (Nitrogen doped CNTs (N-CNTs), and Boron doped CNTs (B-CNTS).

4.3.1. Experimental and results

The CNTs are doped by nitrogen and boron atoms, representing the most widely used p and n type dopants. Structural perfect graphene was also studied for comparison.

The purpose of this work is to gain fundamental insights to the influence of adsorbed molecules on the electronic properties of different defective CNTs, and how these effects could be used to design more sensitive gas sensing devices.

To find the most favorable adsorption configurations, the molecule under investigation is initially placed at different positions above a CNTs sheet with different orientations. After full relaxation, the optimized configurations obtained from the different initial states are compared to identify the most energetically stable one. The most stable configurations of the NO_2, C_2H_2, CO, C_2H_4, NH_3, and H_2O molecules on the pristine (P-CNTs), boron (B-CNTs), nitrogen (N-CNTs) are then determined and exploited for calculating the values of adsorption energy, equilibrium molecule-CNTs distance and the charge state (Mulliken charge), listed in table 1.

ISBN:978-84-694-0326-6/DL:T-207-2011

4.3.2. Discussion:

Herein, the modeling is assuming that the binding is a charge transfer based process, i.e. we stick the molecule on the surface and weak bonding occurs (we have weak covalent binding so included in the calculations – Van der Waals is not included, however the LDA overestimates molecular binding, which to some extent compensates for the lack of Van der Waals).

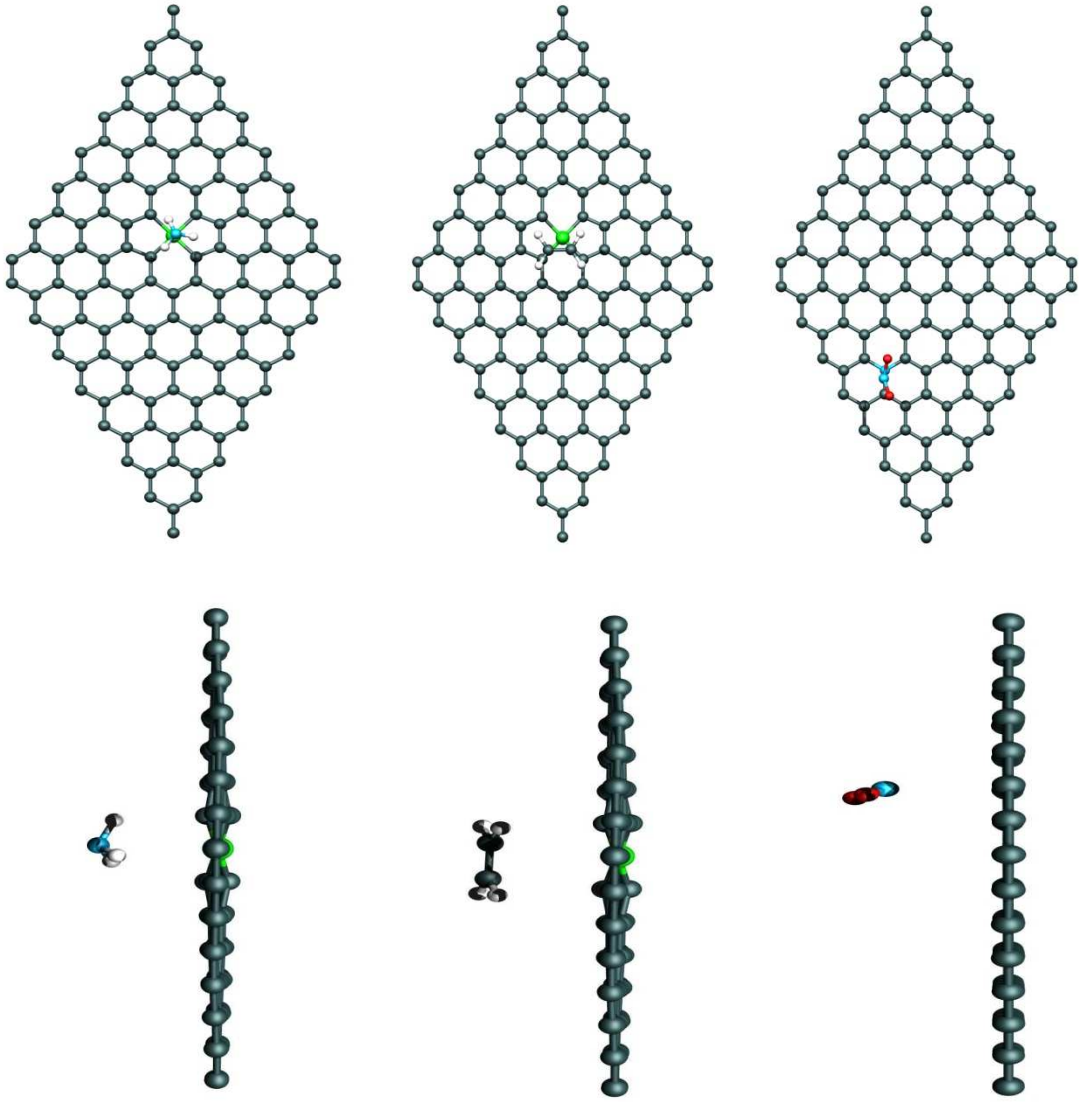

(a) (b) (c)

Figure 1: Schematic view (on the top: front view and on the bottom: side view) of the favorable adsorption configurations of the (a) NH_3, (b) C_2H_4 and (c) NO_2 molecules on the boron vacancy complex, boron vacancy, and substitutional nitrogen-graphenes respectively. C, B, N, O and H atoms are shown as grey, green, blue, red and white, respectively.

What we have not examined here is electrochemical binding mechanisms, whereby the molecules bind to the surface but then overcome some energetic reaction barrier and break

ISBN:978-84-694-0326-6/DL:T-207-2011

down into other components (possibly with the involvement of water molecules too) which stick to the surface. Then, these other components could result in much higher charge transfer than the molecules themselves. This was not performed regarding the lack of time needed for a detailed chemical investigation on a case by case basis.

The results found in table 1 are discussed on the basis of the interaction between each gas molecule with pristine and boron or nitrogen doped graphene using the two different structures either substituted or vacancy doped graphene:

Table. 1: Binding energy, charge state of the gas molecule when bound to the CNT surface, and equilibrium molecule-CNTs distance.

	Binding Energy (eV)				
Gas	Pristine	B-s	B-V	N-s	N-V
NO_2	1.73	2.74	3.55	2.42	1.96
H_2O	0.21	0.33	0.38	0.23	0.44
CO	0.16	0.12	0.23	0.16	0.23
NH_3	0.17	0.71	0.25	0.30	0.27
C_2H_4	0.26	0.25	0.26	0.31	0.30
C_2H_2	0.16	0.21	4.07	0.27	0.26
	Charge state (eV)				
NO_2	-0.353	-0.328	-0.367	-0.134	-0.322
H_2O	-0.077	-0.111	-0.134	-0.026	-0.144
CO	-0.047	-0.062	-0.088	-0.008	-0.060
NH_3	-0.043	+0.350	+0.059	0.015	-0.046
C_2H_4	-0.036	-0.029	-0.028	-0.026	-0.039
C_2H_2	-0.017	-0.004	+0.053	-0.007	-0.075
	CNTs-Molecule distance(A)				
NO_2	2.7	1.69	1.55	1.38	-
H_2O	2.497	3.02	1.78	1.46	-
CO	2.834	2.97	2.86	1.51	-
NH_3	2.78	1.66	2.86	1.546	-
C_2H_4	2.88	3.63	3.13	1.514	-
C_2H_2	3.07	3	band	1.52	-

ISBN:978-84-694-0326-6/DL:T-207-2011

Some exemples of the favorable adsorption configurations for some gas molecules on doped graphene are shown in figue 1.

- ***CO molecule:***

A CO molecule was placed above a carbon, nitrogen or boron atom with the CO molecule oriented perpendicular (with the C or O atom pointing towards the graphene sheet) to the graphene.

After full relaxation, the binding energy on graphene sheet was 0.16 eV, and the molecule-sheet distance was 2.834 Å. The low adsorption energy and long distance indicate a weak interaction (Table 1). In both cases of N-V and B-V, the gas molecules were more close to the graphene sheet than in the other configurations (B-s and N-s). The charge state of CO on B-V and N-V were -0.088 eV and -0.06 eV respectively, which were higher than the other structures. A very small charge (0.008 eV) was transferred from N-s to CO molecule. Compared to pristine graphene, the higher binding energy and higher charge state of B-V and N-V structures indicate a stronger interaction with CO. No improvement in the interaction between CO and substituted B and N structure was noticed.

- ***NO_2 molecule:***

NO_2 is the most reactive molecule with the tested configurations. In fact, in the case of pristine graphene, NO_2 showed the highest binding energy (1.73 eV) and charge state (-0.353 eV) compared to the other gas molecules. These results were improved when using either substitute or vacancy doped boron or nitrogen (fig.1.c) regarding their higher binding energy, higher charge state and smaller molecule/CNT distance as reflected in table 1. In this case, boron showed stronger binding energy and higher charge state than nitrogen. This latter presented results too close to the ones obtained with pristine graphene in terms of binding energy and charge state. However, the distance of gas molecule/CNT was found to be smaller.

- ***NH_3 molecule***

Stronger interaction was in this case noticed using either nitrogen or boron structures compared to pristine graphene (fig.1.a). Better results were obtained with boron compared to nitrogen in the case of the substituted configuration. While very similar results were obtained when working with the vacancy doped nitrogen and boron. In the case of boron, in both configurations, the charge was found to be transferred from NH_3 molecule to B-graphene system reflected by the positive charge state. The same was observed with N-s. While in the

ISBN:978-84-694-0326-6/DL:T-207-2011

case of vacancy doped nitrogen, the negative sign of the charge state indicated a transfer of charge from N-V graphene to NH_3 molecule.

- ***C_2H_2 molecule***

Either substituted boron or nitrogen and vacancy doped nitrogen presented a low interaction towards C_2H_2, but slightly higher than the one obtained with pristine graphene. The best results were achieved by vacancy doped boron. In this case, the binding energy was around 20 times higher than the other materials. In this case, a band was formed between the vacancy doped boron and the gas molecule.

- ***C_2H_4 molecule***

The interaction of the different structures with C_2H_4 seemed to be higher than C_2H_2. In this case, the results obtained with boron were close to pristine graphene suggesting a low interaction with C_2H_4. For either boron or nitrogen, the results obtained with both configurations (Substituted or vacancy doped) were quite similar (fig.1.b). The results obtained with nitrogen suggested a slightly higher interaction than with boron and pristine graphene.

- ***H_2O molecule***

H_2O was found to affect boron and nitrogen structures more than pristine graphene. For either boron or nitrogen, the vacancy doped structure was found to interact more with water rather than the substituted structure.

ISBN:978-84-694-0326-6/DL:T-207-2011

Summary

As general observation from the results reflected in table 1, the interaction of the different molecules with the doped structures was found to be higher than pristine graphene, a part from the case of CO. In this case, the results obtained with the different structures were close to the results obtained with the pristine graphene, and suggested a weak interaction between CO and pristine and doped graphenes.

In general, the results obtained with boron were more interesting than the ones obtained with nitrogen structures for NO_2, H_2O, NH_3 and C_2H_2. Very similar results were obtained with CO, C_2H_4. These results revealed the possibility of designing a selective detection towards the different gases by combining the different materials: pristine, N or B-doped CNTs.

In the case of boron, the interactions observed with substituted structure were weaker than the ones found with the vacancy doped structure exception made of NH_3. This one was found to interact more strongly with substituted boron.

For nitrogen, the results obtained with both structures were quite similar apart for H_2O and CO. In this case, the interaction was more promoted using the vacancy doped structure compared to the substituted structure.

As conclusions, for detection of NO_2 the calculations suggest the best material will be N-V whereas for detection of NH_3, material B-s will be better. Gases like CO, C_2H_4 and C_2H_2 will not be easily detected by any of the materials considered here, according to the calculations. The theoretical results obtained here will be compared to their corresponding experimental results mentioned in chapter 5, section 5.3.

ISBN:978-84-694-0326-6/DL:T-207-2011

References

[1] MJ Rayson, Rapid filtration algorithm to construct a minimal basis on the fly from a primitive Gaussian basis, Computer Physics Comm., 181(6) 1051–1056 (2010)
[2] MJ Rayson and PR Briddon, Highly efficient method for Kohn-Sham density functional calculations of 500-10000 atom systems, Physical Review B, 80 art.no. 205104 (2009)
[3] MJ Rayson and PR Briddon, Rapid iterative method for electronic-structure eigenproblems using localised basis functions, Computer Physics Communications,178(2), 128–134(2008).
[4] MJ Rayson, Lagrange-Lobatto interpolating polynomials in the discrete variable representation, Physical Review E, 76 art.no. 026704 (2007).
[5] JP Goss, MJ Shaw and PR Briddon, Marker-method calculations for electrical levels using Gaussian-orbital basis-sets, Topics in Applied Physics, 104 69–94 (2007).
[6] PR Briddon and R Jones, LDA calculations using a basis of gaussian orbitals, Phys. Status Solidi B-Basic Res. 217, pp.131–171 (2000)

[7] PR Briddon, Ab initio modelling techniques applied to c-Si, in Properties of Crystalline silicon, No. 20 in EMIS Datareviews Series, edited by Robert Hull (INSPEC, Institute of Electrical Engineers, London, 1999), Chap. 6.9, pp. 300–356
[8] R Jones and PR Briddon, The ab initio cluster method and the dynamics of defects in semiconductors, chapter 6 in "Identification of Defects in Semiconductors", volume 51A of Semiconductors and Semimetals (Academic Press, Boston) 1998.
[9] W. Kohn, Nobel Lecture: Electronic structure of matter—wave functions and density functionals, Reviews of Modern Physics 71, 1253-1266 (1999).

[10] W. Kohn and L. J. Sham, Self-Consistent Equations Including Exchange and Correlation Effects, Physical Review 140, A1133-A1138 (1965).

[11] D. C. Langreth and J. P. Perdew, Theory of nonuniform electronic systems. I. Analysis of the gradient approximation and a generalization that works, Physical Review B 21, 5469-5493 (1980).

[12] D. C. Langreth and M. J. Mehl, Beyond the local-density approximation in calculations of ground-state electronic properties, Physical Review B 28, 1809-1834 (1983).

[13] J. P. Perdew and Y. Wang, Accurate and simple density functional for the electronic exchange energy: Generalized gradient approximation, Physical Review B 33, 8800-8802 (1986).

[14] J. P. Perdew, Density-functional approximation for the correlation energy of the inhomogeneous electron gas,, Physical Review B 33, 8822-8824 (1986).

[15] C. Hartwigsen, S. Goedecker, and J. Hutter, Relativistic separable dual-space Gaussian pseudopotentials from H to Rn, Physical Review B 58, 3641-3662 (1998).

[16] H. J. Monkhorst and J. D. Pack, Special points for Brillouin-zone integrations, Physical Review B 13, 5188-5192 (1976).

[17] G. Mazur, P. Petelenz, Charge transfer excitons in perylenetetracarboxylic dianhydride - microelectrostatic calculations, Chemical Physics Letters 324, 161–165 (2000)

UNIVERSITAT ROVIRA I VIRGILI
DESIGN, FABRICATION AND CHARACTERISATION OF GAS SENSORS BASED ON NANOHYBRID MATERIALS
Radouane Leghrib
ISBN:978-84-694-0326-6/DL:T-207-2011

5. SENSOR CHARACTERIZATION

UNIVERSITAT ROVIRA I VIRGILI
DESIGN, FABRICATION AND CHARACTERISATION OF GAS SENSORS BASED ON NANOHYBRID MATERIALS
Radouane Leghrib
ISBN:978-84-694-0326-6/DL:T-207-2011

ISBN:978-84-694-0326-6/DL:T-207-2011

As it was mentioned in the introduction, the aim of this thesis is to produce an efficient gas sensor array based on the combination of different metal decorated carbon nanotubes able to selectively detect target gases at ambient temperature, especially benzene. For that, we need to:

- ✓ Explore theoretically and experimentally the effect of oxygen functionalization and metal decoration on the sensing properties of carbon nanotubes.
- ✓ Understand the interaction mechanism with the studied gases
- ✓ Analyze the effect of the active layer deposition techniques on their sensing properties
- ✓ Select the most interesting materials which will be combined to get a selective gas sensor array for monitoring a few target gases.

In parallel to the development of sensors based on treated carbon nanotubes (e.g, oxygen functionalized and metal decorated MWCNTs), other materials based on nanotube composites were also investigated. These last include: Nitrogen or boron doped CNTs, metal oxide, metal oxides mixed with either metal decorated CNTs or nitrogen/boron doped CNTs, and metal oxides doped CNTs. All the sensors based on the cited materials were characterized towards different gases separately such as NO_2, CO, NH_3, C_2H_4, C_6H_6 and moisture (H_2O), in a dry ambient, and were operated at different temperatures (room temperature (14-28 ºC), 150 ºC and 250 ºC). Two relative humidity levels were measured: the change from 0 % to 50 %, and from 0 % to 80 %.

In this section the sensing properties of different materials will be discussed in detail including: sensitivity, selectivity, linearity, and response and recovery times. Attention will be also given to the detection mechanism based both on the experimental results and some theoretical calculations.

5.1. Gas sensing properties of metal-decorated carbon nanotubes

5.1.1. Reactivity and proposed detection mechanisms

Metal decorated samples show quantum-mechanical attributes by taking advantage of the electron transfer between the metal nanoparticles and the CNTs upon a gas adsorption [1-7] resulting superior to either of its constituent components. In fact, they detect gases that are normally undetectable by pristine or plasma-treated bare CNTs (cf. Annex II).

We found that the sensing properties of each composite (metal/CNT) is affected by many parameters which we need to take into account: the effect of nanoluster size, sensor operating

ISBN:978-84-694-0326-6/DL:T-207-2011

temperature, plasma treatment conditions or precursor type (e,g. in the case of the plasma treatment or plasma metal decoration) and finally the deposition method onto the sensor membrane. All these parameters are very important for determining gas sensing performance. Those preparation conditions effects will be attentively discussed and studied separately. As expected, pristine MWCNTs presented a weak interaction with the tested gases, which was not surprising as pristine CNTs are poorly reactive. For example, they showed a noisy response to high NO_2 concentrations (the most reactive gas among the species tested) and this is the reason why there is intense and competitive researches to make CNTs' surface more reactive.

Responsiveness of the different hybrid materials (metal-decorated CNT) towards the different gases (NO_2, CO, C_2H_4, NH_3, C_6H_6 and moisture) was plotted versus acquisition time and grouped according to the research team that provided each material (LISE, CHANI or SAM team) (cf. Annex II).

As a general overview of the results, sensor resistances decrease with increasing concentrations of NO_2, which is an electron acceptor (cf. Annex II). Hence, upon NO_2 adsorption, electronic charge is transferred from the CNT towards metal clusters [1]. The observed resistance decrease when exposing the CNT networks to NO_2 can be due to a direct electron transfer from the CNTs to the NO_2, or to an indirect electron transfer via metal nanoparticles, which would lead to increased holes concentration in the CNTs, which results in an increase in CNTs conductivity, thereby the resistance decreases. Several mechanisms have been proposed to explain the nature of the CNT-NO_2 interaction [8-13]. While the measured CNT network resistance changes upon exposure to NO_2 can be explained by either proposing NO_2 physical adsorption processes [9] or NO_2 chemical adsorption processes [10-12], the observed long recovery times lead us to suggest that NO_2 chemisorption occurs during the detection experiments described above. This chemisorption may result from the interaction between NO_2 gas molecules and defects in the CNT structure [14-16] or with metal nanoparticles [17]. Peng et al. studied the adsorption, diffusion, and reaction of NO_2 on a SWCNT using ab initio calculations [18]. Since there are catalyst islands on SWCNT, NO_2 molecules are known to interact with catalytic surfaces to form NO and NO3 molecules.

The desorption of NO_2 and NO molecules is very fast (less than 1 second at room temperature), while the desorption of NO_3 molecules is much slower (about 12 hours). They deduced that the slow recovery is due to the difficulty to desorb NO_3 strongly chemisorbed on the SWNT surface.

ISBN:978-84-694-0326-6/DL:T-207-2011

Unlike in the presence of NO_2, upon exposure to C_6H_6, C_2H_4, NH_3 and H_2O, the resistance increases with increasing gas concentration. All these species are electron donors. This suggests that, upon adsorption of electron donor species, a significant amount of electronic charge is transferred from the metal clusters towards the CNT. According to these results, our mats of plasma-treated, metal-decorated MWCNTs behave as p-type semiconductors [19]. Although MWCNTs tend to show a metallic behavior at room temperature [20], the semiconducting behavior observed here can be attributed to the presence of oxygen species adsorbed on CNTs [21] promoted by the oxygen plasma treatment.

Finally, the sign of the sensor response to CO can be sometimes positive or negative (cf. Annex II). This is because this gas can behave either as electron donor or electron acceptor depending on the experimental conditions (such as: oxygen partial pressure) [22-24]. However, more research is needed to obtain a clear explanation for this ambivalent interaction of the CO molecule with CNTs.

The response to gases of all metal decorated samples was increased compared either to plasma-treated or non-treated CNTs. This suggests the importance of metal decoration for enhancing the gas response of CNTs based materials. This was in agreement with theoretical first principles calculations performed on MWCNTs with oxygenated defects or on metal-decorated MWCNTs, in which charge transfer between the adsorbed gas molecule and the nanotube is enhanced by the presence of metal nanoparticles [17]. From the figures of annex II, although the earlier saturation of some sensors in the case of CO detection (figure.1.a) and C_2H_4, most of metal decorated MWCNTs show a good linearity in the case of NO_2 (figure.1.b), C_6H_6, and some cases C_2H_4 with increasing concentrations of tested gases in a given range.

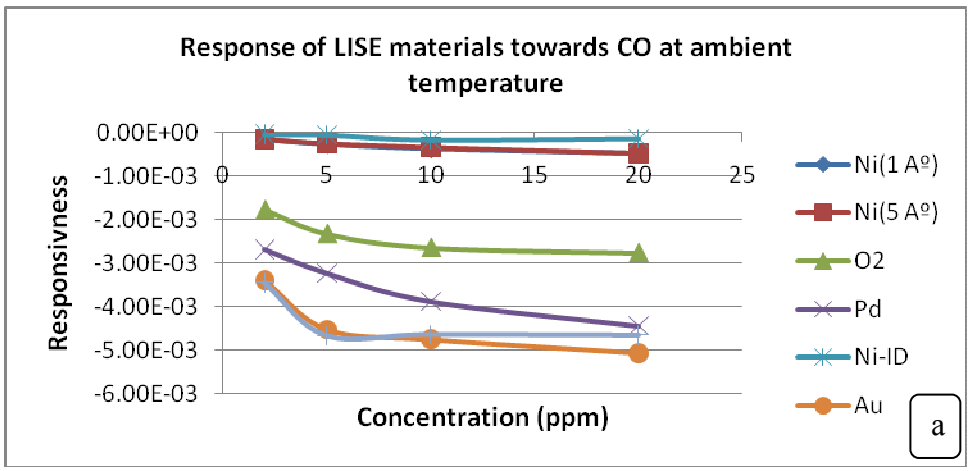

ISBN:978-84-694-0326-6/DL:T-207-2011

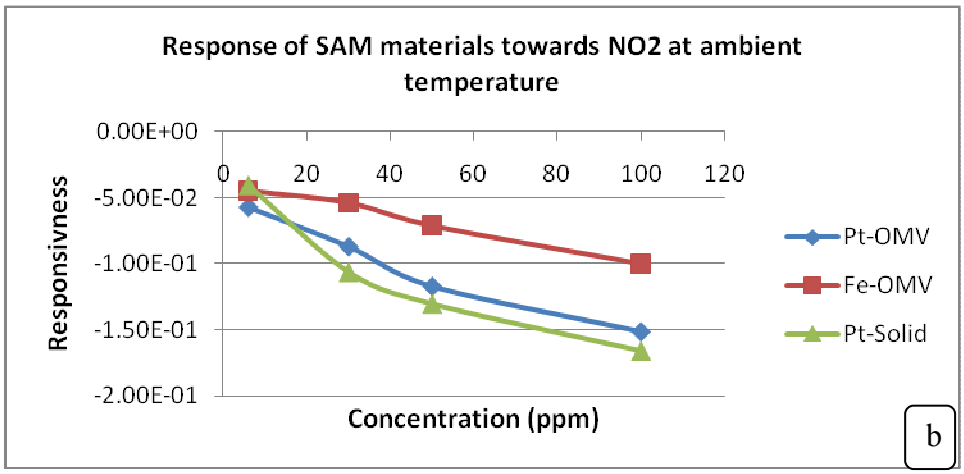

Figure 1: Detection at room temperature of: (a) CO (b) NO_2

In fact, the oxygen plasma treatment of CNTs is important for achieving a good interaction between metal or metal nanoparticles and the CNT surface. This results in a homogeneous dispersion of metal nanoparticles on the CNT sidewalls and in nanoparticles with narrow size distribution. All this helps in enhancing gas sensitivity.

Electrical conductance in CNTs is ballistic even at room temperature, [25, 26] which enables the rapid detection of electron transport through CNTs. The interaction mechanism between a given metal-decorated sample and a given gas remains not well understood by scientists. Several efforts have been devoted to study and understand the interaction between gas molecules and gas sensitive layers. In general, gas molecules tend to react with the active sites situated at the carbon nanotube surface, which can include: defective sites (i.e, existing in the raw material or induced defects) and or species decorating CNTs surface such as metal, metal oxides, polymers, etc. In our case, we proposed two mechanisms that can occur simultaneously or separately during the exposure to the gas [27]. The first one considers that the molecules react with the oxygenated defects created during the oxygen plasma treatment. In other words, CNTs behave like p-type materials due to electron withdrawing by oxygen molecules adsorbed on the CNT surface [25-28]. The gas directly adsorbs onto an oxygenated defect located at the CNT sidewall created by the oxygen plasma treatment, inducing electron transfer and changing the electrical conductivity of the hybrid nanomaterial. In the second mechanism, the gas adsorbs onto a metal nanoparticle and this results in a significant charge transfer between the nanoparticle and the CNT, which eventually changes the electrical conductivity of the hybrid nanomaterial) [1, 27, 29-30].

ISBN:978-84-694-0326-6/DL:T-207-2011

5.1.1.1. Effect of material synthesis conditions

a. plasma treatment conditions

The plasma treatment is important because it enables cleaning, activating, functionalizing and metal decorating CNTs in a more homogeneous way. Oxidative treatments affect the density of states (DOS) of valence bands and increase the work function of purified MWCNTs (4.3 eV) [31], which is close to the work function of the metals considered in this thesis (between 4.9-5.1 eV) [32-36]. The effective electronic interaction between metal nanoparticles and the CNT facilitates the detection of gases through the change in the electrical conductivity of mats formed by these hybrid nanomaterials.

To confirm that effect, the sensing properties of two different rhodium-decorated samples pretreated by different plasmas were compared; the first was treated in the presence of argon (Rh/Ar/MWCNTs) and the second with argon and oxygen plasma (Rh/Ar/O_2/MWCNTs).

Figure 2 shows the responsiveness of both samples towards different concentrations in the range of ppb and ppm of: (a) NO_2, (b) CO (c) C_2H_4, (d) benzene and at room temperature. Figure.2.e. shows the effect of moisture on sensing hybrid film, two relative humidity rates were measured: the change from 0 % to 50 %, and from 0 % to 80 %. The change between 50 % and 80 % was in all cases in order of 10^{-4} which reflect a negligible change when passing from 50 % of humidity rate to 80 %.

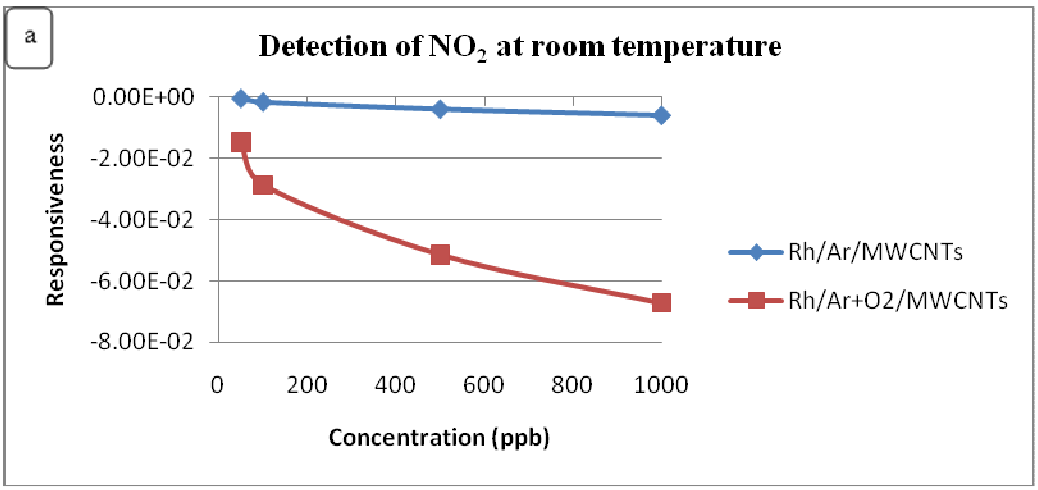

ISBN:978-84-694-0326-6/DL:T-207-2011

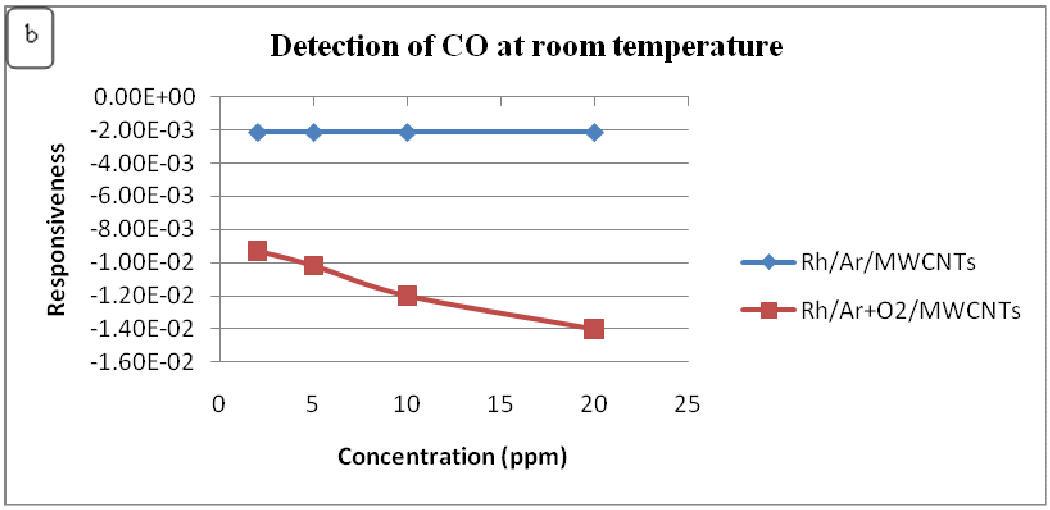

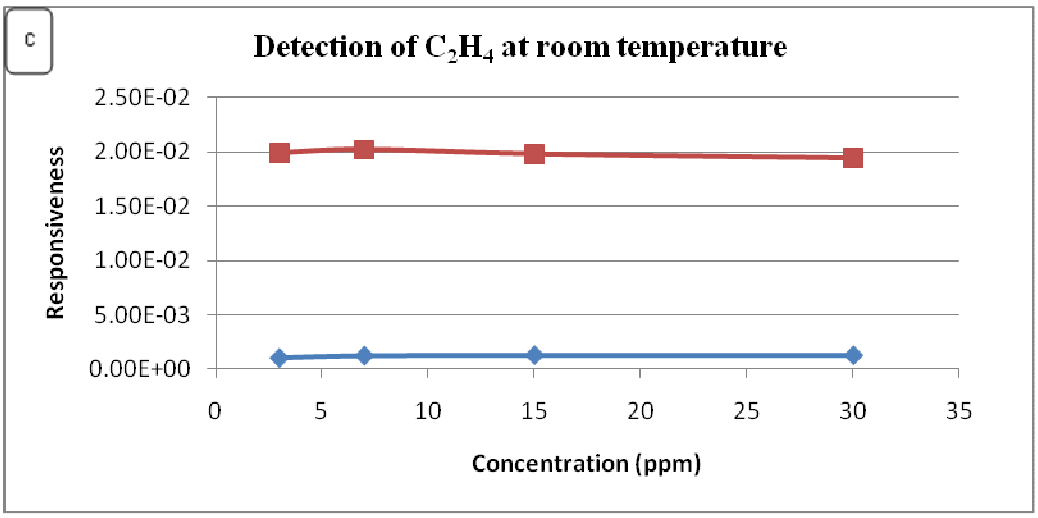

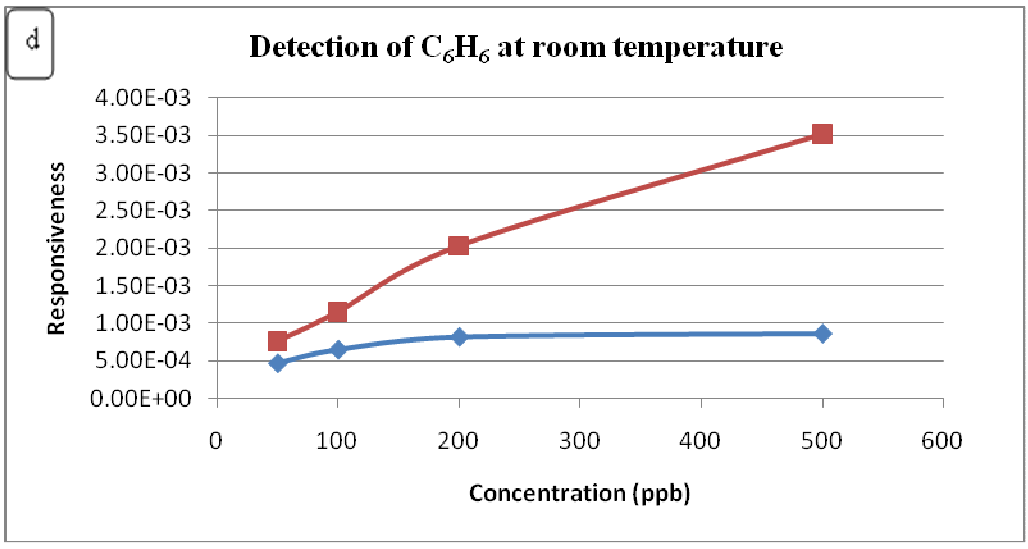

UNIVERSITAT ROVIRA I VIRGILI
DESIGN, FABRICATION AND CHARACTERISATION OF GAS SENSORS BASED ON NANOHYBRID MATERIALS
Radouane Leghrib
ISBN:978-84-694-0326-6/DL:T-207-2011

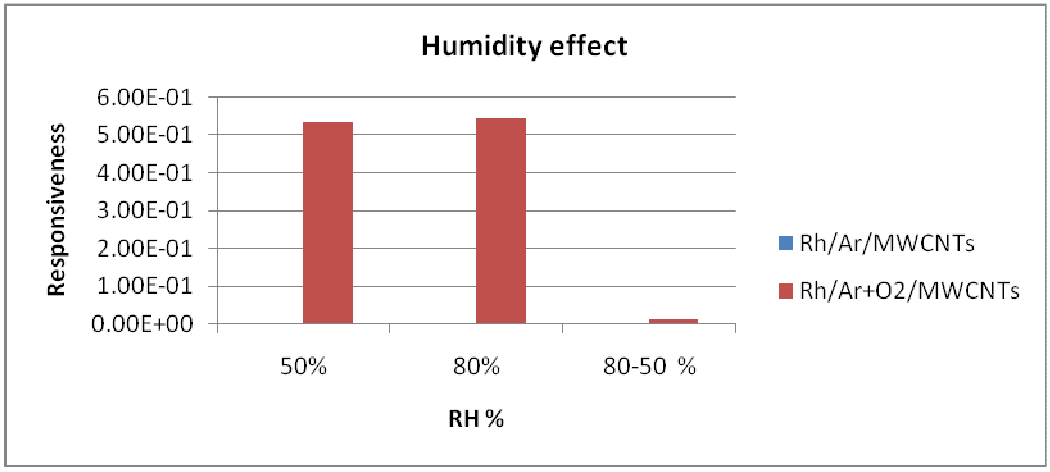

Figure 2: Comparison of responsiveness of Rh/Ar/MWCNTs and Rh/Ar+O2/MWCNTs samples towards (a): NO2, (b): CO (c): C2H4, (d): C6H6 and (e): moisture at room temperature

For all gases, the responses of materials treated in oxygen plasma were higher than those of materials treated in argon plasma by at least a factor of two (Figure 2.a, b and c). These results confirmed the importance of the O_2 plasma treatment prior to metal decoration. In fact, the introduction of oxygen during the CNT plasma treatment leads to the creation of active sites into CNT surface, which improves the metal-CNT surface interaction resulting in a good control of nanocluster size and a homogeneous dispersion of metal nanoclusters over the CNT sidewalls. The amount of metal and its dispersion is higher than in the case of nanotubes treated in an argon plasma [37]. This is in agreement with the results obtained from TEM images (Annex.1). The higher amount and better dispersion of metal nanoparticles decorating CNTs obtained when an oxygen plasma is used results in a higher responsiveness to gases. Furthermore, gas sensors employing materials treated in argon plasma show an early saturation of their response at low gas concentrations, this is not the case of sensors based on materials treated in oxygen plasma (see Fig. 2). Concerning Ethylene detection, both sensors were saturated at the first tested concentration (3 ppm of ethylene). Nanotubes decorated with Rh, in plasma of O_2 and Ar, show good linearity with increasing concentration of tested gases. An inconvenient of oxygen plasma treatment is that the response to moisture is highly enhanced due to the polarity modification induced in the samples. CNTs become more hydrophilic after the oxygen plasma treatment and remain basically hydrophobic if treated in a plasma not containing oxygen (Figure 2.e).

ISBN:978-84-694-0326-6/DL:T-207-2011

b. Effect of the precursors

From the results shown in Annex II, we can notice that even when working with the same metal, the response towards the gases changes depending on the preparation conditions or the metal decoration procedure.

As we already mentioned in the experimental section (Annex.1), some of the decorated samples were prepared from either solid salt or organometallic (OMV) based precursors.

In figure 3 and 4, we compare, for example, the responsiveness of Fe or Pt decorated samples, prepared from different kinds of precursors and deposited by the same deposition technique (Air-brushing).

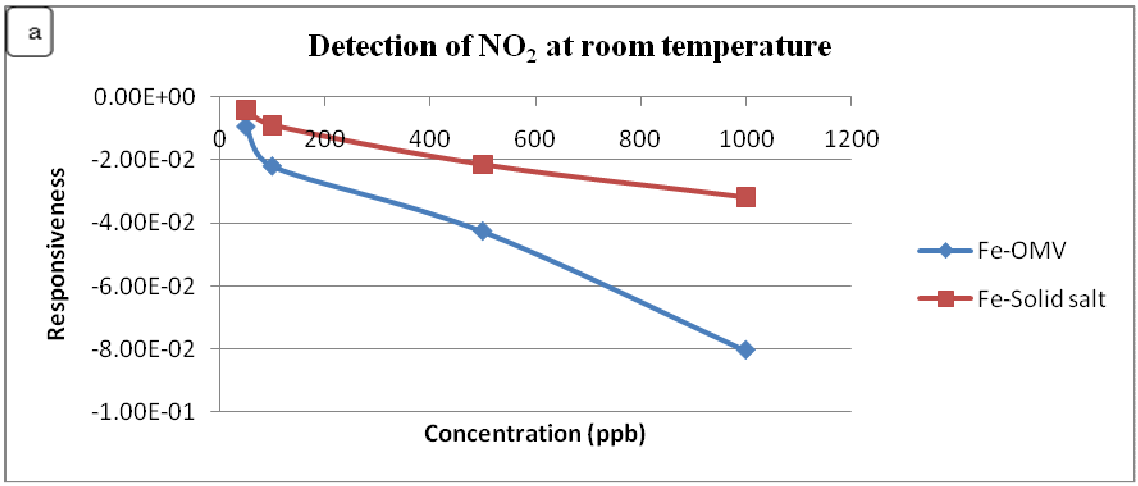

Figure 3: Effect of Fe precursor on the response of Fe/MWCNTs samples towards gases

For both metals, we can notice that the sensors prepared from organometallic precursors present a significantly higher response than the ones prepared from solid salt metal precursors (figure.3 and 4).

From XPS analysis (Table 1), in the case of Pt decorated CNTs, it was found that OMV based precursors allowed to attach the highest amount of metal by comparison to the preparation techniques based on solid salt precursor. In our case, this resulted in a higher sensitivity to the gases tested (Figure 3).

ISBN:978-84-694-0326-6/DL:T-207-2011

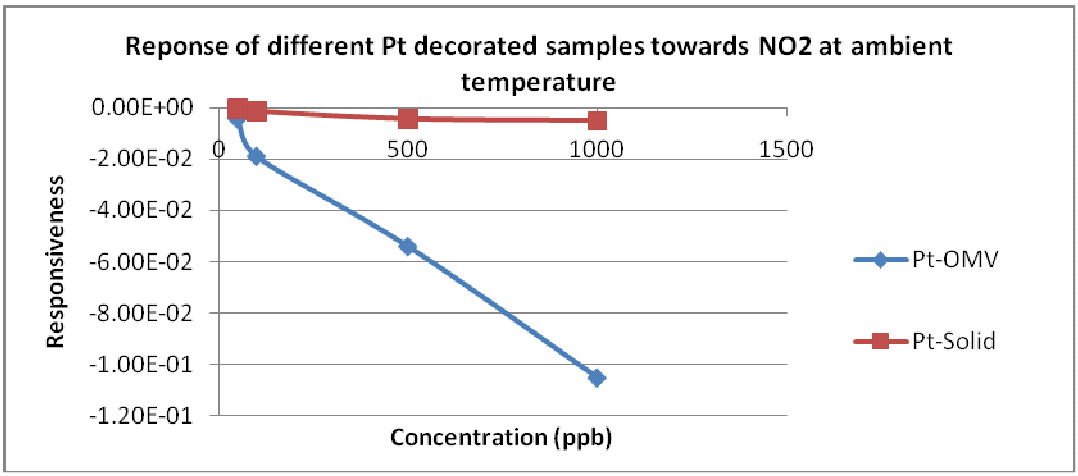

Figure 4: Effect of Fe precursor on the response of Pt/MWCNTs samples towards gases

However, XPS analysis performed by SAM group on Fe decorated CNTs (Table 1), shows that, unlike in the case of platinum, solid salt precursor presents a higher amount of metal attached to the nanotube wall than OMV based precursor. One would expect the sensitivity reached using a solid salt based precursor to be higher than the one reached using an OMV based precursor. However, the OMV material still presents the higher sensitivity.

The higher sensitivity due to OMV based precursors obtained for both metals was then, according to XPS results, surprisingly independent from the amount of metal nanoclusters. To understand this effect, we will focus on the TEM analysis performed on both samples (Figure 5).

Table 1: Elemental chemical composition percentage as derived from an XPS analysis of the metal decorated samples prepared from the two different precursors

Metal precursor	O [%]	N [%]	C [%]	Fe [%]	Pt [%]
Fe-Solid	12.3	0.5	84.2	3	-
Fe-OMV	7.1	0.3	90.7	1.9	-
Pt-Solid	1.7	0.2	95.3	-	2.9
Pt-OMV	2.5	-	92	-	5.2

From the TEM analysis performed by SAM group on platinum decorated samples, (Figure 5), we notice that the use of an organometallic precursor for the metal decoration of nanotubes results in a good and homogeneous dispersion of metal nanoparticles (Figure 5. Right). In contrast, when using solid precursors (Figure 5. Left), residues of the precursor remain in the sample and there was no way to remove them completely. These residues are not chemically reactive but could desactivate the nanohybrid material. In this case, the metal nanoclusters

ISBN:978-84-694-0326-6/DL:T-207-2011

seem to have larger diameter than when OMV precursors are used and the dispersion is not as good as it was before. On the basis of these observations for Pt-CNTs, we can assume that the higher NO_2 sensitivity obtained by the sensor based on Fe-decorated CNTs from an organometallic precursor is due to the good dispersion of metal nanoparticles obtained and to the absence of precursor residues. In Fe-decorated CNTs from solid salt precursor, the presence of residues seems to be more detrimental for sensitivity than the amelioration brought by an increased amount of metal.

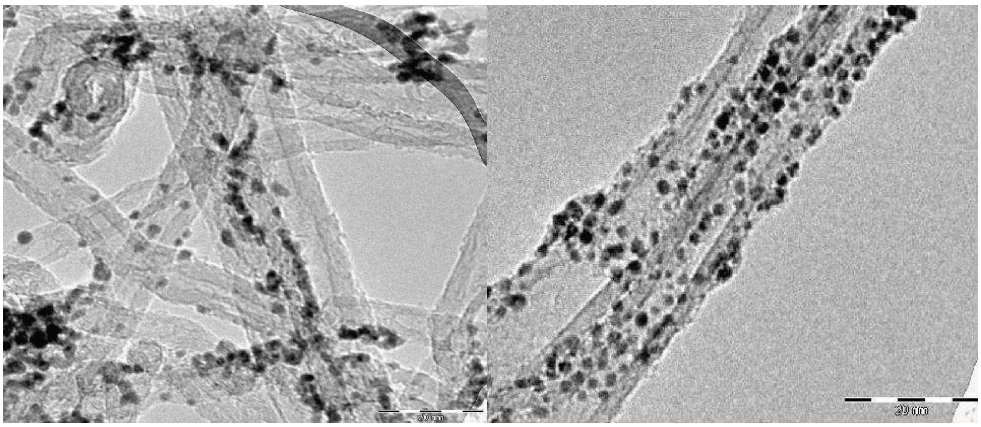

Figure 5: TEM images of Pt-decorated CNT using: right) using organometallic precursor; left) Solid precursor (from SAM Laboratory)

Unfortunately, in the case of Fe decorated CNT, it was not possible to see iron nanoclusters on CNT side wall using High Resolution TEM (HRTEM). But to confirm the deposition of the metal nanoparticles, Energy Dispersive X-ray spectroscopy (EDX) was used and the survey spectrum shows the existence of Fe at the CNT surface.

c. Effect of nanoparticle size

The effect of metal nanoparticle size was studied in the case of MWCNTs samples decorated with nickel by the LISE team using the same precursor and the same sensor coating method (airbrushing).

From heterogeneous catalysis, it is known that the smaller Au nanoparticles are the more reactive. This can be explained by the dependence of the reactivity of Au nanoclusters and the fraction of atoms that are located at either corners, edges, or on surfaces in the top half of a truncated octahedron as a function of the particle diameter [38]. Clearly, the total number of surface atoms changes only slightly when the particle size decreases from 10 nm to 2 nm. However, the fraction of corners increases significantly when the particle size is less than 4 nm and scales approximately as d^{-3} as the diameter of the particles shrinks. The increase in

ISBN:978-84-694-0326-6/DL:T-207-2011

the estimated fraction of corner atoms coincides with a generally observed increase in reactivity to gases with decreasing metal particle size [6].

In our case, three samples of CNTs decorated with nickel of different nanocluster sizes, namely, 1 nm, 5 nm or 10 nm were compared. The nanotubes decorated with nanoclusters of intermediate nanocluster size (5 nm) showed the best results for the gases studied (figures 6.a and 6.b) compared to samples of 1 nm and 10 nm nanoclusters size. Similar results were obtained by Penza and co-workers when producing gas sensors based on Au decorated MWCNT [39]. They found that samples of 5 nm of Au decorated CNTs show the highest gas sensitivity measured, which suggest that the smaller metal nanocluster grains (1 nm in diameter) were highly reactive and this caused their tendency to agglomerate resulting in bigger grains, thereby their sensitivity to gases was closer to the one of big nanoclusters (10 nm in diameter). On the other hand, intermediate particles (5 nm in diameter) remain isolated and show in this way the higher sensitivity to gases.

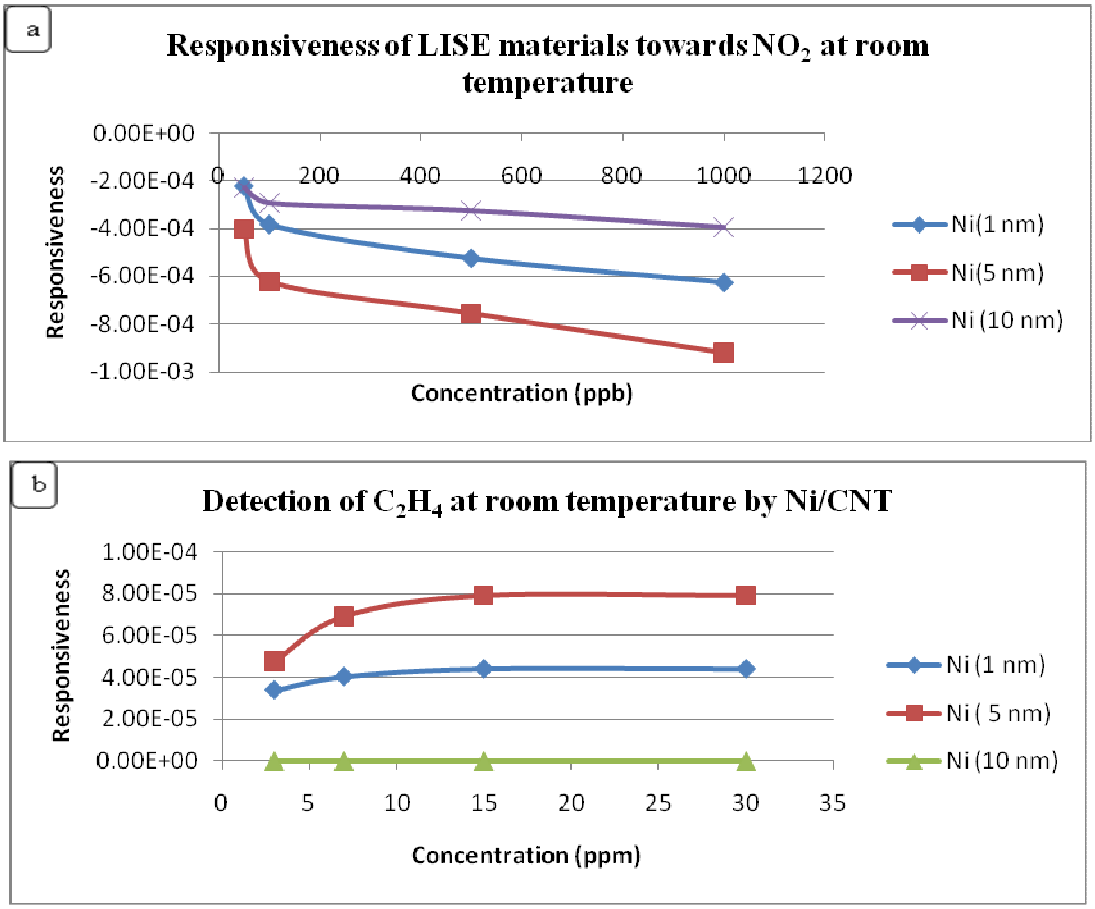

Figure 6: Effect of nanoclusters size on the response for: a) NO2 detection and b) C2H4 detection, at room temperature

ISBN:978-84-694-0326-6/DL:T-207-2011

5.1.1.2. Effect of sensor fabrication conditions

a. Effect of the electrode metal

Many works have been addressed to study the effect of metal electrodes on gas sensor performance [40-42]. They found that the contact resistance (e.g. Schottky, Ohmic) between CNTs and metallic electrode plays a strong role in the sensitivity to NO_2 by revealing a strong dependence of the sensor response and the electrode material (Pd, Cr, Al, Au, Ti, Pt). In this context, we performed some tests using an alumina substrate as testing transducer with screen printed interdigitated Pt and Au electrodes.

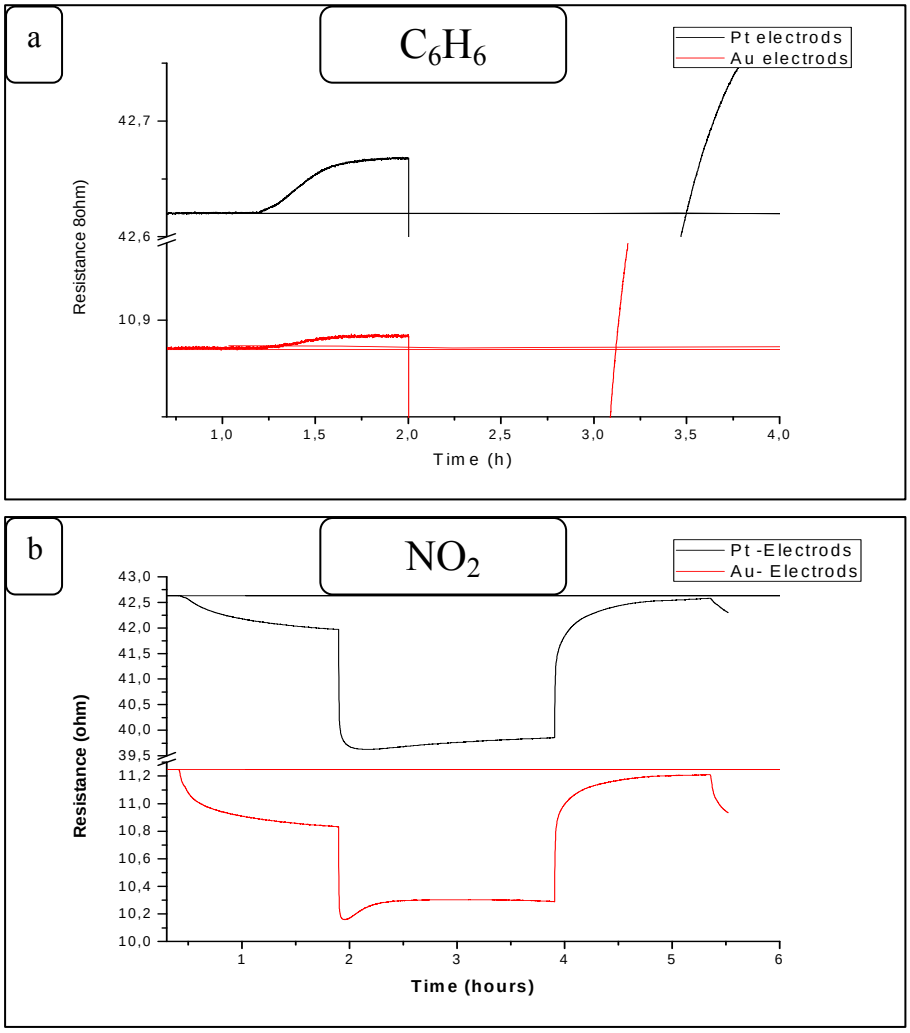

Figure 7: Effect of Pt and Au electrodes for the detection of:a) benzene. b) NO_2 using Rh-MWCNTs

Our main objective from this study was to evaluate the effect of the metal electrodes on the sensing properties of our nanohybrid materials towards benzene, (being benzene the most interesting target gas for our application). NO_2 was tested for comparison. NO_2 and benzene

ISBN:978-84-694-0326-6/DL:T-207-2011

have opposite detection signal signs. Rh-decorated MWCNTs were employed as gas sensitive material in this study.

It was found (figure 7) that when using Pt electrodes, the sensitivity towards benzene was improved compared to the sensitivity obtained by the sensor with Au electrodes. In contrast, NO_2 seems to have better sensitivity using sensor with Au electrodes. In fact, gas detection can occur also at the interface between the nanotubes and the electrodes as suggested by Zhang et al [40]. From these results, it should be taken into account the effect of electrodes for a good selective detection of a given gas depending on the desirable application. In our case, Pt electrodes seem a good choice since they enhance benzene responsiveness.

b. Effect of the deposition method

We will focus now on CNTs decorated with the same metal (i.e, Au) and same preparation method (i.e, thermal evaporation), and having the same nanoparticle size, but deposited by two different techniques. For this comparison, we will take the example of two different metal decorated samples, Au/MWCNTs.

We will use following abbreviations to refer to the deposition methods: DD: will refer to the direct drop coating method; and ID to the inverse drop coating method.

We have already shown in the experimental section (3.2.2.2) that the stability of the nanoclusters is affected by the deposition method. In fact, when using inverse drop coating method instead of direct drop coating, it was demonstrated that the stability of the nanoclusters is enhanced. For example, for Au nanoparticles, it is known that they have a weak interaction energy with carbon nanotubes (this explains why Au nanoparticles are formed on the tube wall rather than obtaining a complete wetting of the tubes when gold is thermally evaporated) [6, 8-18]. The thermal treatment employed in the drop coating fabrication step induces some gold nanoparticles to leave the carbon nanotube sidewalls. In contrast, when the inverse drop coating fabrication procedure was employed, this thermal treatment was previous to the plasma treatment and Au decoration steps. As a result, the inverse drop coating avoids the detachment of metal nanoparticles for the carbon nanotube wall.

We investigated the effects on the sensing properties towards NO_2 and CO of different methods employed for fabricating gas sensor based on gold decorated MWCNTs. Direct and inverse drop coating methods have been used to deposit gold decorated, oxygen plasma treated MWCNTs onto interdigitated sensor electrodes. While the preparation method does not significantly influences NO_2 detection (Figure 8.a and 8.b), a clear improvement in CO

ISBN:978-84-694-0326-6/DL:T-207-2011

sensitivity is observed when the inverse drop coating method is employed (Figure 8.c). The inverse drop coating method prevents gold nanoparticles from leaving the nanotube surface during the fabrication of the sensor, resulting in sensors with enhanced CO responsiveness.

- **Understanding the interaction mechanism of NO_2 and CO with Au and/or oxygen treated carbon nanotubes:**

For the treated samples, all sensors were more responsive to NO_2 than to CO. Figures 8.a and 9 show the response to increasing concentrations of NO_2 for Au-decorated MWCNT sensor prepared by the direct drop coating method and operated at room temperature. The observed resistance decreases when exposing the CNT networks to NO_2 can be due to a direct electron transfer from the CNTs to the NO_2, or to an indirect electron transfer via Au nanoparticles, which would lead to increased holes concentration in the CNTs, which leads to increase the CNTs conductivity, thereby the resistance decreases. While in the first mechanism NO_2 adsorbs on the nanotube sidewalls, in the second one NO_2 adsorbs on Au nanoparticles.

The measured CNT network resistance changes upon exposure to NO_2 can be explained by either proposing NO_2 physical adsorption processes or NO_2 chemical adsorption processes [8-18], the observed long recovery times lead us to suggest that NO_2 chemisorption occurs during the detection experiments described above. NO_2 chemisorption may result from the interaction between NO_2 gas molecules and defects in the CNT structure or with metal nanoparticles.

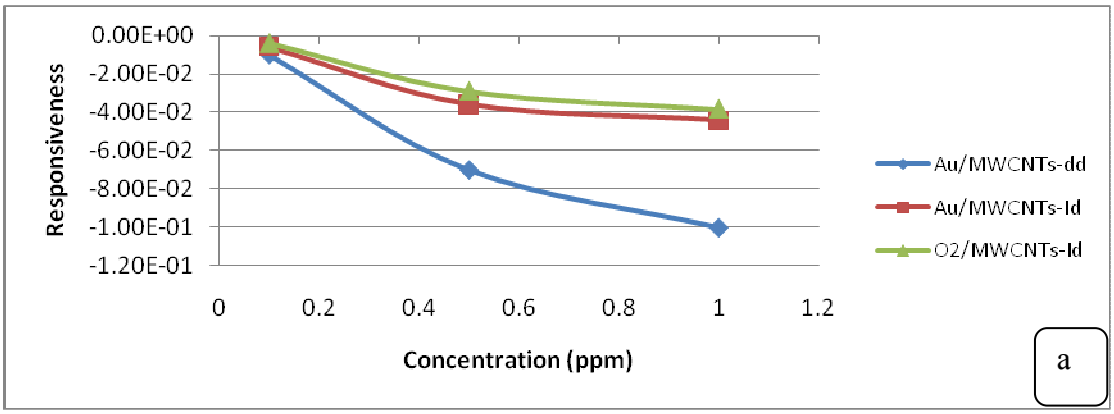

ISBN:978-84-694-0326-6/DL:T-207-2011

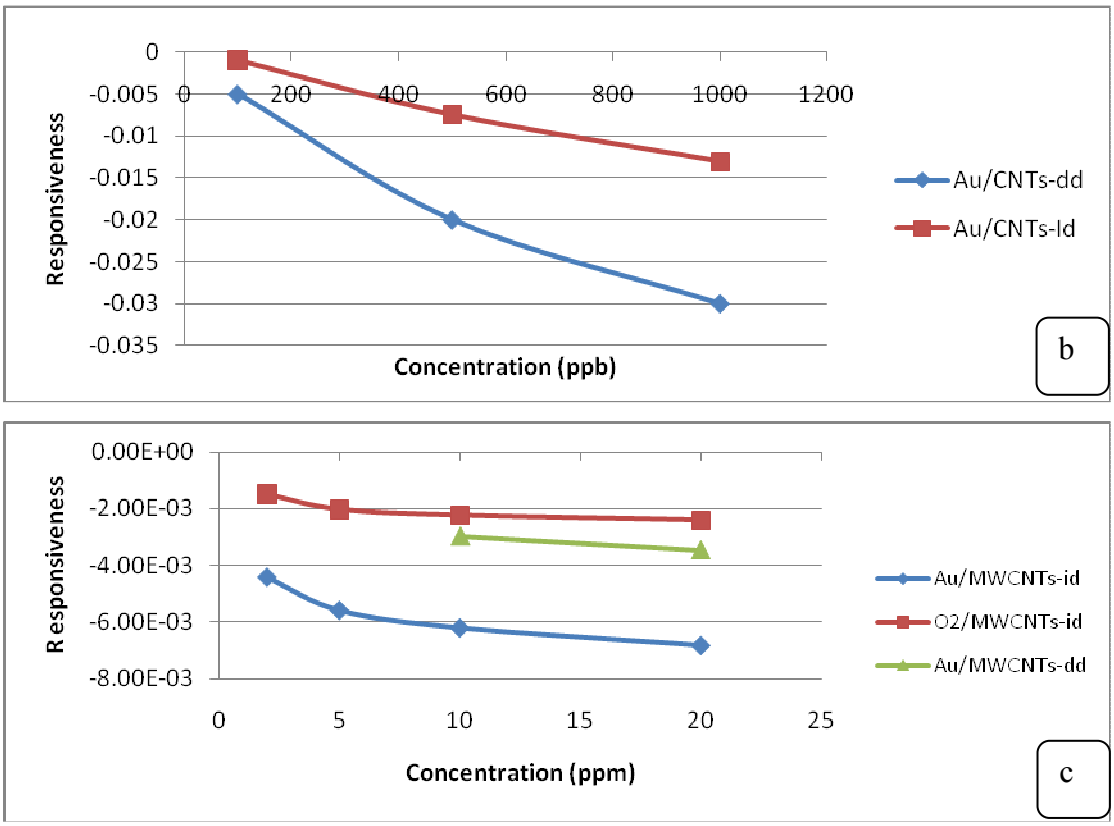

Figure 8: a) Average responsiveness of Au/CNTs (dd-id) and O_2/CNTs sensors for the detection of NO_2 at room temperature. b) Average responsiveness of Au/CNTs (dd-id) sensor for the detection of NO_2 at 150 ºC. c) Average responsiveness of Au/CNTs (dd-id) and O_2/CNTs sensor for the detection of CO at room temperature.

Figures 8.a and 8.b shows the responsiveness towards increasing concentrations of nitrogen dioxide of the different sensors tested when operated at room temperature and at 150ºC, respectively, and the responsiveness towards carbon monoxide at room temperature.

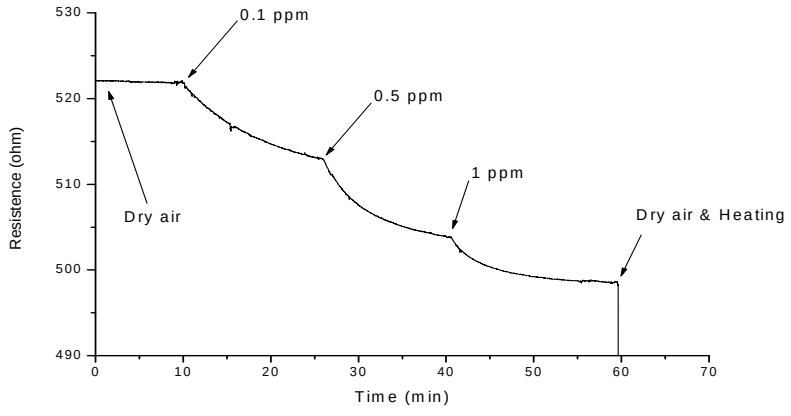

Figure 9: Resistance change of Au/CNTs based gas sensor for NO2 detection at room temperature (Direct drop coating).

In figure 8.a, the responsiveness of Au decorated MWCNTs deposited by the inverse drop coating method is slightly higher than the responsiveness of oxygen functionalized MWCNTs

ISBN:978-84-694-0326-6/DL:T-207-2011

for NO_2 detection at room temperature. This is in agreement with theoretical first principles calculations performed on MWCNTs with oxygenated defects or on Au-decorated MWCNTs, in which charge transfer between the adsorbed gas molecule and the nanotube is enhanced by the presence of Au nanoparticles. In contrast, Au decorated MWCNTs deposited by the direct drop coating method show the highest responsiveness toward NO_2. In these sensors, carbon nanotubes are decorated with some Au nanoparticles but also present oxygenated vacancies, since the thermal treatment removed many gold nanoclusters from the nanotube sidewalls. The presence of such oxygenated vacancies is more important and homogeneously distributed than in sensors deposited by the inverse method. This is due to the fact that the oxygen plasma treatment is performed on nanotube powders and these are stirred during the treatment when the direct drop coating method is employed. Instead, in the inverse drop coating method, nanotubes form a mat already deposited on the sensor substrate when they undergo oxygen plasma treatment and stirring is not possible. As it is known that NO_2 adsorbs both on oxygenated vacancies as gold nanoparticles, the higher and more homogeneous presence of oxygenated vacancies in the direct drop coated sensors could be the reason for the higher responsiveness toward NO_2 found in Au decorated MWCNTs deposited by the direct drop coating method.

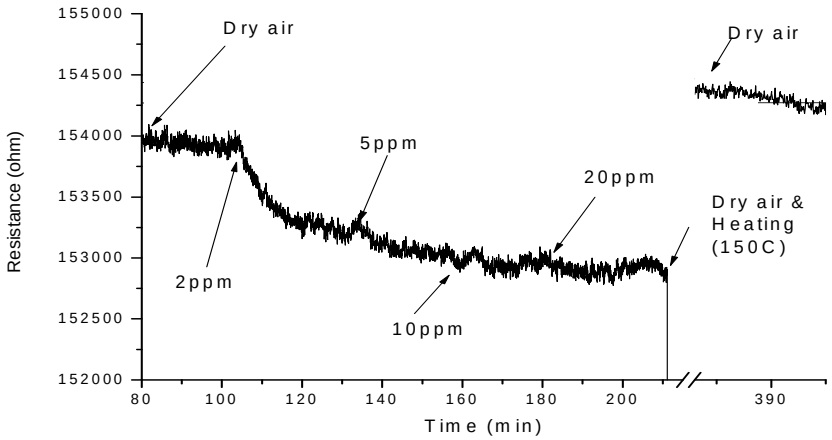

Figure 10: Resistance change of Au/CNTs based gas sensor for CO detection at room

The sensors were far less responsive to CO than to NO_2. The best responsiveness at room temperature towards CO was obtained by sensors based on gold decorated MWCNTs deposited by the inverse drop coating method, while at 150ºC no sensor detected CO. Figure 10 shows the response at room temperature towards increasing concentrations of carbon monoxide for a sensor based on Au decorated multi-walled carbon nanotubes deposited by inverse drop coating. Unlike in the detection of NO_2, the presence of gold nanoparticles on the

ISBN:978-84-694-0326-6/DL:T-207-2011

carbon nanotube sidewalls seems to be essential for enhancing the detection of CO. When CO molecules adsorb at gold nanoparticles, there is an important charge transfer that affects nanotube conductivity. However, gold nanoparticles have a weak interaction with the surface of plasma treated nanotubes. When the film is thermally treated during the process of sensor fabrication in the direct drop coating, nanoparticles are easily removed from CNTs, which causes the number of Au nanoparticles to diminish and so does sensor responsiveness towards CO. In contrast, in sensors fabricated by the inverse drop coating method, carbon nanotubes remain decorated with Au nanoparticles because Au decoration happens after the thermal treatment employed for nanotube deposition onto the sensor substrate.

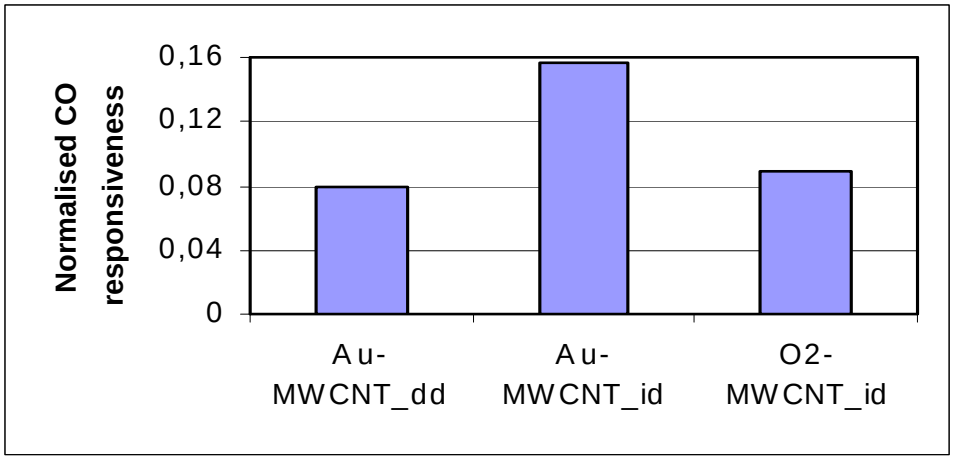

Figure 11: Normalised average responsiveness to CO 20 ppm (normalised to the response towards NO_2, 1 ppm for each sensor considered)

Figure 11 illustrates the normalised responsiveness towards CO for the different types of sensors studied. In this figure, for a given sensor type, CO responsiveness is divided by its NO_2 responsiveness. This confirms that Au-decorated MWCNTs sensors prepared by the inverse drop coating method show the highest responsiveness to CO.

So, from these last results, we can notice that:

- The inverse drop coating method prevents the detachment of metal nanoparticles from the nanotube wall.
- The presence of a high number of metal nanoparticles is essential for enhancing CO detection. The highest CO to NO_2 responsiveness ratio is obtained with the inverse drop coating preparation method. That is, the one that lead to sensing films based on MWCNTs well decorated with Au nanoparticles.
- Selectivity may probably be reached for some gases using array of sensors fabricated by both methods.

ISBN:978-84-694-0326-6/DL:T-207-2011

5.1.1.3. Effect of the operating temperature

The effect of the operating temperature on the sensing properties of active layers has been investigated. It was found that the responsiveness at 150ºC of metal decorated CNT for the tested gases, at the exception of Rh and Pd decorated CNTs, was lower than at room temperature (cf. Annex II). Figure 12.a shows an example of the responsiveness of a Pt/MWCNT sensor towards different concentrations of NO_2 when operated at room temperature and at 150ºC. Figure 12.c shows the responses obtained in the case of a Rh/MWCNT sensor detecting benzene at room temperature and at 150ºC.

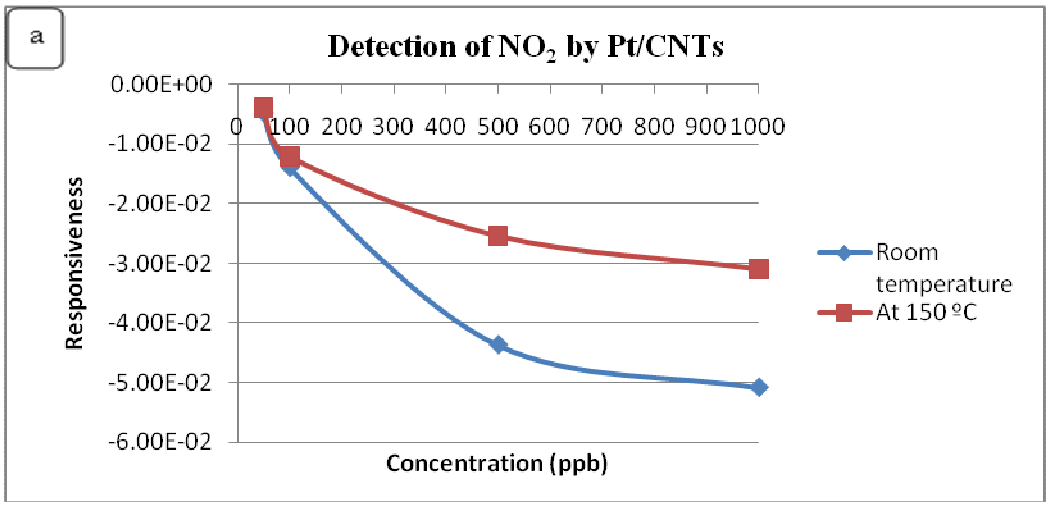

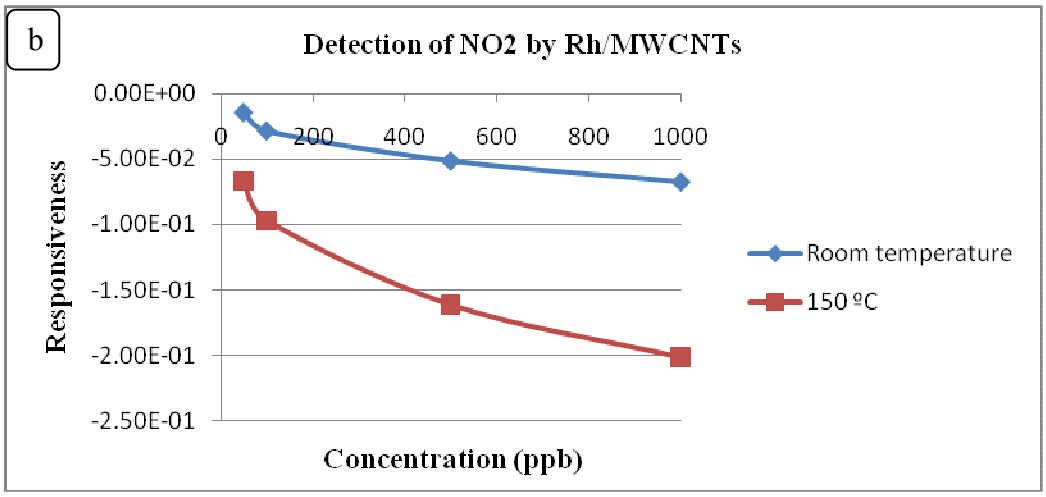

ISBN:978-84-694-0326-6/DL:T-207-2011

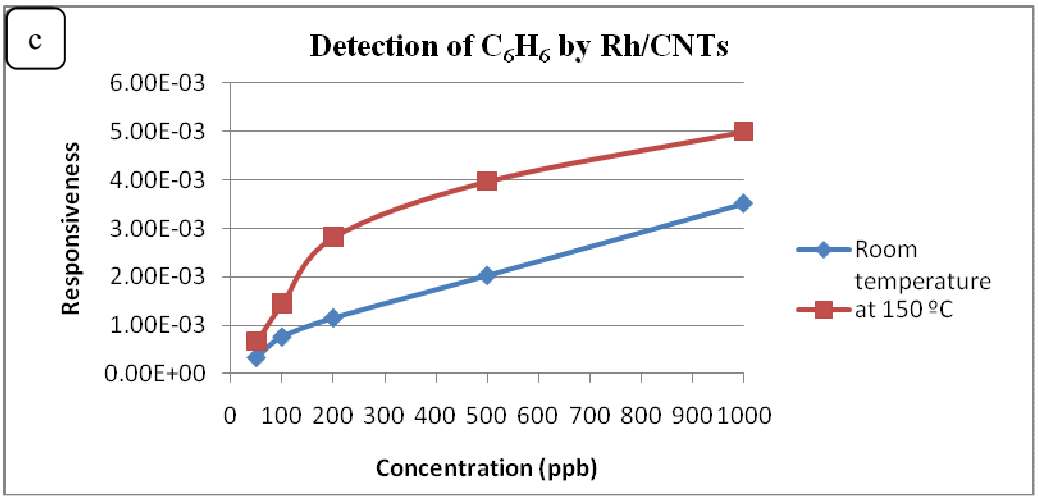

Figure 12: Comparison between the detection at room temperature and 150 ºC for the same metal decorated sample: (a) Example of NO_2 detection using Pt/MWCNTs, (b) Example of NO_2 detection using Rh/MWCNTs and (c) benzene detection using Rh/MWCNTs

An explanation for the behaviour shown in Fig. 12.a is that there are more NO_2 molecules adsorbed on the gas sensitive material at room temperature than at 150ºC, which explains the higher sensor response obtained at room temperature. This was theoretically demonstrated. In fact, it was suggested that at 150 ºC, NO_2 leaves the CNT-surface [1], which is qualitatively in agreement with our experimental results. Peng et al [44], found also experimentally that rising the operating temperature of the sensors up to 150 ºC results in the partial desorption of NO_2 molecules from the surface of metal-doped nanotubes. Penza et al [45] suggested that the lowered gas response of metal-functionalized CNTs at elevated temperatures should be attributed to the reduced catalytic activity of the nanosized catalysts under test.

Unlike with Ni, Pt, Au or Fe decorated CNTs and oxygen functionalized CNTs, the interaction between gas molecules and Rh and Pd decorated CNTs is increased by operating the sensors above room temperature (Figure 12.b).

Rh and Pd decorated CNT have a better sensitivity at 150 ºC than at room temperature, while by contrary, the sensitivity of the other materials drop at 150 ºC compared to room temperature. This seems very interesting from the point of view of selectivity. However, this effect remains not clearly explained in literature. This effect depends on the interaction energy between the metal-decorated CNT and gas molecule. So, the energy given by 150 ºC to the system (gas molecule-(metal decorated CNT)), in some cases, favorizes the interaction between the two systems (gas molecule and metal decorated CNT), while in others, this energy causes the partial desorption of gas molecule. So, further investigation is needed to highlight this point.

ISBN:978-84-694-0326-6/DL:T-207-2011

We have found that most metal decorated CNT sensors decrease their responsiveness when their operating temperature is increased above room tempersture. This is why the final sensor characterization will be performed at room temperature only, which is more interesting from the point of view of lowering power consumption in view of designing a hand-held, battery operated detector.

Summary

In this section, the performance of the sensors towards the different gases tested in terms of sensitivity, reactivity mechanism and response linearity were compared:

- ✓ The importance of oxygen plasma prior to metal decoration was demonstrated.
- ✓ The humidity effect was found to considerably affect the response of those samples due mainly to the presence of oxygen.
- ✓ The interaction mechanism with gases is not totally understood yet, for that reason, two possible mechanisms were proposed here.
- ✓ The reactivity of the different samples was shown to depend on different parameters:

- The nature of the precursors was found to affect the responsiveness of the samples. In fact, organometallic precursors were found to be more suitable for enhancing the sensitivity of the metal decorated samples than solid salt precursors. This was due to the more homogenous distribution of the nanoclusters in the nanotubes surface than to the amount of metal attached.
- Smaller are the metal nanoparticles, higher is their reactivity, but the best response to gases, is achieved by the most isolated nanoclusters which is the case of intermediate sizes (i.e., 5 nm).
- The higher is the amount of nanoclusters of the optimized size, the higher the responsiveness to gases is..
- Finally, the deposition method can tune the response towards a gas or another depending on the gas adsorption site. For example, direct drop coating is preferred for gases like NO_2 which prefers oxygen sites, while inverse drop coating is better for the gases which react more with the metal nanoclusters such as CO.
- The type of the metallic electrodes affects the sensitivity to gases. In fact, some interaction can occur at the interface between the electrodes and active layer resulting in change in the conductivity of the materials. This interaction was found to depend on the target gas (e.g, benzene prefers Pt electrodes while NO_2 prefers Au electrodes). Certain selectivity can be derived from such an effect.

ISBN:978-84-694-0326-6/DL:T-207-2011

- For a given metal decorated sample, the response at ambient temperature was much generally much higher than at 150 ºC, by contrary to Rh and Pd/MWCNTs which need more investigation on their behaviour.
- By adjusting all these parameters, we found good responses to gases which are reported to have weak or no interaction with pristine carbon nanotubes based materials, such as benzene. Also, the detection limits in this case are quite small around 50 ppbs.

✓ Gas sensor based on CNTs, usually present large recovery times at ambient temperature. By subjecting our sensors to heating at 150 ºC, we could diminish the recovery time from 3h at ambient temperature to 15 min under 150 ºC. The desorption can be further quickened by illuminating the sensor using Ultra-Violet (UV) light.

✓ Although sensors are subjected to some baseline drift in some cases, which is often experienced with CNT based chemo-resistive sensors [46], their effects can be minimized in a detector by employing simple baseline correction techniques [47].

We will take advantage from the differences found in the behaviour of the previously studied sensors in order to check the possibility of selectively detecting the different gases tested. An array of sensors using metal decorated MWCTNs will be optimized for attempting this task. This study will be carried out through a PCA analysis.

5.1.2. Evaluation of the selectivity of the nanohybrid sensors through Principal Component Analysis (PCA).

The final aim is to select the best sensors in terms of sensitivity, selectivity and reproducibility towards the gases of interest and to assemble them in an integrated microsensor array. The responsiveness and linearity results were already presented in the previous section (5.1) and annex. II.

The responses obtained from sensors made of 12 different materials were gathered into a database to undergo a PCA analysis (cf. Table 2). In total, 21 sensors were tested towards different gases (NO_2, CO, C_2H_4 and C_6H_6). And for each sensor and gas concentration, four replicate measurements were made in order to better assess the reproducibility of results.

After collection, the raw data was plotted without any previous processing. Since each vapor/gas is unique, each sensing element within the 21 sensors produces a different response and the resulting response vector provides a response signature characteristic of the sample being measured. The principal component analysis was applied to the data set for pattern

ISBN:978-84-694-0326-6/DL:T-207-2011

recognition and or/gas discrimination. PCA was performed employing standard routine from MATLAB.

In this section, we will proceed to the analysis of data taking as variables the 21 loadings (metal decorated samples) in order to check the contribution of each hybrid material in term of sensitivity and the reproducibility of results obtained from the same sensor's material (figure 13.a). This will allow to eliminate the less performant gas sensors, in terms of reproducibility and sensitivity (figure.13.b). The sensor with weak information shown in zone B-figure 13, are eliminated. The 15 remaining sensor's data in loading plots will be plotted in scores plot taking as variables the four tested gases (NO_2, CO, C_2H_4 and C_6H_6). From this plot, we check the discrimination of the different gases. Figure 14 shows that the discrimination of the different gases was reached. In order to select the most four selective sensors towards the gases, we chose from the loading plots of 15 remaining sensor, which give an acceptable information about gases detection, the most separated materials which have the best results in terms of gases sensitivity, response reproducibility and linearity. Thereby, we will chose four materials, by combining them we will produce a sensor array with high sensitivity, good selectivity, response reproducibility and linearity

5.1.2.1. PCA of sensors sorted by metals

- **21 sensors:**

Figure 13 shows the first two principal components for the data of the 21 sensors. In this case, the *X* is a matrix of 21 sensor responses to the different gases. The sensors responses are labeled in table 2 as:

Table 2: The different CNT sensors subjected to PCA with their corresponding new adopted annotations.

X-CNTs	Providing team	New annotation in PCA
O_2	LISE	OxNa
Au	LISE	AuNa
Pd	LISE	PdNa
Ni (1Aº)	LISE	N1Na
Ni (5Aº)	LISE	N5Na
Ni (ID)	LISE	NNa1
Ni (ab)	LISE	NNa2
Rh(5 nm)/Ar+O_2	CHANI	Rh4U1, Rh4U2,

ISBN:978-84-694-0326-6/DL:T-207-2011

		Rh4U3 , Rh4U4
Pt	CHANI	PtU1, PtU2, PtU3
Ni (OMV)	CHANI	NiU1, NiU2, NiU3
Ni (5 nm)	CHANI	N5U1, N5U2, N5U3
Pt (solid)	SAM	PtAl

Figure 13.a shows the PCA results of the 21 sensors sorted by metals, while Figures 13.b and c represents a zoom on zone A and B respectively:

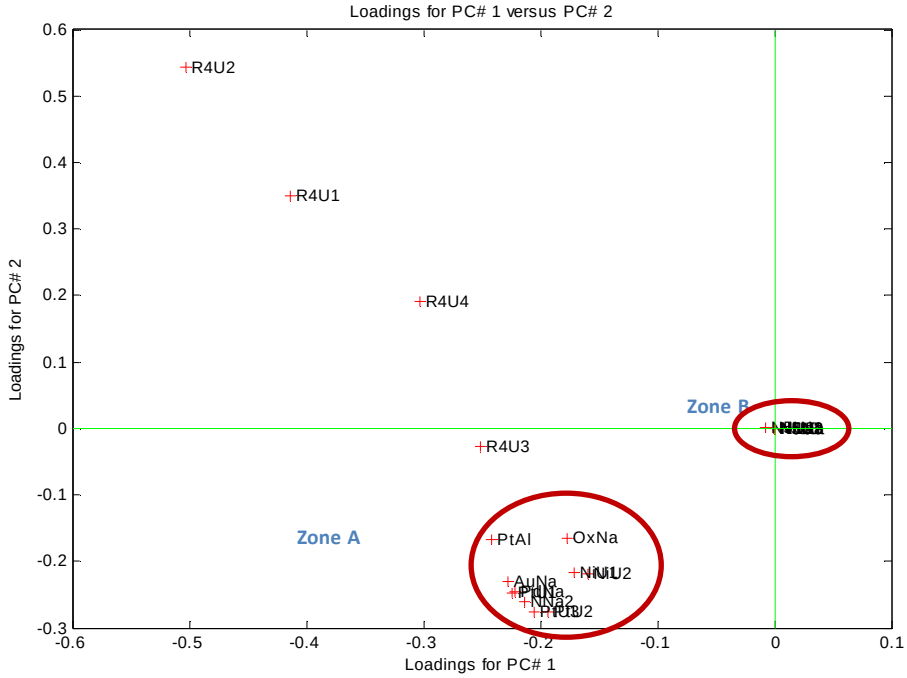

- **Zone A:**

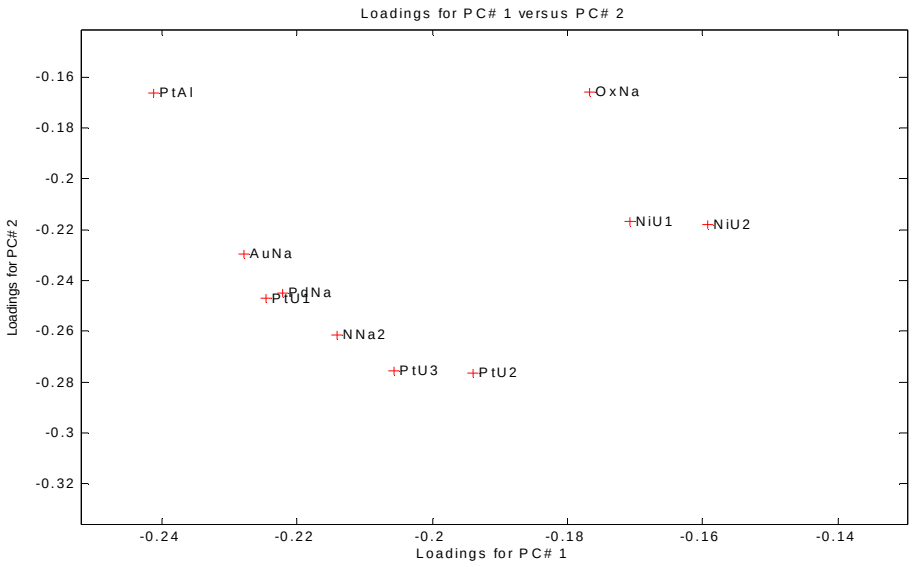

ISBN:978-84-694-0326-6/DL:T-207-2011

- **Zone B:**

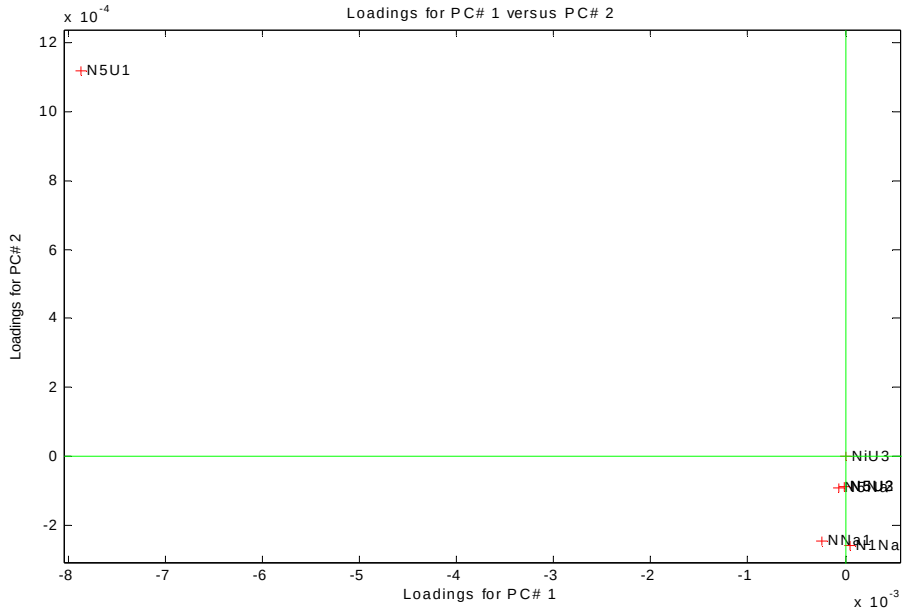

Figure 13: PCA of 21 sensors sorted by metals: (a) The whole plot (b): Zoom Zone A; (c): Zoom Zone B

➢ From the previous results (Figure 13), we can notice that:

- From Zone A, the results obtained with O_2, NiU, PtU, PtAl samples are quite separated.
- Especially, NiU and PtU give quite reproducible results, reflected by the fact that their representing points are overlapped.
- From Zone B, N5U, NNa give non reproducible results and weak information

⇨ For that reason, NNa, N5U will be eliminated.

The PCA analysis will be then repeated for the 15 remaining sensors (Figure 14):

ISBN:978-84-694-0326-6/DL:T-207-2011

- **15 sensors**:

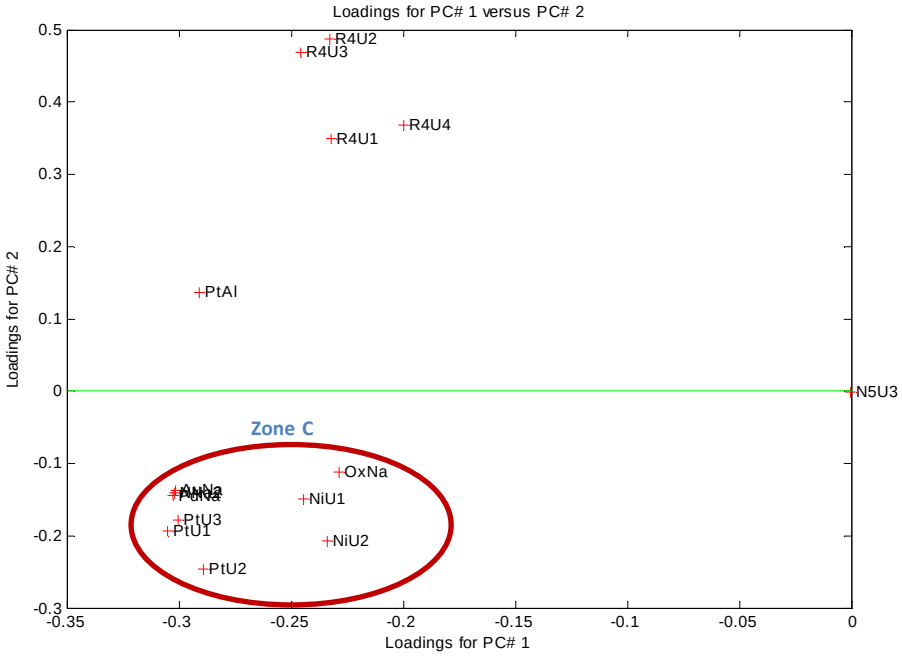

- **Zone C**

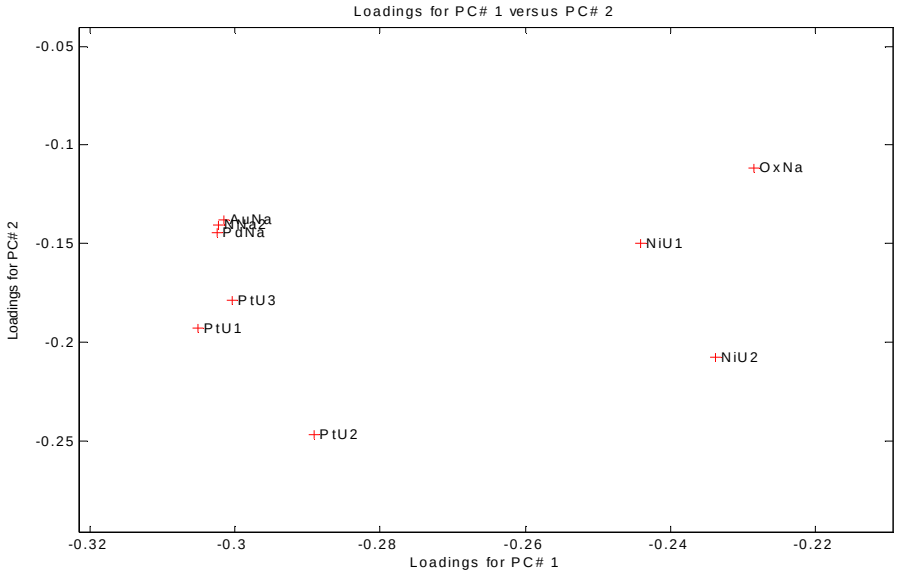

Figure 14: PCA of 15 remaining sensors sorted by metals: (a) The whole plot (b): Zoom Zone C

➢ From these results (Figure 14) , we can notice that:

- Rh based samples give quite reproducible results
- Pd and Au based samples results are quite similar

ISBN:978-84-694-0326-6/DL:T-207-2011

5.1.2.2. PCA of the sensors sorted by gas (scores plot):

- **21 sensors**

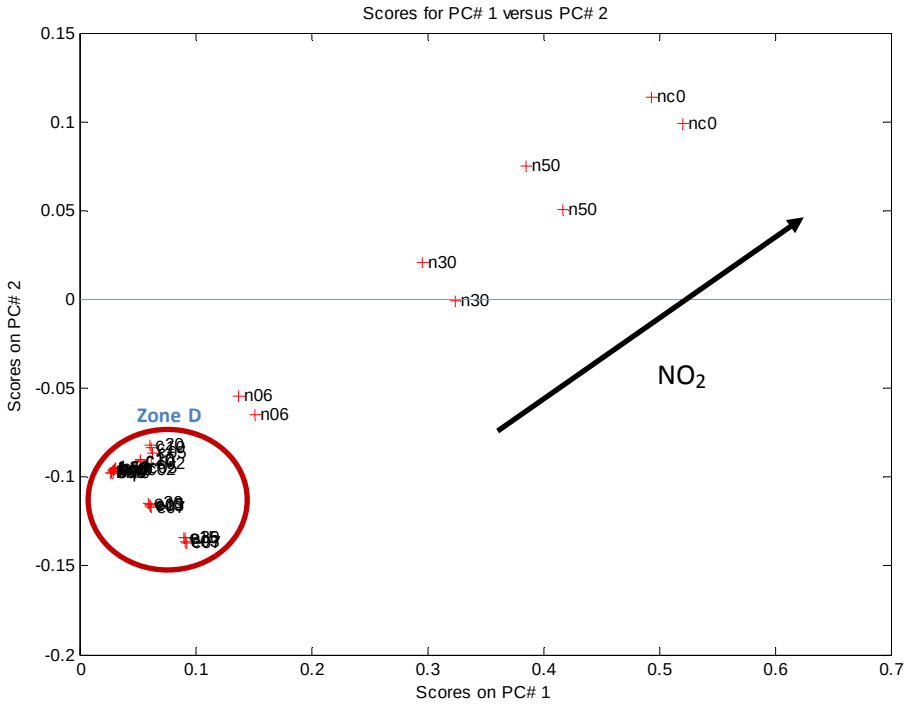

- **Zone D:**

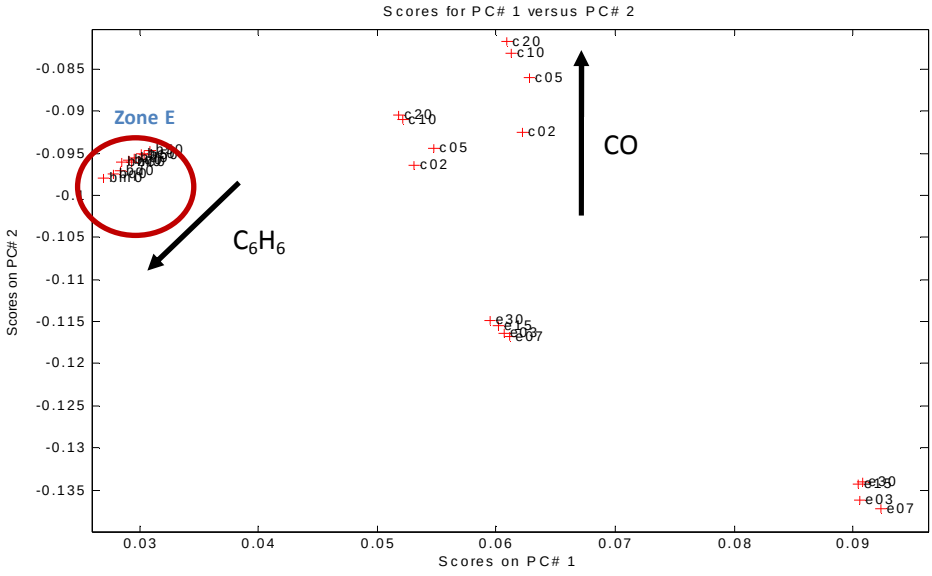

ISBN:978-84-694-0326-6/DL:T-207-2011

- **Zone E:**

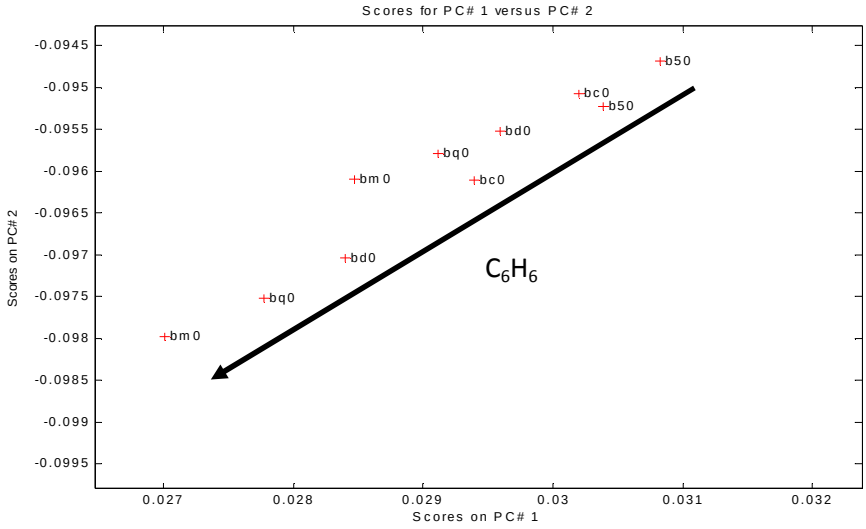

Figure 15: PCA of 15 remaining sensors sorted by metals: (a) The whole plot (b): Zoom Zone D (c): Zoom Zone E

➢ From these results (Figure 15), we can notice that:

- For all sensors, the increase of gas concentration induces response increase.
- PCA shows separation between gases.

- **15 sensors:**

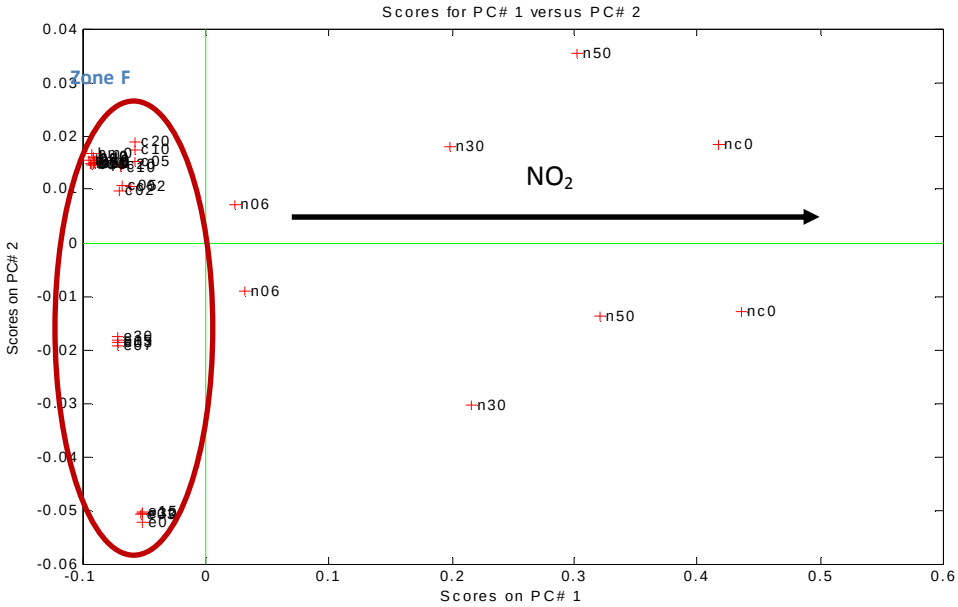

ISBN:978-84-694-0326-6/DL:T-207-2011

- **Zone F:**

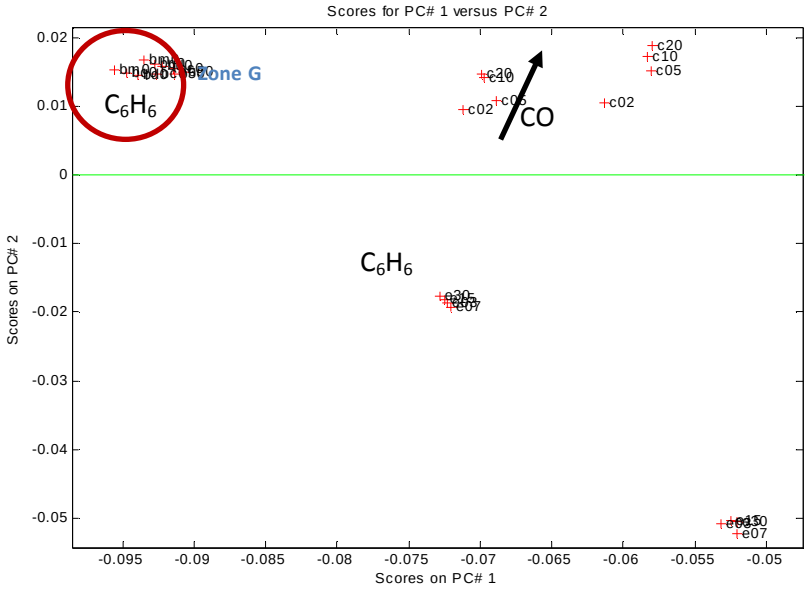

- **Zone G:**

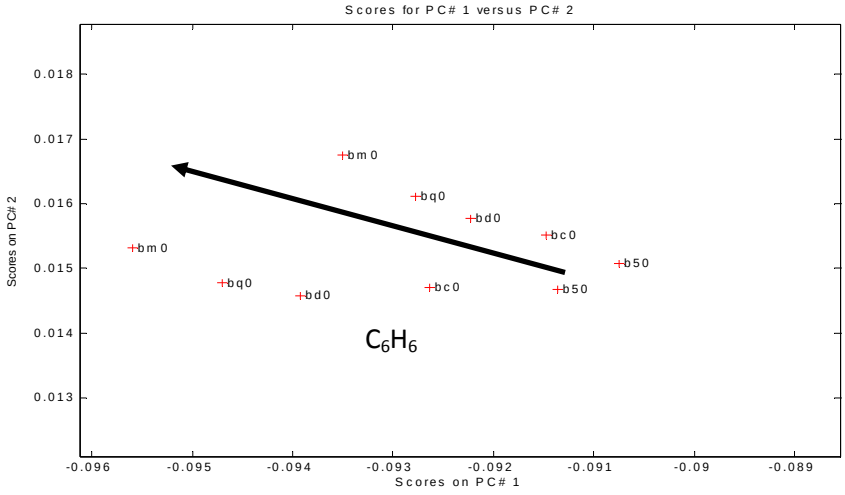

Figure 16: PCA of 15 remaining sensors sorted by metals: (a) The whole plot (b): Zoom Zone F (c): Zoom Zone G

- From the plot of the 15 sensors (Figure 16), we can get the same conclusions as in the case of 21 sensors (Figure 15).

In general, from the PCA plots sorted by metals and by gases, we can see that the most promising results in terms of gases separation and results reproducibility are achieved by: Rh-ULB; Pt-ULB; OxNa; Pt-Al.

We will perform PCA analysis on these four materials.

ISBN:978-84-694-0326-6/DL:T-207-2011

5.1.2.3. Selection of the metal decorated samples for benzene selective detection:

- **PCA on Rh-ULB; Pt-ULB; OxNa; Pt-Al sorted by gases**

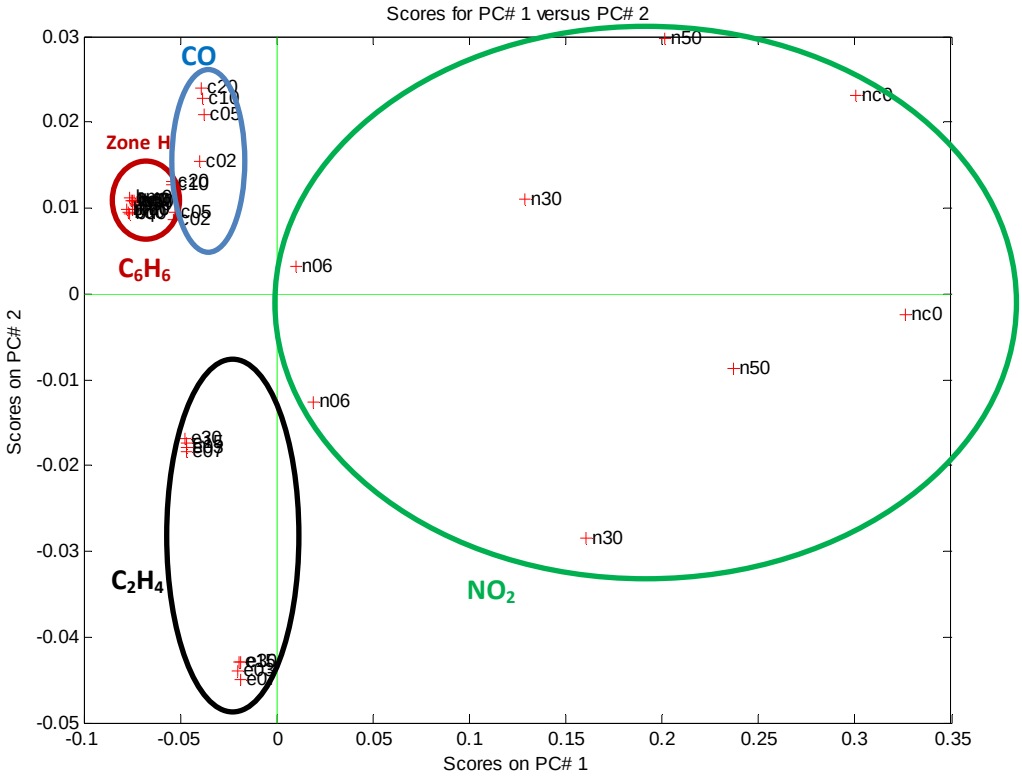

- **Zone H**

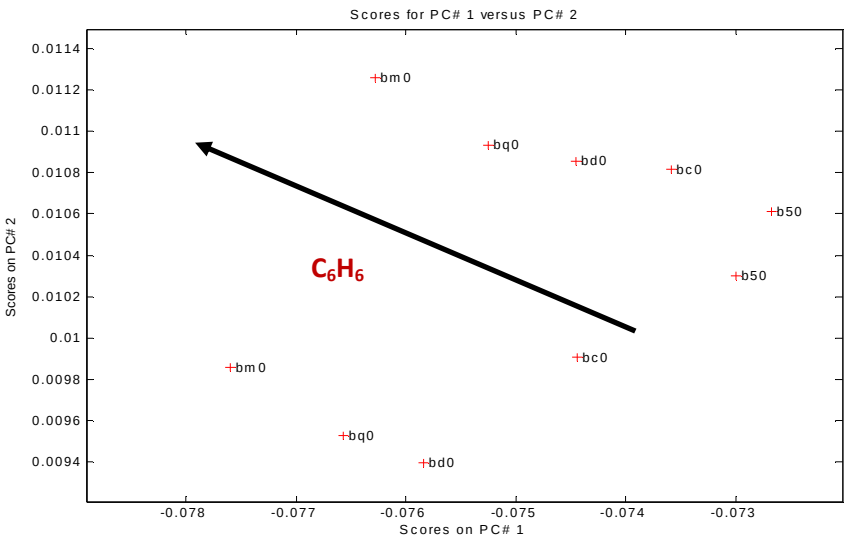

Figure 17: PCA of the four selected sensors sorted by gases: (a) The whole plot (b): Zoom Zone H

ISBN:978-84-694-0326-6/DL:T-207-2011

- From the PCA results (Figure 17), the combination of : Rh-ULB, Pt-ULB, Pt-SAM and O_2-LISE provides a selective response to benzene.
- Rh and Pt are necessary for sensitivity and selectivity reasons. While O_2-LISE can be substituted by Au-LISE or Pd-LISE with similar results.

We have demonstrated a selective detection at room temperature by the combination of four hybrid nanomaterials:

- The sensing performance of the hybrid nanomaterials could be mainly attributed to the different effectiveness of electron transfer between different metal nanoclusters and MWCNTs, to specific reactivities of metal cluster surfaces and, finally, to an increase in the specific surface area of our hybrid nanomaterials.
- When combined in a microsensor array, the use of these benzene-sensitive and benzene-insensitive metal-decorated MWCNTs can provide selective detection of benzene at trace levels (ppb concentration).

Once we have identified the four materials able to selectively detect benzene, the next step consists of preparing the final device based on a miniaturized, four-element, integrated gas sensor array. These materials are (Rh, Pt and Pd decorated MWCNTs and oxygen plasma treated MWCNTs.

A deeper study will be performed on those sensors. Other gases such as H_2S will be tested and the effect of the moisture will be also taken into account. Indeed, the final device will be tested towards the mixture of the previous tested gases in a dry and humid air ambient. The fabrication of the final sensing array and its characterization towards the different gas mixtures will be presented in chapter 6.

Before, we will present the results obtained with other hybrid materials such as metal oxide doped and nitrogen or boron doped carbon nanotubes.

5.2. Gas sensing properties of metal oxide-doped carbon nanotubes

5.2.1. Materials based on commercial metal oxides

The gas sensing properties of the different hybrid materials produced (section 3.1.2) (Au-MWNTs; Ag-MWNTs; SnO_2; WO_3; Au-MWNTs/SnO_2; Ag-MWNTs/WO_3) (Annex III) were evaluated in terms of responsiveness. Sensors based on SnO_2 mixed with Au-decorated MWCNT hybrids were the most sensitive to NO_2 among the different materials studied,

ISBN:978-84-694-0326-6/DL:T-207-2011

outperforming the responsiveness of either pure SnO_2 or pure Au-decorated MWCNT materials when operating both at 250 and 150 ºC. Typical responses of metal-decorated MWCNT/SnO_2 gas sensors to NO_2 are shown in Figure 17. The fluctuation in the response signal that occurs at high NO_2 concentrations is due to the increased effect of noise when sensor resistance becomes very high (i.e. comparable in magnitude to the input impedance of the multimeter employed to acquire it).

5.2.1.1. Effect of the doping ratio respect to the sensing temperature

The quantity of nanotubes dispersed in the SnO_2 matrix was found to play a determinant role in the responsiveness of the hybrid materials to NO_2. At a concentration ratio of 1/250 wt%, the responsiveness of the hybrids made of metal decorated MWCNTs (either using Au or Ag dopants) and SnO_2 was significantly superior to that with the 1/500 wt% ratio when the detection of NO_2 was performed at 250 ºC. When the operating temperature of sensors was lowered to 150 ºC, the particular type of metal decorating the carbon nanotubes played also an important role in the NO_2 detection. Thus, at 150 ºC a concentration ratio of 1/250 wt% of carbon nanotubes dispersed in the SnO_2 matrix was the most appropriate when Au was used as a dopant, while 1/500 wt% of Ag-decorated MWCNT added to SnO_2 was the most suitable for this latter case. On the other hand, similar values of responsiveness were found at 150 ºC for both Au-MWCNT/SnO_2 and Ag-MWCNT/SnO_2 (1/500 wt%) materials. Furthermore, it is worth mentioning that the response of the hybrid films based on SnO_2 became already saturated after the injection of only 500 ppb of NO_2 at the working temperature of 150 ºC (Figure 17 b).

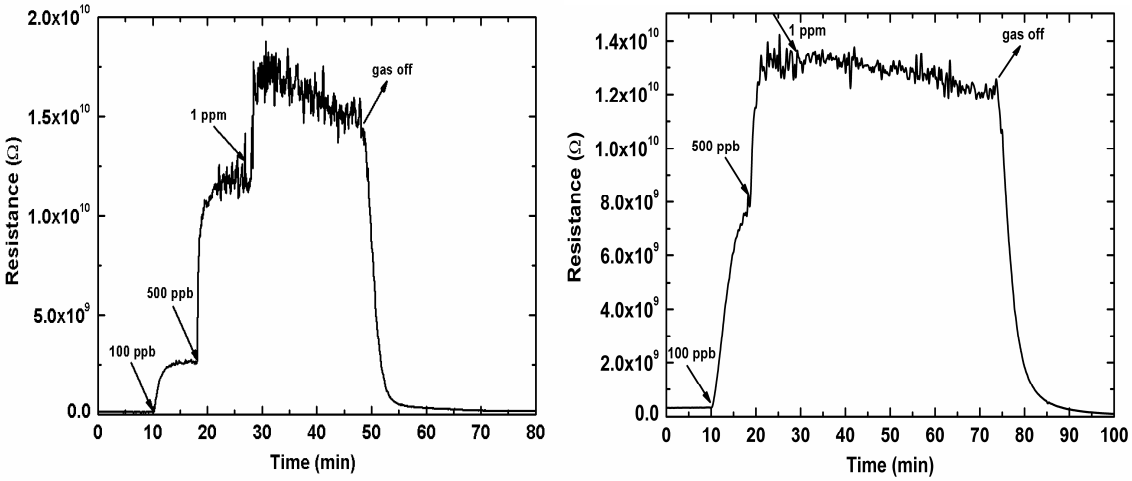

Figure 17. Response to NO_2: (a) detection at 250 ºC with Au-MWCNT/SnO_2 (1/250 wt%) sensor; (b) detection at 150 ºC with Au- MWCNT/SnO_2 (1/250 wt%).

ISBN:978-84-694-0326-6/DL:T-207-2011

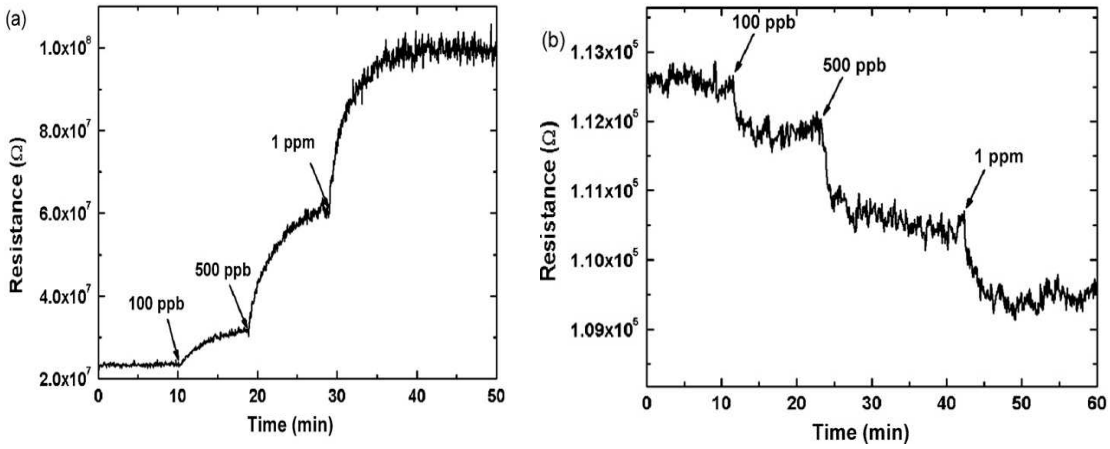

Figure 18. (a)NO_2 detection at 150 ºC with Ag-MWCNT/WO_3 (1/500 wt%) sensor; (b) NO_2 detection at 150 ºC with Ag-MWCNT/WO_3 (1/250 wt%) sensor.

Regarding the responsiveness towards NO_2 of the hybrid materials based on WO_3 (see Fig. 18), it was at least one order of magnitude below the one obtained by the hybrids based on SnO_2. The quantity of nanotubes embedded in WO_3 was of important relevance. Thus, when the sensors were operated at 250 ºC, only metal-decorated MWCNT dispersed in the WO_3 matrix in a concentration ratio of 1/500 wt% were able to detect NO_2 (the metal used as a dopant did not change sensor performance in this case), while at 150 ºC, the semiconducting behavior of the metal-decorated MWCNT/WO_3 hybrids changed from n-type at a concentration ratio of 1/500 wt% to p-type at 1/250 wt%. For the measurements performed at 250 ºC, the response time to 100 ppb and to 500 ppb of NO_2 was around 2 min both for the hybrid materials based on WO_3 and for the pure WO_3 sensors. It rose to 3 min in the case of hybrids based on SnO_2, but in this latter case it compared very favorably to the one of pure SnO_2 sensors, which did not reach completely a steady state regime 15 min after gas injection. When the sensor operating temperature was lowered and NO_2 test measurements were performed, the sensors needed a longer time to reach the steady state. The response times varied between 6 and 10 min for hybrid sensors and were over 15 min for pure metal oxide sensors. Recovery time varied between 10 and 20 min for Au-based hybrid sensors (see Fig. 17) and was over 30 min for Ag-based hybrids and pure metal oxide sensors. The second air pollutant tested was carbon monoxide. The highest responsiveness in the case of the CO tests was again achieved by the hybrid sensors based on Au-decorated MWCNT and SnO_2 in a concentration ratio of 1/250 wt%, operated at 250 ºC (see Fig. 19). Although lower, some responsiveness was also obtained at 150 ºC by the hybrid sensors containing SnO_2. Similarly to the detection of NO_2, when CO was tested Au based hybrid sensors showed response and

ISBN:978-84-694-0326-6/DL:T-207-2011

recovery times of about 5 min (operated at 250 ºC), while the response and recovery times of pure metal oxides was higher than 15 min. When the metal oxide employed was WO_3, the only hybrid based on this material that responded to CO was Ag-MWCNT/WO_3 in the concentration ratio of 1/500 wt% at an operating temperature of 250 ºC. When the Ag-MWCNT/WO_3 sensor (concentration ratio 1/250 wt%) was operated at 250 ºC, it behaved as an n-type semiconductor in the presence of CO; operated at 150 ºC it did not respond at all to CO; while at room temperature its behavior was equivalent to an n-type semiconductor.

- This behavior clearly suggests that not only the amount of carbon nanotubes present determines the semiconducting character of the resulting hybrid material, but also that the operating temperature can play an important role in the sensing mechanism. Unlike oxygen-functionalized MWCNT/SnO_2 hybrid materials, which showed good responsiveness to NO_2 at room temperature [48], metal-decorated MWCNT/metal oxide hybrid materials were not responsive at room temperature. Regarding the response of the gas sensors to the other two pollutants tested (i.e., benzene and ammonia), they were not able to detect the presence of these two contaminants at a concentration level up to 10 ppm in the case of NH_3 and up to 150 ppm in the case of C_6H_6, for the operating temperatures investigated.

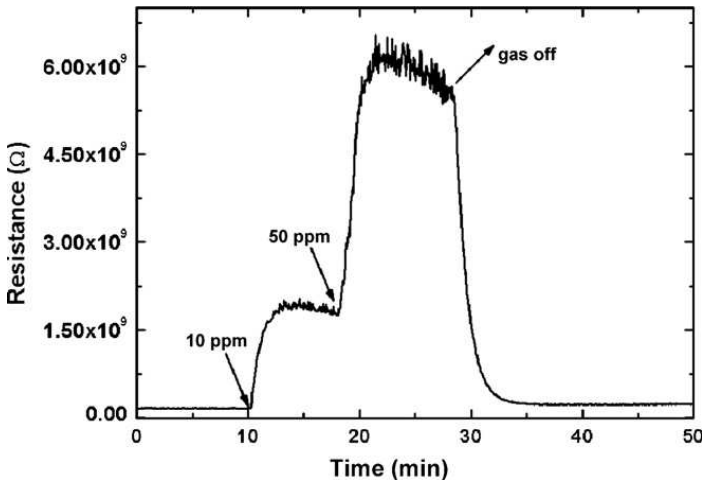

Figure. 19. CO detection at 250 ºC with Au-MWCNT/SnO2 (1/250 wt%) sensor

ISBN:978-84-694-0326-6/DL:T-207-2011

5.2.1.2. Understanding the detection mechanism of metal oxide doped carbon nanotubes

On the basis of the images of the hybrid films recorded by SEM analyses (Fig 1, section 3.1.2.), it can be derived that MWCNTs are embedded within the metal oxide matrix. It has been reported that in hybrid films, two different depletion layers (and associated potential barriers) co-exist [49-50]: one depletion layer is located at the surface of the grains of the metal oxide film and the other one at the interface between MWCNT and metal oxide films. Since SnO_2 or WO_3 films behave as n-type semiconductors and MWCNT films behave as p-type semiconductors [51-52], it can be suggested that the hetero-structure n-SnO_2/p-MWCNT (n-WO_3/p-MWCNT) is formed at the interface between tin oxide (tungsten oxide) and carbon nanotubes. Furthermore, our results indicate that the addition of metal nanoclusters at the CNT surface plays a fundamental role in improving the sensing properties. Studies are being performed to establish if the metal clusters at the CNT surface act lowering the potential barrier of the depletion layers and/or enhancing specific gas adsorptions or promoting specific chemical reactions.

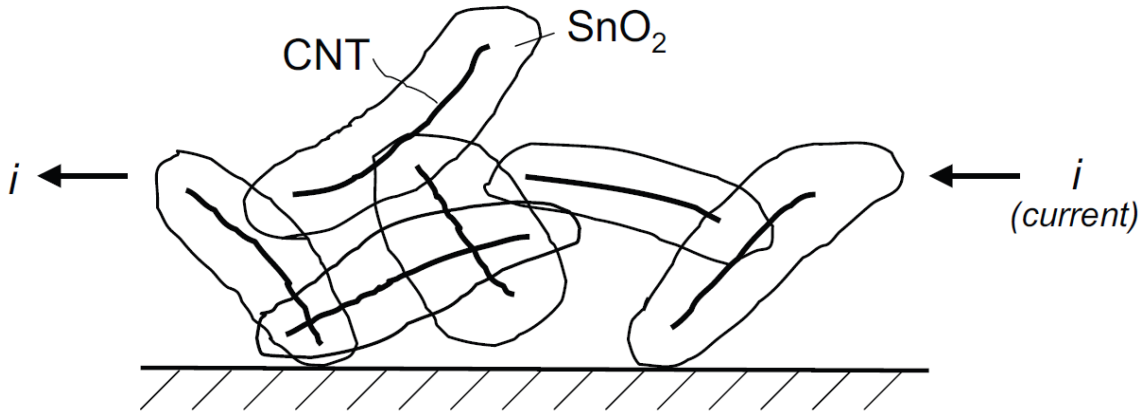

Figure. 20. Schema suggesting how the CNTs are imbedded in metal oxides based on SEM images [49]

Considering the sensitivity of the hybrid films (see Table 3), it can be derived that the adsorption of NO_2 or CO at the metal oxide modifies the depletion layer at the surface of its grains and also at the n-metal oxide/p-MWCNT heterostructures. This combined effect may explain the improvement in responsiveness shown by tin or tungsten oxide-based hybrid sensors as compared with either pure metal oxides, metal decorated CNT based gas sensors [53] or WO_3 or SnO_2 metal oxides doped with Au or Ag noble metals [54-56]. The results obtained indicate also that the number of CNT added to the metal oxide matrix has to be

ISBN:978-84-694-0326-6/DL:T-207-2011

extremely small. The best results were obtained with the SnO_2/CNT hybrids, when the presence of the carbon nanotubes was undetectable by normal SEM analysis. This is in concordance with the results published by Wei et al. [49]. We expect that keeping extremely low the number of CNT added to the metal oxide matrix, improved results in terms of sensitivity to NO_2 and CO can be obtained.

The lack of responsiveness observed for NH_3 and C_6H_6 by the new hybrid sensors can be associated to the non-appropriateness of the used combination of materials for detecting such species, as suggested by Penza et al. [57] who found that Au-CNT is an appropriate material for detecting NO_2 while Pt-CNT is more suitable for detecting benzene or ammonia.

❖ **Conclusion**

- In this section, we have shown that the addition of a small quantity of metal-decorated MWCNT to metal oxides can significantly improve the detection capability of metal oxide based sensors and lower the operating temperature.
- In particular, micro-sensors based on Au-MWCNT/SnO_2 hybrid films in a concentration ratio of 1/250 wt% showed the highest sensitivity towards NO_2 and CO, among the different materials studied.
- The response mechanism is fully reversible, since the sensors can recover their baseline resistance after each exposure to pollutant gases. Our results suggest that there is an optimum amount of carbon nanotubes to be added to each particular metal oxide in order to enhance the responsiveness.
- Material characterization analysis (performed by SEM and TEM) showed that the nanotubes endured the process of deposition and subsequent annealing at 450 ºC in air, but at the same time, part of the metal nanoclusters decorating the nanotube surface was detached.
- Based on these results, the modulation of the width of two depletion layers existing at the surface of metal oxide grains and at the interface of metal oxide grains and MWCNT, respectively, is postulated as the mechanism that could explain the enhanced performance of hybrid metal oxide/MWCNT sensors in comparison with pure metal oxide or pure MWCNT sensors.

ISBN:978-84-694-0326-6/DL:T-207-2011

5.2.2. Materials based on home-synthesized metal oxide

5.2.2.1. Comparison of the sensing properties of pure and doped materials

The gas sensing properties of the different materials were investigated. In addition to the sensors based on SnO_2-decorated plasma-treated carbon nanotube hybrid materials, sensors based on pure tin oxide nanoparticles and on pure plasma-treated carbon nanotubes were also fabricated and characterized. This enables comparing the performance of the different materials, and better understanding the gas sensing behavior of hybrid materials.

In the case of the nanotubes mixed with commercial metal oxides, it was found that the nanotubes are embedded in the metal oxide (see section 3.1.2.). The scheme of figure 20 gives an idea of how could be the morphology of the mixture. By contrast, in the case of carbon nanotubes decorated with homemade metal oxide, it was found that isolated nangraines are attached to the nanotubes walls (see section 3.2.2, figure.2.b). The scheme in figure 21 shows how could be the morphology of the composite. This difference in the morphology of the composites can result in different sensing mechanism, which we will discuss later.

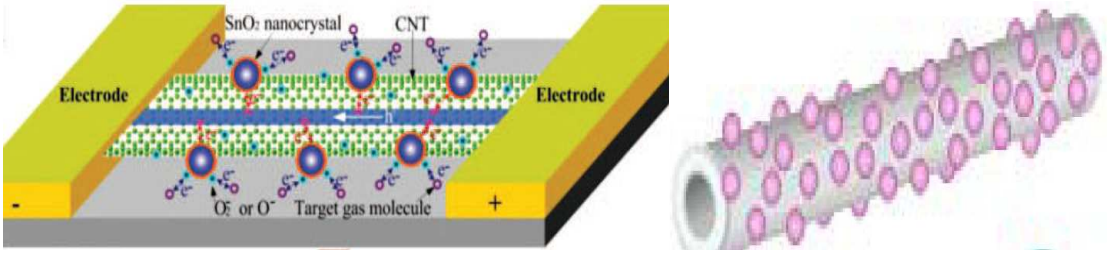

Figure. 21. Scheme suggesting how the CNTs are decorated with discrete metal oxides nano-grains [64]

Pure tin oxide gas sensors did not show responsiveness to any of the species tested, namely, nitrogen dioxide (up to 1 ppm) and carbon monoxide (up to 20 ppm). This result is not surprising because sensors were operated either at room temperature or at 150ºC and it is well known that pure tin oxide films are not responsive to gases at such low operating temperatures [58]. On the other hand, when operated at room temperature, sensors based on pure oxygen plasma-treated MWCNTs were responsive to nitrogen dioxide and carbon monoxide (Figure 22). When operated at 150 ºC, these sensors were not responsive to any of the species tested. This suggests that the interaction between nitrogen dioxide or carbon monoxide and plasma-treated MWCNTs is mild (i.e., mainly physisorption) and involves a small amount of charge

ISBN:978-84-694-0326-6/DL:T-207-2011

transfer between adsorbed species and carbon nanotubes [59]. As said in section 5.1.1, when the surface of carbon nanotubes is heated to 150 ºC, the amount of species physisorbed at the tube sidewalls is significantly reduced and the electrical conductivity of the tubes is not affected to a measurable extent.

Hybrid nanomaterials are remarkably sensitive to nitrogen dioxide and carbon monoxide, especially when the sensors based on such materials are operated at room temperature.

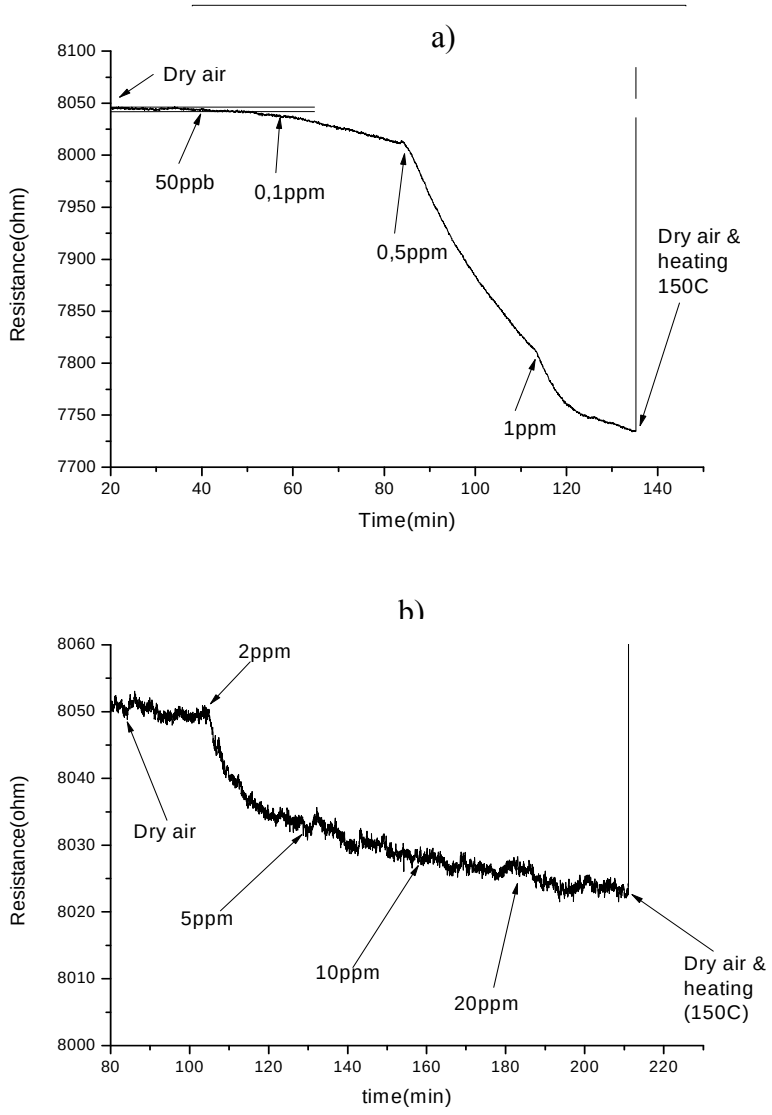

Figure 22: Response of oxygen plasma treated carbon nanotube towards increasing concentrations of: a) nitrogen dioxide and b) carbon monoxide, at room temperature .

5.2.2.2. Effect of the doping ratio

At room temperature, the highest responsiveness to these gases was obtained for sensors that contained an intermediate amount of tin oxide (i.e., prepared with 12 mg of plasma treated

ISBN:978-84-694-0326-6/DL:T-207-2011

nanotubes dispersed in 20 ml of the precursor solution). While sensors based on hybrid nanomaterials with the lowest content of tin oxide (i.e., 10 ml of the precursor solution) showed diminished responsiveness to nitrogen dioxide and carbon monoxide, the sensors employing nanomaterials with the highest content of tin oxide (i.e. 40 ml of the precursor solution) showed a dramatically reduced sensitivity to these gases. When operated at 150 ºC, all sensors based on hybrid nanomaterials decreased their responsiveness to nitrogen dioxide and carbon monoxide. Table 3 summarizes these results. For carbon monoxide, saturation in sensor response is observed in some cases. From the results reported in Table 3, it can be derived that there is an optimal ratio between the amounts of oxygen plasma functionalized carbon nanotubes and tin oxide precursors in order to maximize the responsiveness towards carbon monoxide and nitrogen dioxide. If the amount of tin oxide is too low, the sensors based on the resulting hybrid nanomaterial show a responsiveness that is only slightly ameliorated when compared to the one of sensors based on pure carbon nanotubes. However, when the amount of tin oxide is too high, sensors dramatically reduce their responsiveness, approaching the behavior of pure tin oxide sensors.

5.2.2.3. Detection mechanism of metal oxide doped carbon nanotubes towards NO_2 and CO

Figure 23 shows the response towards increasing concentrations of nitrogen dioxide for two sensors based on carbon nanotube and tin oxide hybrid nanomaterials. Both sensors employ the same gas sensitive material resulting from the mixture of an intermediate amount of tin dioxide precursor (i.e. 20 ml) with 12 mg of oxygen plasma treated MWCNTs (i.e., close to the optimal ratio).

Figure 23. a. shows the response of a sensor operated at room temperature. The sensor is based on hybrid material prepared with an intermediate amount of tin oxide precursor (i.e. 20 ml). Sensor resistance decreases when the concentration of NO_2 increases. Tin dioxide is an *n*-type semiconductor, oxygen plasma treated carbon nanotubes behave as mild *p*-type semiconductors [60] and NO_2 is an oxidising gas (i.e. upon adsorption, it accepts electron charge from carbon nanotubes or tin oxide nanoclusters). Considering these aspects, room temperature detection mechanisms can be postulated as follows. NO_2 can physisorb on the carbon nanotube sidewalls and on tin oxide nanoclusters. In the former case, each adsorbed molecule traps electrons from the nanotube, which results in a conductivity increase for the nanotube (*p*-type). This is the mechanism that explains why nitrogen dioxide can be detected by plasma treated carbon nanotubes at room temperature.

ISBN:978-84-694-0326-6/DL:T-207-2011

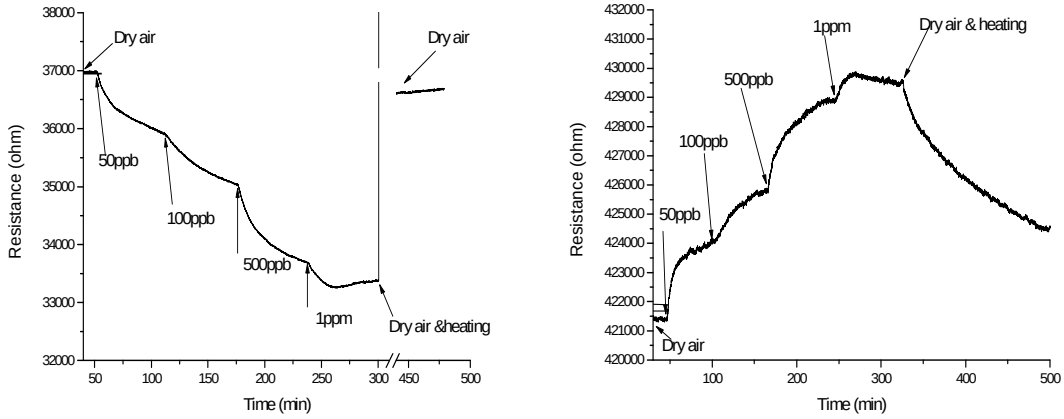

Figure 23: Response of tin oxide decorated oxygen plasma treated carbon nanotube hybrids towards increasing concentrations of nitrogen dioxide. Sensors were operated at room temperature (a) and at 150ºC (b).

In the latter case, adsorbed nitrogen dioxide accepts electrons from the tin dioxide nanocluster and this in turn causes an effective electronic charge transfer from the carbon nanotube towards the tin oxide nanocluster. Once again this charge transfer causes the conductivity of the nanotube to rise. Macroscopically, both mechanisms contribute to a decrease in sensor resistance, but the second mechanism explains why sensors based on hybrid tin oxide and CNT materials are more responsive than those based on pure CNT materials.

Figure 23 *b* shows the response of a similar sensor operated at 150ºC. Unlike when operated at room temperature, the sensor resistance increases when the concentration of nitrogen dioxide increases. This is too high a temperature for sensors based on our pure CNT materials to detect NO_2 (see Table 3), possibly due to temperature-favored NO_2 desorption from CNT sidewalls. Additionally, this is too low a temperature for sensors based on our pure tin oxide nanoparticles to detect NO_2 (see Table 3). Assuming that in a film of tin oxide nanoparticles, conductivity is mobility-limited by the potential barriers that develop at the boundaries of nanograins [61-63], higher operating temperatures (than 150ºC) are needed to ensure that a significant amount of electrons can tunnel potential barriers at grain boundaries and contribute to the overall conductance of the film. In other words, to ensure that free carriers are effectively collected by the electrodes. Therefore, when our hybrid CNT-SnO_2 materials are operated at 150ºC, the nitrogen dioxide detection mechanism is based on the change in the number of conduction electrons available after NO_2 is adsorbed on tin oxide nanoparticles (adsorbed NO_2 traps electrons).

ISBN:978-84-694-0326-6/DL:T-207-2011

Table 3: Average responsiveness (and associated standard deviation) towards different concentrations of nitrogen dioxide and carbon monoxide for the different sensors developed. Sensors were operated at room temperature and at 150 ºC

Temperature	Species	Concentration	SnO_2	CNT/SnO2_low	CNT/SnO2_mid	CNT/SnO2_high	CNT
R.T.	NO_2	50 ppb	< 0.01	0.68 (0.0027)	2.77 (0.0003)	< 0.01	< 0.01
		100 ppb	< 0.01	1.24 (0.0050)	4.59 (0.0046)	0.039 (0.00004)	< 0.01
		500 ppb	< 0.01	2.29 (0.0035)	8.12 (0.0050)	0.065 (0.00004)	0.69 (0.0002)
		1000 ppb	< 0.01	2.94 (0.0006)	10.20 (0.0031)	0.088 (0.00009)	1.56 (0.0019)
	CO	2 ppm	< 0.01	0.45 (0.0014)	3.39 (0.0029)	< 0.01	0.15 (0.0004)
		5 ppm	< 0.01	0.59 (0.0006)	4.04 (0.0024)	0.012 (0.00001)	0.20 (0.0004)
		10 ppm	< 0.01	0.65 (0.0004)	4.29 (0.0005)	0.017 (0.00002)	0.22 (0.0006)
		20 ppm	< 0.01	0.69 (0.0012)	4.20 (0.0002)	0.022 (0.00001)	0.24 (0.0005)
150ºC	NO_2	50 ppb	< 0.01	0.63 (0.0008)	0.06 (0.0001)	< 0.01	< 0.01
		100 ppb	< 0.01	1.02 (0.0013)	0.17 (0.0001)	< 0.01	< 0.01
		500 ppb	< 0.01	1.76 (0.0023)	0.41 (0.0002)	< 0.01	< 0.01
		1000 ppb	< 0.01	1.95 (0.00031)	0.46 (0.0002)	< 0.01	< 0.01
	CO	2 ppm	< 0.01	0.41 (0.0004)	< 0.01	< 0.01	< 0.01
		5 ppm	< 0.01	0.39 (0.0004)	< 0.01	< 0.01	< 0.01
		10 ppm	< 0.01	0.39 (0.0002)	< 0.01	< 0.01	< 0.01
		20 ppm	< 0.01	0.41 (0.0003)	< 0.01	< 0.01	< 0.01

ISBN:978-84-694-0326-6/DL:T-207-2011

Unlike when pure tin oxide was employed, in our hybrid material the presence of a mesh of multiwall carbon nanotubes embedded within the tin oxide nanoparticles helps reducing the number of potential barriers. A conduction electron needs to cross to reach the electrodes. Although meshes of oxygen plasma treated MWCNT behave macroscopically as mild *p*-type semiconductors, many nanotubes present are of metallic nature, which explains this reduction in the number of potential barriers an electron needs to cross. In such a situation, even a small change in the number of charge carriers available (caused by NO_2 adsorption) can be easily detected as a resistance change, which explains the macroscopically observed *n*-type nature of our hybrid nanomaterials when operated at 150ºC. This is further supported by the fact that the baseline resistance of sensors based on hybrid nanomaterials is significantly lower than the one of those based on pure tin oxide nanoparticles (carbon nanotubes are responsible for lowering the overall resistance of the gas sensitive film).

Sensor based on the mixture of an intermediate amount of tin dioxide precursor (i.e. 20 ml) with 12 mg of oxygen plasma treated MWCNTs (i.e., close to the optimal ratio) which shows a highest response towards CO detection (figure.24), shows a decrease in its resistance when exposed to CO. in contrast CO is considered as reducing gas. So, because of p-type of the sensor active layer, the conductivity should decrease. This new result has been observed by Ganhua Lu et al [64]. They have attributed such reaction behaviour to the presence of CO that leads to more O_2 adsorption (higher saturation concentration of oxygen adsorbates) due to a decrease in the work function of SnO_2 nano-grains [65] which leads to the increase of sensor conductivity. However, this mechanism has not yet been proved and more investigation is needed to understand the exact sensing mechanism,.

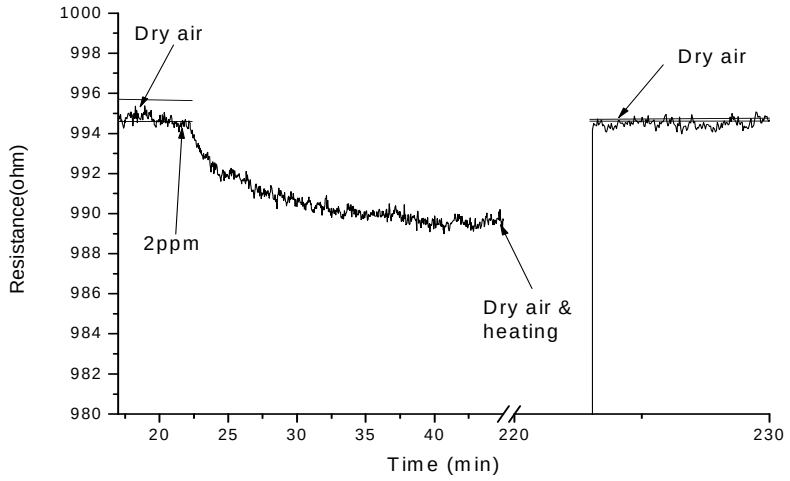

Fig.24. Response of tin oxide decorated oxygen plasma treated carbon nanotube Hybrids (mid) towards 2ppm of CO operated at room temperature.

ISBN:978-84-694-0326-6/DL:T-207-2011

5.2.2.4. Effect of moisture

The responses induced by changes in ambient moisture from 0% to 50% and from 0 % to 80 % relative humidity were investigated, than we had a look on the effect of humidity passing from 50 % to 80 %. Measurements were conducted at room temperature only, since this was optimal for reaching the highest responsiveness towards nitrogen dioxide or carbon monoxide. These results are summarized in Figure 25. It is well-known that tin oxide is highly sensitive to ambient moisture [62, 66]. A different behavior can be identified for tin oxide-rich sensors and tin-oxide lean sensors. Indeed, sensors based on pure tin oxide and those based on tin oxide carbon nanotube hybrids containing the highest amount of tin oxide (i.e. tin oxide-rich sensors) are the most responsive to moisture changes (0 %- 50 % and 0 % - 80 %), the change between 50 % -80 % was very small. On the other hand, sensors based on pure carbon nanotubes or on hybrid nanomaterials with lowest or intermediate amounts of tin oxide (i.e., tin oxide-lean sensors) show a more than one order of magnitude lower moisture responsiveness that the one of tin oxide-rich sensors.

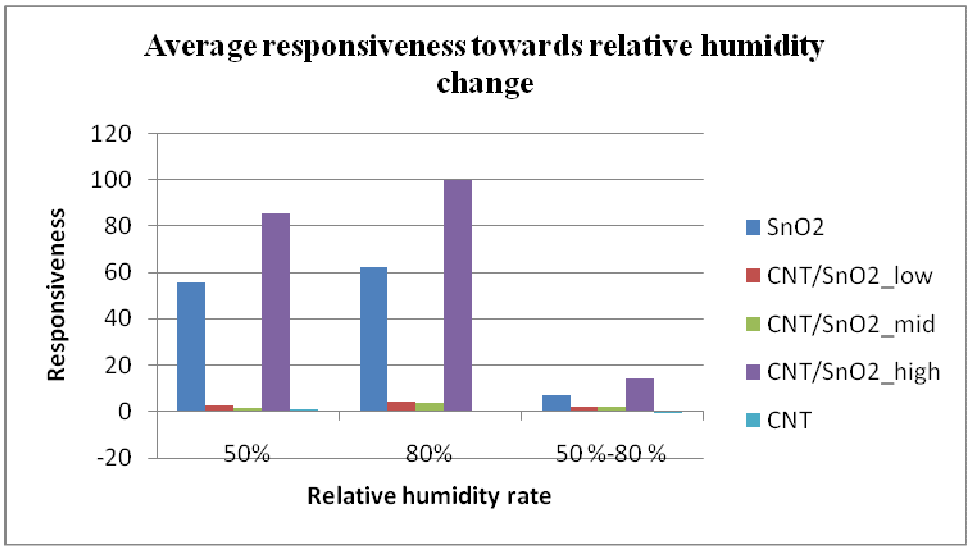

Figure.25. Average responsiveness (and associated standard deviation) towards relative humidity changes (from dry air to 50% R.H. and to 80% R.H.) for the different sensors developed. Sensors were operated at room temperature

5.2.2.5. Conclusion

- The gas sensing properties of the hybrid materials were investigated and compared against the sensing properties of sensors based on pure tin oxide nanoparticles or on pure oxygen plasma treated multiwall carbon nanotubes. It was found that at low operating temperatures (room temperature and 150ºC) hybrid nanomaterials were

ISBN:978-84-694-0326-6/DL:T-207-2011

significantly more responsive to nitrogen dioxide and carbon monoxide than pure nanomaterials (pure tin oxide or pure MWCNTs). Additionally, there is an optimal ratio between the amount of tin oxide precursor and carbon nanotubes to be used during the hybrid preparation procedure in order to maximize responsiveness.

- The optimal hybrid materials show a moderate moisture cross-sensitivity, much lower than the one found in pure tin oxide or in hybrids with rich content of tin oxide.
- Based on the nature of the sensor response to nitrogen dioxide and on previous first principles calculation results, different mechanisms for detection depending on the operating temperature have been identified. At room temperature, the optimal hybrid material behaves as a *p*-type semiconductor, which indicates that upon adsorption of nitrogen dioxide molecules either on nanotube sidewalls or on tin oxide nanoclusters, a significant amount of electronic charge is transferred from nanotubes to the adsorbed NO_2 and also from nanotubes to tin oxide nanoclusters, affecting nanotube conductivity. On the other hand, when hybrid materials are operated at 150ºC, these behave as an *n*-type semiconductor. Nitrogen dioxide adsorbs onto tin oxide nanoclusters trapping electrons and, therefore, increases the resistance of the hybrid film. Conductivity is mobility-limited by the presence of potential barriers at tin oxide inter-grain contacts. This effect is measurable at low temperatures (i.e., 150ºC) because the presence of embedded MWCNTs helps reducing the number of potential barriers a conduction electron needs to cross to reach the electrodes.
- The presence of different detection mechanisms activated at different operating temperatures opens an opportunity to tune the selectivity of carbon nanotube based sensors.

❖ **Comparison of commercial and home-made metal oxides:**

- Metal decorated CNT mixed with commercial metal oxides present higher sensitivity at room Temperature and 150 ºC compared to the home-made metal oxide decorated oxygen functionalized CNT, this can be explained by the existence of metal in the first composite which improve the conductivity through the compound active layer.
- The addition of a small quantity of metal-decorated MWCNT to metal oxides can significantly improve the detection capability of metal oxide based sensors and lower the operating temperature.
- The modulation of the width of two depletion layers existing at the surface of metal oxide grains and at the interface of metal oxide grains and MWCNT, respectively, is

ISBN:978-84-694-0326-6/DL:T-207-2011

postulated as the mechanism that could explain the enhanced performance of hybrid metal oxide/MWCNT sensors in comparison with pure metal oxide or pure MWCNT sensors.

- It was found that the sensing mechanism depends on the morphology the nanotubes/ metal oxide composites. While The sensing performance of the hybrid nanostructure sensor could be attributed to the effective electron transfer between SnO2 nanocrystals and MWNTs and to the increase in the specific surface area of hybrid nanostructures in the case of homemade metal oxide decorated CNTs, the modulation of the width of two depletion layers existing at the surface of metal oxide grains and at the interface of metal oxide grains and MWCNT, respectively, in the case of CNTs mixed with metal oxides.
- The presence of different detection mechanisms activated at different operating temperatures opens an opportunity to tune the selectivity of carbon nanotube based sensors.

5.3. Gas sensing properties of N or B-doped carbon nanotubes

In the following sections, the doping effect of nitrogen and boron on the sensing properties of MWCNTs is discussed based on the characterization of the sensors towards many gases and on theoretical LDA/DFT calculations (Chapter 4).

5.3.1. Reactivity towards gases

N- and B-doped CNT sensors responded to NO_2, CO and C_2H_4 (Figures 26-31). Such sensors responded to NO_2 both when operated at room temperature or at 150ºC (Figures.26-28). However, N-doped CNT's responsiveness was higher when operated at room temperature (Figure.26). This behavior has been already explained in section 5.1.1.3. Figure 26 shows the detection of increasing concentrations of NO_2 by a N-doped nanotube sensor operated at room temperature. Low concentrations (i.e. 50 ppb) can be easily detected. This figure shows also that heating speeds up baseline recovery after NO_2 has been removed. Figure 27 shows three cycles of detection and baseline recovery for increasing concentrations of NO_2. While detection is performed at room temperature for higher sensitivity, during recovery, heating at 150ºC is employed to speed up the process. The fact that NO_2 is detected by N-doped CNT sensors and not by pristine CNT sensors and that heating helps in recovering the sensor baseline indicates that NO_2 chemisorbs into defects (e.g. pyridine defects) caused by the

ISBN:978-84-694-0326-6/DL:T-207-2011

substitutional N atoms present in the structure of the CNTs. So, N-doped CNTs can be employed as a good gas sensor for NO_2.

B-doped CNT strongly reacts with the testing gases, even more than N-doped CNT. NO_2 strongly chemisorbs in B-doped CNT layers. The sensor did not regain its baseline after its cleaning, which confirms the change in the chemical composition of the sensing layer after NO_2 detection (figure.28). It was found also by performing theoretical simulations that effectively NO_2 chemisorbed into B-doped CNT with a binding energy of 3.55 eV, resulting in an important charge transfer between NO_2 molecule and B-doped CNT. Furthermore, the sensitivity towards NO_2 detection increases by increasing temperature (Table.4.). This too strong binding of NO_2 with B-doped CNTs results in a non-reversible detection, which makes B-doped CNTs an unsuitable material for NO_2 sensing.

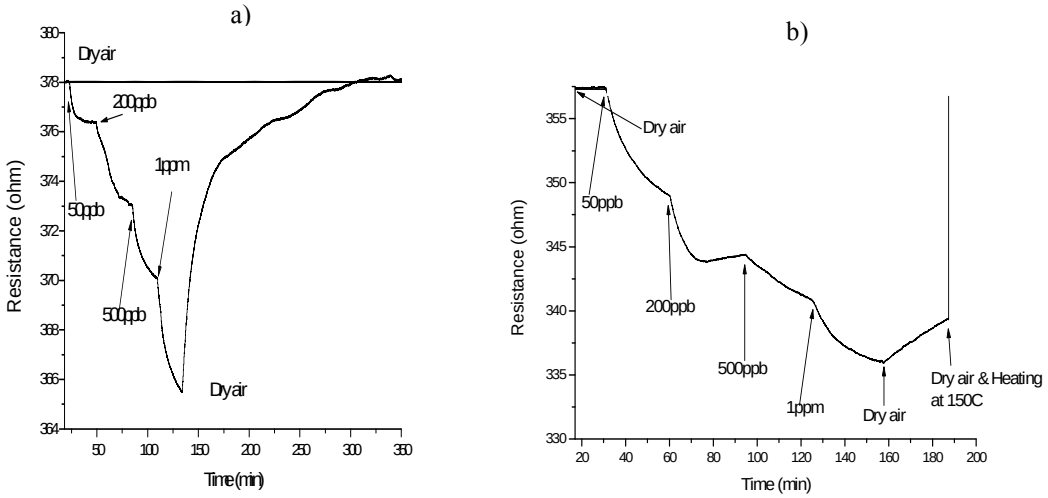

Figure.26. Response of N-doped CNT-based sensor to successively increasing concentrations of nitrogen dioxide when operated at room temperature (a) and operated at 150ºC (b). For a faster and full recovery of the sensor baseline resistance in dry air, heating at 150ºC is necessary

ISBN:978-84-694-0326-6/DL:T-207-2011

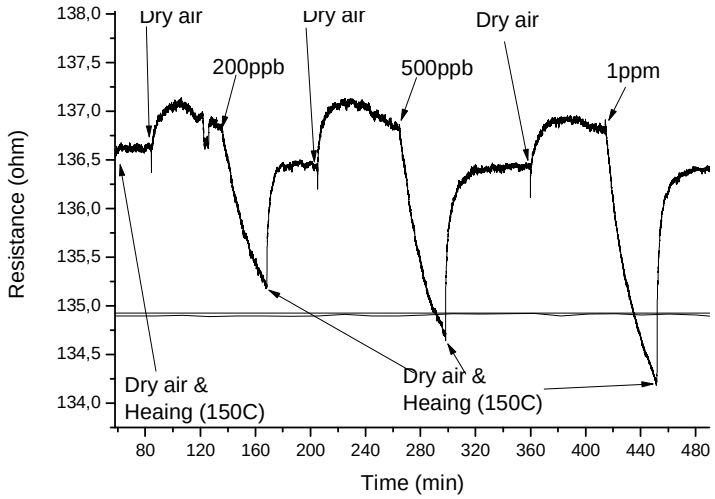

Figure.27. Detection of increasing concentrations of NO_2 at ambient temperature by a N-doped CNT-based sensor. Baseline recovery is speeded up by heating at 150ºC.

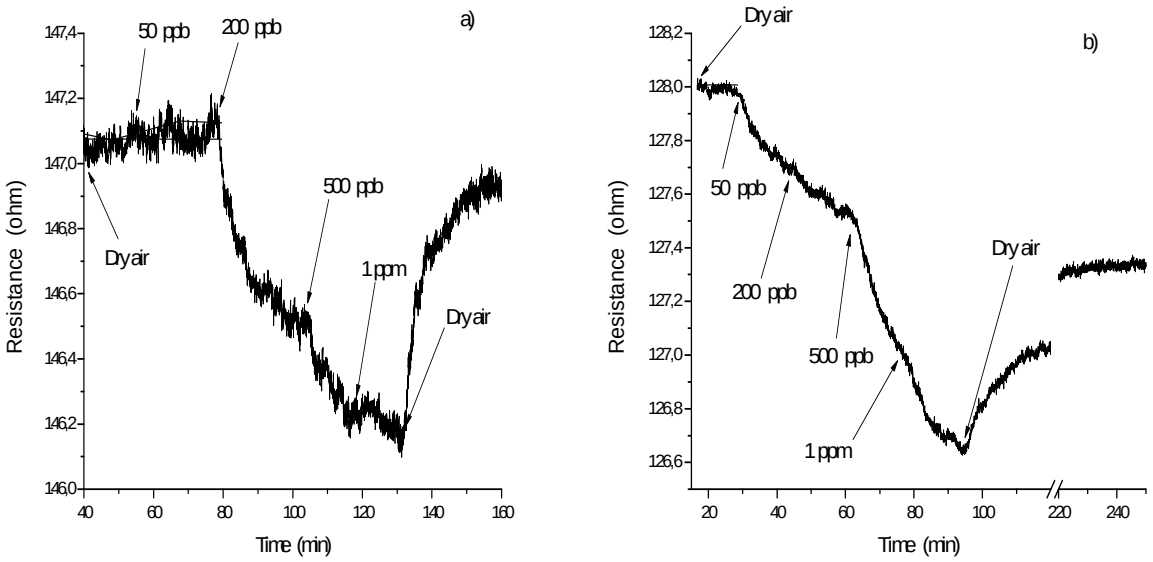

Figure.28. Response of a B-doped CNT-based sensor to successively increasing concentrations of nitrogen dioxide when operated at room temperature (a) and operated at 150ºC (b). For a faster and full recovery of the sensor baseline resistance in dry air, heating at 150ºC is necessary

Carbon monoxide was detected by N- and B-doped CNT sensors, provided these were operated at room temperature (see Figures.29, 30). Similarly to NO_2, temperature favors desorption of CO from the CNT walls, which results in diminished responsiveness. In the particular case of CO, heating at 150ºC seems enough for the complete desorption of this species and, therefore, no response is obtained. Like for NO_2, CO interacts with defects, but

ISBN:978-84-694-0326-6/DL:T-207-2011

this interaction is milder since lower responses are obtained for significantly higher concentrations (e.g. CO was measured at concentrations ranging from 2 up to 20 ppm).

A covalent binding of CO molecule with the boron-doped CNTs was observed, which indicates that this molecule undergoes chemical adsorption, while non-covalent binding occurred when CO molecule adsorbed on the nitrogen-doped CNTs indicating the occurrence of a physical adsorption. Boron-doped CNTs show stronger binding energies and shorter binding distance for CO sensing than pristine carbon nanotubes. The stronger binding energies and shorter binding distance are consistent with the larger charge transfer between molecules and doped CNT systems. This indicates that the binding characteristic between molecules and doped CNT system is an ionic type. And the electron charge transfer is an important mechanism in changing the conductivity in the doped CNTs when adsorbed with CO molecule.

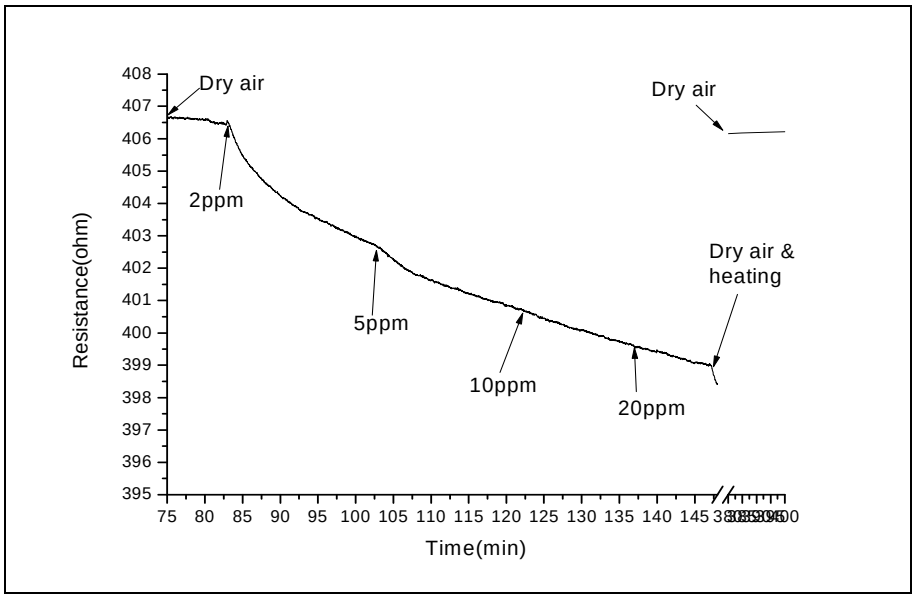

Figure.29. Detection of increasing concentrations of CO at ambient temperature by a N-doped CNT-based sensor.

ISBN:978-84-694-0326-6/DL:T-207-2011

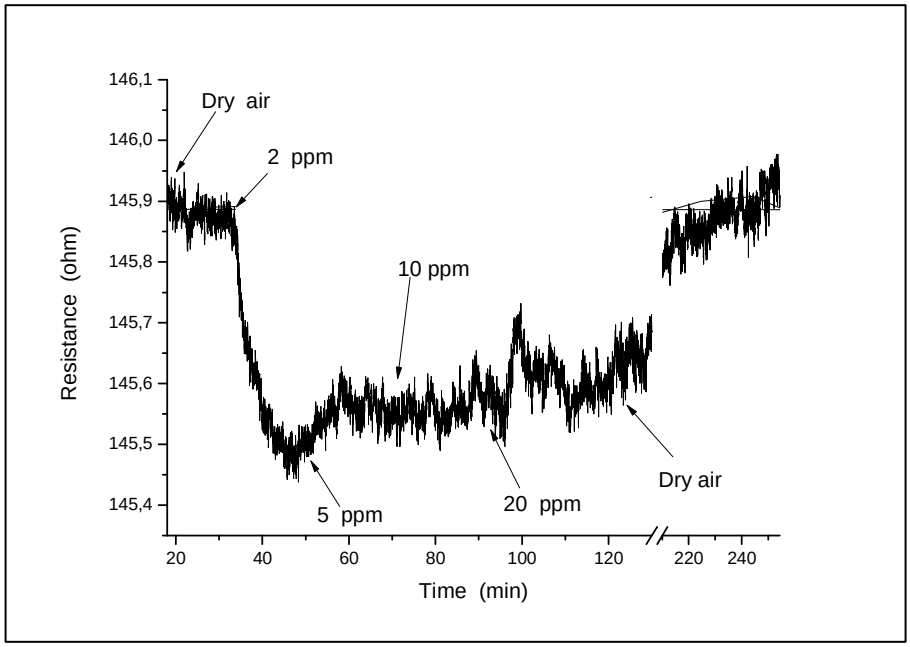

Figure.30. Detection of increasing concentrations of CO at ambient temperature by a B-doped CNT-based sensor.

Ethylene was detected by N-doped CNT sensors only, provided these were operated at 150ºC. Unlike for NO_2 and CO, the chemisorption of ethylene onto CNT defects (and associated charge transfer between adsorbate and nanotube) is increased by operating the sensors above room temperature. On the other hand, ethylene was detected only at room temperature by B-doped CNTs (see Table.4).

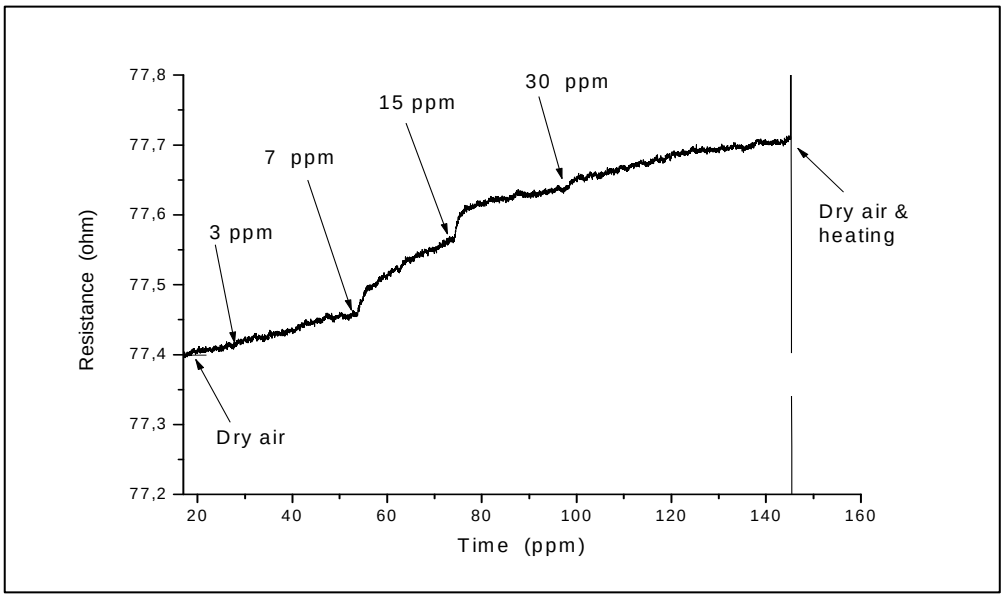

Figure.31. Detection of increasing concentrations of C2H4 at ambient temperature by a B-doped CNT-based sensor.

UNIVERSITAT ROVIRA I VIRGILI
DESIGN, FABRICATION AND CHARACTERISATION OF GAS SENSORS BASED ON NANOHYBRID MATERIALS
Radouane Leghrib
ISBN:978-84-694-0326-6/DL:T-207-2011

5.3.2. Effect of moisture

Un-doped nanotube sensors did not respond to CO (up to 20 ppm) or C_2H_4 (up to 30 ppm) when operated at room temperature or at 150ºC. The lack of responsiveness towards NO_2 (up to 10 ppm) and NH_3 (up to 200 ppm) of gas sensors prepared with pristine carbon nanotubes had already been verified experimentally and explained by employing density functional theory calculations [51]. However, sensors based on un-doped nanotubes were responsive to humidity changes. This was evaluated by exposing the sensors to step changes in R.H. from 0 to 50% and from 50 to 80% (at 30ºC). The response to humidity was very similar for un-doped and N- or B-doped nanotubes (figure.32).

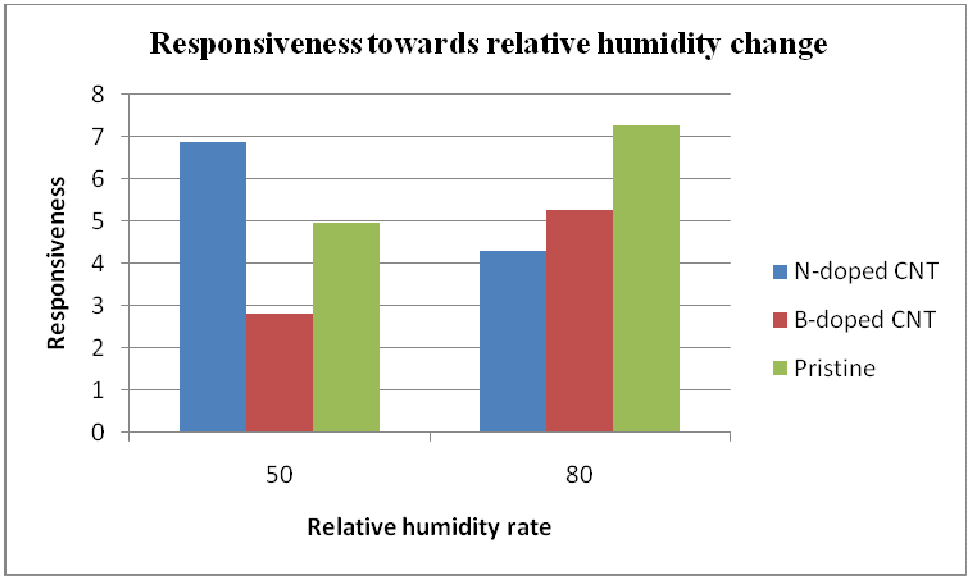

Figure.32. Response to step changes in relative humidity for un-doped, nitrogen an boron doped carbon nanotube sensors operated at room temperature

Figure.32 summarizes humidity responsiveness results for the sensors studied and figure.33 shows a typical response to humidity changes when sensors are operated at room temperature. The rightmost part of the response transient shows the initial recovery of the sensor in dry air. Even if heat is applied (150ºC) to promote desorption, a full recovery of the sensor baseline takes about 2.5 h. Even though different authors have reported that water physisorbs on the surface of carbon nanotubes [67-69] , the fact that both un-doped, N- and B-doped CNT sensors show a high response to humidity and take time to regain their baseline suggests that a strong interaction exists between water molecules and the CNT studied.

ISBN:978-84-694-0326-6/DL:T-207-2011

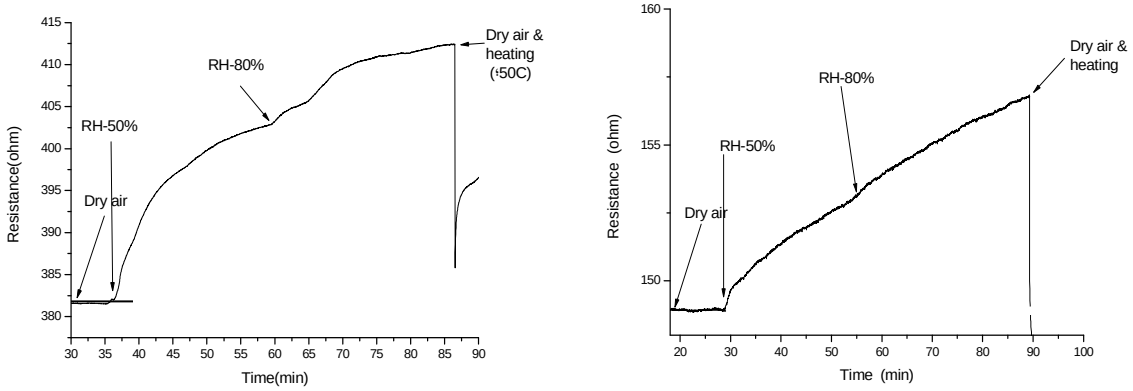

Fig.33. Response when relative humidity is step-changed from 0 to 50% and from 50 to 80%, of : a) N-doped sensor and b) B-doped sensor.

❖ *Summary*

- B- or N-CNTs are cheap and require no post-growth treatment. Sensors based on these materials are very sensitive and present a rapid response, and good recovery time.
- B-doped CNTs showed a high interaction towards gases which is undesirable in some cases such as NO_2 detection as the reaction becomes irreversible.
- N-doped SWCNTs should be good NO_2 sensors with quick response and short recovery time

UNIVERSITAT ROVIRA I VIRGILI
DESIGN, FABRICATION AND CHARACTERISATION OF GAS SENSORS BASED ON NANOHYBRID MATERIALS
Radouane Leghrib
ISBN:978-84-694-0326-6/DL:T-207-2011

Table 4: Summary of responsiveness results.

Sensor Type	Operating Temperature	NO_2 (ppm)				CO (ppm)				Ethylene (ppm)			
		0.05	0.2	0.5	1	2	5	10	20	3	7	15	30
N-CNT	Ambient	-1.70	-3.24	-4.75	-6.70	-0.862	-1.38	-1.89	-2.22	0	0	0	0
N-CNT	150ºC	-0.615	-1.48	-2.28	-3.47	0	0	0	0	0.100	0.160	0.217	0.258
B-CNT	Ambient	-0.8	-3.97	-5.66	-6.21	-2.59	-2.16	-2.13	-2.01	0.74	2.14	3.02	3.91
B-CNT	150ºC	-2.44	-3.7	-7.84	-10.6	0	0	0	0	0	0	0	0
CNT	Ambient	0	0	0	0	0	0	0	0	0	0	0	0
CNT	150ºC	0	0	0	0	0	0	0	0	0	0	0	0

ISBN:978-84-694-0326-6/DL:T-207-2011

References

[1] Z. Zanolli and J.C. Charlier. Detective carbon nanotubes for single-molecule sensing. Phys. Rev. B 2009; 80: 155447-155453.

[2] A. Felten, C. Bittencourt, and J.-J. Pireaux, Gold clusters on oxygen functionalized CNTs: XPS and TEM studies, Nanotechnology **17** (2006) 1954

[3] C. Bittencourt, A. Felten, B. Douhard, J.-F. Colomer, G. Van Tendeloo, W. Drube, J. Ghijsen, and J.-J. Pireaux, Metallic nanoparticles on plasma treated carbon nanotubes: Nano2hybrids, SurfaceScience 601 (13) 2007; 2800-2804

[4] C. Bittencourt, A. Felten, J. Ghijsen, J.-J. Pireaux, W. Drube, R. Erni, and G. Van Tendeloo, Decorating Carbon Nanotubes with Nickel Nanoparticles Chem. Phys. Lett. 436 (2007) 368

[5] F, Banhart, interaction between metal and carbon nanotubes: at the interface between old and new materials, nanoscale 1 (2) (2009) 201-213

[6] Britt Hvolbæk, Ton V. W. Janssens, Bjerne S. Clausen, Hanne Falsig, Claus H. Christensen, and Jens K. Nørskov, Catalytic activity of Au nanoparticles, nanotoday, 2 (4) (2007) 14-18

[7] I. Suarez-Martinez, C. Bittencourt, X. Ke, A. Felten, J.J. Pireaux, J. Ghijsend, W. Drube, G. Van Tendeloo, C.P. Ewels, Probing the interaction between gold nanoparticles and oxygen functionalized carbon nanotubes, Carbon 47 (2009) 1549 – 1554

[8] J. Kong, N.R. Franklin, C. Zhou, M.G. Chapline, S. Peng, K. Cho, H. Dai, nanotube molecular wires as chemical sensors, Science 287 (2000) 625–662.

[9] H. Chang, J.D. Lee, S.M. Lee, Y.H. Lee, Adsorption of NH3 and NO2 molecules on carbon nanotubes, Appl. Phys. Lett. 79 (2001) 3863–3865.

[10] W.-L. Yim, X.G. Gong, Z.-F. Liu, chemisorption of NO2 on carbon nanotubes, J. Phys. Chem. B 107 (2003) 9363–9369.

[11] M.D. Ellison, M.J. Crotty, D. Koh, R.L. Spray, K.E. Tate, Adsorption of NH3 and NO2 on single-walled carbon nanotubes, J. Phys. Chem. B 108 (2004) 7938–7943.

[12] A. Ricca, C.W. Bauschlicher Jr., the adsorption of NO_2 on (9,0) and (10,0) carbon nanotubes, Chem. Phys. 323 (2006) 511–518.

[13] H.-Q. Nguyen, J.-S. Huh, behaviour of single walled carbon nanotubes based gas sensors at various temperature of treatment and operation, Sens. Actuator B 117 (2006) 426–430.

[14] S. Santucci, S. Picozzi, F. Di Gregorio, L. Lozzi, C. Cantalini, L. Valentini, J.M. Kenny and B. Delley, NO_2 and CO gas adsorption on carbon nanotubes: experiment and theory, Journal of Chemical Physics, 119 (20), (2003) 10904-10910.

[15] L. Valentini, L. Lozzi, C. Cantalini, I. Armentano, J.M. Kenny, L. Ottaviano, S. Santucci, Effects of oxygen annealing on gas sensing properties of carbon nanotube thin films, Thin Solid Films 436 (2003) 95–100.

[16] L. Valentini, F. Mercuri, I. Armentano, C. Cantalini, S. Picozzi, L. Lozzi, S. Santucci, A. Sgamellotti, J.M. Kenny, Role of defects on the sensing properties of carbon nanotubes thin films: Experiment and Theory, Chemical Physics Letters 387 (2004) 356–361.

ISBN:978-84-694-0326-6/DL:T-207-2011

[17] A. Starr, V. Joshi, S. Skarupo, D. Thomas, J.C.P. Gabriel, Gas sensor array based on Metal decorated carbon nanotubes, J. Phys. Chem. B 110 (2006) 21014–21020.

[18] S. Peng, K. Cho, P. Qi, and H. Dai, "Ab initio study of CNT-NO_2 gas sensor," Chemical Physics Letters, vol. 387, no. 4–6, pp. 271–276, 2004

[19] Radouane Leghrib, Roman Pavelko, Alexandre Felten, Alexey Vasiliev, Carles Cané, Isabel Gràcia, Jean Jacques Pireaux, Eduard Llobet, Gas sensors based on multiwall carbon nanotubes decorated with tin oxide nanoclusters, Sensors and Actuators B 145 (2010) 411–416

[20] T. W. Odom, J. L. Huang, P. Kim, C. M. Lieber. Atomic structure and electronic properties of siingle-walled carbon nanotubes . Nature 1998; 391 (6662): 62-64.

[21] P. G. Collins, K. Bradley, M. Ishigami, A. Zettl, Extreme oxygen sensitivity of electronic properties of carbon nanotubes, Science 2000, 287(2000) 1801-1804

[22] D. R. Kauffman, D. C. Sorescu, D. P. Schofield, B. L. Allen, K. D. Jordan, and A. Star, Understanding the Sensor Response of Metal-Decorated Carbon Nanotubes, Nano Letters 2010, 10 (2010) 958–963

[23] J-X. Zhaoa, Y.H. Ding, Theoretical study of the interactions of carbon monoxide with Rh decorated (8,0) singlewalled carbon nanotubes, Materials Chemistry and Physics 110 (2008) 411–416

[24] F. P. Rouxinol, R V. Gelamo and S. A. Moshkalev, Gas sensors based decorated carbón nanotubes, http://sciyo.com/download/pdf/pdfs_id/10008

[25] Q. Cao, J. A. Rogers. Ultrathin films of single-walled carbon nanotubes for electronics and sensors: A review of fundamental and Applied aspects. Advanced Materials (2009) 21- 29.

[26] P. Poncharal, C. Berger, Y. Yi, Z. L. Wang, W. A. de Heer, Room temperature ballistic conduction in carbon nanotubes, Journal of Physical Chemistry B 106 (2002) 12104.

[27] R. Ionescu, E.H. Espinosa, E. Sotter, E. Llobet, X. Vilanova, X. Correig, A. Felten, C. Bittencourt, G. Van Lier, J.-C. Charlier, d, J.J. Pireaux, Oxygen functionalisation of MWNT and their use as gas sensitive thick-film layers, Sensors and Actuators B 113 (2006) 36–46

[28] N.Peng and Q. Zhang, Sensing mechanisms of carbon nanotube based NH_3 gas detectors, http:/*sciyo.com/download/pdf/pdfs_id/10004*

[29] I. Sayago, H. Santos, M.C. Horrillo, M. Aleixandrea, M.J. Fernández, E. Terrado, I. Tacchini, R. Arozc,W.K. Maser, A.M. Benito, M.T. Martínez, J. Gutiérrez, E. Muñoz, Carbon nanotube networks as gas sensors for NO_2 detection, Talanta 77 (2008) 758–764

[30] Douglas R. Kauffman and Alexander Star, Chemically Induced Potential Barriers at the Carbon Nanotube Metal Nanoparticle Interface, NANO LETTERS 2007 Vol. 7, No. 7 1863-1868

[31] Y. Li, H. Wang, Y. Chen, M. Yang, A multi-walled carbon nanotube/palladium nanocomposite prepared by a facile method for the detection of methane at room temperature, Sensors and Actuators B 132 (2008) 155–158

[32] H. Ago, T. Kugler, F. Cacialli, W. R. Salaneck, M. S. P. Shaffer, A. H. Windle, R. H. Friend. Work Functions and Surface Functional Groups of Multiwall Carbon Nanotubes., Journal of Physical chemistry B, 103 (1999) 8116-8121.

ISBN:978-84-694-0326-6/DL:T-207-2011

[33] O. Koppius. A comparison of the thermionic photo-electric work function for platinum. Physical Review18 (1921) 443-455.

[34] P.A. Anderson, Work function of gold, Physical Review 115 (1959) 553-554.

[35] R. Jaeckel, B. Wagner, Photo-electric measurement of the work function of metals and its alteration after gas adsorption, Vacuum 13 (1-12): (1963) 509-511.

[36] D. E. Eastman. Photoelectric work function of transition, Rare-Earth, and Noble metals. Physical Review B 2 (1970) 1-2.

[37] Claessens, N., Demoisson, F , Dufour, T, Mansour, Ali, Felten, A, Guillot, J, Pireaux, J-J, Reniers, F, Carbon nanotubes decorated with gold, platinum and rhodium clusters by injection of colloidal solutions into the post-discharge of an RF atmospheric plasma, Nanotechnology, 21(38) (2010) [0957-4484]

[38] E.H. Dixon, Some photoelectric and thermionic properties of rhodium, Physical Review 37 (1931) 60-69.

[39] T V. W. Janssens, B. S. Clausen, B. Hvolbæk, H. Falsig, C. H. Christensen, T. Bligaard and J. K. Nørskov , Insights into the reactivity of supported Au nanoparticles: combining theory and experiments, Topics Catalysis, 44 (1-2) (2007), 15-26

[40] M. Penza, R. Rossi, M. Alvisi, G. Cassano, E. Serra, Functional characterization of carbon nanotube networked films functionalized with tuned loading of Au nanoclusters for gas sensing applications, Sensors and Actuators B 140 (2009) 176–184

[41] J. Zhang, A. Boyd, A. Tselev, M. Paranjape and P. Barbara, Mechanism of NO_2 interaction in carbon nanotube field effect transistor chemical sensors, Applied Physics Letters **88** (2006) 123112.

[42] P. Bondavalli, P. Legagneux and D. Pribat, carbon nanotubes as gas sensors: state of the art critical review, Sensors Actuators B 140 (2009) 304.

[43] P. Bondavalli, P. Legagneux, D. Pribat, A. Balan and S. Nazeer, 2008 'Gas fingerprinting using carbon nanotubes transistor arrays', Journal of Experimental Nanoscience, 3 (4), (2008) 347 - 356

[44] N. Peng, Q. Zhang, Y. C. Lee, H. Huang, O. K. Tan, J. Tian, and L. Chan, Humidity and Temperature Effects on Carbon Nanotube Field-Effect Transistor-Based Gas Sensors, SENSOR LETTERS Vol. 6 (2008) 796–799.

[45] M. Penza, R. Rossi, M. Alvisi, M.A. Signore, G. Cassano, D. Dimaio, R. Pentassuglio, E. Piscopiello, E. Serra, M. Falconieri, Characterization of metal-modified and vertically-aligned carbon nanotube films for functionally enhanced gas sensor applications, Thin Solid Films 517 (2009) 6211–6216.

[46] T. C. Pearce, J. W. Gardner, Predicting organoleptic scores of sub-ppm flavor notes Part 2, computational analysis and results, Analyst 123 (1998) 2057-2055.

[47] C. T. White, T. N. Todorov, carbon nanotubes as long ballistic conductors, Nature 393 (1998) 240.

[48] E.H. Espinosa, R. Ionescu, B. Chambon, G. Bedis, E. Sotter, C. Bittencourt, A. Felten, J.-J. Pireaux, X. Correig, E. Llobet, Low temperature gas detection with hybrid metal oxides/MWCNTs, in: XX Eurosensors Conference Aniversary, Goteborg, Sweden, September 17–20, 2006.

ISBN:978-84-694-0326-6/DL:T-207-2011

[49] B.Y. Wei, M.C. Hsu, P.G. Su, H.M. Lin, R.J. Wu, H.J. Lai, A novel SnO_2 gas sensor doped with carbon nanotubes operating at room temperature, Sensors and Actuators B 101 (2004) 81–89.

[50] Y. Chen, C. Zhu, T. Wang, The enhanced ethanol sensing properties of multi-walled carbon nanotubes/SnO_2 core/shell nanostructures, Nanotechnology 17 (2006) 3012–3017.

[51] R. Ionescu, E.H. Espinosa, E. Sotter, E. Llobet, X. Vilanova, X. Correig, A. Felten, C. Bittencourt, G. Van Lier, J.-C. Charlier, J.J. Pireaux, Oxygen functionalisation of MWNT and their use as gas sensitive thick-film layers, Sensors and Actuators B 113 (2006) 36–46.

[52] L. Valentini, I. Armentano, J.M. Kenny, C. Cantalini, L. Lozzi, S. Santucci, Sensors for sub-ppm NO_2 gas detection based on carbon nanotube thin films, Applied Physics Letters 82 (2003) 961–963.

[53] E.H. Espinosa, R. Ionescu, C. Bittencourt, A. Felten, R. Erni, G. Vantendeloo, J.-J. Pireaux, E. Llobet, Metal-decorated multi-wall carbon nanotubes for low temperature gas sensing, Thin Solid Films 515 (2007) 8322–8327.

[54] P. Ivanov, E. Llobet, F. Blanco, A. Vergara, X. Vilanova, I. Gracia, C. Can´e, X. Correig, On the effects of the materials and the noble metal additives to NO_2 detection, Sensors and Actuators B 118 (2006) 311–317.

[55] M. Stankova, X. Vilanova, J. Calderer, E. Llobet, J. Brezmes, I. Garcia, C. Cané, X. Correig, Sensitivity and selectivity improvement of rf sputtered WO_3 microhotplate gas sensors, Sens. Actuators B 113 (2006) 241–248.

[56] M. Penza, G. Cassano, F. Tortorella, Gas recognition by activated WO_3 thin-film sensors array, Sensors and Actuators B 81 (2001) 115–121.

[57] M. Penza, G. Cassano, R. Rossi, M. Alvisi, A. Rizzo, M.A. Signore, Th. Dikonimos, E. Serra, R. Giorgi, Enhancement of sensitivity in gas chemiresistors based on carbon nanotube surface functionalized with noble metals (Au, Pt) nanoclusters, Applied Physics Letters 90 (2007) 173–176.

[58] D.G. Rickerby, N. Wätchter, M.C. Horrillo, J. Gutiérrez, I. Gràcia, C. Cané, Structural and dimensional control in micromachined integrated solid state gas sensors, Sensors and Actuators B 69 (2000) 314–319.

[59] R.G. Pavelko, A.A. Vasiliev, V.G. Sevastyanov, F. Gispert Guirado, X. Vilanova, N.T. Kuznetsov, Studies of thermal stability of nanocrystalline SnO2, ZrO_2, and SiC for semiconductor and thermocatalytic gas sensors, Russian Journal of Electrochemistry 45 (2009) 470–475.

[60] F.J. Humphreys, M. Haterly, Recrystallization and Related Annealing Phenomena, Elsevier, 2004.

[61] I. Simon, N. Barsan, M. Bauer, U. Weimar, Micromachined metal oxide gas sensors: opportunities to improve sensor performance, Sensors and Actuators B 73 (2001) 1–26.

[62] R. Ionescu, E.H. Espinosa, R. Leghrib, A. Felten, J.J. Pireaux, R. Erni, G. Van Tendeloo, C. Bittencourt, N. Ca˜ nellas, E. Llobet, Novel hybrid materials for gas sensing applications made of metal decorated MWCNTs dispersed on nanoparticles metal oxides, Sensors and Actuators B 131 (2008) 174–182.

ISBN:978-84-694-0326-6/DL:T-207-2011

[63] S. Mishra, C. Ghanshyam, N. Ram, R.P. Bajpai, R.K. Bedi, Detection mechanism of metal oxide gas sensor under UV radiation, Sensors and Actuators B 97 (2004) 387–390.

[64] G. Lu, L. E. Ocola, and J. Chen, Room-Temperature Gas Sensing Based on Electron Transfer between Discrete Tin Oxide Nanocrystals and Multiwalled Carbon Nanotubes, Advanced Materials, 21 (2009) 2487–2491

[65] L. Zhao, M. Choi, H.S. Kim, S.H. Hong, The effect of multiwalled carbon nanotubes doping on the CO gas sensitivity of SnO_2 based nanomaterials, Nanotechnology 18 (2007) 445501.

[66] P. Moseley, B. Tofield, Solidstate Gas Sensors, Adam Hilger, Bristol, UK, 1987

[67] P. S. Na, H. Kim, H.M. So, K.J. Kong, H. Chang, B.H. Ryu, B.K. Kim, J.J. Kim and J. Kim, Investigation of the humidity effect on the electrical properties of single-walled carbon nanotube transistors, Applied Physics Letters 87, 093101-1-3 (2005).

[68] D. Sung, S. Hong, Y.H. Kim, N. Park, S. Kim, S.L. Maeng, K.C. Kim, ***Ab initio*** study of the effect of water adsorption on the carbon nanotube field-effect transistor, Applied Physics Letters 69 (2006) 243110

[69] L. Liu, X. Ye, K. Wu, R. Han, Z. Zhou, T. Cui, Humidity Sensitivity of Multi-Walled Carbon Nanotube Networks Deposited by Dielectrophoresis, Sensors, 9 (2009) 1714-1721

UNIVERSITAT ROVIRA I VIRGILI
DESIGN, FABRICATION AND CHARACTERISATION OF GAS SENSORS BASED ON NANOHYBRID MATERIALS
Radouane Leghrib
ISBN:978-84-694-0326-6/DL:T-207-2011

6. DEVELOPMENT OF A NANO2HYBRID SENSOR ARRAY FOR SELECTIVE BENZENE DETECTION

UNIVERSITAT ROVIRA I VIRGILI
DESIGN, FABRICATION AND CHARACTERISATION OF GAS SENSORS BASED ON NANOHYBRID MATERIALS
Radouane Leghrib
ISBN:978-84-694-0326-6/DL:T-207-2011

ISBN:978-84-694-0326-6/DL:T-207-2011

In chapter 5, section 5.1.2, it was demonstrated that the combination of benzene sensitive and insensitive materials based metal decorated CNTs sensors allowed the selective detection of benzene by detecting simple gases. Due to requirement of the real applications, it is important to check the validation of the selective detection performance of benzene in gas mixture and in different humid ambient.

Herein, we will show the final validation results obtained for the prototype of benzene detector employing an integrated microarray of 4 sensors with 4 different hybrid materials selected in chapter 5 (Rh, Pt, Pd, and O_2 or Au/ MWCNTs) which were deposited by drop coating method (see section 3.2.2.2.a).

The detection performance in terms of reproducibility, sensitivity, limit of detection, selectivity, response and recovery times will be shown in three steps: by working with simple gases, and with binary gas mixture either in dry or humid ambient. The concentrations measured in each measurement were:

Single gas measurements: Benzene (100, 250, 500 and 1000 ppb), nitrogen dioxide (100 and 500 ppb), hydrogen sulphide (5 and 10 ppm), carbon monoxide (2 and 5 ppm).

Binary gas mixtures measurements are reflected in the table below.

***Table 1*: Binary gas mixture measurements performed**

	NO_2 (ppb)		H_2S (ppm)		CO (ppm)	
C_6H_6 (ppb)	100	500	5	10	2	5
100	☑	☑	☑	☑	☑	☑
250	☑	☑	☑	☑	☑	☑
500	☑	☑	☑	☑	☑	☑

This gave a total of 28 different gases or gas mixtures generated within each database. Since every measurement was replicated 4 times, 112 measurements were performed for each database and 336 measurements were performed in total. These measurements were performed with 16 microsensors (i.e. 4 replicated microsensor arrays were characterized for each one of the 4 hybrid materials selected. These measurements spanned during nearly 3 months.

Experimental sensors characterisation was performed using the automatized testing circuit as was described previously in section 3.3.2 (Procedure.2).

ISBN:978-84-694-0326-6/DL:T-207-2011

6.1. Results and discussion

6.1.1. Measurements in dry ambient

In this case the carrier gas was pure synthetic air containing 10 % of relative humidity.

Figure 2 shows typical sensor response and recovery cycles employing the measurement/ baseline recovery procedure described above for the detection of NO_2 (figure 2.left) by Rh/CNTs and the detection of H_2S (figure 2.right) by Pd/CNTs.

The response time for benzene detection was defined as the time needed for the response to sweep from 10% to 90% of its final value. Similarly, recovery time was defined as the time needed for the resistance to sweep from 90% down to 10% of its initial value. Figure 3 right shows the response towards benzene of a Rh-MWCNT sensor. Response time was estimated to be 60 s and recovery time (after switching off the heater) was estimated to be 5 min.

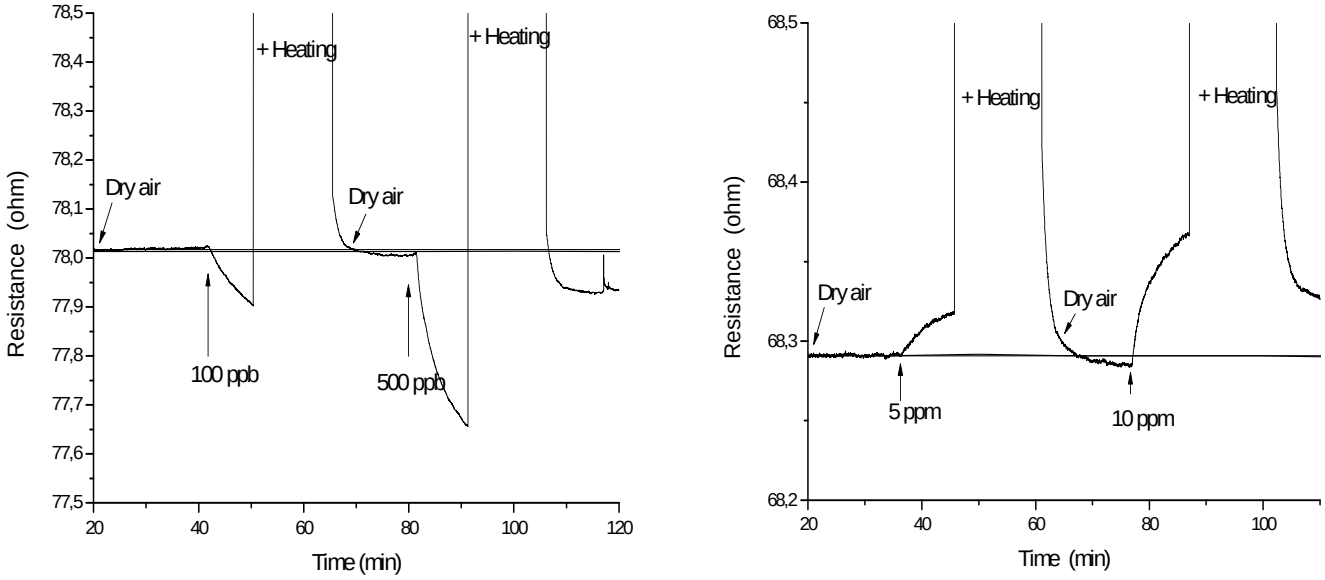

Figure 2: Typical measurement and recovery cycles of hybrid sensors. The species measured were nitrogen dioxide (left) and hydrogen sulphide (right).

ISBN:978-84-694-0326-6/DL:T-207-2011

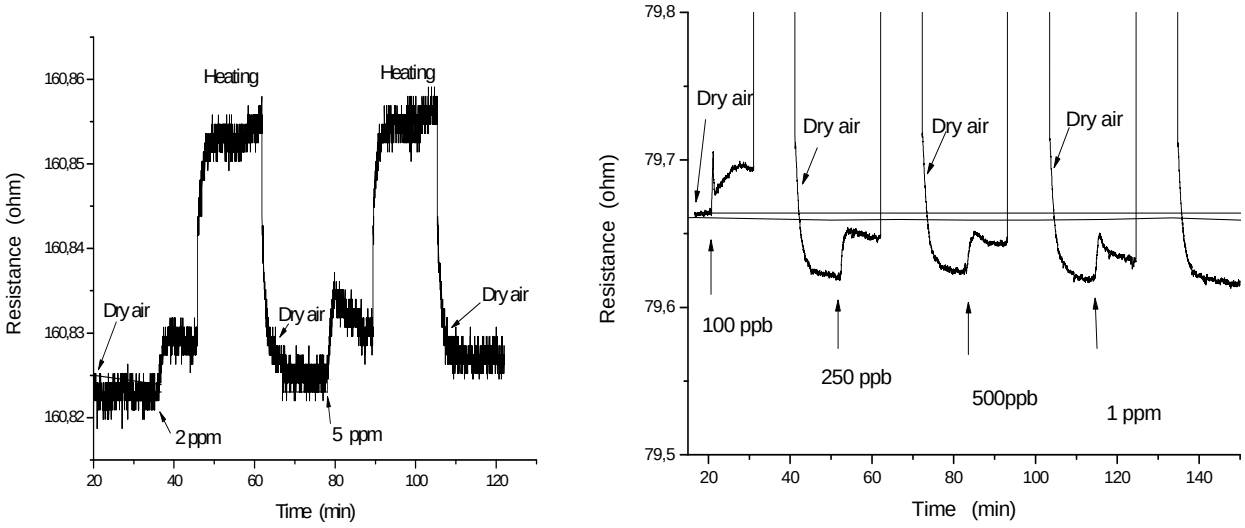

Figure 3: Successive responses of: Pt-MWCNTs sensor to CO(left), and Rh-MWCNT sensor to benzene (right).

❖ **Sensor reproducibility**

By studying the response towards 100 ppb of benzene obtained with replicated sensors (i.e. sensors that employed the same hybrid material coated employing the same technique), it was possible to assess how reproducible was the sensor fabrication technique. Four replicate sensors were prepared from each hybrid material assessed in this study. A given hybrid material employed to fabricate 4 replicated sensors was produced in the same batch. Therefore, the fluctuations in performance for sensors based on colloidal suspensions or organometallic precursors can be attributed exclusively to the deposition method (drop coating) and not to plasma treatment and metal decoration. Unlike in the previous case, for materials deposited with the alternative drop coating method, not only the deposition but also the plasma treatment and metal decoration can be sources of fluctuations.

Reproducibility was estimated by calculating the ratio between the mean of the responses and the standard deviation. The higher the value of this ratio is, the more reproducible the fabrication procedure is. For the four materials considered (i.e. 16 sensors evaluated), the values of the ratio ranged between 4.2 and 6.4. The higher values corresponded to sensors fabricated employing the alternative drop coating method. In such sensors, MWCNTs were airbrushed onto the sensor substrates. For sensors fabricated employing the drop coating method, reproducibility is lower. This confirms that the airbrush method leads to a better control in the amount of material deposited, which results in better reproducibility. However, these figures are low enough for a

ISBN:978-84-694-0326-6/DL:T-207-2011

calibration of each sensor produced to be needed before being integrated in a benzene detector. This problem is also encountered with standard metal oxide sensors.

❖ **Reproducibility of measurements**

By studying the response of a given sensor towards 4 independent replicated measurements of benzene 100 ppb, it was possible to assess how reproducible the measurements were. Reproducibility was estimated by calculating the ratio between the mean of the responses and the standard deviation. The higher the value of this ratio is, the more reproducible the measurement is. For the 16 sensors evaluated, the values of the ratio ranged between 4.2 and 11.1. Most of the sensors showed a value close to 10. Even though, a low concentration of benzene was used to estimate reproducibility (low responses are prone to be affected by noise), the reproducibility of measurements is fair.

❖ **Benzene sensitivity and limit of detection**

Rh-decorated MWCNT showed the highest sensitivity towards benzene. Sensors responded to 50 ppb of benzene, therefore, the lower limit of detection is below this concentration. This is further discussed when the quantitative estimation of benzene concentration is showed here.

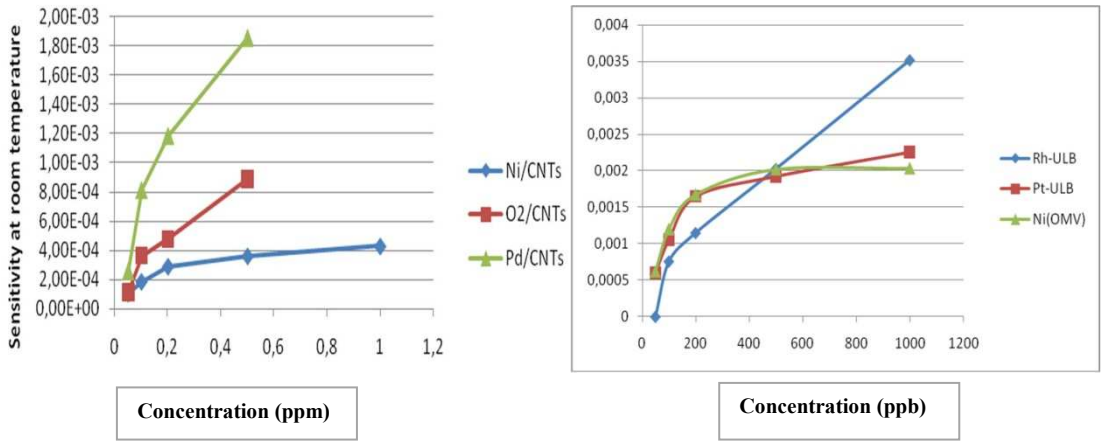

Figure 4: Benzene sensitivity at room temperature of some hybrid materials employed

❖ **Selectivity**

As before, selectivity was assessed employing principal component analysis (PCA). The response matrix was constructed as follows. Given the fact that four replicated sensors were available, each response was defined as the average value over the 4 replicated sensors. This sensor response was pre-processed by applying a mean-centering. Mean centering removes offsets and seems the most appropriate technique here, since all

ISBN:978-84-694-0326-6/DL:T-207-2011

sensors are based on similar gas-sensitive materials (metal-decorated MWCNTs). The first two principal components were retained for data representation. These accounted for over 98% of variance in the data (89.0% PC1 and 9.3% PC2). The scores of the PCA are shown in Figure 5.

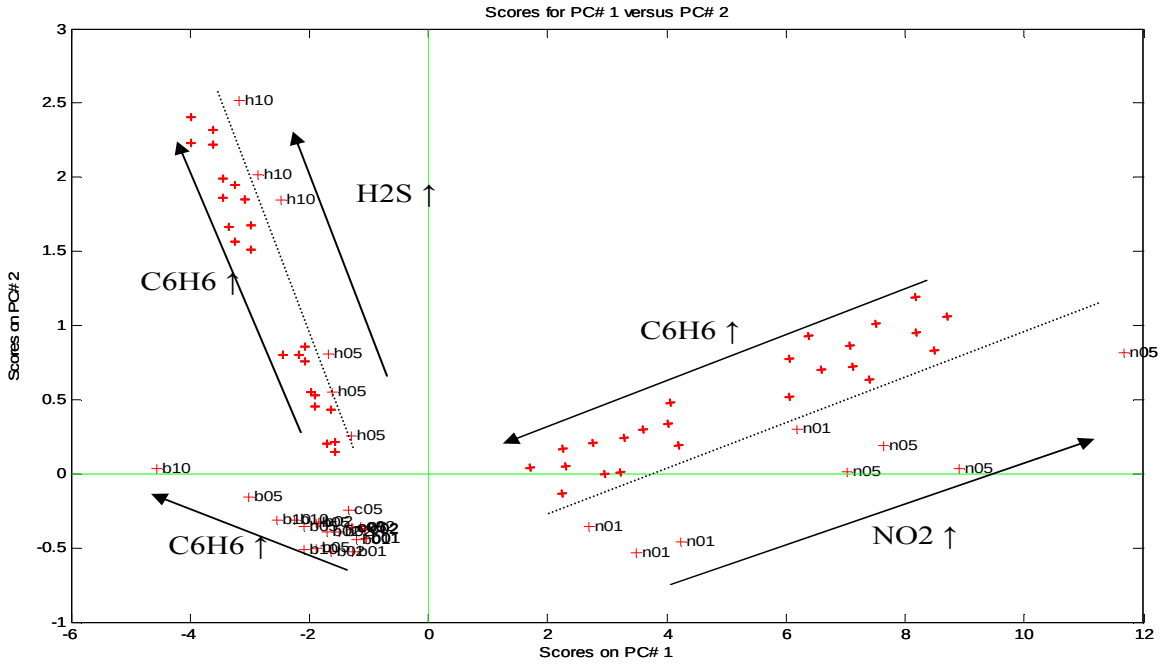

Figure 5: Score plot of the PCA analysis performed on the response matrix employing the first database (single gases and binary mixtures measured at 10% R.H.)

The score plot shows that benzene can be distinguished from hydrogen sulfide and nitrogen dioxide, even when it appears in mixtures. The arrows indicate how measurements are sorted in the score plot according to increasing concentrations of the different species. Sensors are very responsive to NO_2 and H_2S, this explains why mixtures of these gases containing benzene appear rather close to measurements of pure NO_2 and H_2S. Pure benzene measurements appear rather close to CO measurements. This sector of the score plot is shown magnified in Figure 6. The magnified score plot shows that it is possible to discriminate benzene from CO.

ISBN:978-84-694-0326-6/DL:T-207-2011

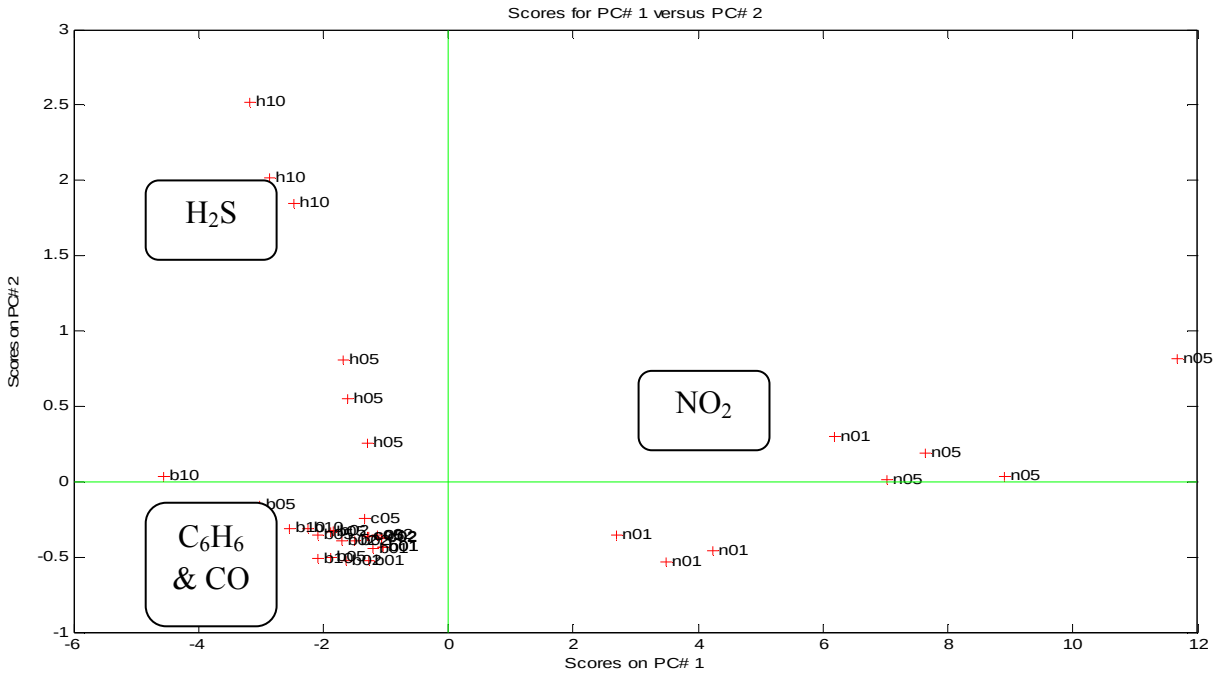

Figure 6.a: The score plot showing the discrimination of single gases.

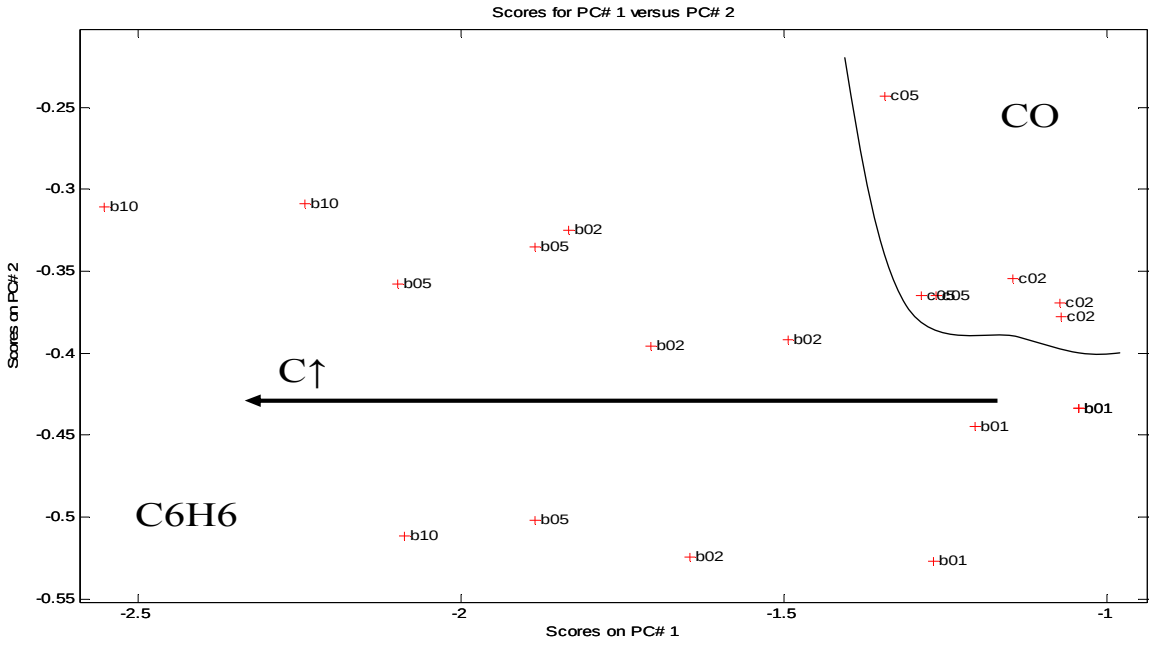

Figure 6.b: Magnification of the score plot showing that benzene can be discriminated from CO. The arrow indicates increasing benzene concentrations

Given the results of the PCA analysis shown in figures 5 and 6, the strategy to analyze benzene with the detector is as follows. Given a new measurement, the scores of this measurement on the PCA are found by appropriately scaling the measurement vector employing the calibration set means (mean-centering pre-processing step) and multiplying the mean-centered response vector by the PCA loadings (or eigenvectors).

ISBN:978-84-694-0326-6/DL:T-207-2011

Once the scores are found, the measurement is projected onto the PCA score plot. Depending on the scores associated to the new measurement, it is possible to identify (employing a distance metric) whether the measurement corresponds to NO_2, H_2S or CO / C_6H_6 (or benzene in a mixture). This is illustrated in Figure 7, where simple decision boundaries have been indicated.

For determining the presence of benzene and estimating its concentration, specific calibration models have been built in each zone. In the CO/Benzene and the H_2S/Benzene zones, a simple partial least squares (PLS) model is enough to quantify benzene. However, in the NO_2/Benzene zone a nonlinear model such as a multilayer perception (MLP) performs slightly better. This is possibly due to the fact that NO_2 and benzene have opposite effects on the change in sensor resistance (benzene is electron donator and NO_2 is electron acceptor).

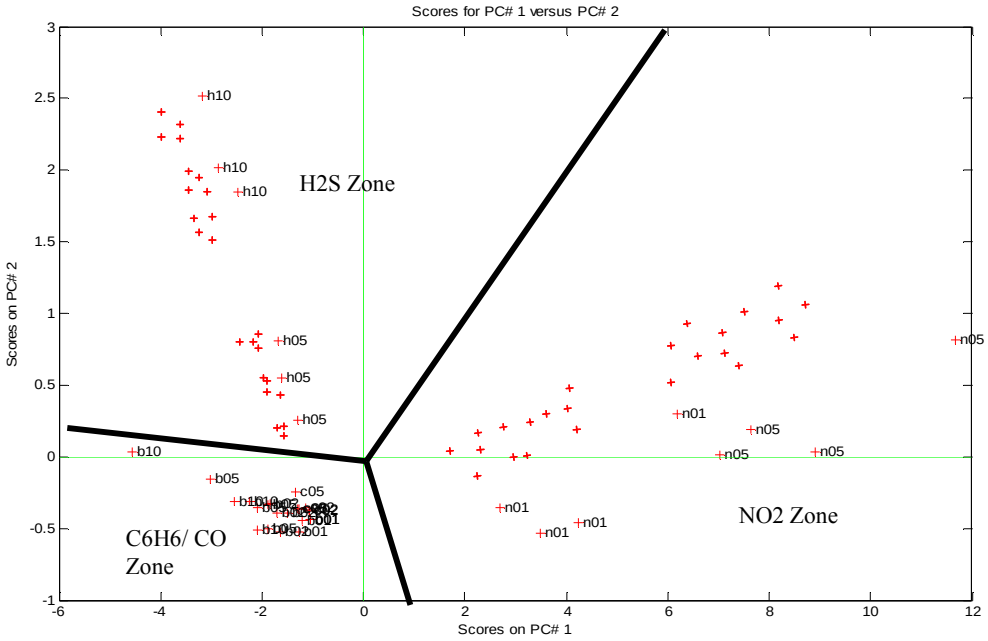

Figure 7: Score plot showing decision boundaries. See main text for details

Figure 8 shows the performance of two of such dedicated models. The one aimed at quantifying benzene in the presence of CO and the one aimed at quantifying benzene in the presence of NO_2. Both figures show validation results. A 4-fold cross-validation strategy was employed. It consists of removing one measurement per concentration for evaluation and the three replicate measurement left are used for training. This process is repeated 4 times, each time selecting a different replicate for the validation process.

ISBN:978-84-694-0326-6/DL:T-207-2011

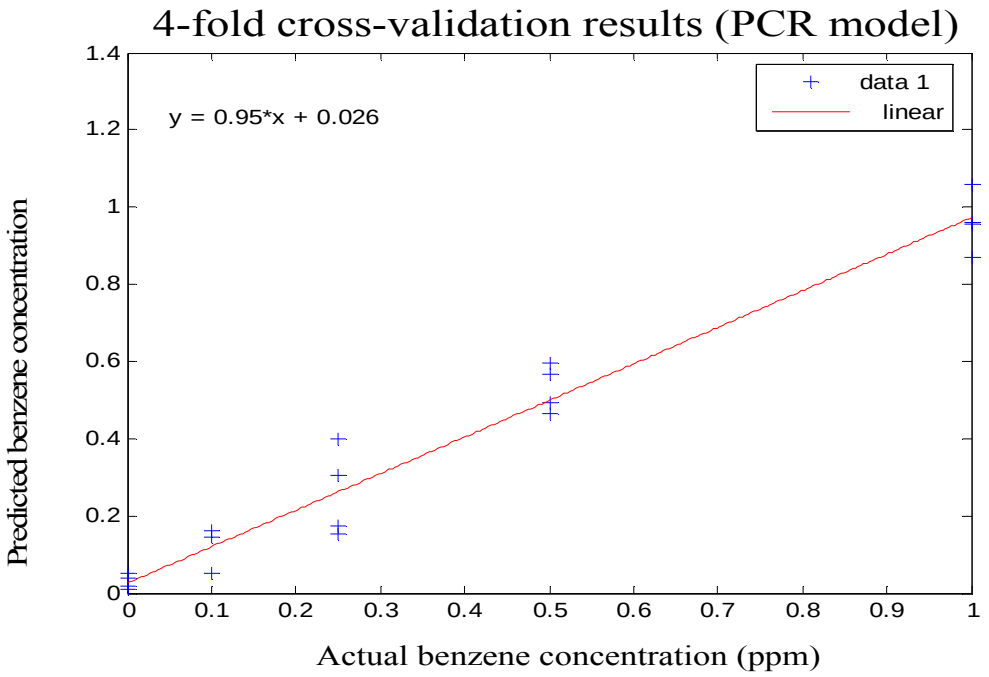

Figure 8.a: Validation results obtained for specific benzene quantification in CO mixtures.

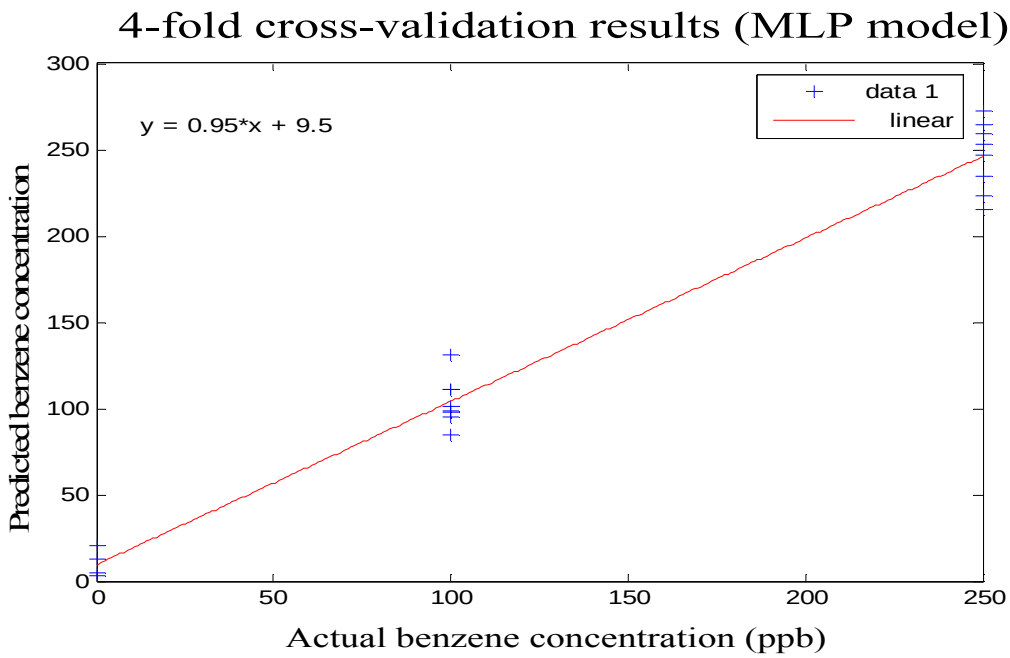

Figure 8.b: Validation results obtained for specific benzene quantification in NO_2 mixtures

The slopes of the fittings shown in Figure 8 are 0.95 (which are close to the ideal 1). The correlation coefficients of the linear regression between the real and predicted benzene concentrations are 0.982 and 0.987 respectively. Finally the intercept shows the minimum error in the concentration estimation (or the lower limit of detection). This

ISBN:978-84-694-0326-6/DL:T-207-2011

error is 26 ppb, which implies that the lower limit of reliable detection for benzene is about 25 ppb.

Prior to use one of the three specific benzene quantification models with a new sensor array response, it is necessary to determine to which zone the measurement belongs (defined in Figure 7). This approach was validated employing a leave-one out cross-validation on the measurements in the database. A 100% success rate in zone recognition was obtained.

The following figures show typical sensor responses and recovery cycles under dry ambient conditions for different gas mixtures (Benzene/CO, benzene/H_2S, and Benzene/NO_2). The measurement/ baseline recovery procedure described previously was employed and different carbon nanotubes based sensors were studied.

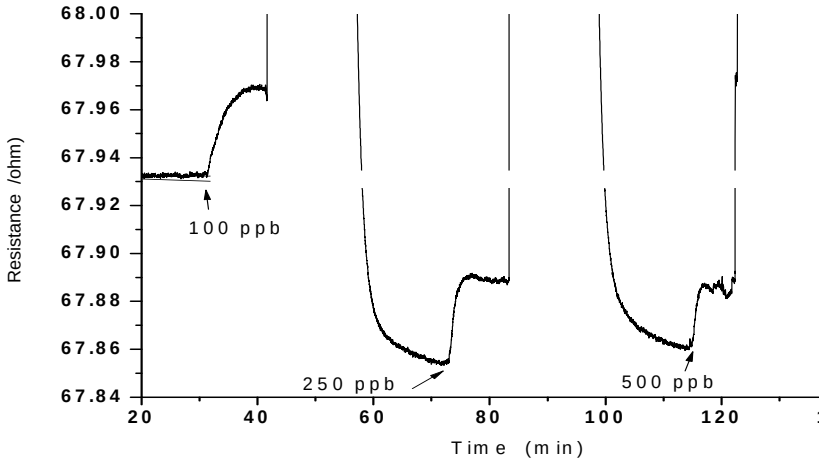

Figure 9: Detection of benzene in the presence of 2 ppm of CO at room temperature in dry air by Rh/CNTs

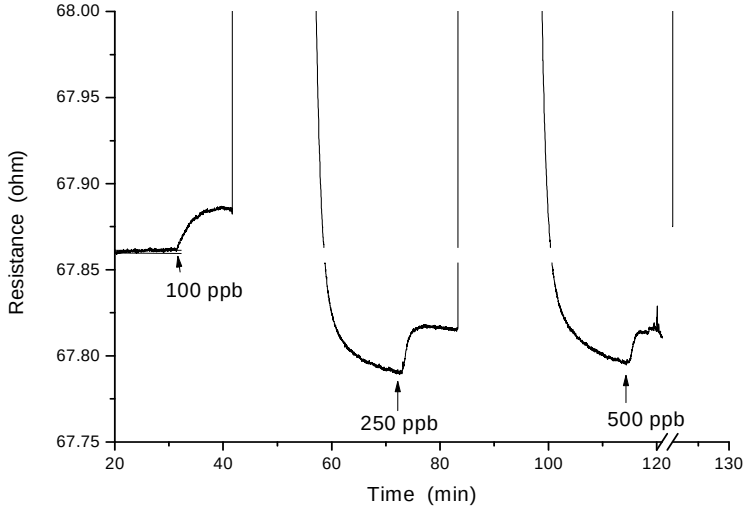

Figure 10: Detection of benzene in the presence of 2 ppm of CO at room temperature in dry air by Pd/CNTs

ISBN:978-84-694-0326-6/DL:T-207-2011

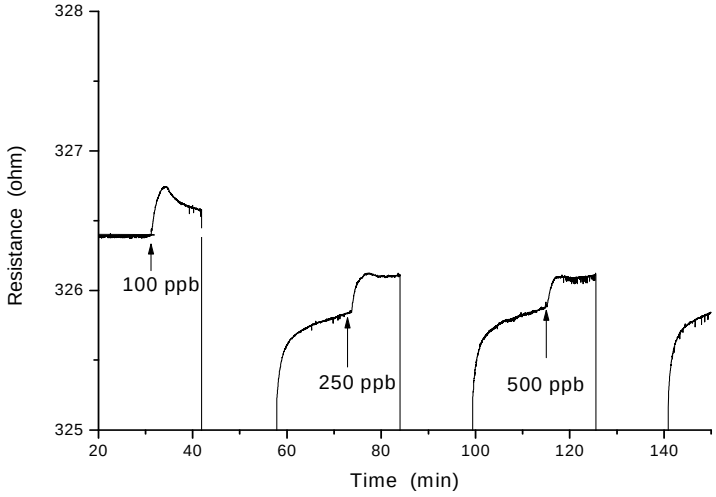

Figure 11: Detection of benzene in the presence of 5 ppm of CO at room temperature in dry air by O_2/CNTs

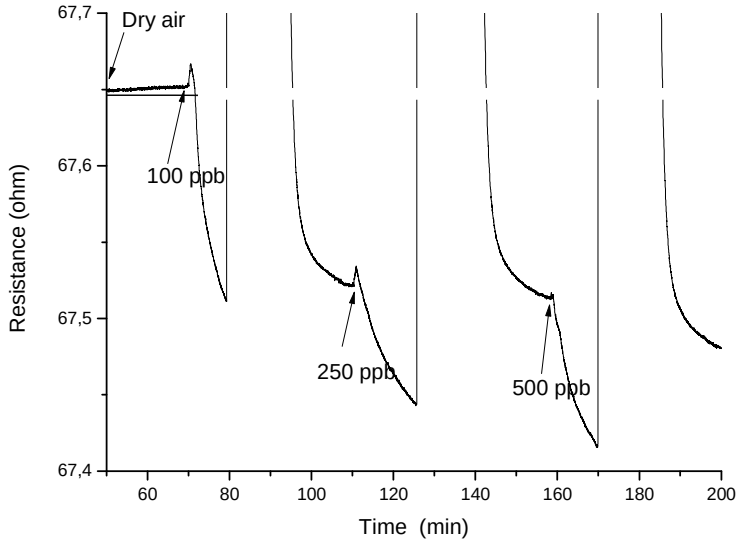

Figure 12: Detection of benzene in the presence of 500 ppb of NO_2 at room temperature in dry air by Pd/CNTs

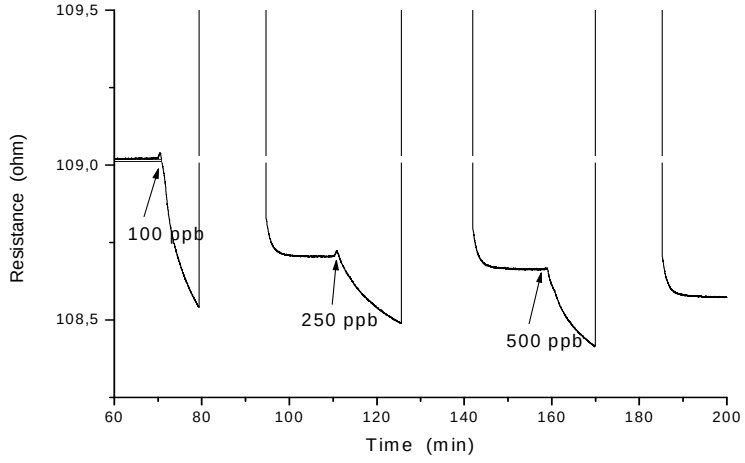

Figure 13: Detection of benzene in the presence of 500 ppb of NO_2 at room temperature in dry air by Pt/CNTs

ISBN:978-84-694-0326-6/DL:T-207-2011

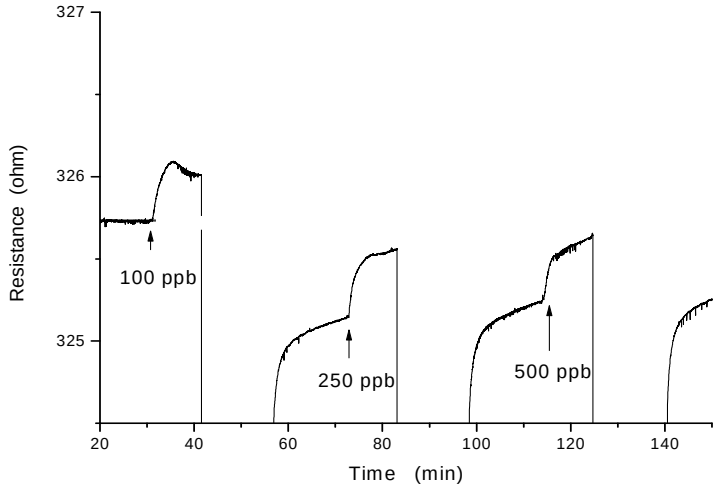

Figure 14: Detection of benzene in the presence of 10 ppm of H_2S at room temperature in dry air by O_2/CNTs

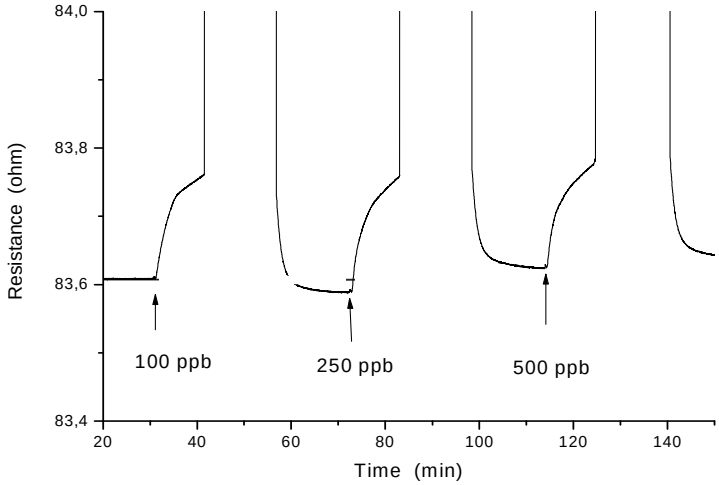

Figure 15: Detection of benzene in the presence of 10 ppm of H_2S at room temperature in dry air by Pt/CNTs

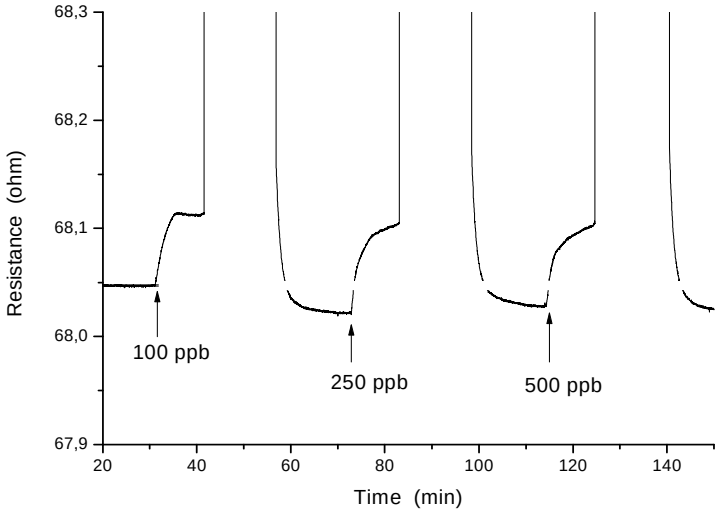

Figure 16: Detection of benzene int the presence of 10 ppm of H_2S at room temperature in dry air by Pd/CNTs

ISBN:978-84-694-0326-6/DL:T-207-2011

6.1.2. Measurments in humid ambient

In this section, we will investigate the effect of humidity on the sensing properties of the benzene detector. To do so, the benzene detector will be exposed to single gases and binary mixtures summarized in table 1in the presence of 50 % and 80 % of humidity in the carrier gas and during gas detection. These two rates are auto-generated by an Environics system and they were chosen in order to include the whole range of humidity from the low to the maximum level.

The measurements at different humidity levels were performed working under the same conditions as before and also employing the same testing circuit (see section 6.1.).

In this case, the carrier gas was pure synthetic air containing 50 % and 80 % of relative humidity. The following figures show typical sensor response and recovery cycles employing the measurement/ baseline recovery procedure described previously for the detection of benzene, H_2S and their mixtures employing different sensing materials, at a humidity level of 50 %. Even though the possibility to detect benzene in H_2S in the presence of 80 % relatve humidity was investigated, results are not shown because it was not possible to detect benzene at such a high humidity level.

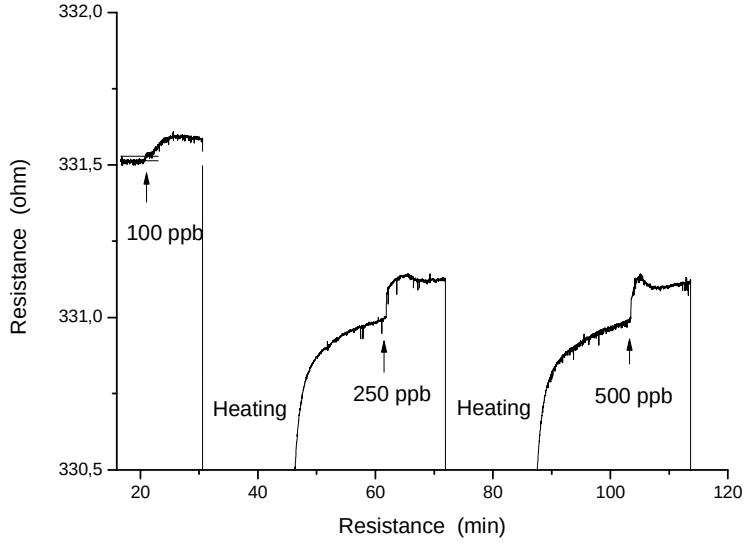

Figure 17: Detection of benzene at room temperature in humid air 50 % by O_2/CNTs

ISBN:978-84-694-0326-6/DL:T-207-2011

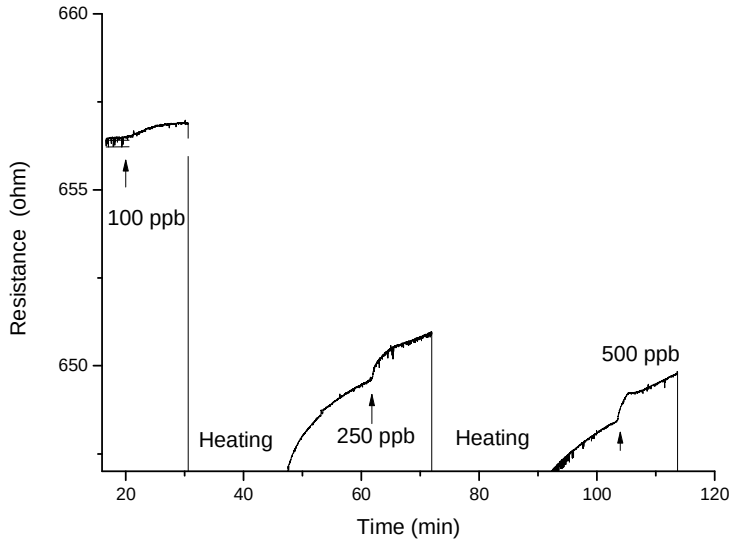

Figure 18: Detection of benzene at room temperature in humid air 50 % by Pt/CNTs

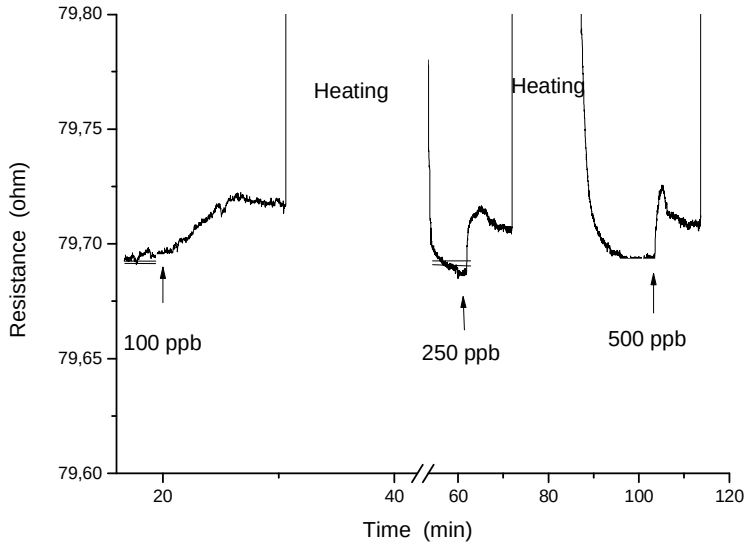

Figure 19: Detection of benzene at room temperature in humid air 50 % by Rh/CNTs

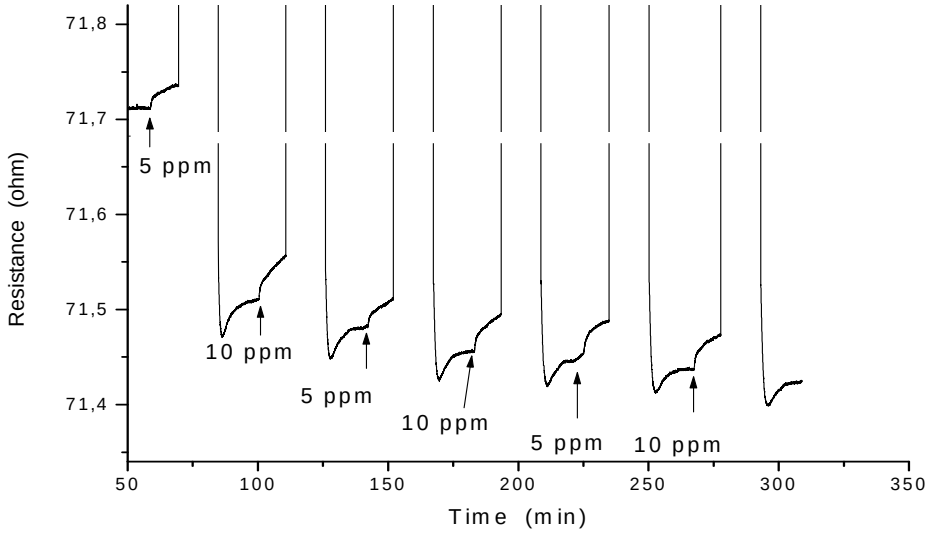

Figure 20: Detection of H_2S at room temperature in humid air 50 % by O_2/CNTs

ISBN:978-84-694-0326-6/DL:T-207-2011

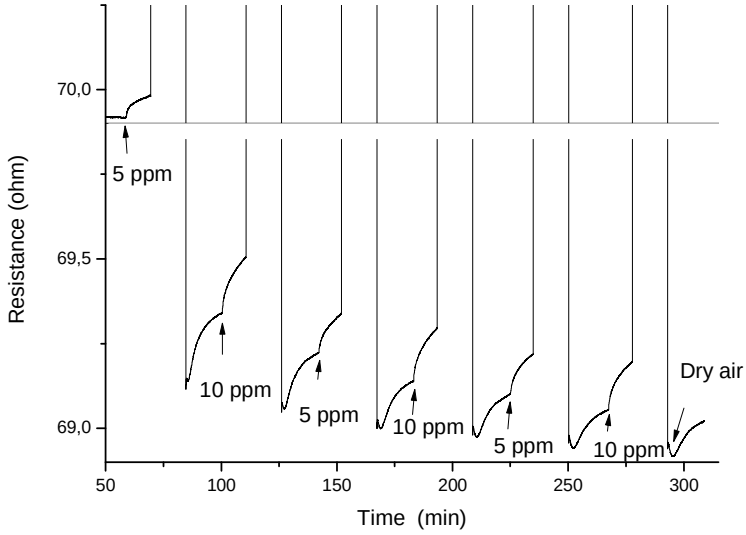

Figure 21: Detection of H_2S at room temperature in humid air 50 % by Pd/CNTs

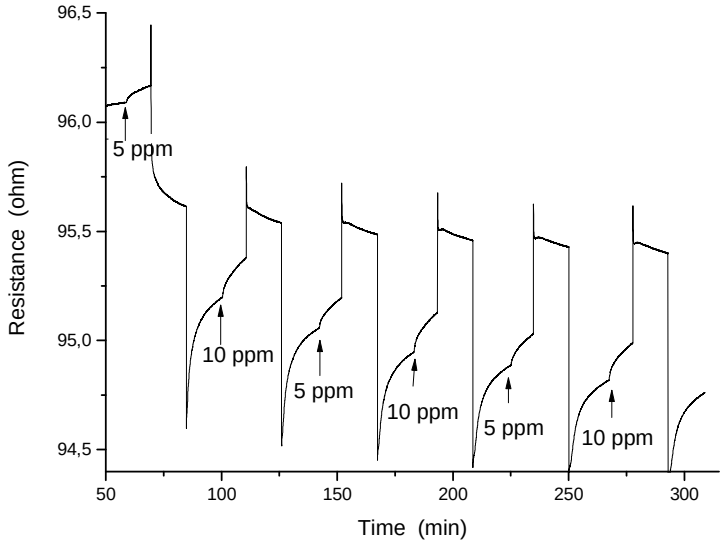

Figure 22: Detection of H_2S at room temperature in humid air 50 % by Pt/CNTs

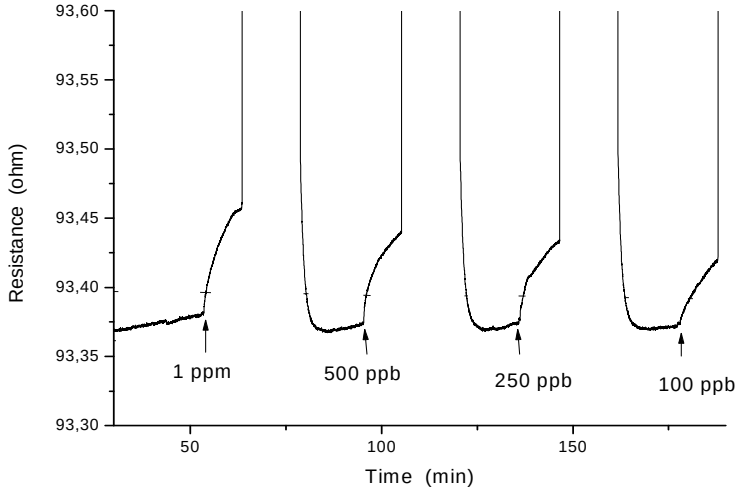

Figure 23: Detection of benzene at the presence of 5 ppm of H_2S at room temperature in humid air 50 % by Pt/CNTs

UNIVERSITAT ROVIRA I VIRGILI
DESIGN, FABRICATION AND CHARACTERISATION OF GAS SENSORS BASED ON NANOHYBRID MATERIALS
Radouane Leghrib
ISBN:978-84-694-0326-6/DL:T-207-2011

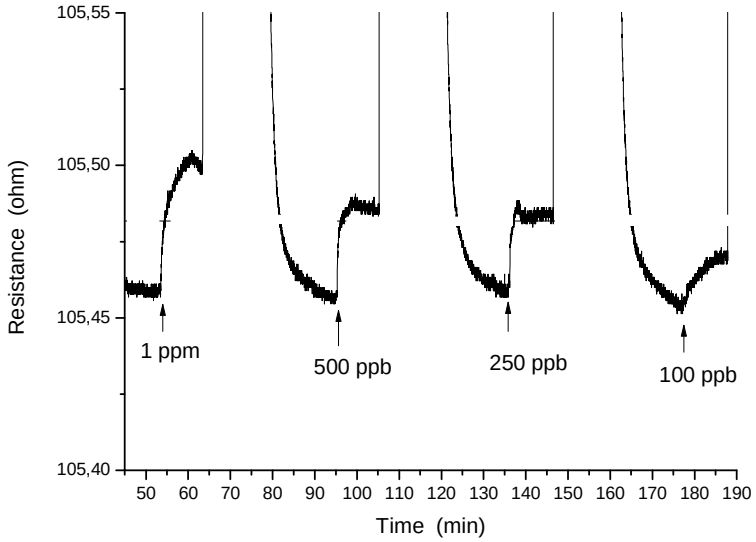

Figure 24: Detection of benzene at the presence of 5 ppm of H_2S at room temperature in humid air 50 % by Rh/CNTs

The response time of the sensors was defined as the time needed for the response to sweep from 10% to 90% of its final value. Similarly, recovery time was defined as the time needed for the resistance to sweep from 90% down to 10% of its initial value. From the figures above, the response time was estimated to range between 60 s to 120 s while recovery time (after switching off the heater) was estimated to be 5 min.

Given the large amount of information resulting from the characterization the sensors, a mathematical processing is needed in order to have a more clear vision about the sensors selectivity, and reproducibility. Annex IV summarizes the scripts used in MATLAB to perform such processing which used classical algorithms such as principal component analysis, linear discriminant, partial least squares or a multilayer perceptron neural network.

A linear discriminant analysis was performed using the responses of a 4-element sensor array based on Rh, Pt, Pd decorated MWCNTs and oxygen functionalized MWCNTs. We did not specify if the experiment was in dry or humid ambient. So, a total discrimination between benzene, H_2S, and their mixture is achieved. Regarding the discrimination between H_2S and its mixture with benzene, two points of the mixture were very near from the points of H_2S detection but they did not overlap. This can be the result of an error in these specific measurements (outliers). It is important to stres that we did not define the concentrations or the nature of the measuring ambient (dry or humid ambient). Even if we did not take into account this last factor we can see from figure 25, in which we present the results of LDA processing ,that for each species two

ISBN:978-84-694-0326-6/DL:T-207-2011

groups of points are clearly visible, which correspond to different humidity levels. Figure 25 shows that the selective detection of benzene at trace levels (detection limit below 50 ppb) is possible. Within the cluster of a given species, data points are replicate measurements of different concentrations.

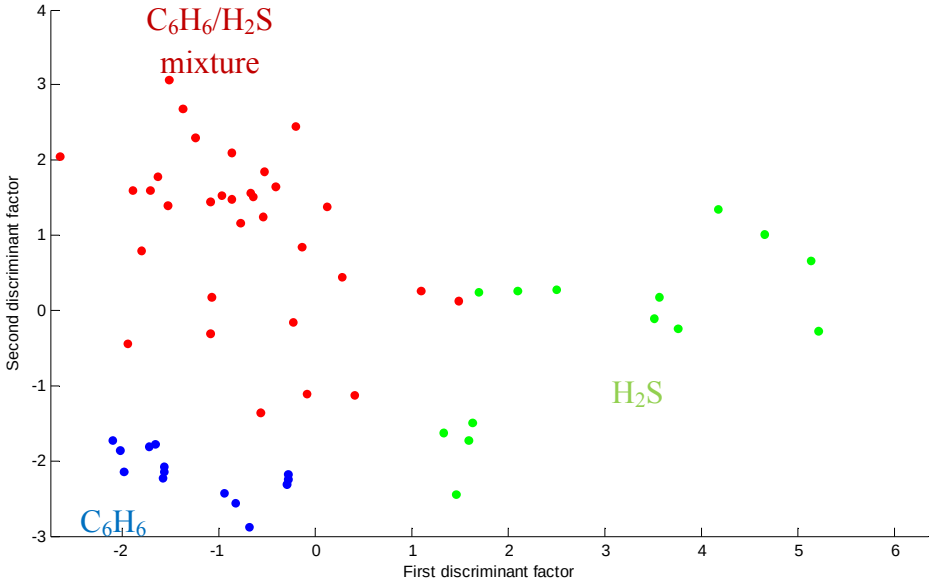

Figure 25. LDA performed on the responses in both dry and humid ambient of a 4-element microsensor array coated with MWCNTs decorated with 4 different metal nanoparticles.

To verify the presence of benzene and then estimate its concentration, specific calibration models have been built in the zone of the mixture with H_2S. Regarding the number of variables that we are processing here (e.g, gases concentration, and the humidity rate), we performed at first, a simple partial least squares (PLS) model aimed at predicting benzene concentration regardless the presence of H_2S or the humidity level. However, the correlation coefficient (0.842) of the linear regression between the real and predicted benzene concentrations was not good enough (fig. 26). In the second step, we processed the data gathered under humid ambient conditions and the result was more acceptable since the correlation coefficient of the linear regression between the real and predicted benzene concentrations was 0.959 (fig. 27). The data for dry ambient conditions was also processed, and in this case the correlation coefficient of was 0.883, which is worse than in the case of humid ambient (fig. 28). Since humidity seems to play a major role in the accuracy of the benzene predictive models, a multilayer perceptron (MLP) neural network was trained and validated on the data. Once more, the MLP model was aimed at estimating benzene concentration regardless the presence of

ISBN:978-84-694-0326-6/DL:T-207-2011

H_2S or the humidity level. The MLP had as inputs the response of the sensors and an extra input with the humidity level. During the training phase, the MLP is expected to learn compensate humidity changes. The results were very encouraging and the correlation coefficient of the linear regression between the real and predicted benzene concentrations was 0.994. Figure 29 shows the performance of such dedicated model. It shows the final validation results of the benzene detector.

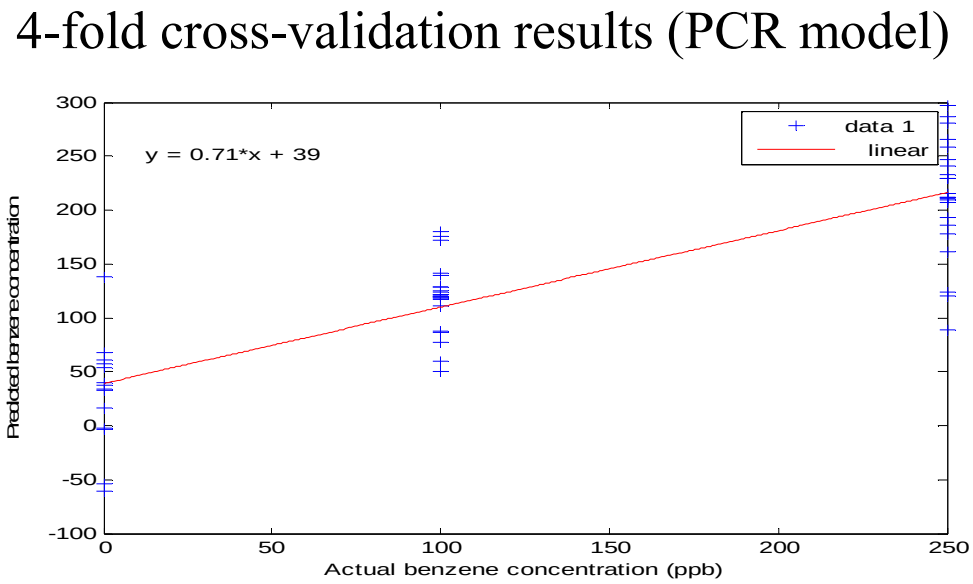

Figure 26: Validation results obtained for specific benzene quantification in H_2S mixtures in both dry and humid ambient.

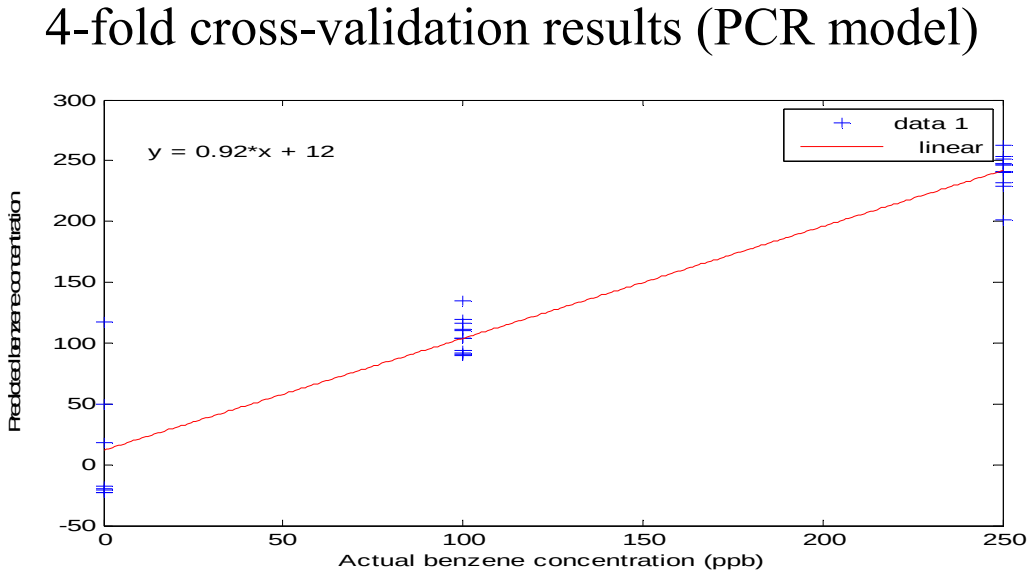

Figure 27: Validation results obtained for specific benzene quantification in H_2S mixtures in humid ambient.

ISBN:978-84-694-0326-6/DL:T-207-2011

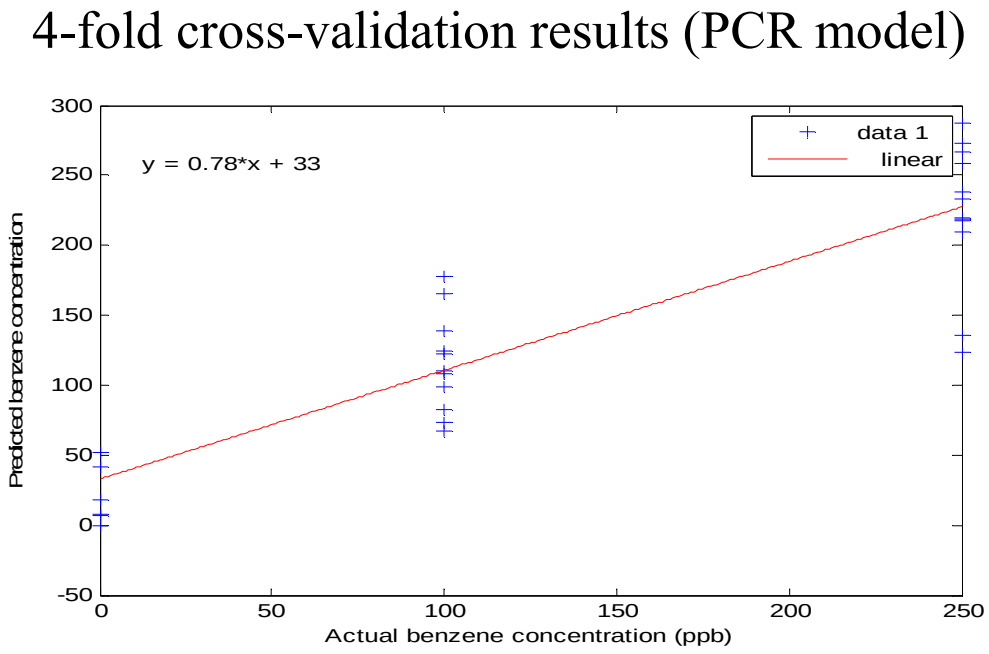

Figure 28: Validation results obtained for specific benzene quantification in H_2S mixtures in dry ambient.

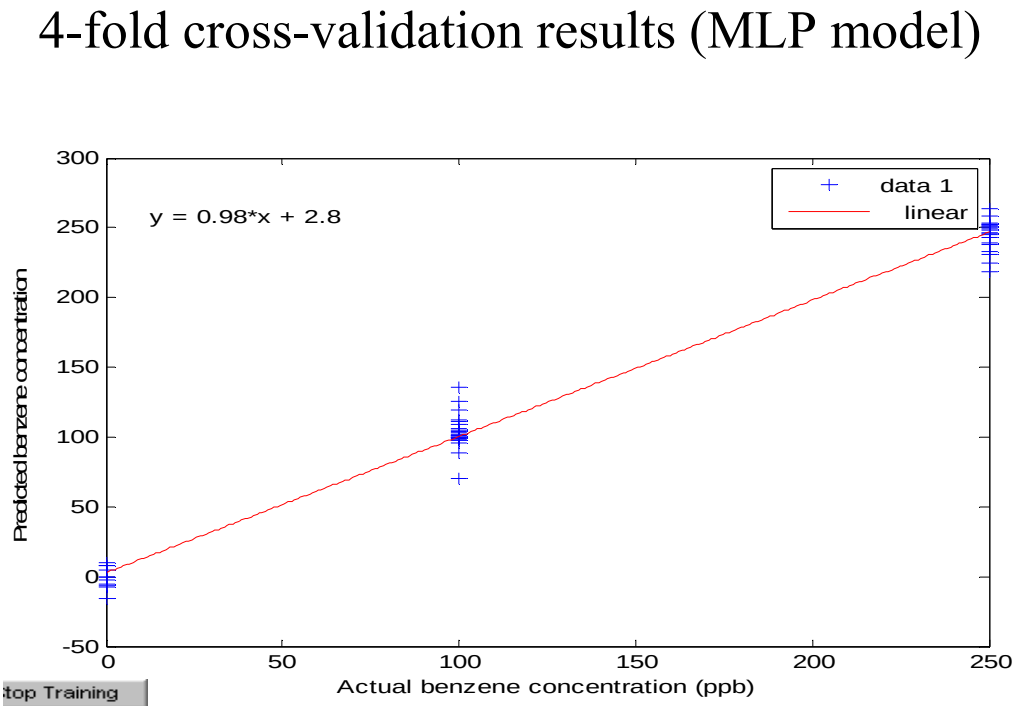

Figure 29: Validation results obtained for specific benzene quantification in H_2S mixtures in both dry and humid ambient.

UNIVERSITAT ROVIRA I VIRGILI
DESIGN, FABRICATION AND CHARACTERISATION OF GAS SENSORS BASED ON NANOHYBRID MATERIALS
Radouane Leghrib
ISBN:978-84-694-0326-6/DL:T-207-2011

To summarize, the obtained results which we showed above validate the strategy of selective benzene detection and show that benzene concentration can be estimated with fair accuracy.

Concerning the commercialization of the benzene detector, more studies are needed in terms of testing a wider range of gases, better fighting humidity effects and further studying sensor lifetime.

6.2. Final prototype

The final proposed detector prototype (hand-held unit) which will host our sensor array is shown in figure 30. The fabrication of this prototype is being carried out by Sensotran Company. It is expected that the air-flow can be set externally or an air pump can be operated. In the first tests, the measurement procedure has been shortened to 5 min data acquisition and 5 minutes of cleaning (including heating for baseline recovery). Therefore the detector can perform a measurement every 10 minutes. But still more work is needed before the benzene detector can be marketed.

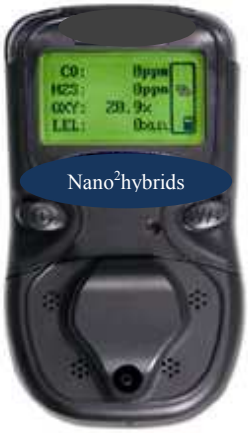

Figure 30: first prototype hand-held unit ***for selective benzene detection***

UNIVERSITAT ROVIRA I VIRGILI
DESIGN, FABRICATION AND CHARACTERISATION OF GAS SENSORS BASED ON NANOHYBRID MATERIALS
Radouane Leghrib
ISBN:978-84-694-0326-6/DL:T-207-2011

UNIVERSITAT ROVIRA I VIRGILI
DESIGN, FABRICATION AND CHARACTERISATION OF GAS SENSORS BASED ON NANOHYBRID MATERIALS
Radouane Leghrib
ISBN:978-84-694-0326-6/DL:T-207-2011

CONCLUSIONS AND FUTURE PROSPECTS

UNIVERSITAT ROVIRA I VIRGILI
DESIGN, FABRICATION AND CHARACTERISATION OF GAS SENSORS BASED ON NANOHYBRID MATERIALS
Radouane Leghrib
ISBN:978-84-694-0326-6/DL:T-207-2011

ISBN:978-84-694-0326-6/DL:T-207-2011

In this thesis, a wide variety of gas sensors using CNT materials have been studied. The nanomaterials employed included pristine, oxygen functionalized, metal or metal oxide decorated carbon nanotubes, metal oxide and CNT mixtures and finally, nitrogen or boron substituted multi-walled carbon nanotubes. The sensors were tested towards different toxic gases such as benzene, carbon monoxide, nitrogen dioxide, ethylene, hydrogen sulfide, ammonia in dry and humid conditions and their performances were compared in terms of reactivity, responsiveness, stability, reproducibility, response and recovery times. As a main conclusion of this thesis, it was found possible to design a sensitive and selective benzene detector employing an array of four sensors that used MWCNT decorated with four different metal nanoclusters. Partial conclusions are as follows.

➲ In what concerns sample preparation:

- Different metal decorated samples were prepared from different precursors and different nanocluster sizes (samples prepared by other partners).
- Different metal oxide decorated samples were prepared from different commercial and home-made precursors and using different doping ratios.

➲ In what concerns the sensor fabrication:

- A device based on a silicon four-element integrated micro-sensor array was fabricated in the “Centro National de Microelectronica” in Barcelona to host the prepared carbon nanotubes active layers.
- Deposition of CNTs in a desired position and formation of reliable electrical contacts are among the biggest challenges on the way to mass production of CNTs-based devices. In fact, the electrical transport properties of a CNT-based device are dependent on the metal-CNT contact properties. For metal electrodes, a junction with semiconductor CNT may result in a Schottky barrier (SB) and a junction with metallic CNT may produce an Ohmic contact. To develop and design CNT-based devices, low values of contact resistances are required, because high resistances result in higher noise, especially at elevated working temperatures.
- Prior to deposition, it is important to select a suitable organic solvent for the dispersion of the carbon nanotube samples. Indeed, the solvent must be able to

ISBN:978-84-694-0326-6/DL:T-207-2011

separate to the maximum the agglomerated carbon nanotubes of the as received powder into isolated ones, if not the deposited layer will not be very homogeneous. Layer homogeneity is in fact important for gas sensing applications, because it influences the gas sensing properties (e.g. adsorption and diffusion phenomena are affected). Furthermore, good homogeneity of the active layers is necessary for reaching good sensor reproducibility.

- The selection of the organic solvent was found to depend on the deposition method to be used. Dimethylformamide was found to be better for the dispersion of oxygen functionalized carbon nanotubes, while acetone dispersed better the pristine ones.
- Different deposition techniques were tested: Direct drop coating, inverse drop coating and direct and inverse airbrushing:

-After the CNTs have been deposited using previous techniques (Drop coating, airbushing, screen printing, etc) onto the metal electrodes, the resistance of the device is generally high. One way to reduce the contact resistance is to perform a thermal treatment. In fact, it was found in the literature that by performing a thermal treatment of the CNTs layer, the sensor contact resistance diminishes.

-By drop coating the metal decorated samples onto the sensor, the thermal treatment performed after the deposition was found to affect the adhesion of the nanoclusters onto the MWCNT walls.

-To prevent the partial removal of the metal nanoclusters during the deposition process said above, inverse drop coating method was tested as alternative. This method consists of employing the drop coating technique to deposit untreated carbon nanotubes dispersed in acetone on the silicon substrate. In this way, the thermal treatment is performed on the pristine CNTs prior to the functionalization in oxygen plasma followed by metal decoration. TEM analysis confirmed the non detachment of metal nanoclusters from the nanotube sidewalls thanks to this method.

-After the deposition, the thermal treatment can vary from a solvent to another but must be selected so as not to affect the properties of the active material. This thermal treatment was already adjusted using DTA-TGA analysis.

-By comparing the advantages and drawbacks of each technique (in terms of compatible solvents, homogeneity of the resulting films, etc.), it is evident that the air-brushing method remains the best one for gas sensor fabrication using the

ISBN:978-84-694-0326-6/DL:T-207-2011

nano-hybrid materials. Indeed, this technique makes a good match between good uniformity of the deposited layer, good definition of the deposited area, absence of impurities after the deposition, and the possibility to adjust the resistance of the active layer. The inverse airbrushing technique is preferred.

➲ In what concerns the sensor characterization:

➢ For the metal decorated samples:

- The response behavior to gases changes depending on the binding energy of the metal with the carbon nanotubes. The higher this energy is, the stronger the interaction is.
- The interaction mechanism with gases is not totally understood yet, for that reason, two possible mechanisms were proposed here, which can occur simultaneously or separately during the exposure to the gas:

  - The first one considers that the molecules react with the oxygenated defects created during the oxygen plasma treatment. In other words, CNTs behave like p-type materials due to electron withdrawing by oxygen molecules adsorbed on the CNT surface. The gas directly adsorbs onto an oxygenated defect located at the CNT sidewall created by the oxygen plasma treatment, inducing electron transfer and changing the electrical conductivity of the hybrid nanomaterial. In the second mechanism, the gas adsorbs onto a metal nanoparticle and this results in a significant charge transfer between the nanoparticle and the CNT, which eventually changes the electrical conductivity of the hybrid nanomaterial.
- The reactivity of the different samples was shown to depend on different parameters:

  -Effect of the material synthesis:

  - The importance of oxygen plasma prior to metal decoration was demonstrated. In fact, the plasma treatment is important because it enables cleaning, activating, functionalizing and metal decorating CNTs in a more homogeneous way. Oxidative treatments affect the density of states (DOS) of valence bands and increase the work function of purified MWCNTs, which is close to the work function of the metal considered in this thesis. The effective electronic interaction between metal nanoparticles and the CNT facilitates the detection of gases through the

ISBN:978-84-694-0326-6/DL:T-207-2011

change in the electrical conductivity of mats formed by these hybrid nanomaterials.

- The functionalization of the nanotubes was also tried with argon instead of oxygen. This resulted in a lower response to moisture, however, the response to the gases was diminished. An inconvenient of oxygen plasma treatment is that the response to moisture is highly enhanced due to the polarity modification induced in the samples. CNTs become more hydrophilic after the oxygen plasma treatment and remain basically hydrophobic if treated in a plasma not containing oxygen.
- The nature of the precursors was found to affect the responsiveness of the samples. In fact, organometallic precursors were found to be more suitable for enhancing the sensitivity of the metal decorated samples than solid salt precursors. This was more due to the more homogenous distribution of the nanoclusters in the nanotubes surface than to the amount of nanoclusters attached.
- Smaller are the metal nanoparticles, higher is their reactivity, but the best response to gases is achieved by the most isolated nanoclusters which is the case of intermediate sizes (i.e., 5 nm).
- The higher is the amount of nanoclusters of the optimized size, the higher the responsiveness to gases is.

-Effect of the sensor fabrication:

- The effect of the deposition method on the sensing properties of the materials was investigated. The deposition method can tune the response towards a gas or another depending on the gas adsorption site. For example, direct drop coating is preferred for gases like NO_2 which prefers oxygen sites, while inverse drop coating is better for the gases which react more with the metal nanoclusters such as CO. The highest CO to NO_2 responsiveness ratio is obtained with the inverse drop coating preparation method. That is, the one that lead to sensing films based on MWCNTs well decorated with Au nanoparticles. Selectivity may probably be reached for some gases using an array of sensors fabricated by both methods.
- The type of the metallic electrodes affects the sensitivity to gases. In fact, some interaction can occur at the interface between the electrodes and

ISBN:978-84-694-0326-6/DL:T-207-2011

active layer resulting in change in the conductivity of the materials. This interaction was found to depend on the target gas (e.g, benzene prefers Pt electrodes while NO_2 prefers Au electrodes). Some selectivity can be derived from such an effect.

-Effect of sensor working conditions:

- For a given metal decorated sample, the response at ambient temperature was much higher than at 150 ºC a part for Rh and Pd decorated MWCNTs. This effect can be due to the partial desorption of some molecules at 150 ºC but it remains not well understood.
- The carrier gas flow is reported to have certain effect on the kinetic interaction of gas molecules with the active layer. The higher is the flow, the faster is the interaction and desorption. This improvement also depends on the design of the sensing chamber inlet and outlet. The flow used in our case was adjusted to 100 ml/min for the requirements of the application even if higher flows would be preferred for a faster response and recovery.
- Gas sensor based on CNTs, usually present large recovery times at ambient temperature. By subjecting our sensors to heating at 150 ºC, we could diminish the recovery time from 3 h at ambient temperature to 15 min under 150 ºC. Desorption can be further quickened by illuminating the sensor using Ultra-Violet (UV) light.
- Although sensors are subjected to some baseline drift in some cases, which is often experienced with CNT based chemo-resistive sensors, their effects can be minimized in a detector by employing simple baseline correction techniques.
- The sensing performance of the hybrid nanomaterials could be mainly attributed to the different effectiveness of electron transfer between different metal nanoclusters and MWCNTs, to specific reactivities of metal cluster surfaces and, finally, to an increase in the specific surface area of our hybrid nanomaterials. By adjusting all these parameters, we found good responses to gases which are reported to have weak or no interaction with pristine carbon nanotubes based materials, such as benzene. Also, the detection limits in this case were quite small around 50 ppb.

ISBN:978-84-694-0326-6/DL:T-207-2011

- When combined in a four microsensor array, the use of these benzene-sensitive and benzene-insensitive metal-decorated MWCNTs provided a selective detection of benzene at trace levels (ppb concentration) confirmed by PCA o LDA analyses. These materials can be for example: Rh, Pt and Pd decorated MWCNTs and oxygen plasma treated MWCNTs, even if other combinations remain possible. This result is very interesting since no benzene sensor has been reported until now with these combined features: Selective, sensitive, miniaturized (Portable), low cost, and operating at room temperature (low power consumption).
- A selective gas sensor array based on Rh, Pd, Pt, and O_2 modified CNTs was successfully implemented at room temperature and showed good discrimination between NO_2, H_2S, C_6H_6, and CO in mixture at dry ambient and 50 % humid ambient.
- The obtained results validated the strategy of selective benzene detection and showed that benzene concentration can be estimated with fair accuracy. The final benzene detector was used in a demonstration prototype devoted to the selective detection of benzene in industrial applications.

➢ For the metal oxide doped or mixed with MWCNTs:

- The gas sensing properties of the hybrid materials were investigated and compared against the sensing properties of sensors based on pure tin oxide nanoparticles or on pure oxygen plasma treated multiwall carbon nanotubes. It was found that at low operating temperatures (room temperature and 150ºC) hybrid nanomaterials were significantly more responsive to nitrogen dioxide and carbon monoxide than pure nanomaterials (pure tin oxide or pure MWCNTs). Even if the response at 150 ºC is higher than at room temperature.
- Additionally, there is an optimal ratio between the amount of tin oxide precursor and carbon nanotubes to be used during the hybrid preparation procedure in order to maximize responsiveness.
- The response mechanism is fully reversible, since the sensors can recover their baseline resistance after each exposure to pollutant gases.

ISBN:978-84-694-0326-6/DL:T-207-2011

- Based on these results, the modulation of the width of two depletion layers existing at the surface of metal oxide grains and at the interface of metal oxide grains and MWCNT, respectively, is postulated as the mechanism that could explain the enhanced performance of hybrid metal oxide/MWCNT sensors in comparison with pure metal oxide or pure MWCNT sensors.
- The optimal hybrid materials showed a moderate moisture cross-sensitivity, much lower than the one found in pure tin oxide or in hybrids with rich content of tin oxide.
- For home made metal oxides doped CNTs, based on the nature of the sensor response to nitrogen dioxide and on previous first principles calculation results, different mechanisms for detection depending on the operating temperature have been identified. At room temperature, the optimal hybrid material behaves as a *p*-type semiconductor, which indicates that upon adsorption of nitrogen dioxide molecules either on nanotube sidewalls or on tin oxide nanoclusters, a significant amount of electronic charge is transferred from nanotubes to the adsorbed NO_2 and also from nanotubes to tin oxide nanoclusters, affecting nanotube conductivity. On the other hand, when hybrid materials are operated at 150ºC, these behave as an *n*-type semiconductor. Nitrogen dioxide adsorbs onto tin oxide nanoclusters trapping electrons and, therefore, increases the resistance of the hybrid film. Conductivity is mobility-limited by the presence of potential barriers at tin oxide inter-grain contacts. This effect is measurable at low temperatures (i.e., 150ºC) because the presence of embedded MWCNTs helps reducing the number of potential barriers a conduction electron needs to cross to reach the electrodes.
- Metal decorated CNT mixed with commercial metal oxides present higher sensitivity at room Temperature and 150 ºC compared to the home-made metal oxide decorated oxygen functionalized CNT, this can be explained by the existence of metal in the first composite which improve the conductivity through the compound active layer.

ISBN:978-84-694-0326-6/DL:T-207-2011

- The presence of different detection mechanisms activated at different operating temperatures opens again an opportunity to tune the selectivity of carbon nanotube based sensors.
- Ternary hybrid materials based on metal decorated carbon nanotubes mixed with commercial metal oxides offered the possibility to further enhance the responsiveness towards gases. In particular, micro-sensors based on Au-MWCNT/SnO_2 hybrid films in a concentration ratio of 1/250 wt% showed the highest sensitivity towards NO_2 and CO, among the different materials studied.

➢ For the nitrogen or boron doped MWCNTs:

- B- or N-CNTs are cheap and require no post-growth treatment. Sensors based on these materials are very sensitive and present a rapid response, and good recovery time compared to pristine CNTs.
- B-doped CNTs showed a high interaction towards gases which is undesirable in some cases such as NO_2 detection as the reaction becomes irreversible. While N-doped SWCNTs should be good NO_2 sensors with quick response and short recovery time.
- The experimental results obtained with boron and nitrogen doped CNTs followed the tendency of the theoretical results obtained using vacancy doped boron and nitrogen structures.

These results were among the best found in literature. However, other improvements are worth of investigation:

➲ In what concerns sample preparation:

- Other hybrid samples can be prepared by combining the different materials tested during this thesis. The use of ternary hybrids will be interesting for further increasing the sensitivity towards gases. For example:
  - The metal decorated samples such as Rh, Pd, Pt, etc can be mixed with the metal oxides.
  - The N or B doped CNTs can be decorated with different metallic nanoclusters.
  - SWCNTs can be used instead of MWCNTs for their many advantages (Higher surface area, higher number of semi-conductor tubes, etc)

ISBN:978-84-694-0326-6/DL:T-207-2011

➲ In what concerns sensor fabrication:

- The inverse airbrushing technique can be used to prepare the final selective device. A better alternative could be to use the dielectrophoresis method in order to fix, separate and align at the same time the carbon nanotubes on top of the sensor membrane and electrodes. Other research teams have shown that the alignment of nanotubes further improves the electrical transport through the nanotubes layer. This method is also useful for a good adhesion of the active layer to the substrate.
- Another possibility is to deposit the electrodes above the carbon nanotubes sensing layer already deposited onto the sensor membrane. This is expected to promote the contact between the active layer and the electrodes.
- Finally the thermal treatment can be optimized for all sensing materials including the metal decorated CNTs, metal oxide doped or ternary hybrids CNTs. This will also decrease sensor resistance.

➲ In what concerns sensor characterization:

- The sensor operating conditions can be also improved. In fact, the design of the gas inlet can be perpendicular instead of laminar in order to increase the pressure of the gas above the sensor. This will aid to improve the interaction of the gas with the sensing layer and lower the response and recovery times.
- As reported in literature, the sensors can be recovered by ultraviolet light illumination instead of thermal desorption, for reaching recovery times in the order of seconds. However careful checking whether UV light modifies the CNT surface is needed, otherwise unwanted response drift or irreversible changes in sensor response would arise.

UNIVERSITAT ROVIRA I VIRGILI
DESIGN, FABRICATION AND CHARACTERISATION OF GAS SENSORS BASED ON NANOHYBRID MATERIALS
Radouane Leghrib
ISBN:978-84-694-0326-6/DL:T-207-2011

UNIVERSITAT ROVIRA I VIRGILI
DESIGN, FABRICATION AND CHARACTERISATION OF GAS SENSORS BASED ON NANOHYBRID MATERIALS
Radouane Leghrib
ISBN:978-84-694-0326-6/DL:T-207-2011

ANNEX I:

Nano^{2}hybrids materials: Materials preparation and characterization carried out by LISE, SAM, and CHANI laboratories

UNIVERSITAT ROVIRA I VIRGILI
DESIGN, FABRICATION AND CHARACTERISATION OF GAS SENSORS BASED ON NANOHYBRID MATERIALS
Radouane Leghrib
ISBN:978-84-694-0326-6/DL:T-207-2011

ISBN:978-84-694-0326-6/DL:T-207-2011

1. Pristine carbon nanotubes fabrication

Commercially available carbon nanotubes provided by Nanocyl, S. A were selected regarding their low cost and high purity (Table 1). The presence of impurities being an inconvenient for gas sensors [1].

Carbon nanotubes sold by Nanocyl were produced by catalytic chemical vapour deposition (CCVD) process (Nanocyl-3100) [2]. Their main characteristics are cited in the following table:

Table 1: Main characteristics of the pristine MWCNTs provided by Nanocyl

Property	Value
Average diameter (nm)	Inner: 3-7 Outer:3-15
Average length (µm)	50
Surface area (m^2/g)	200- 300
Carbon purity (%)	95

The pristine carbon nanotubes were subjected to a surface functionalization and decoration in order to increase their surface reactivity as was explained in section 2.1.2.

2. Carbon nanotubes functionalization and decoration

a. Basic concepts about plasma treatment

The plasma treatment refers to the use of an ionized gas (the 4th state of matter in which gas molecules come apart and become intensely reactive) at either low pressure or atmospheric pressure [3-5].

In general, the plasma treatment process can involve many applications such as surface decontamination, fine etching of the surface to create greater surface area, grafting of new functional groups or chemical species on the surface, and the deposition of coatings on the surface, etc [3].

Compared to some conventional chemical treatment methods: Wet chemistry [6], reactive gas atmosphere [7], and electrochemistry [8], etc, plasma treatment exhibits many important advantages. In fact, it is:

- ✓ Environmentally friendly: They do not use a large quantity of polluting chemicals.
- ✓ Requiring short time of treatment: Only a few seconds or minutes are needed to achieve their full treatment (surface cleaning, surface activation,

ISBN:978-84-694-0326-6/DL:T-207-2011

functionalization, defects creation), compared to the large time (hours or days) required by classical methods to functionalize CNTs

- ✓ Highly controllable: Operating plasma parameters (gas composition, pressure, plasma power, duration …etc) confirmed that it is possible to control the interfacial properties [9]. So the use of plasma allows at the same time to: control, select and finely tune the reactivity of the active layer.
- ✓ Multifunctional methods: Plasma treatment is not limited only to the application of active layers treatment for gas sensors, but it can be used in catalytic systems, fuel cells, biosensor, …etc
- ✓ Scalable to industrial production (treatment of large quantity): The industrial production is achieved by some companies [2]. Furthermore, large scale applications are foreseeable in catalysis [10], fuel cells [11], gas sensors [12], biomaterials [13], etc.

When dealing with a plasma treatment system, the main parameters that can be controlled are:

- ✓ The plasma power
- ✓ The treatment time
- ✓ The pressure and nature of the plasma gas
- ✓ The position of the sample

Three different plasma treatment systems were used by the three different partners. The main difference being the working pressure and the sample position inside the plasma reactor.

In the next part, the plasma system used by each member of the three groups will be described and some of their corresponding results will be also presented.

b. LOW PRESSURE PLASMA (LISE)

In this case, the carbon nanotubes are treated in a home-made chamber using inductively coupled plasma [9] (Fig. 1).

The proposed plasma treatment is performed at low pressure in two steps: surface cleaning, activation then metal thermal evaporation. The samples have been characterized by TEM and XPS analysis.

❖ **Surface functionalization**

A controlled flow of gas (oxygen, ammonia, tetrafluoromethane, nitrogen, hydrogen) can be introduced depending on the type of functionalization we want to get.

ISBN:978-84-694-0326-6/DL:T-207-2011

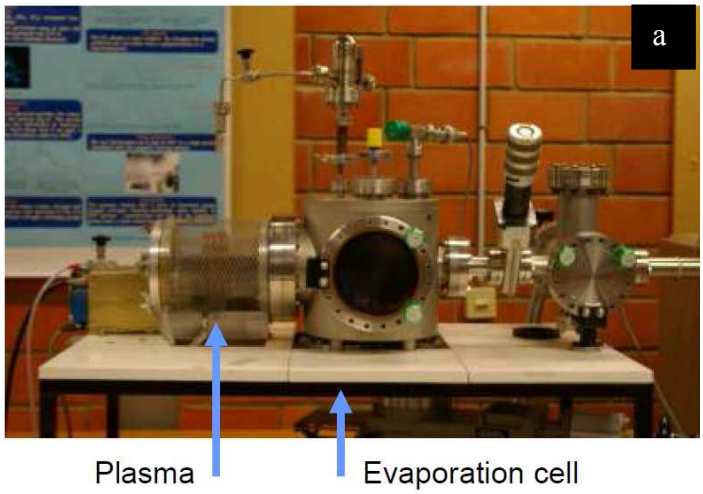

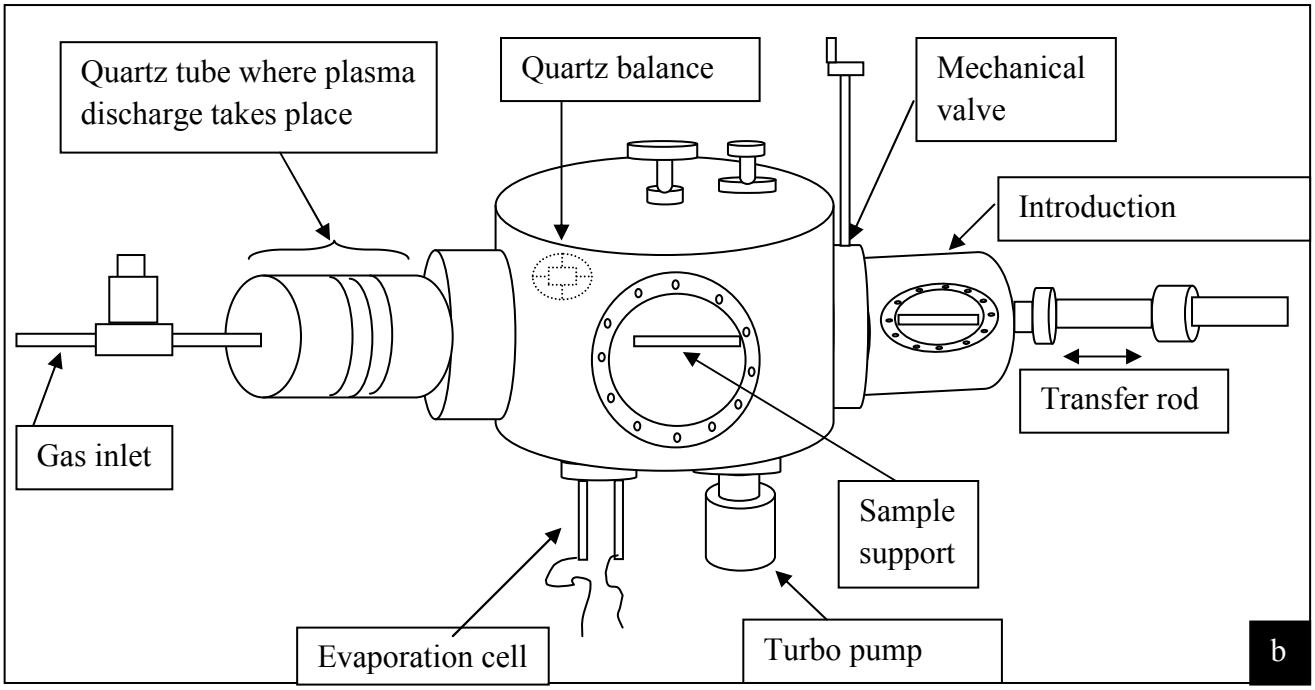

Figure 1: (a) Picture of the plasma evaporation cell from LISE laboratory (b) Scheme of the vacuum chamber used for plasma treatment and metal evaporation

The as-provided MWCNTs were placed inside a glass vessel and a magnet, externally controlled from the plasma chamber, was used to stir the nanotubes powders during the plasma treatment. Inductively coupled plasma at a RF frequency of 13.56 MHz was used during the process [9]. Once the MWCNTs powder was placed inside the plasma glow discharge, the treatment was performed at a pressure of 0.1 Torr, using a determined power, while the processing time was adjusted. A controlled flow of gas

ISBN:978-84-694-0326-6/DL:T-207-2011

(Argon, Helium, oxygen, etc) was introduced inside the chamber, which gave rise to functional species attached to the CNT walls.

The effect of plasma parameters variation on the MWCNTs treatment was widely studied [9, 14].

First, to investigate the effect of plasma treatment on CNTs, different plasmas of different gases (oxygen, argon, hydrogen, ammonia, etc) were tested. X-ray photoelectron spectroscopy technique (XPS) was used to study the elemental composition of each type of treatment of MWCNTs. Oxygen plasma was selected because it allows to attach functional groups such as hydroxyl, carbonyl and carboxyl known to be reactive sites to increase interaction with gases [14].

A complete study on oxygen functionalisation of MWCNTs has been performed. As it is known, oxygen plasma is quite aggressive towards carbon nanotubes. So, it is necessary to analyze the effect of the oxygen plasma treatment by varying the treatment conditions (Plasma power, treatment time and the position inside the chamber).

After carbon nanotubes functionalization using oxygen plasma, the samples were decorated with metal nanoclusters.

- **Surface decoration**

In the second processing step, different metals such as Au, Ag, Ni, Ti, Pd, Pt, Rh were thermally evaporated from a metal wire over O_2/CNT samples. The processing parameters were adjusted to be sufficient enough in order to obtain a fair dispersion of few metallic nanoclusters decorating the MWCNT, but at the same time to avoid the formation of a metallic layer covering the carbon nanotube, non-convenient for semiconducting gas sensors because of turning their behavior into metallic.

The influence of the amount of metal evaporated and plasma treatment on the dispersion and size of the metal nanoparticles was studied by TEM.

c. ATMOSPHERIC PLASMA (CHANI)

The CHANI team focused on the surface functionalization and metal deposition on the carbon nanotubes by a plasma home-made chamber at atmospheric pressure. Figure 2 shows the image of the plasma reactor used by CHANI team. In this case also, the sample is first cleaned and activated and then decorated with metal nanoparticles (using either chemical bubblers, spraying system or micro-droping system depending on the metallic precursor) [15].

ISBN:978-84-694-0326-6/DL:T-207-2011

Different reagents can be injected in the post-discharge during plasma treatment:

- ✓ Organometallic molecules
- ✓ Metal salt solutions
- ✓ Colloidal metal solution (with the help of a spraying system)

The system is operated at 80 W and the plasma is formed by feeding the process gas or gases into the system upstream of the electrodes at the flow rate of 30 L/min. More details about the plasma system can be found elsewhere [15].

Different samples were prepared by CHANI team, which were treated in two different gas atmospheres (Argon or Argon/Oxygen). Then, those samples were decorated by different metal nanoclusters provided by different metal precursors: Ni, Fe, Pt, Rh and Au.

In the case of organometallic precursors (Volatile precursors), the decoration was made by chemical bubblers placed in a thermostated bath. While in the case of colloidal solution, either a spraying system or a dropping system was used.

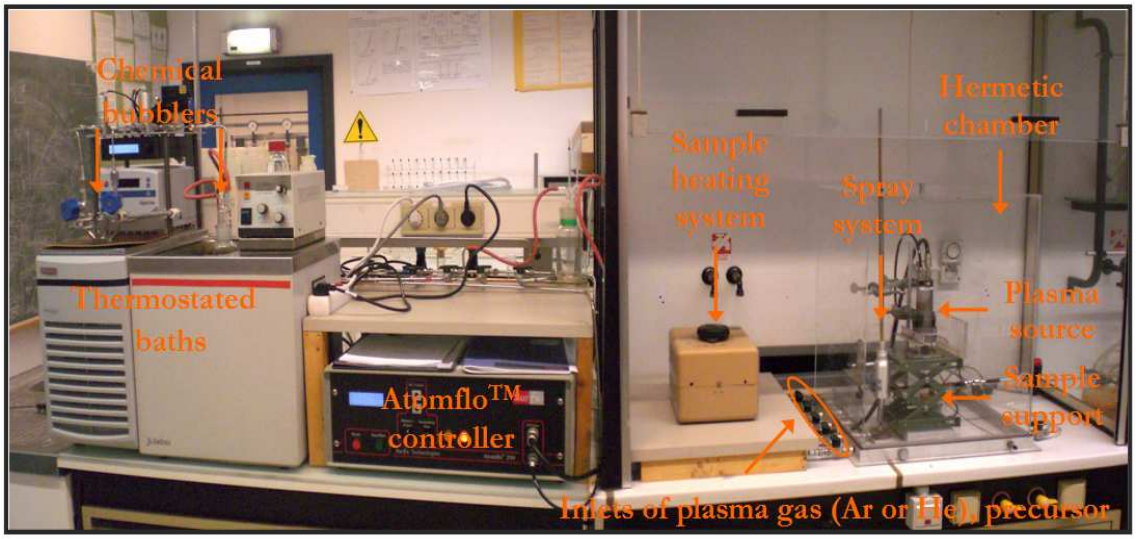

Figure 2: Lab-built atmospheric plasma apparatus used by CHANI team

d. ATMOSPHERIC PLASMA (SAM)

The surface treatments of the samples were performed in a Dielectric-barrier discharge (DBD) Axcys chamber at atmospheric pressure (Fig. 3).

The CNT samples were first treated by helium plasma at a frequency of 20 kHz. And then decorated with different metal nanoclusters (Pt, Ni, Fe, Pd, Ti) using either

ISBN:978-84-694-0326-6/DL:T-207-2011

organometallic or metal salt solution precursors. In this case, the treatments were performed at a power adjusted between 100 to 150 W during from 2.5 to 10 min.

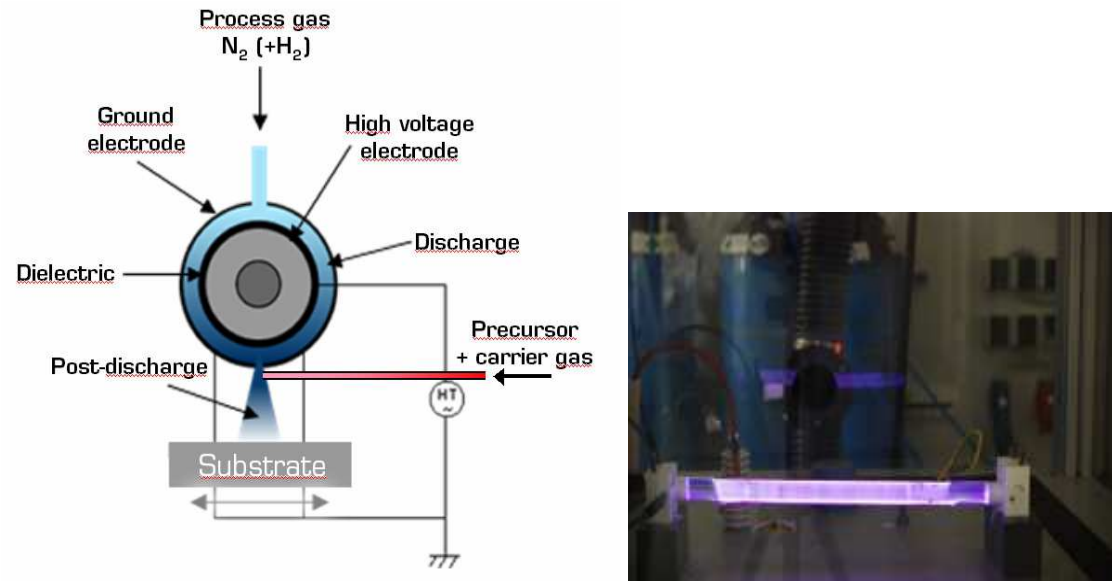

Figure 3: left) Scheme, and right) image of the DBD Axcys atmospheric plasma chamber from SAM laboratory.

3. Materials properties and instrumentation for sample's characterization

a. Basic concepts about material characterization techniques

For a successful functionalization and decoration of the MWCNT samples, it is important to follow, in parallel, the evolution of the treated samples and the quantification of the chemical elements attached to the treated surface using many techniques which will be described in the following section:

- **X-ray Photoelectron Microscopy (XPS)**

It is a surface chemical analysis technique that can be used to analyze the surface chemistry of a material.

XPS spectra are obtained by irradiating a material with a beam of X-rays while simultaneously measuring the kinetic energy and number of electrons that escape from the top 1 to 10 nanometers of the material being analyzed (Fig. 4). XPS requires ultrahigh vacuum conditions. XPS spectroscopy makes it possible to measure the electrons emitted in an interval of energy according to the binding energy of the electrons. Each chemical element being characterized by a single spectrum, this spectroscopic method makes it possible to precisely analyze the chemical nature of a given material. The identification of the chemical state of an element can be obtained

ISBN:978-84-694-0326-6/DL:T-207-2011

starting from the exact measurement of the position of the peaks and their separations in energy.

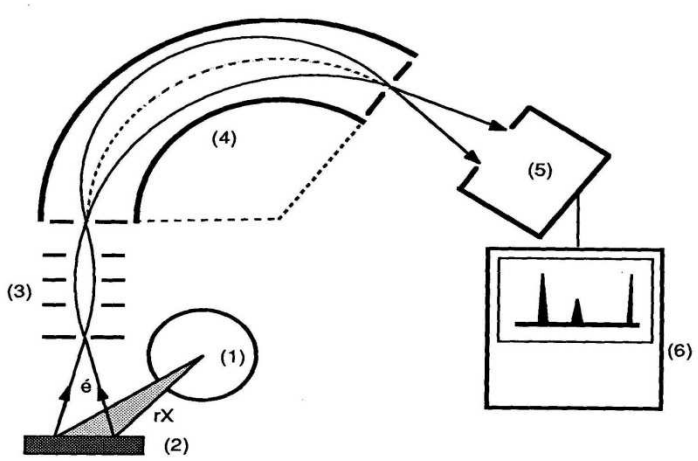

Figure 4: Diagram of X photoelectrons spectrometry system.
(1) X-rays tube; (2) Sample; (3) Electronic focusing system; (4) Spectrometer; (5) Electrons detector (channeltron); (6) Data acquisition.

This technique was implemented in our case in order to quantify the atoms composing the treated CNTs surfaces (oxygen, Nitrogen, etc), the metal deposition and possible contaminations. The characteristics of the equipments used are shown in table 2:

Table 2: Characteristics of the characterization XPS equipment used

Analytical tool	**Instrument**	**Spectral resolution**	**Spatial resolution**	**Software of data processing**
XPS-LISE	HP5950A SSX100 Scienta 300	1 eV 0.8 eV 0.5 eV	Surface analyzed Some mm^2 1 mm^2 1 mm^2	Winspec. CasaXPS (Official license)
Synchrotron photoemission	2 beamlines	0.6 eV And 0.2 eV	Surface analyzed 1 mm^2	Axis 2000 (Free software)

❖ Transmission Electron Microscopy (TEM)

The microscope used is a JOEL 1011 model. It allows studying the morphology of the particles of a sample with a resolution of 0.2 nm and an image amplification ranging between 200 and 1000000 x.

ISBN:978-84-694-0326-6/DL:T-207-2011

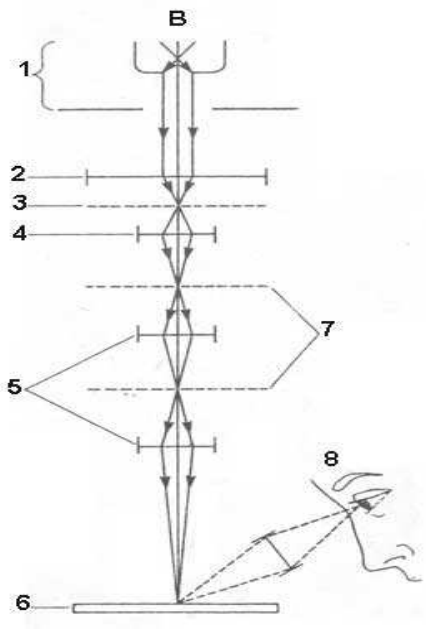

Figure 5: Diagram of TEM system.
(1) Electron gun; (2) Condenser lens; (3) Specimen plane; (4) Objective lens; (5) Projector lens system; (6) Fluorescent screen; (7) Intermediate image planes; (8) Binocular viewer

The transmission electron microscope (TEM) uses a high voltage electron beam to create an image. The electrons are emitted by an electron gun, commonly fitted with a tungsten filament cathode as the electron source. The electron beam is accelerated by an anode at high voltages with respect to the cathode, focused by electrostatic and electromagnetic lenses, and transmitted through the specimen that is in part transparent to electrons and in part scatters them out of the beam. When it emerges from the specimen, the electron beam carries information about the structure of the specimen that is magnified by the objective lens system of the microscope (Fig. 5). The spatial variation in this information (the "image") is viewed by projecting the magnified electron image onto a fluorescent viewing screen coated with a phosphor material. The image can be photographically recorded by exposing a photographic film or plate directly to the electron beam, or a high-resolution phosphor may be coupled by means of a lens optical system or a fiber optic light-guide to the sensor of a CCD (charge-coupled device) camera. The image detected by the CCD may be displayed on a monitor or computer.

In our case, the sample must be deposited on a copper mesh and TEM enables to see isolated MWCNTs, measure the diameter and length of the tube and visualize the dispersion of the nanoclusters on the tube wall. In some cases, high resolution TEM is

ISBN:978-84-694-0326-6/DL:T-207-2011

used for further enhancing image clarity and for identifying how metal nanoparticles sit on nanotube sidewalls.

❖ **Environmental Scanning Electron Microscopy (ESEM)**

The scanning electron microscope is a type of electron microscope that images the sample surface by scanning it with a high energy beam of electrons (Fig. 6). The electrons interact with the atoms that make up the sample producing signals that contain information about the sample's surface topography, elemental composition.

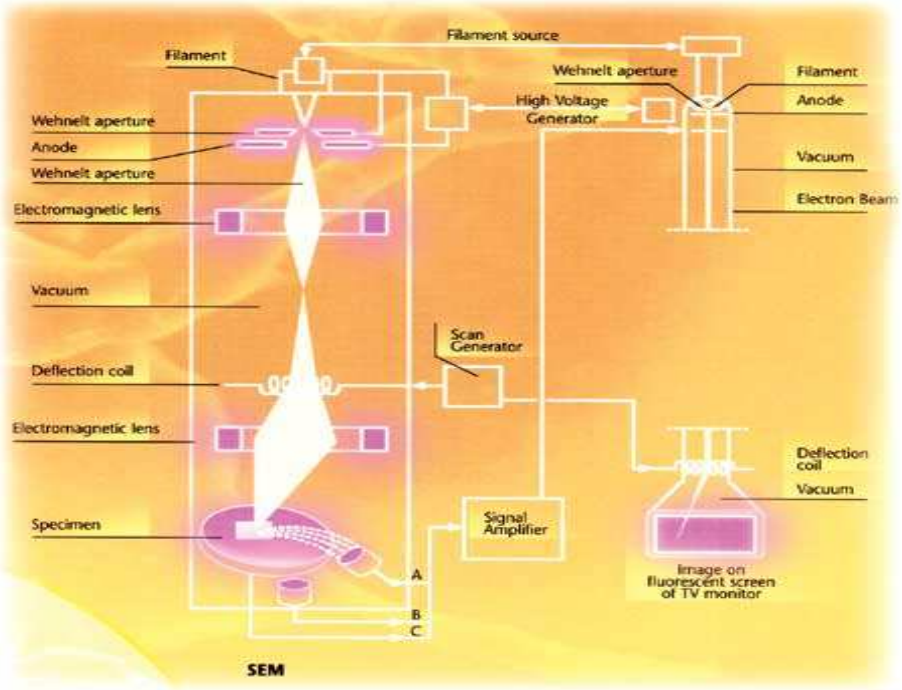

Figure 6: Diagram of Scanning Electron microscope.

ESEM is a scanning electron microscope that allows a gaseous environment in the specimen chamber. In our case the MWCNTs treated samples did not emit any vapours under vacuum conditions during the sample analysis. However, the ESEM was used instead of SEM technique only from a resolution point of view.

The characteristics of the equipment used in our case are summarized in table 3:

ISBN:978-84-694-0326-6/DL:T-207-2011

Table 3: Characteristics of the characterization ESEM equipment used

Model	FEI QUANTA 600
Resolution (nm)	3.0
Magnification	15 - 3000000 x
Voltage (kV)	0.5 - 30
Sample rotation (º)	360
Sample inclination (º)	70
Detector of retro-dispersed electrons	Yes

In the case of weakly conductive samples, it is usual to coat their surface with a thin layer of electrically conductive material, commonly gold. In our case, our samples are quite conductive but we tend to coat them with a gold layer, by low vacuum sputtering, for improving signal and surface image resolution. The samples are then mounted in a specimen holder called a specimen stub prior to analysis.

b. Characterization of LISE materials (

Finally, oxygen plasma was selected because it allows attaching functional groups such as hydroxyl, carbonyl and carboxyl (Table 4) known to be reactive sites to increase interaction with gases [16].

Relative concentrations of the functional groups are observed to vary with the plasma parameters. Oxygen grafting can be obtained at up to 23 % in different conditions [14].

The idea is to attach a maximum amount of functional groups without destroying the surface of the carbon nanotube. Higher power or longer treatment duration can damage the nanotube surface. For that, it was decided to keep the plasma power below 15 W and the time treatment below 60 s inside the discharge. TEM images of the oxygen-treated samples in the different treatment conditions (Fig. 7) confirmed the XPS results (Table 4).

Table 4 summarized the effect of treatment time and power in the percentage of functional groups attached to the surface of the carbon nanotube.

ISBN:978-84-694-0326-6/DL:T-207-2011

Table 4: The effect of different plasma treatment conditions (Duration, sample position and power) in the percentage of functional groups attached to CNTs surface.

	Oxygen %	CNTs %	C-O % (hydroxyl)	C=O % (carbonyl)	CO-O % (carboxyl)
Effect of the treatment time (5 W)					
5 s	11,8	77,9	14,3	4,2	3,6
30 s	**15,7**	**80,0**	**8,2**	**10,2**	**1,6**
2 min	17,2	72,1	6,5	18,1	3,3
Effect of the plasma power (30 s)					
5 W	**15,7**	**80,0**	**8,2**	**10,2**	**1,6**
15 W	16,1	75,1	4,6	17,3	3,0
50 W	16,1	Fe and Co observed by XPS (i.e., CNT wall damaged)			

❖ Surface decoration

The plasma treatment was found to increase the interaction between metal nanoclusters and CNTs and, at very low metal coverage, chemical bonds could be induced [17] that led to a more uniform cluster dispersion. This suggests the occurrence of a stronger interaction between the metal atom and the oxygen plasma treated CNTs. Figure 8 shows an example of gold nanoclusters deposited on pristine carbon nanotubes (Fig 8.a) compared to O_2-treated samples (Fig 8.b). In this case, the results suggested that gold atoms deposited on the non treated CNTs migrate and merge together to form large clusters. This indicates that there is weak interaction energy between gold atoms and the nanotube surface [18].

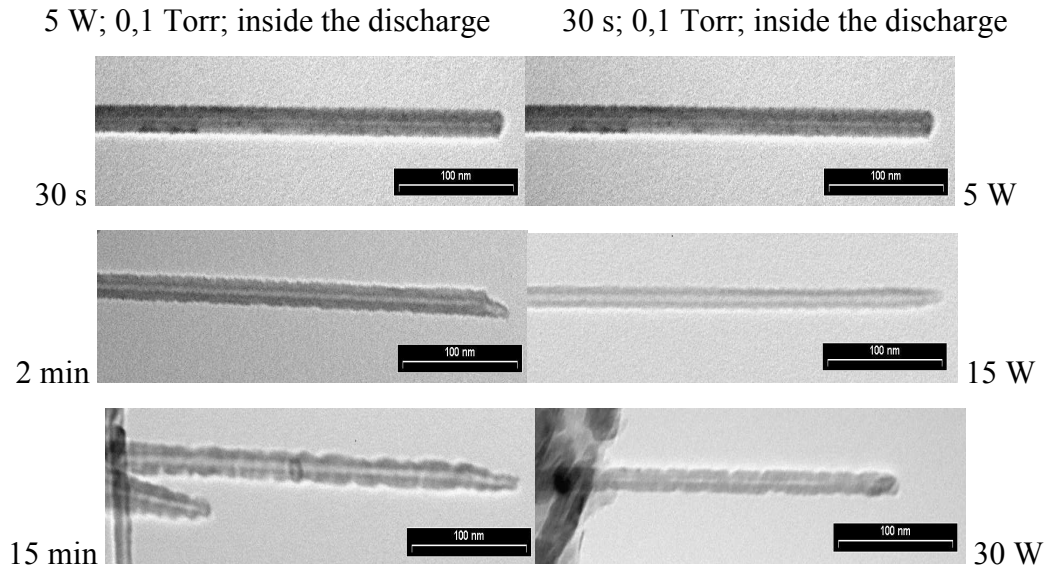

Figure 7: TEM images of O_2-fuctionalized CNTs in different treatment conditions [14].

ISBN:978-84-694-0326-6/DL:T-207-2011

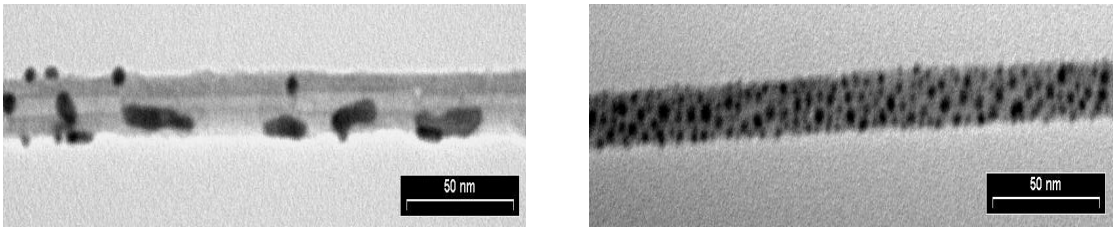

(a) (b)

Figure 8[17-18]: TEM images of Au on CNT's samples (a) as synthetised (b) O_2-Treated

The influence of the evaporation time and plasma treatment on the metal nanoparticles morphology was studied by TEM. Figure 9 shows TEM images of different amounts of gold on O_2-treated carbon nanotubes. Longer decoration time increases the metal coating amount and the size of the nanoclusters [19]. So it is important to control the treatment time because if not the surface of the CNTs can be completely covered by the metal nanclusters leading to a loss of the semiconductive character of the nanotubes (Fig. 9.d) [19].

So, for gas sensor application, it is important to get a small size distribution and a homogeneous dispersion of metal nanoclusters on the surface of nanotubes. In this case, few seconds of metal evaporation are enough to get good decoration results.

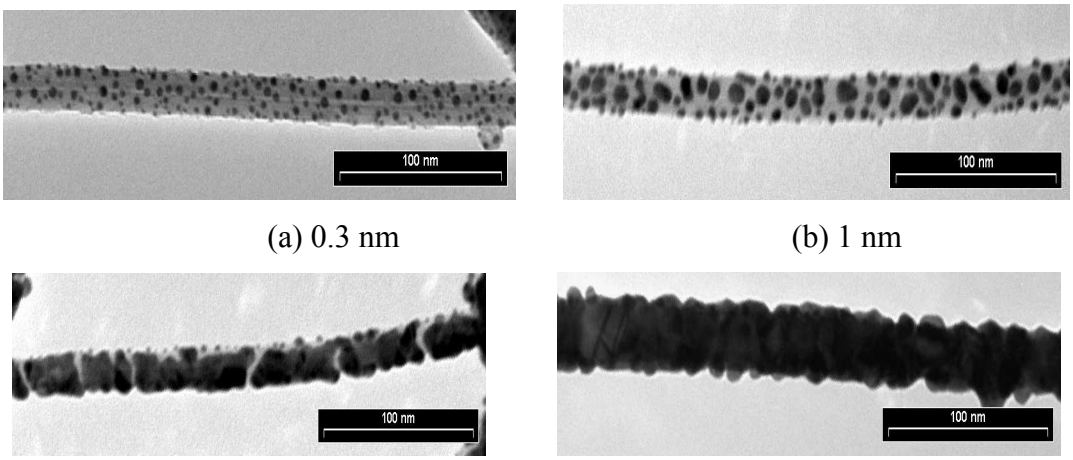

(a) 0.3 nm (b) 1 nm

(c) 4 nm (d) 10 nm

Figure 9: TEM images of Au evaporated on CNT's samples for different treatment times. Thicknesses estimated by a QCM device in the evaporation chamber.[19]

Different metals such as Au, Ag, Pd, Pt, Ni, Ti, Rh were successfully deposited over O_2/CNT samples by thermal evaporation technique. Figure 10 shows some TEM images and XPS analysis of the metal-decorated MWCNTs. For the samples decorated with Pd, Ni, Ti, Rh, different amounts of metal atoms were deposited (Table 5).

ISBN:978-84-694-0326-6/DL:T-207-2011

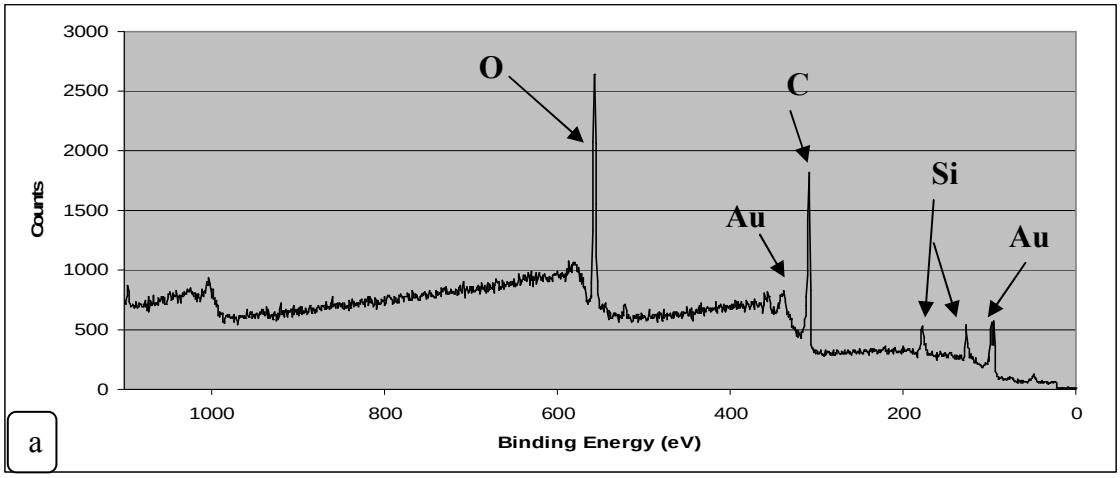

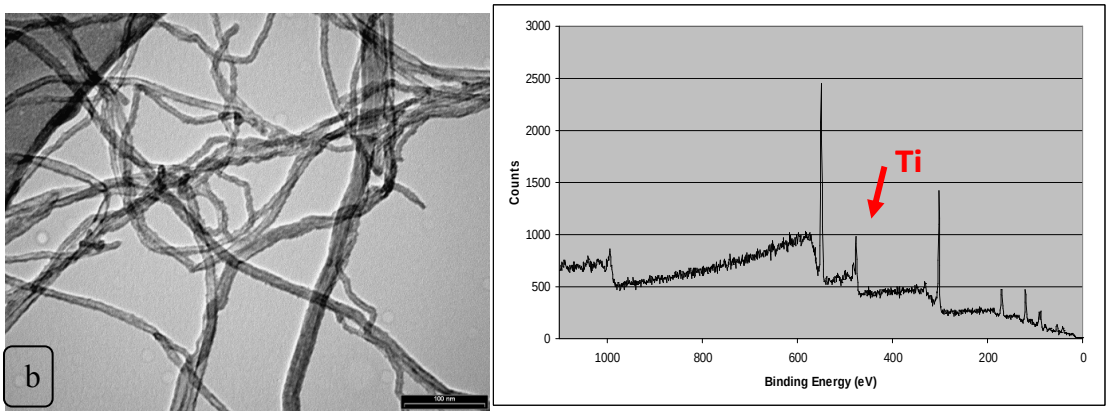

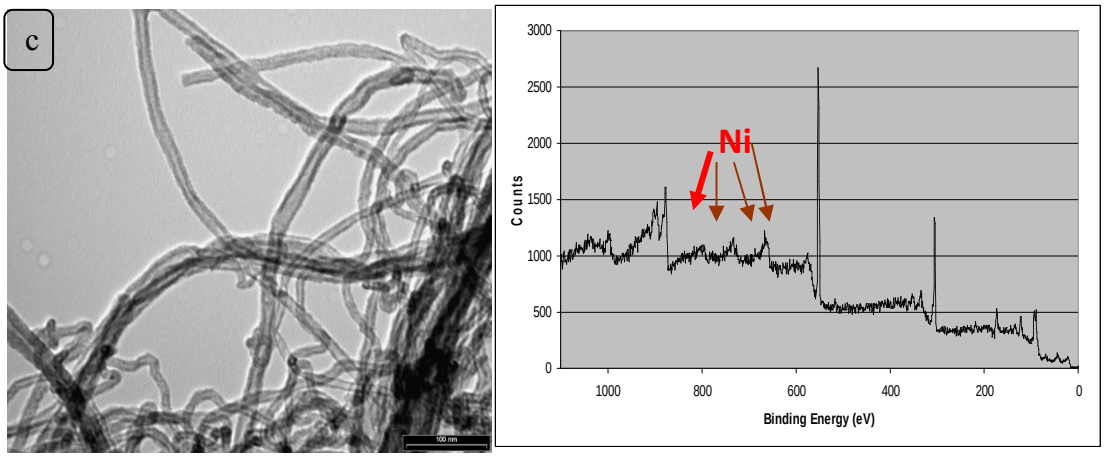

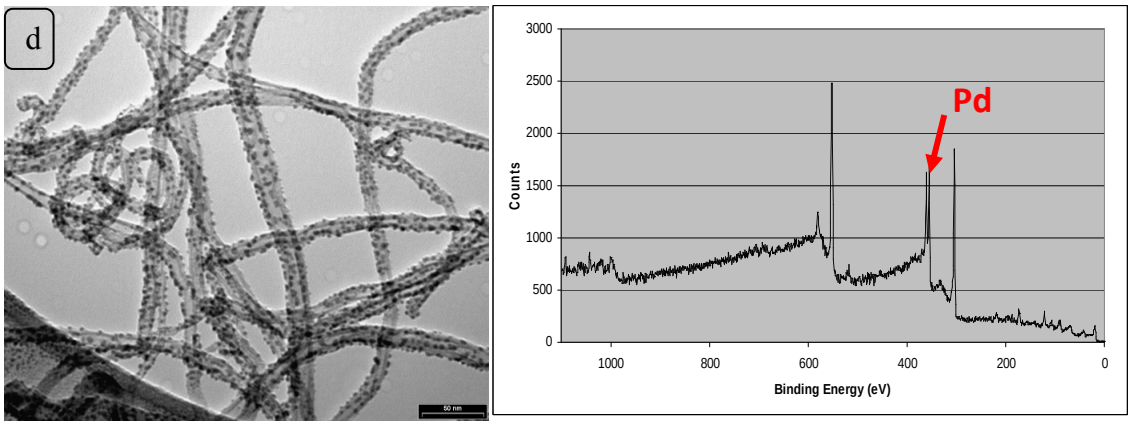

ISBN:978-84-694-0326-6/DL:T-207-2011

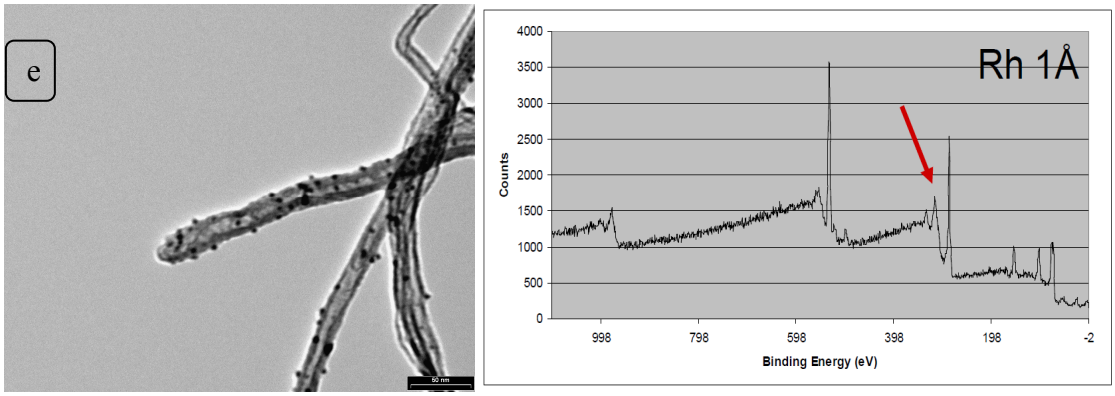

Figure 10:
a) XPS analysis of Au decorated O_2/MWCNTs
b) TEM image and XPS analysis of Ti (5 Å) decorated O_2/MWCNTs
c) TEM image and XPS analysis of Ni (5 Å) decorated O_2/MWCNTs
d) TEM image and XPS analysis of Pd (5 Å) decorated O_2/MWCNTs
e) TEM image and XPS analysis of Rh (1 Å) decorated O_2/MWCNTs

Table 5: Summary of the different metal decorated samples and the size of the metallic nanoclusters deposited.

Metal	Sample Nº	Nanocluster size (nm)
Au	1	10
Ag	2	10
Pd	5	2 -4
Pt	6	4-8
Ni	3	1 ; 5 ; 0,2
Ti	4	0,2
Rh	7	0,2 and 1

c. Characterization of CHANI materials

Table 6 shows the average size of the nanocluster obtained for each metal and the nature of the metal precursor used.

The different obtained samples of metal-decorated MWCNTs were analyzed by XPS and TEM techniques in order to study the elemental composition in each case and to look for the sticking behavior of the nanoparticles in the both treatment plasmas (Ar and O_2/Ar) (Fig. 11) [15]. The metal nanoclusters stick more uniformly and strongly to O_2/Ar treated CNTs than to Ar-treated CNTs.

ISBN:978-84-694-0326-6/DL:T-207-2011

Table 6: Summary of the decorating metal precursors nature and the average nanocluster size obtained

Metal	Sample Nº	Metal precursor	Nanocluster size (nm)
Au	6	Colloidal solution (10 nm, 26 g Au/L)	5
	7		10
Pt	4	Colloidal solution (<10 nm, 3,7 g Pt/L)	4
Ni	1	Colloidal suspension <7nm; $[Ni(Oleate)_2]=10^{-2}$ M; $[NaBH_4]=0,2$ M	5
	2	Organometallic (1,5-cyclooctadiene)nickel(0), 95%	5
FeO	3	Colloidal solution 6,5 nm	7
Rh	5	Colloidal solution (<10 nm, 0,31 g Rh/L)	4

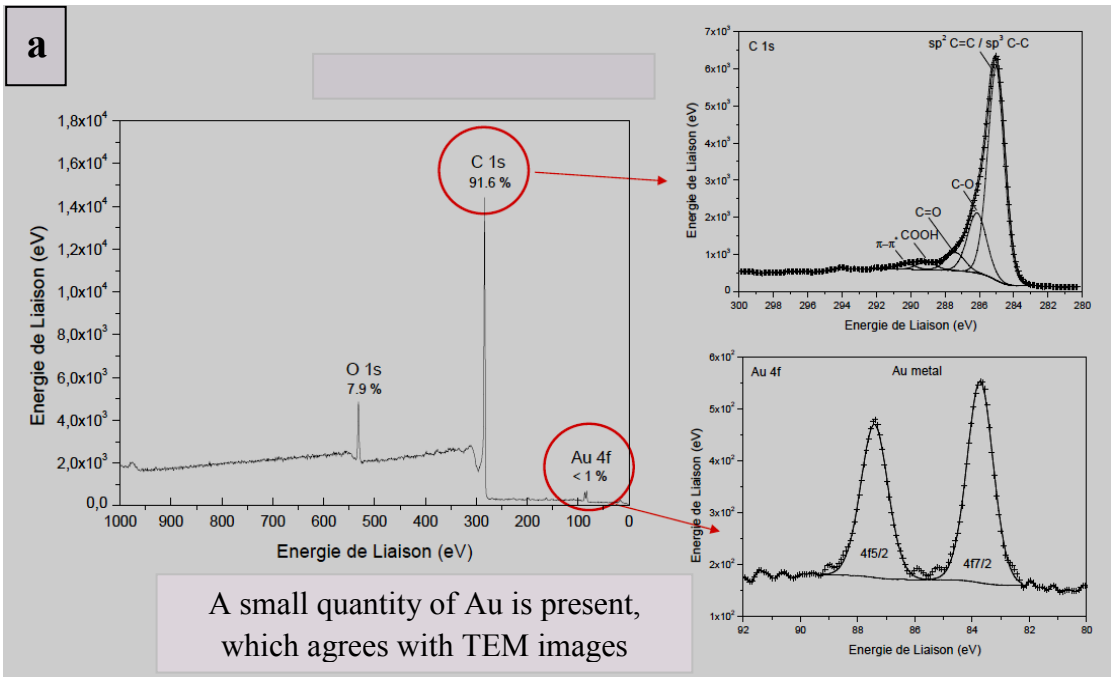

ISBN:978-84-694-0326-6/DL:T-207-2011

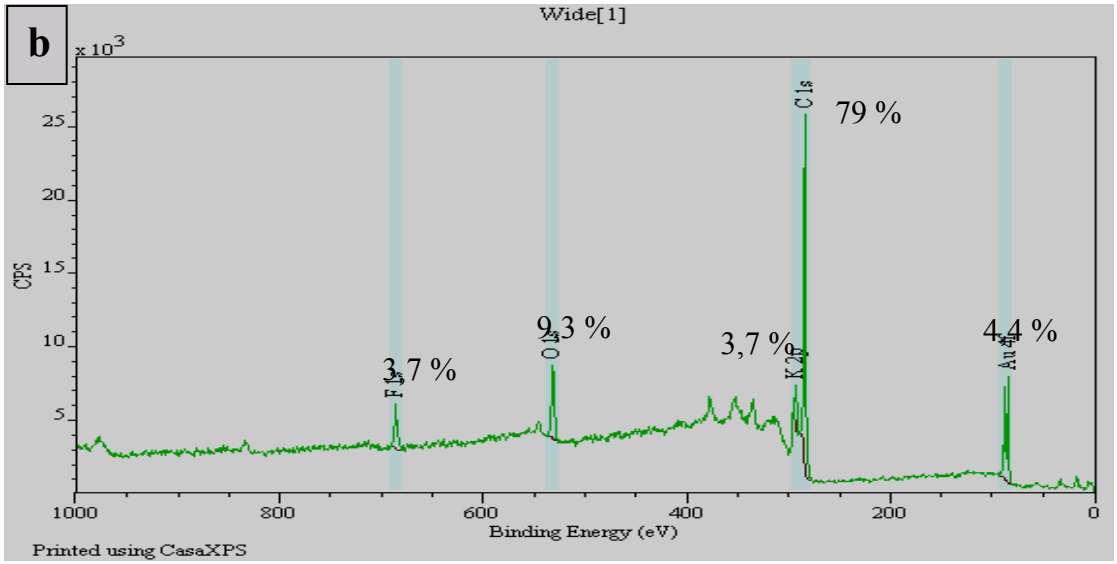

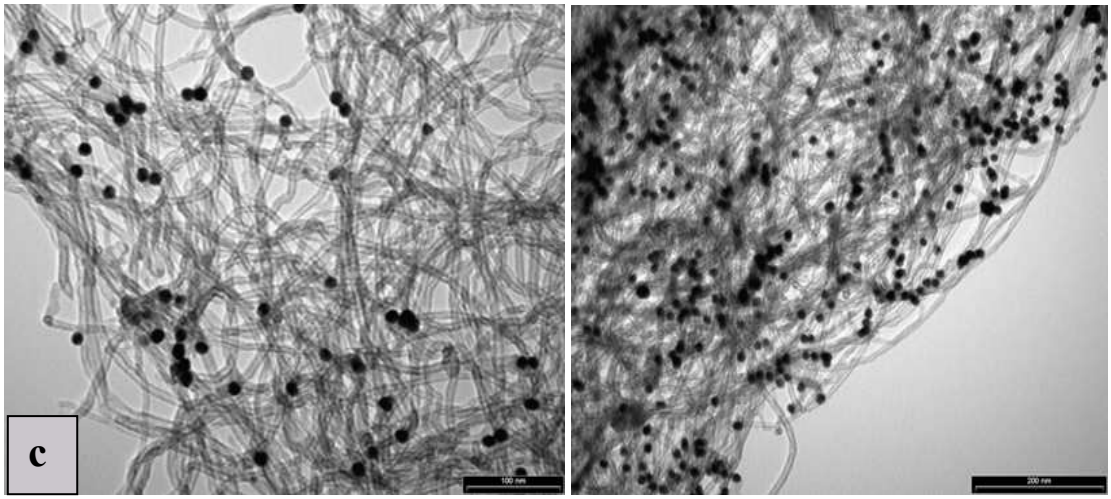

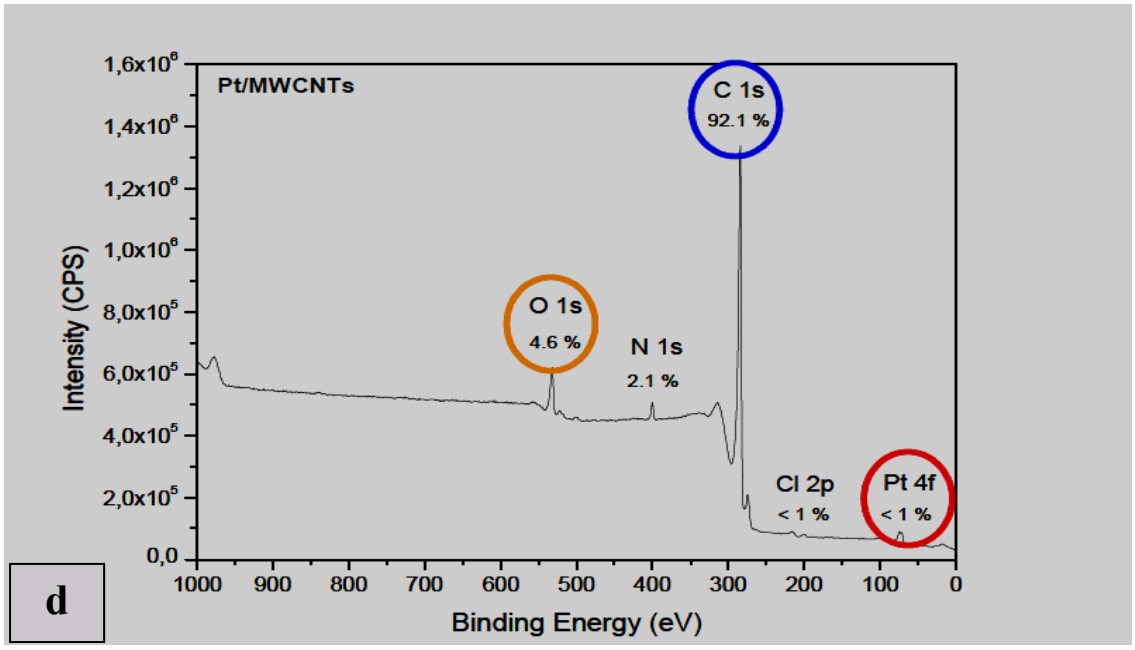

ISBN:978-84-694-0326-6/DL:T-207-2011

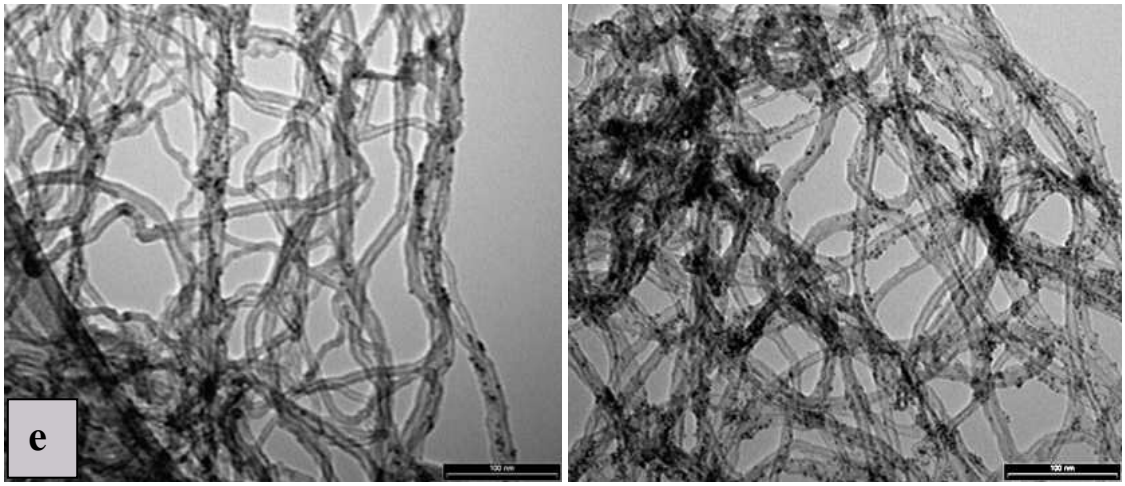

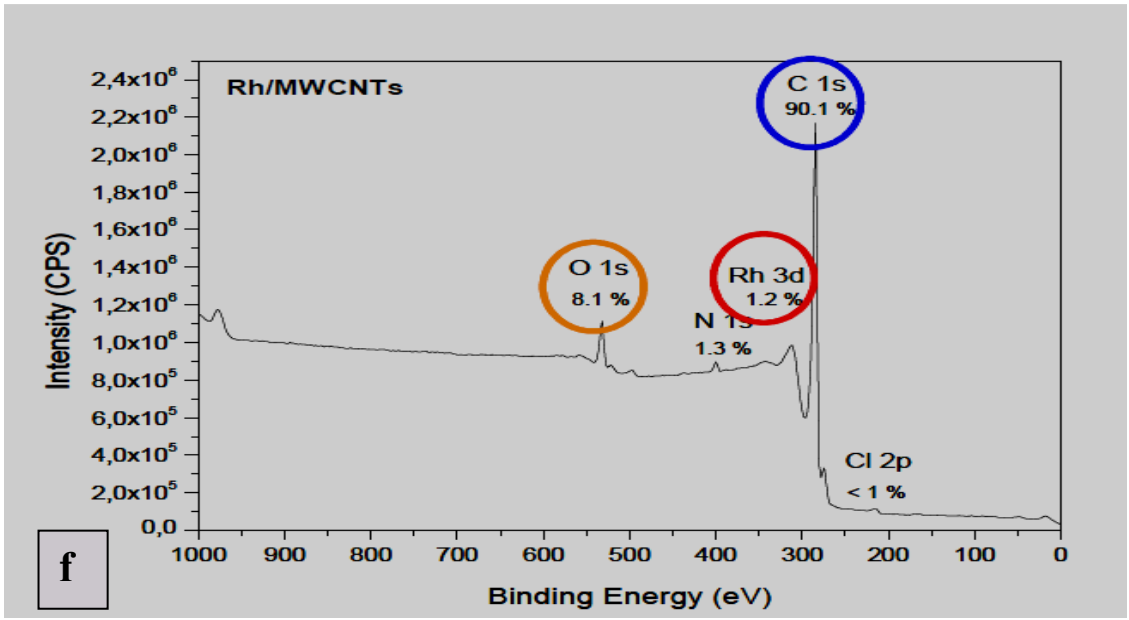

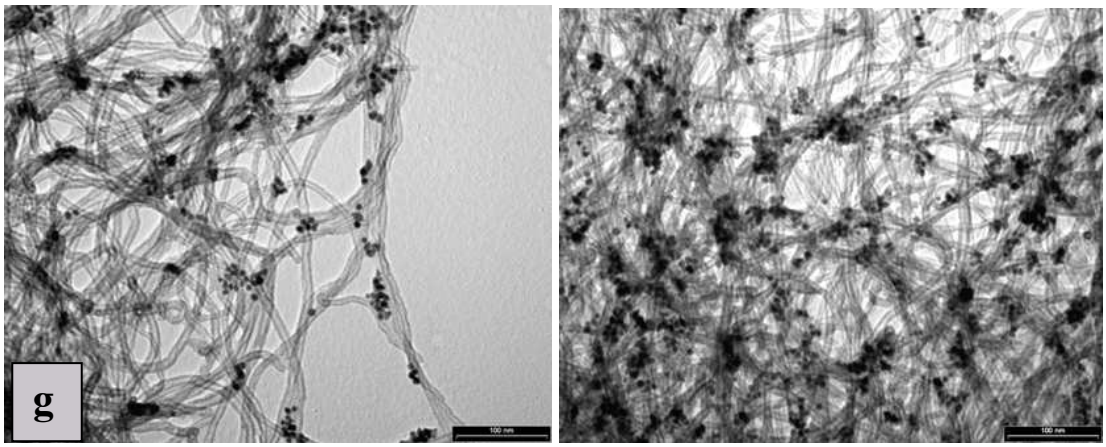

ISBN:978-84-694-0326-6/DL:T-207-2011

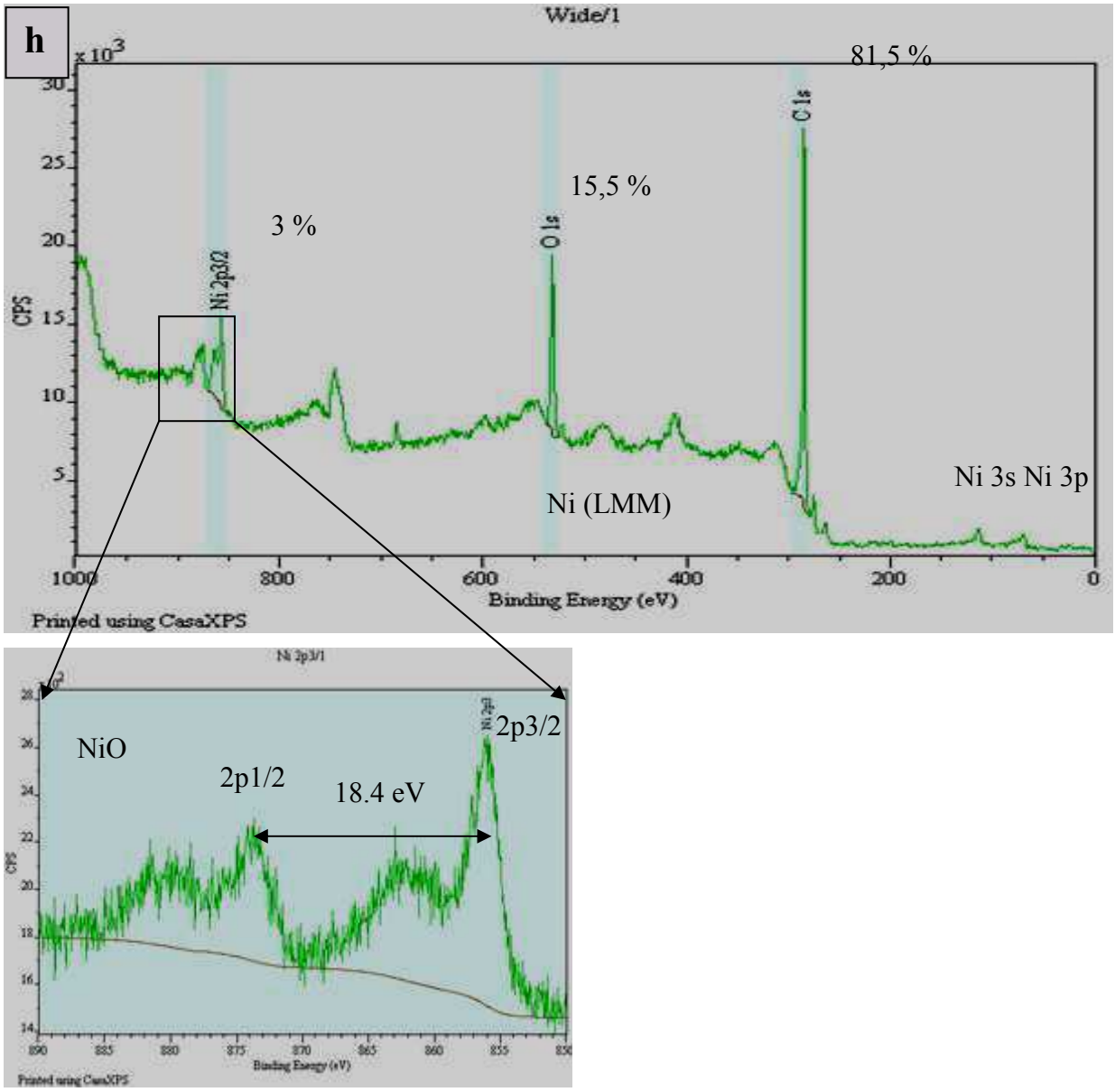

ISBN:978-84-694-0326-6/DL:T-207-2011

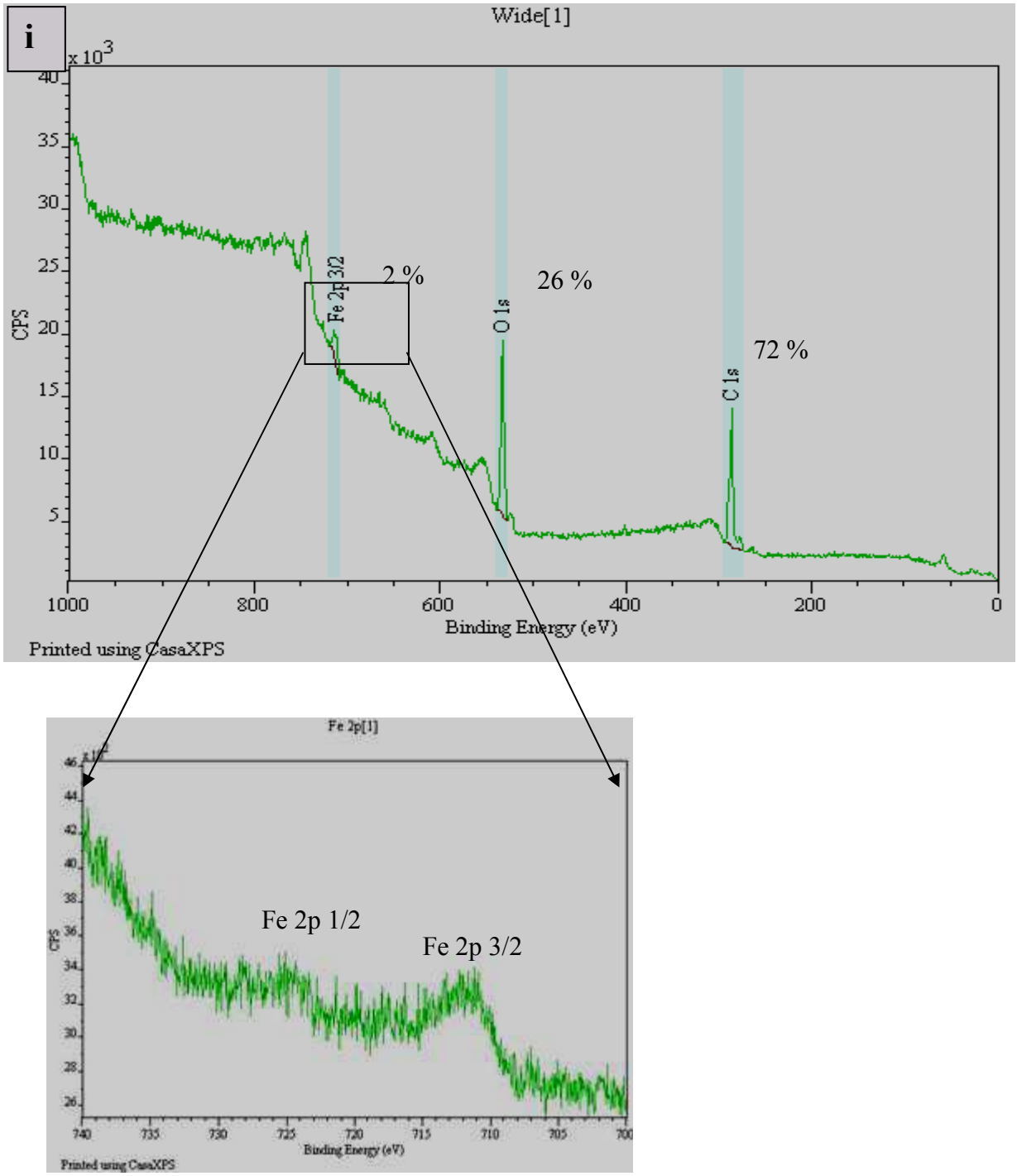

Figure 11:
a) XPS analysis of Au decorated MWCNTs in Ar plasma
b) XPS analysis of Au decorated MWCNTs in O_2/Ar plasma
c) TEM images Au decorated MWCNTs: left) in Ar plasma, right) in O_2/Ar plasma
d) XPS analysis of Pt decorated MWCNTs in Ar plasma
e) TEM images Pt decorated MWCNTs: left) in Ar plasma, right) in O_2/Ar plasma
f) XPS analysis of Rh decorated MWCNTs in Ar plasma
g) TEM images Rh decorated MWCNTs: left) in Ar plasma, right) in O_2/Ar plasma
h) XPS analysis of Ni (OMV) decorated MWCNTs in Ar plasma
i) XPS analysis of FeO decorated MWCNTs in Ar plasma

ISBN:978-84-694-0326-6/DL:T-207-2011

d. Characterization of SAM materials

The presence of the metals was confirmed by High resolution TEM. As an example, figures 12 and 13 show the presence of Pt nanoclusters on the surface of a CNT sample.

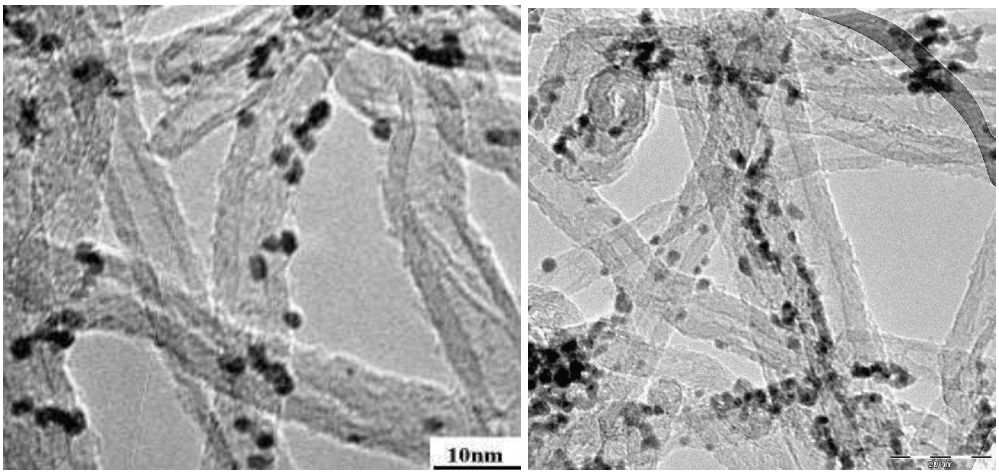

Figure 12: HRTEM images of MWCNTs covered with ~2 nm -sized platinum nanoparticles (~10% volume) after the plasma treatment: left) (100W, 10min, He, 20kHZ, 5 SLM), right) (100W, 10min, He-O_2, 20kHZ, 5 SLM), using platinum solid precursor.

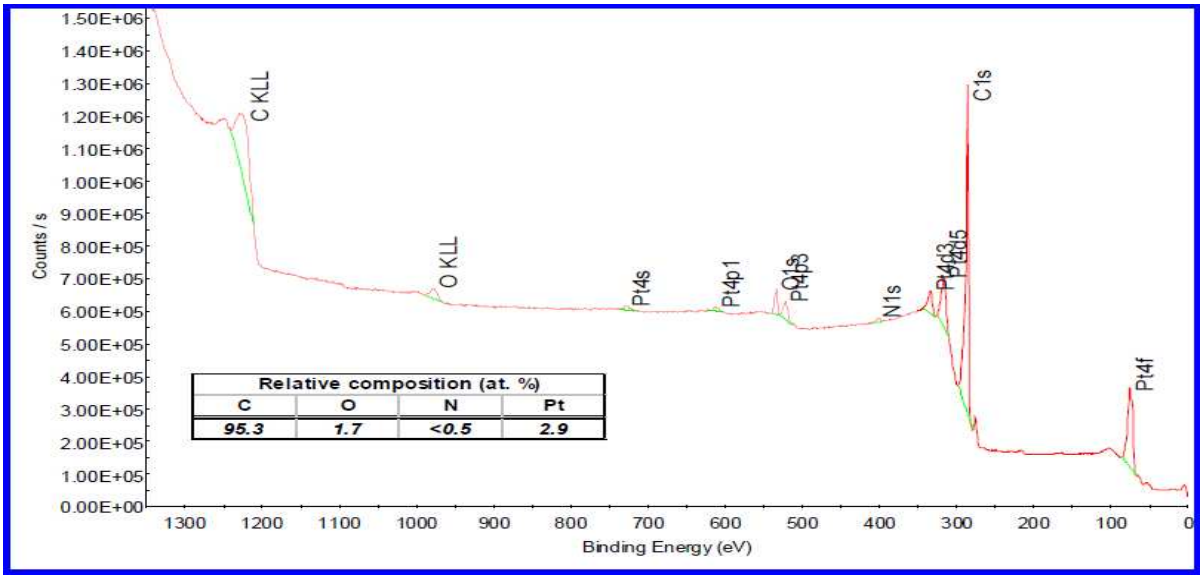

Figure 13: XPS for Pt decorated MWCNTs

For each treated sample, the elemental composition was determined by XPS analysis. Table 7 shows the percentage of each element in the sample.

ISBN:978-84-694-0326-6/DL:T-207-2011

Table 7: Decoration conditions and elemental composition of the CNT treated samples

Metal	Sample Nº	Power (W)	Time (min)	% O	% C	% N	% Metal	Nanocluster size (nm)
Pt	1(solid)	100-150	10	1.7	95.3	0.2	2.9	2
	2(liquid)	150	5	2.5	92	-	5.2	2
	3(lquid)	150	5	2.85	94.11	-	3	2
Ni	4	150	5	20.6	74	-	5	10
	5	150	5	23.5	69.2	0.9	6.4	10
Fe	6	150	5	12.3	84.2	0.5	3	-
	7	150	10	7.1	90.7	0.3	1.9	-

4. Sensor substrate fabrication

The whole device consists of an array of four integrated micro-sensors fabricated on a double-side polished p-type <1 0 0> silicon substrates, 300 μm thick (4-40 Ω·cm).

The structure of each micro-sensor basically consists of interdigitated electrodes, insulating layers and a poly-silicon heater. The technological process needed to fabricate the sensors comprises the following steps [20-22]:

- Deposition of the membrane layer: Dielectric membranes consisting in a 0.3 μm thick Si_3N_4 layer grown by LPCVD are deposited prior to the heater deposition. This layer will act as etch stop during the backside etching employed to form the sensor membranes. Each chip has 4 membranes, the size of which was 900 × 900 μm^2.
- Deposition and patterning of a $POCl_3$-doped poly-silicon heating meander of 6 Ω/sq of resistance. The temperature coefficient of resistivity (TCR) of poly-silicon depends on the doping level, and for the doping level achieved, a value of 6.79×10^{-4} was measured for our devices. The heater can also be used as a temperature sensor.
- Deposition of a 0.8 μm thick SiO_2 layer to insulate the heater from the electrodes and the sensing film.
- Opening of contacts for the heater bonding pads to be accessible.
- Deposition of comb 0.2 μm thick Pt electrodes, patterned by lift-off. A thin layer (20 nm) of Ti was deposited prior to Pt to promote electrode adhesion. The

ISBN:978-84-694-0326-6/DL:T-207-2011

electrode area was 400 × 400 μm^2. A planar view of the membrane showing heater and electrode configuration is shown in figure 16 (top).

- Patterning of the backside etch mask.
- Backside silicon etching with KOH at 70^{o}C (40% wt.) to create the thermally-insulated membranes.
- Wire bonding and packaging: Each array was mounted on a TO-8 package. Gold wires of 25 μm of diameter were used for standard ultrasonic wire bonding. For preventing the membranes to break due to air expansion in the cavity below the membranes when the device is heated, the membranes were not glued directly to the surface of the metallic package but kept elevated by using two lateral silicon spacers. Figure 14 (middle) shows a view of a packaged chip where the 4 membranes are clearly visible.

N.B: There are two options for making sensors. The gas sensitive material can be deposited directly onto the already packaged chip or can be also deposited before packaging is performed. In the last case, the wire bonding step is realized after the deposition of the sensing material.

After the packaging of the silicon substrate in the TO-8 support, thermo-electrical characterization is performed in order to calibrate the heating temperature of the sensor versus the voltage applied to the heater.

ISBN:978-84-694-0326-6/DL:T-207-2011

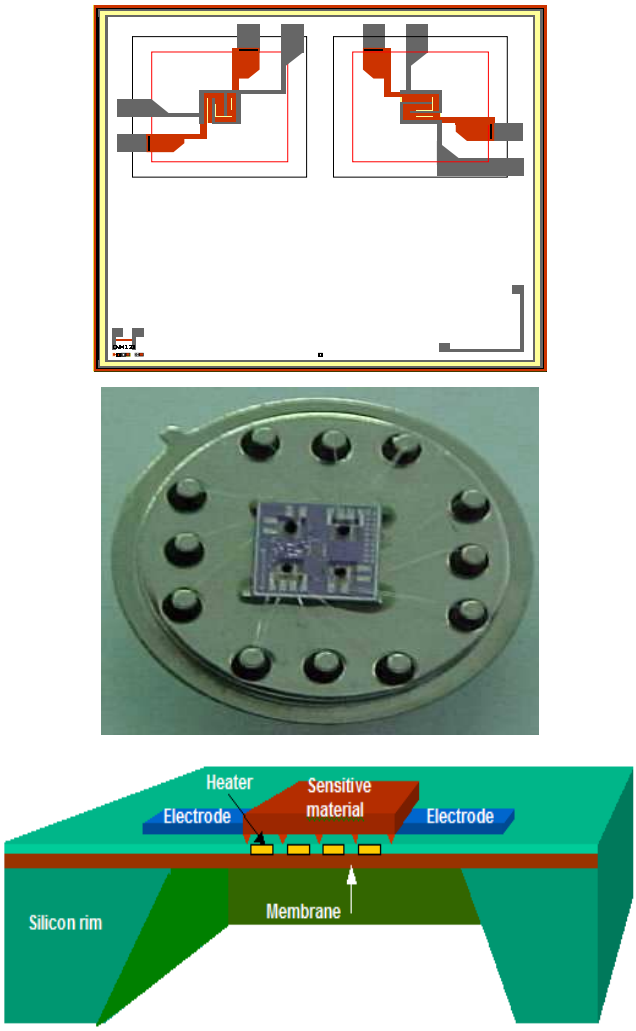

Figure 14: Layout of the silicon-based substrate, which contains 4 integrated membranes with electrodes and heaters stacked on top (top). Image of a packaged silicon substrate (middle). Structure of the micromachined sensor (bottom)

ISBN:978-84-694-0326-6/DL:T-207-2011

References

[1] M. Chen, H-W. Yu, J-H. Chen, H-S. Koo, Effect of purification treatment on adsorption characteristics of carbon nanotubes, Diamond & Related Materials 16, 1110–1115 (2007)

[2] www.nanocyl.com

[3] C. Tendero, C. Tixier, P. Tristant, J. Desmaison, P. Leprince, Atmospheric pressure plasmas: A review, Spectrochimica Acta Part B 61, 2 – 30 (2006)

[4] B. Kegel, H. Schmid, Low-pressure plasma cleaning of metallic surfaces on industrial scale, Surface and Coatings Technology 112, 63–66 (1999)

[5] L. Bárdos, H. Baránková, Plasma processes at atmospheric and low pressures, Vacuum 83, 522–527 (2009)

[6] B. C. Satishkumar, E. M. Vogl, A. Govindaraj and C. N. R. Rao, The decoration of carbon nanotubes by metal nanoparticles, Journal of Phyisics. D: Applied Physics. 29, 3173 (1996)

[7] K.H. An, J.G. Heo, X-ray photoemission spectroscopy study of fluorinated single-walled carbon nanotubes, Applied Physical Letters, 80, 4235-4237 (2002)

[8] Y. Wang, S. V. Malhotra, F. J. Owens, Z. Iqbal, Electrochemical nitration of single-wall carbon nanotubes, Chemical Physics Letters, 407, 68-72 (2005)

[9] A. Felten, C. Bittencourt, J.-J. Pireaux, G. Van Lier, and J.-C. Charlier, RF plasma functionalization of CNTs surface by O2, NH3 and CF4 treatments, J. Appl. Phys. 98, 074308 (2005)

[10] S.F. Yin, Q.H. Zhang, B.Q. Xu, W.X. Zhu, C.F. Ng and C.T. Au, Investigation on catalysis of COx-free hydrogen generation from ammonia, Journal of Catalysis 224, 384-396 (2004).

[11] Baughman, Carbon nanotubes_the route toward applications, Science, 297,787-792 (2002)

[12] Q. Zhao, M. B. Nardelli, W. Lu and J. Bernholc, Carbon Nanotube−Metal Cluster Composites: A New Road to Chemical Sensors?, Nanoletters 5, 847-851 (2005)

[13] J. Meng, L.Song, H. Xu, H.Kong, C. Wang, X. Guo, S. Xie,, Effects of single-walled carbon nanotubes on the functions of plasma proteins and potentials in vascular prostheses, Nanomedicine: Nanotechnology, Biology and Medicine, 1 (2), 136-142 (2005).

[14] A. Felten, J. Ghijsen, J-J. Pireaux, R. L. Johnson, C. M. Whelan, D. Liang, G. Van Tendeloo and C. Bittencourt, Effect of oxygen rf-plasma on electronic properties of CNTs, JOURNAL OF PHYSICS D-APPLIED PHYSICS 40, 23, 7379-7382 (2007)

[15] F. Reniers, F. Demoisson and J.J. Pireaux, Procédé de dépôt de nanoparticules sur un support. (2007)

[16] R. Ionescu, E.H. Espinosa, E. Sotter, E. Llobet, X. Vilanova, X. Correig, A. Felten, C. Bittencourt, G. Van Lier, J.-C. Charlier, J.J. Pireaux, Oxygen functionalisation of MWNT and their use as gas sensitive thick-film layers, Sensors and Actuators B: Chemical 113, 1, 36-46 (2006)

ISBN:978-84-694-0326-6/DL:T-207-2011

[17] I. Suarez-Martineza, C. Bittencourt, X. Kec, A. Feltend, J.J. Pireauxd, J. Ghijsend, W. Drubee, G. Van Tendelooc, C.P. Ewels, Probing the interaction between gold nanoparticles and oxygen functionalized carbon nanotubes, Carbon 47, 1549 – 1554 (2009)

[18] J-C. Charlier, L. Arnaud, I .V. Avilov, M. Delgado, F. Demoisson, E. H. Espinosa, C. P Ewels, A. Felten, J. Guillot, R. Ionescu, R. Leghrib, E. Llobet, A. Mansour, H-N. Migeon, J-J. Pireaux, F. Reniers, I. Suarez-Martinez, G. E. Watson and Z Zanolli, Carbon nanotubes randomly decorated with gold clusters: from nano2hybrid atomic structures to gas sensing prototypes, Nanotechnology 20, 375501 (2009)

[19] C. Bittencourt, A. Felten, B. Douhard, J.-F. Colomer, G. Van Tendeloo, W. Drube, J. Ghijsen, J.-J. Pireaux, Metallic nanoparticles on plasma treated carbon nanotubes: Nano2hybrids, Surface Science 601, 2800–2804 (2007)

[20] R. Ionescu, E.H. Espinosa, E. Sotter, E. Llobet, X. Vilanova, X. Correig, A. Felten, C. Bittencourt, G. Van Lier, J.-C. Charlier, J.J. Pireaux, Oxygen functionalisation of MWNT and their use as gas sensitive thick-film layers, Sensors and Actuators B 113, 36–46 (2006).

[21] M.C. Horrillo, I. Sayago, L. Arés, J. Rodrigo, J. Gutiérrez, A. Götz, I. Gràcia, L. Fonseca, C. Cané, E. Lora-Tamayo, Detection of low NO_2 concentrations with low power micromachined tin oxide gas sensors, Sensors and Actuators B 58 325–329 (1999).

[22] D.G. Rickerby, N. Wätchter, M.C. Horrillo, J. Gutiérrez, I. Gràcia, C. Cané, Structural and dimensional control in micromachined integrated solid state gas sensors, Sensors and Actuators B, 69 314–319 (2000).

UNIVERSITAT ROVIRA I VIRGILI
DESIGN, FABRICATION AND CHARACTERISATION OF GAS SENSORS BASED ON NANOHYBRID MATERIALS
Radouane Leghrib
ISBN:978-84-694-0326-6/DL:T-207-2011

UNIVERSITAT ROVIRA I VIRGILI
DESIGN, FABRICATION AND CHARACTERISATION OF GAS SENSORS BASED ON NANOHYBRID MATERIALS
Radouane Leghrib
ISBN:978-84-694-0326-6/DL:T-207-2011

ANNEX II:

RESULTS OF THE RESPONSE OF METAL DECORATED CARBON NANOTUBE SENSORS TOWARDS GASES

UNIVERSITAT ROVIRA I VIRGILI
DESIGN, FABRICATION AND CHARACTERISATION OF GAS SENSORS BASED ON NANOHYBRID MATERIALS
Radouane Leghrib
ISBN:978-84-694-0326-6/DL:T-207-2011

ISBN:978-84-694-0326-6/DL:T-207-2011

❖ Responsiveness of the metal-decorated carbon nanotubes towards gases and reproducibility results

-NO_2 detection

- At room temperature

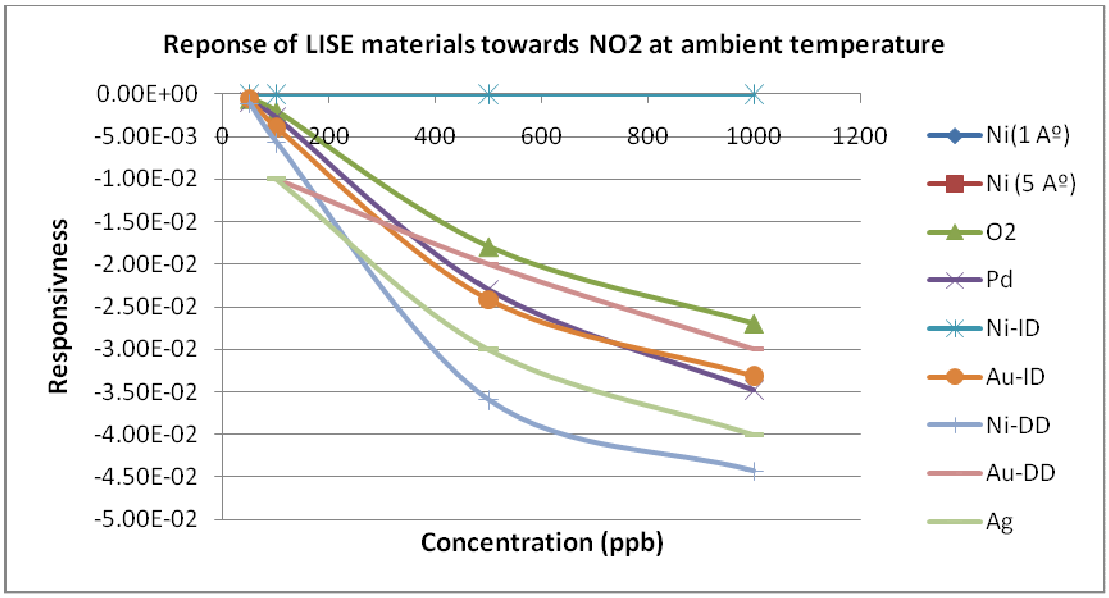

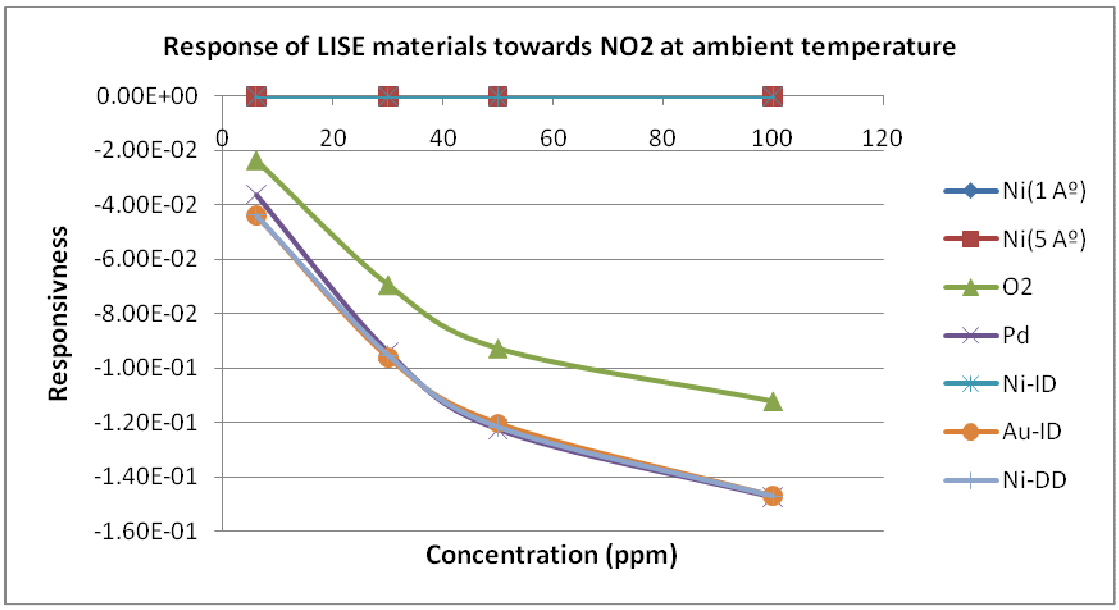

ISBN:978-84-694-0326-6/DL:T-207-2011

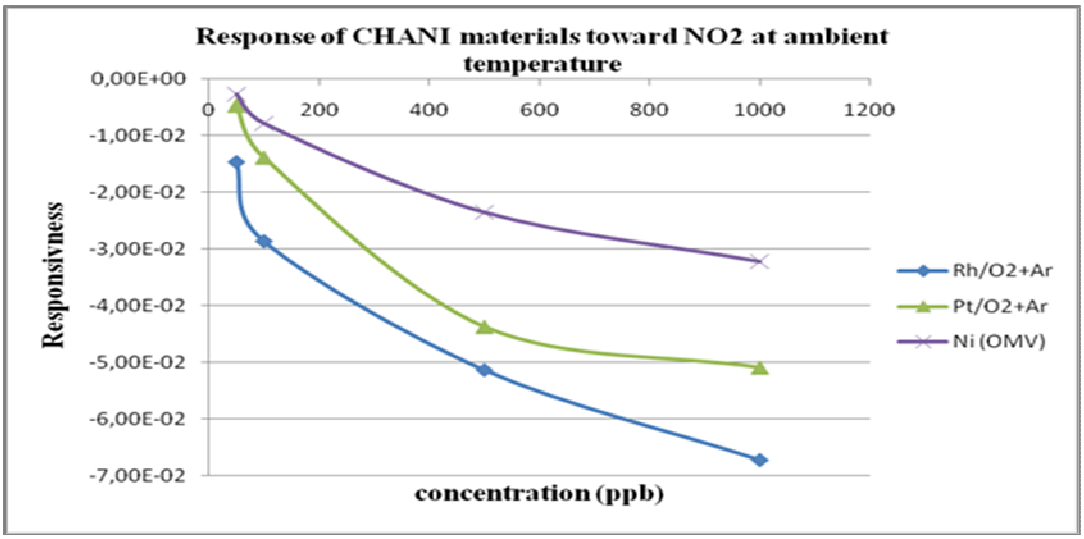

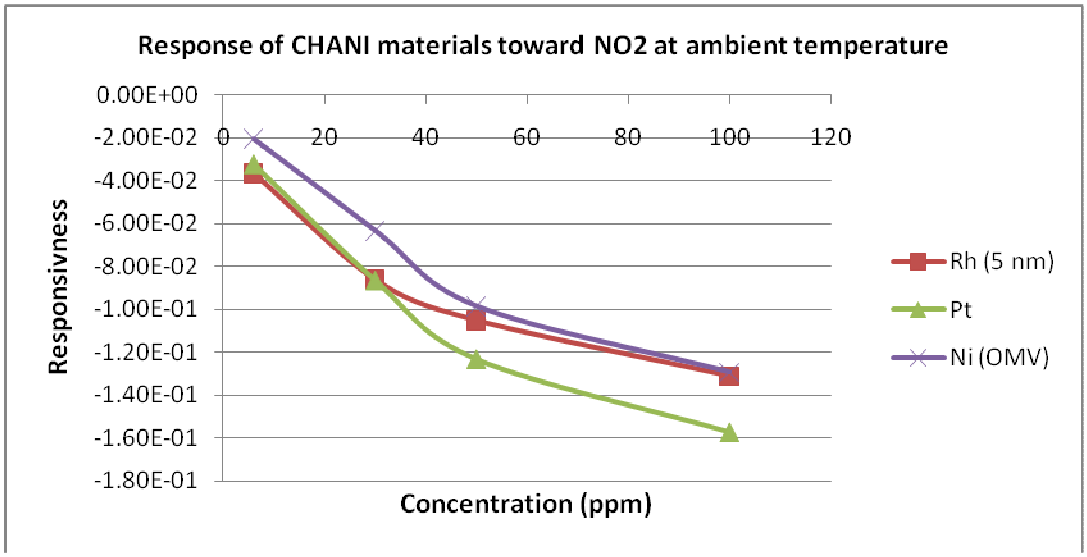

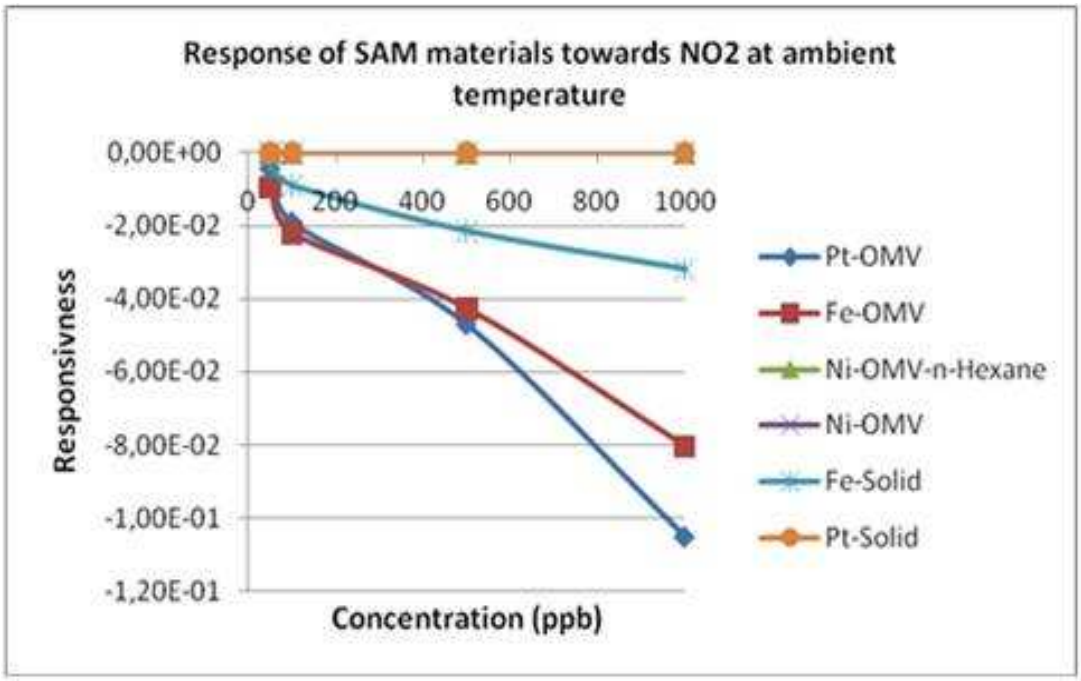

ISBN:978-84-694-0326-6/DL:T-207-2011

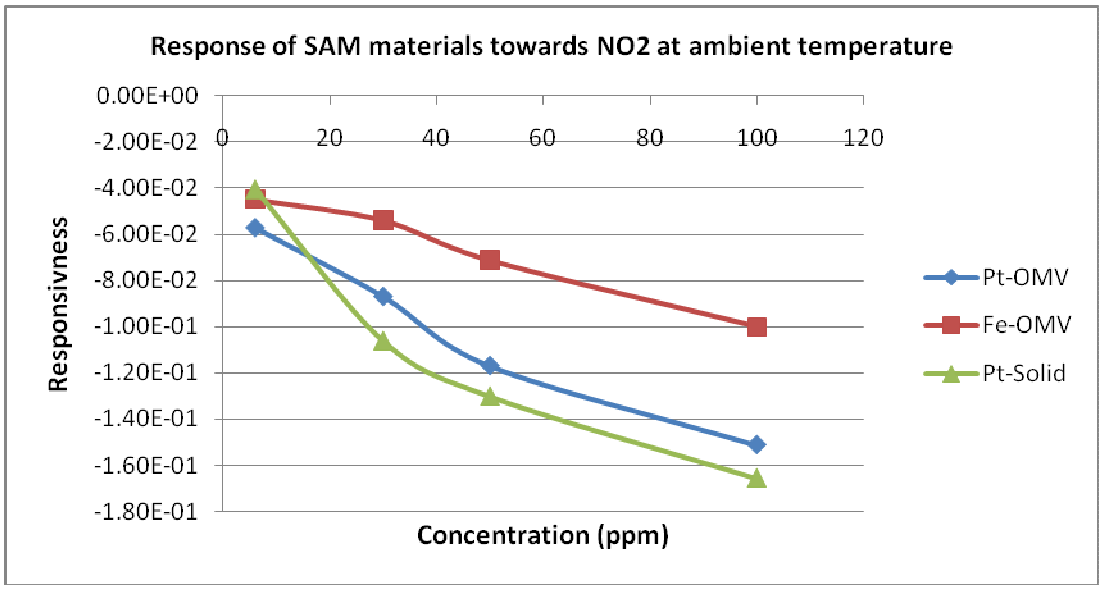

- At 150 ºC

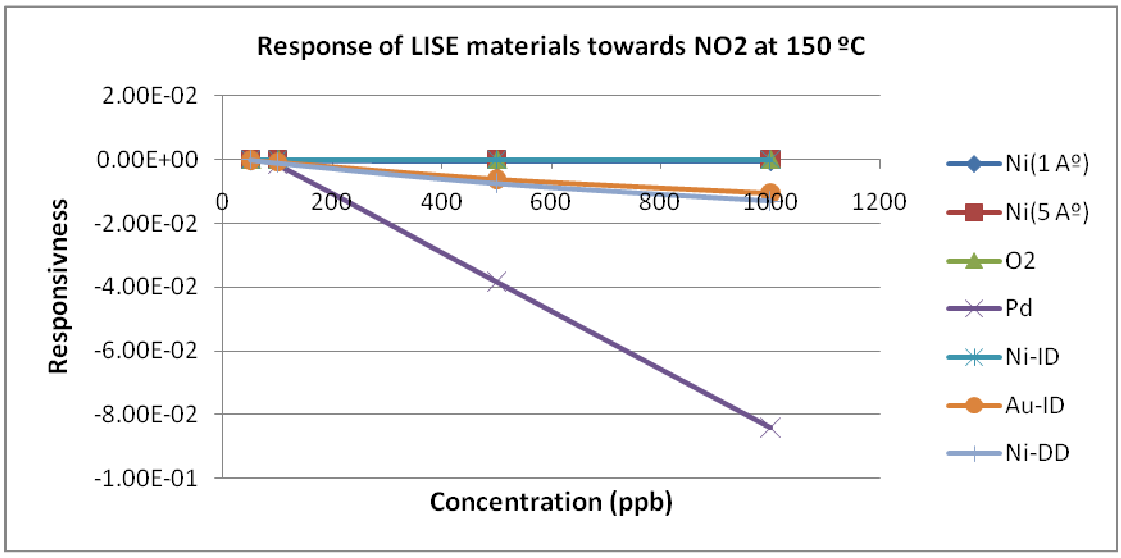

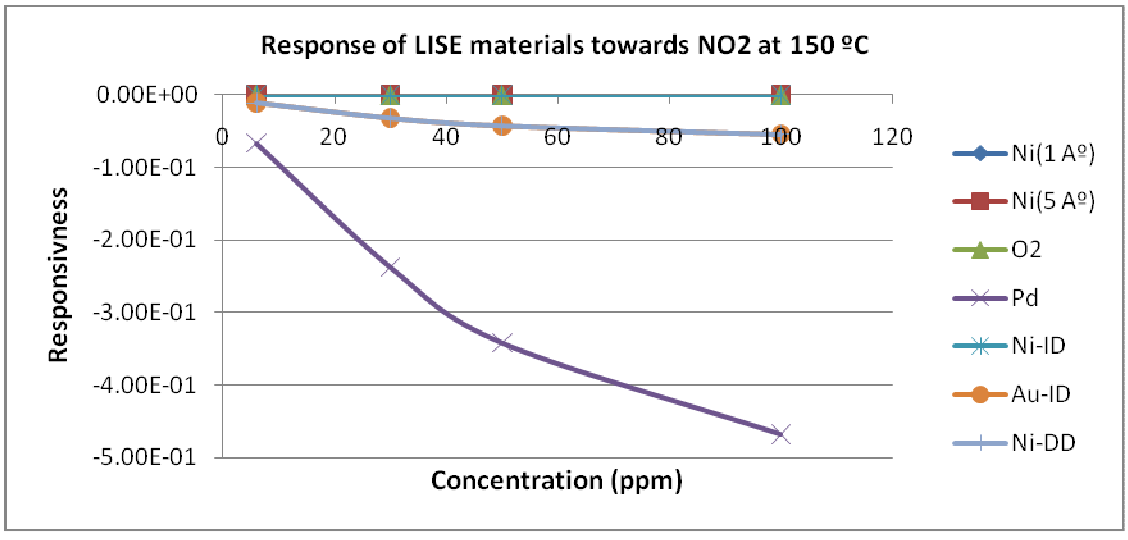

ISBN:978-84-694-0326-6/DL:T-207-2011

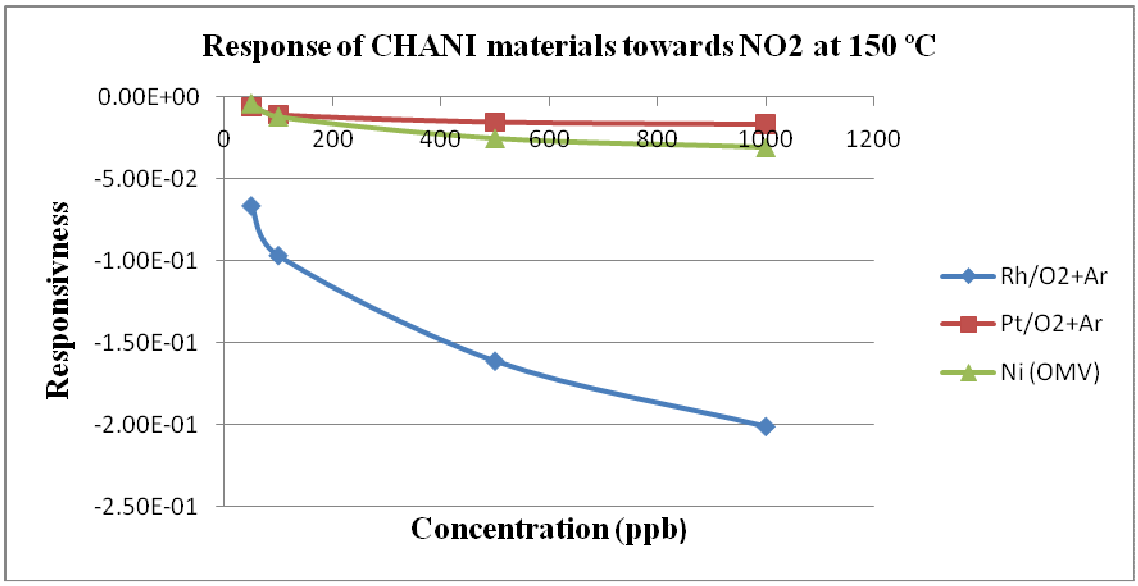

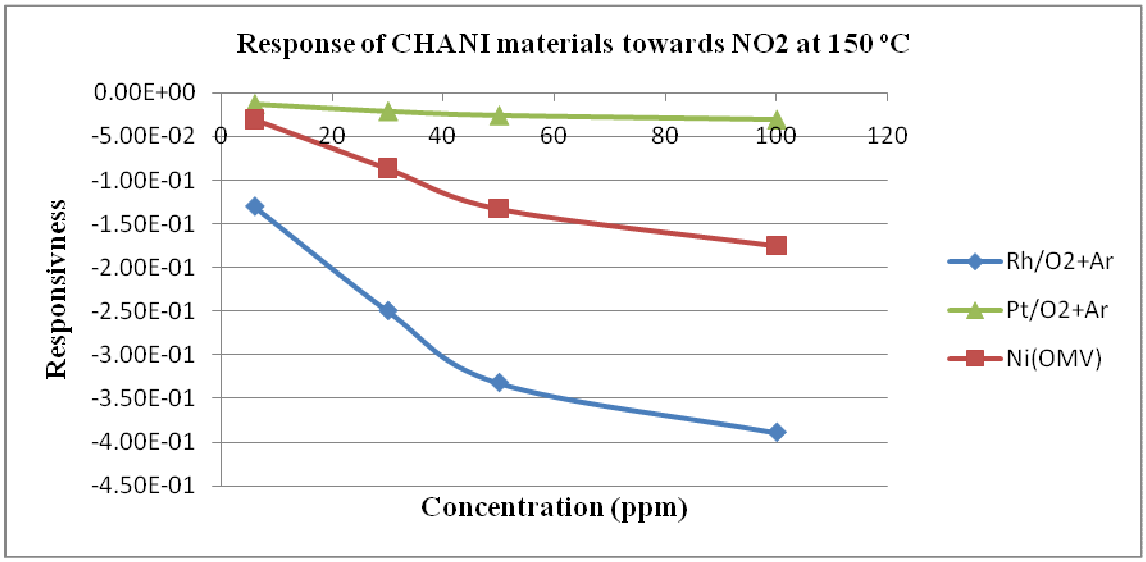

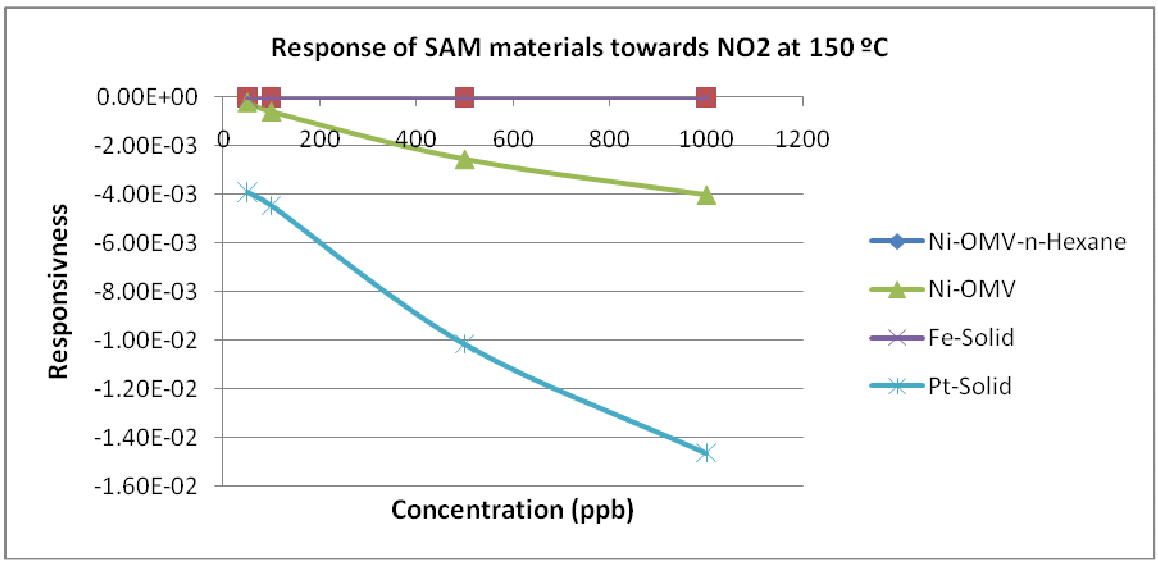

ISBN:978-84-694-0326-6/DL:T-207-2011

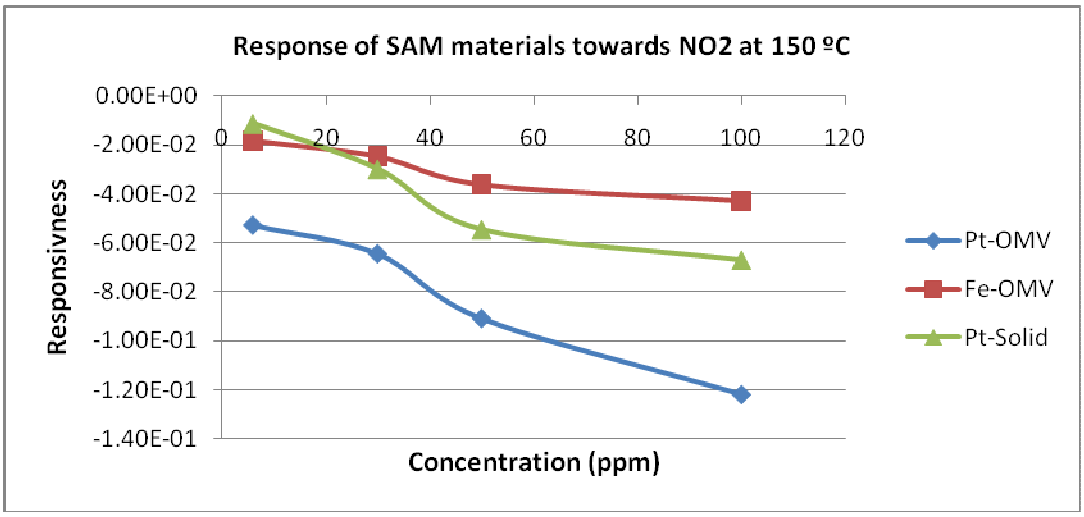

-CO detection

- At room temperature

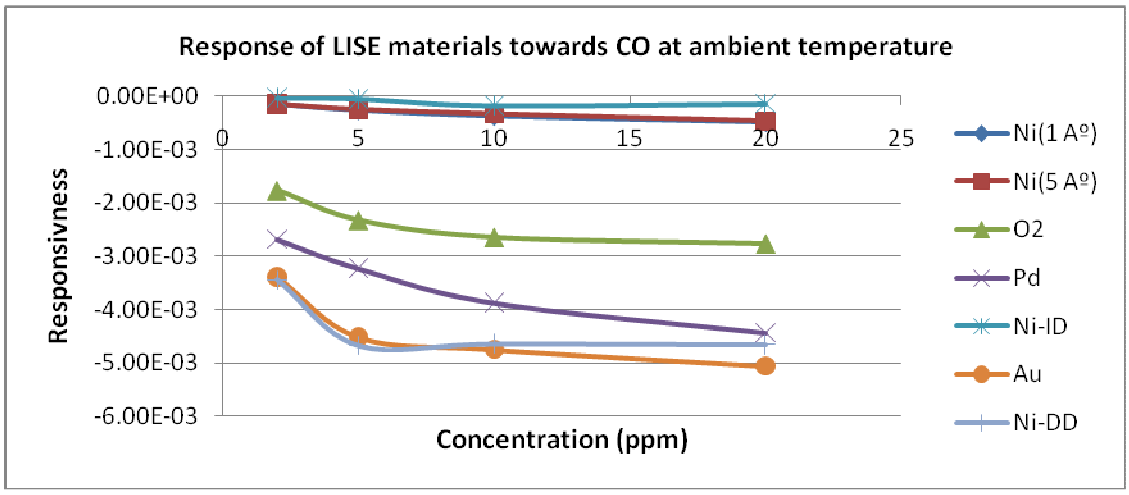

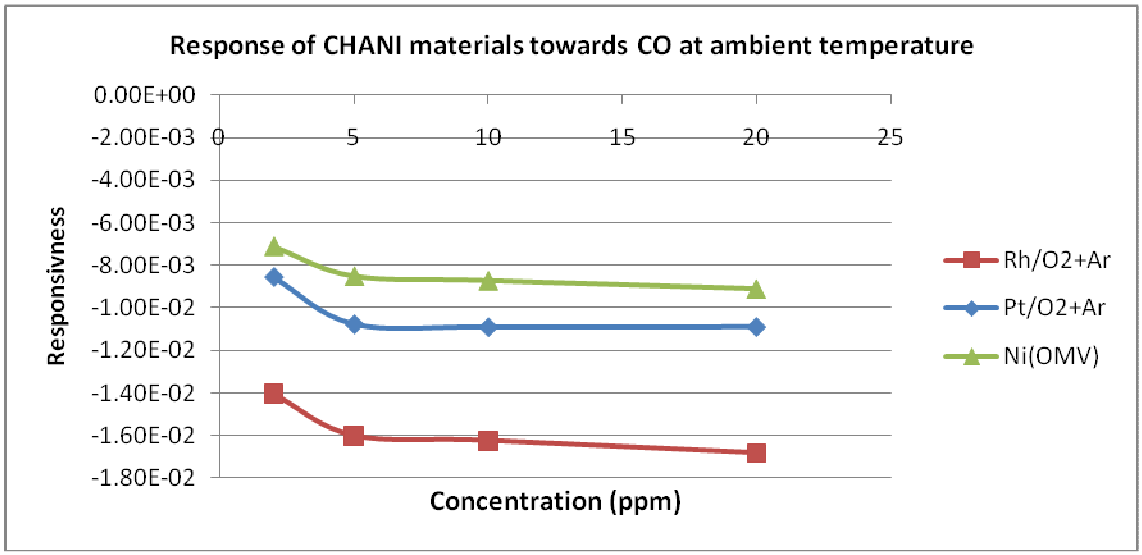

ISBN:978-84-694-0326-6/DL:T-207-2011

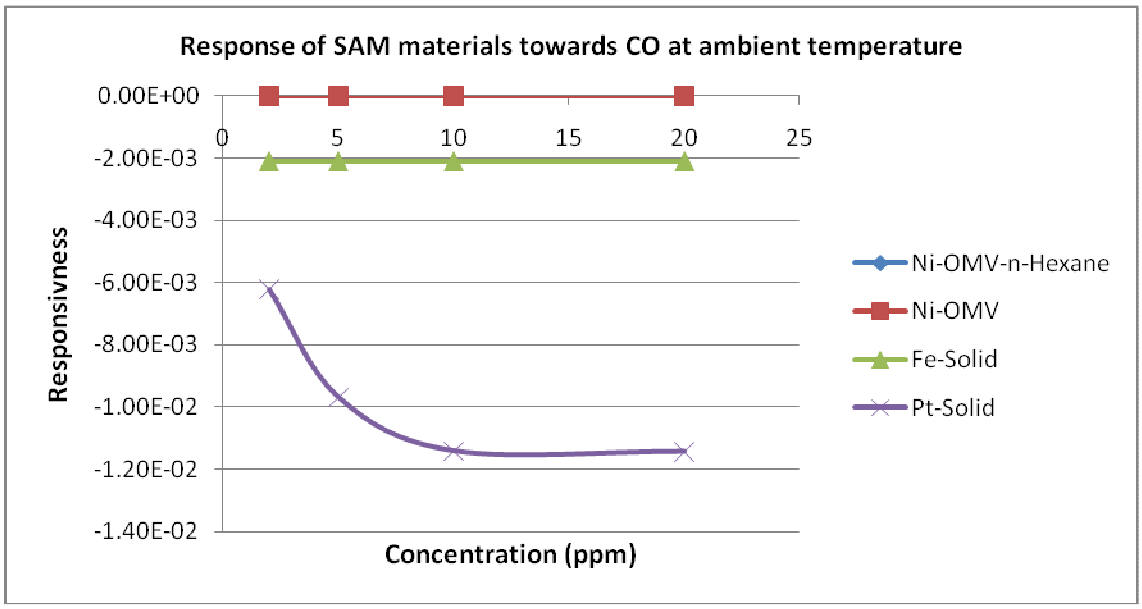

- At 150 ºC

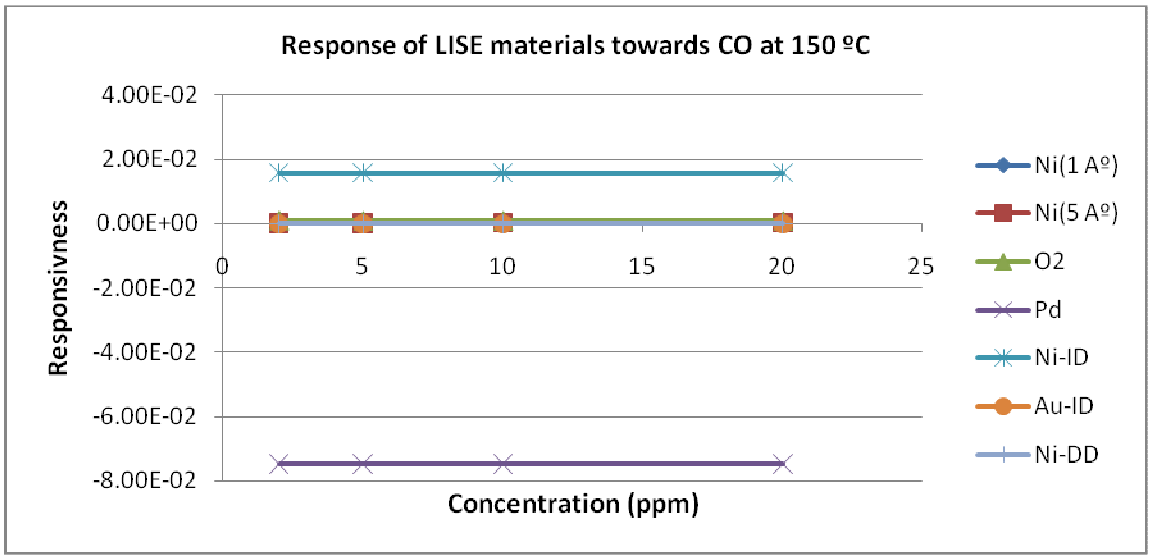

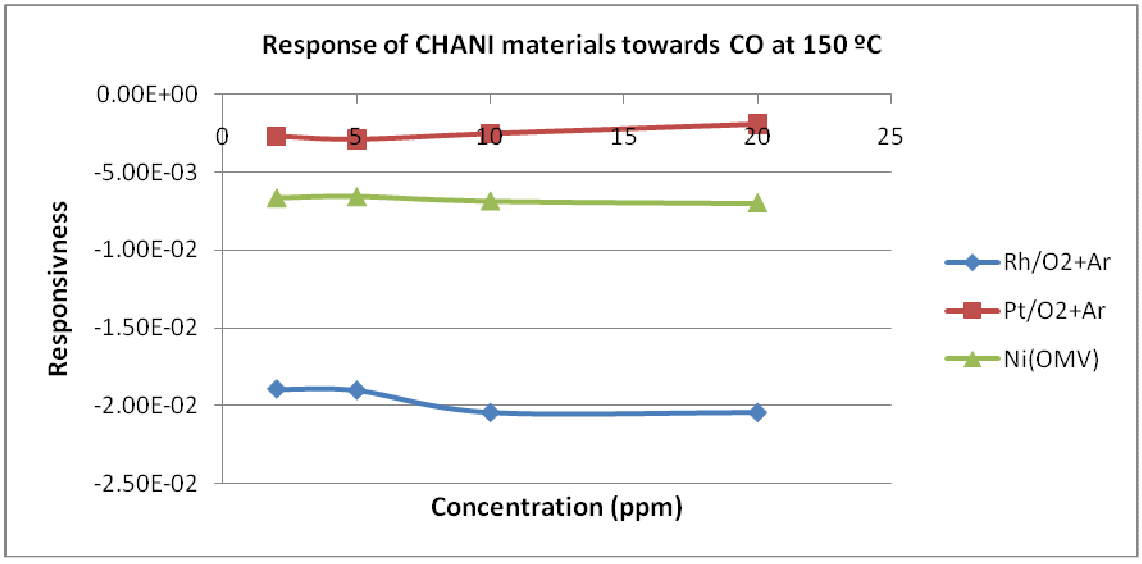

ISBN:978-84-694-0326-6/DL:T-207-2011

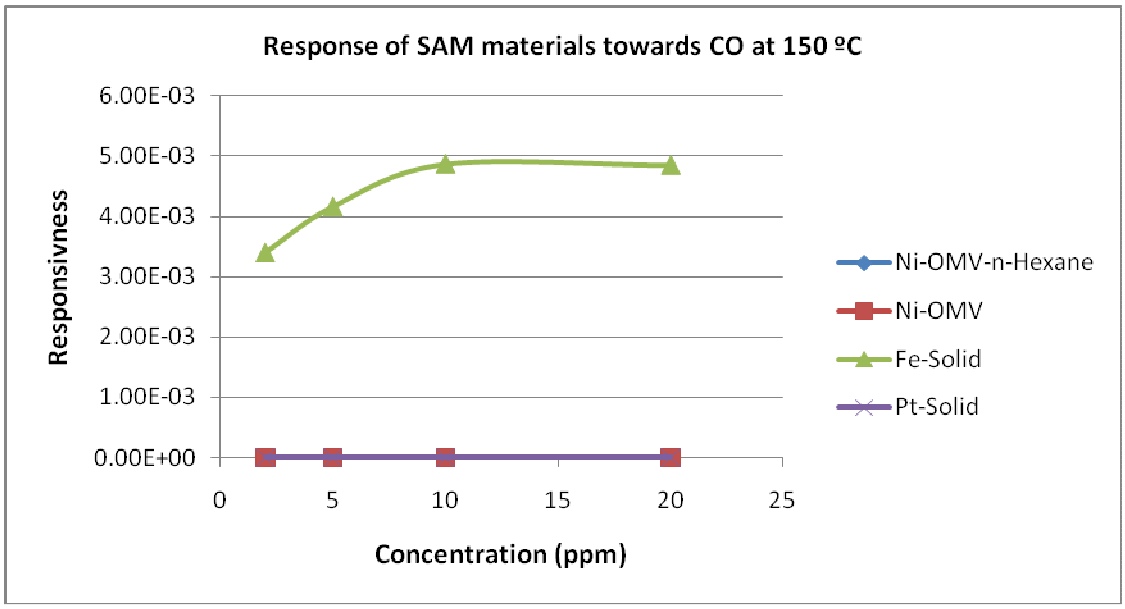

-C_2H_4 detection

- At room temperature

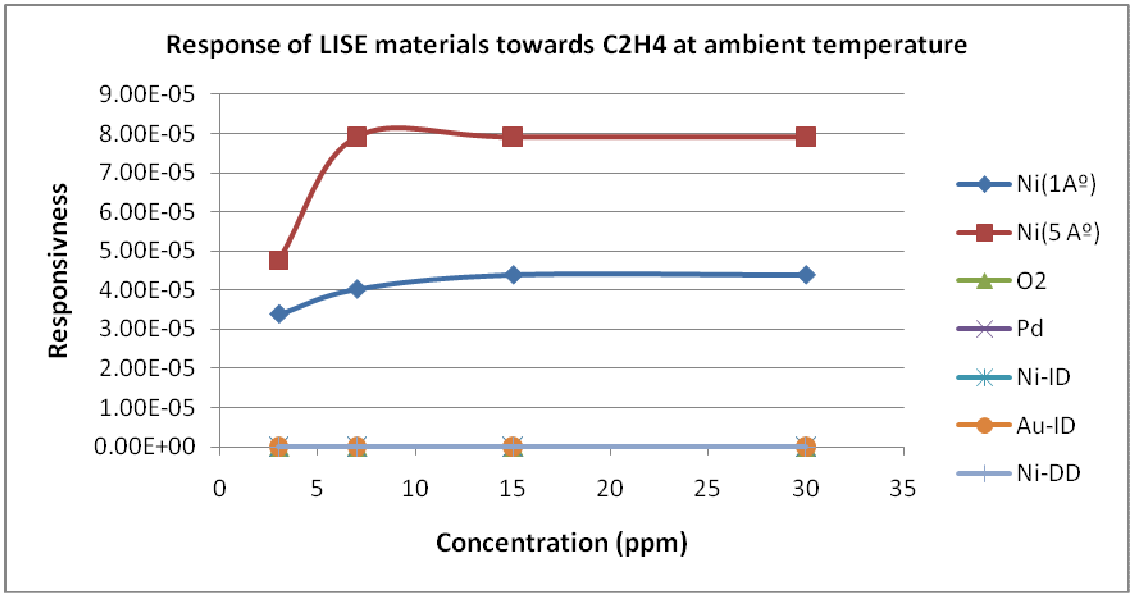

ISBN:978-84-694-0326-6/DL:T-207-2011

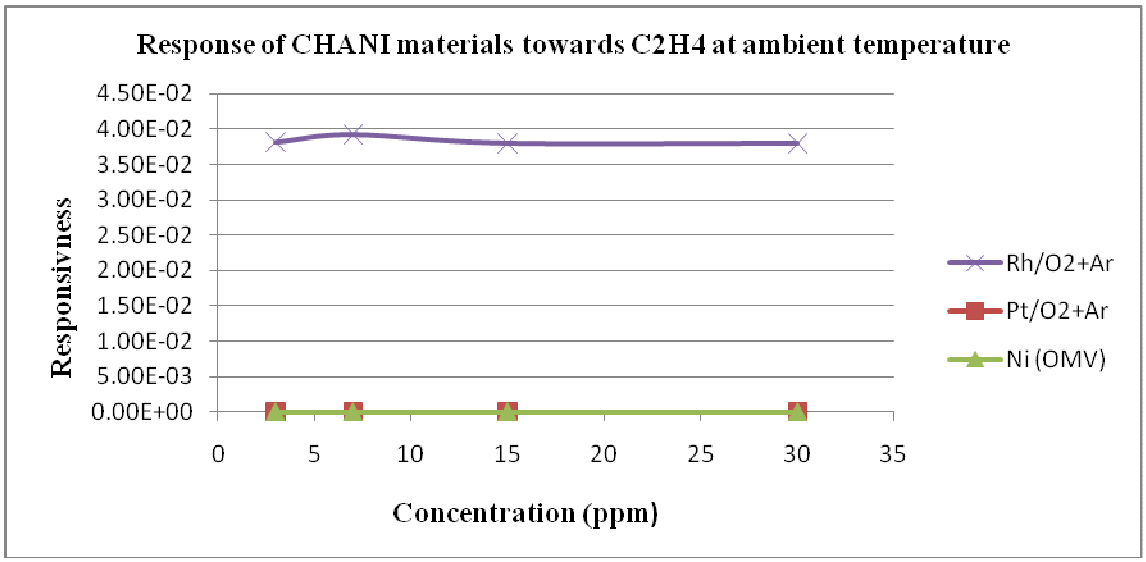

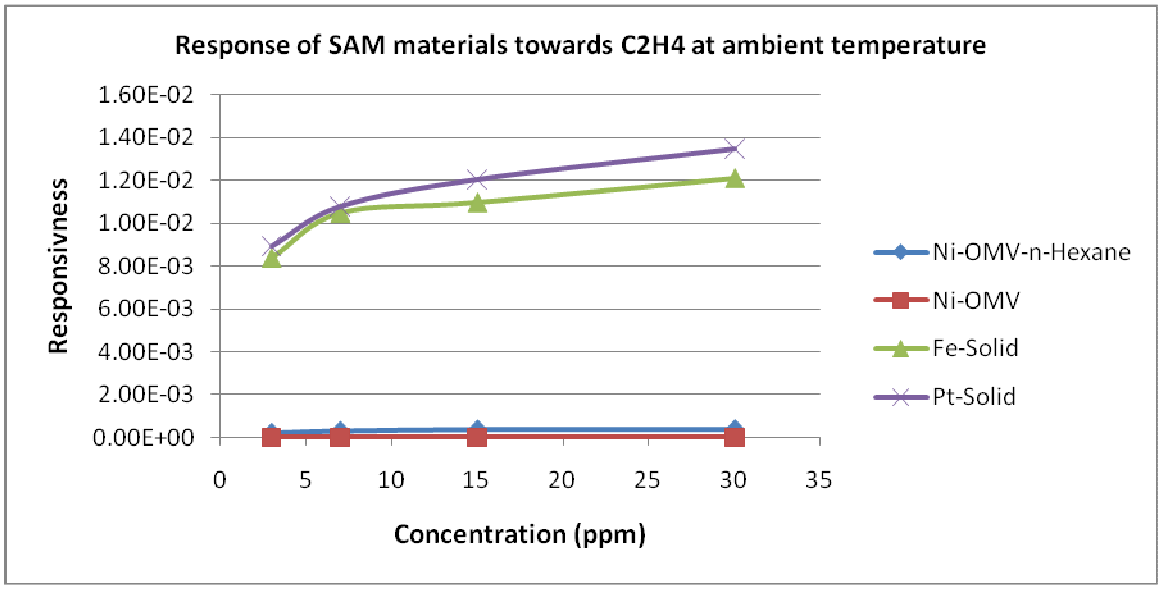

- At 150 ºC

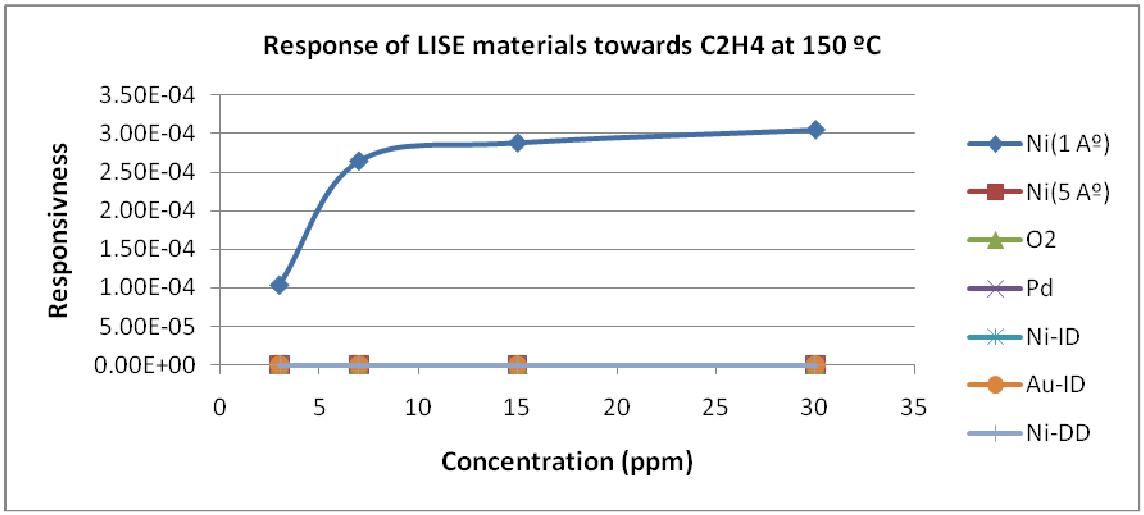

ISBN:978-84-694-0326-6/DL:T-207-2011

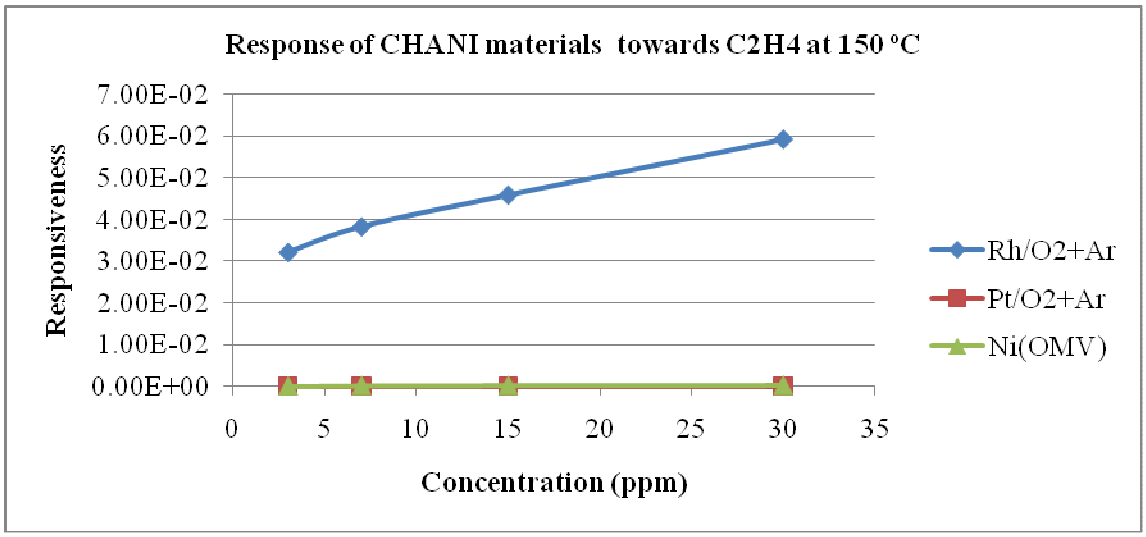

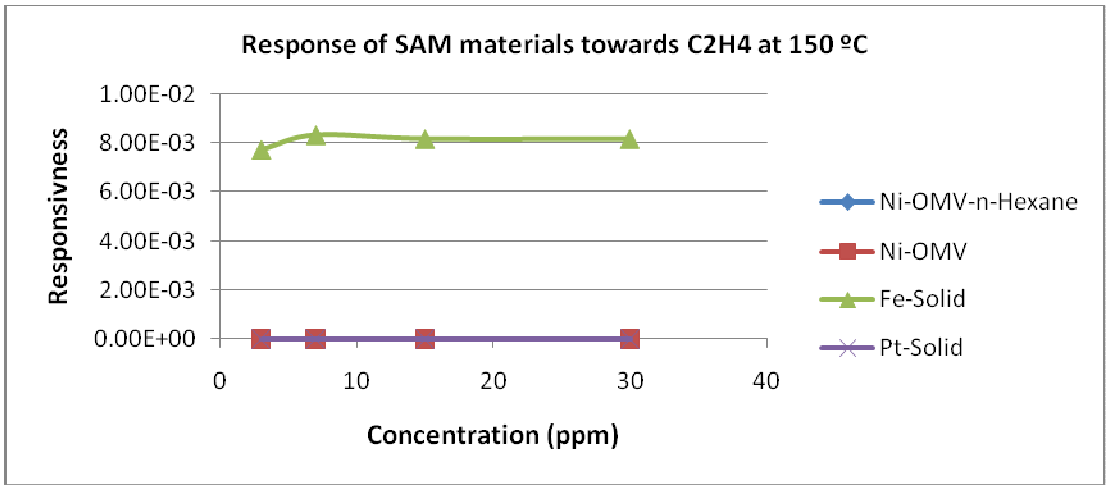

-C_6H_6 detection

- At room temperature

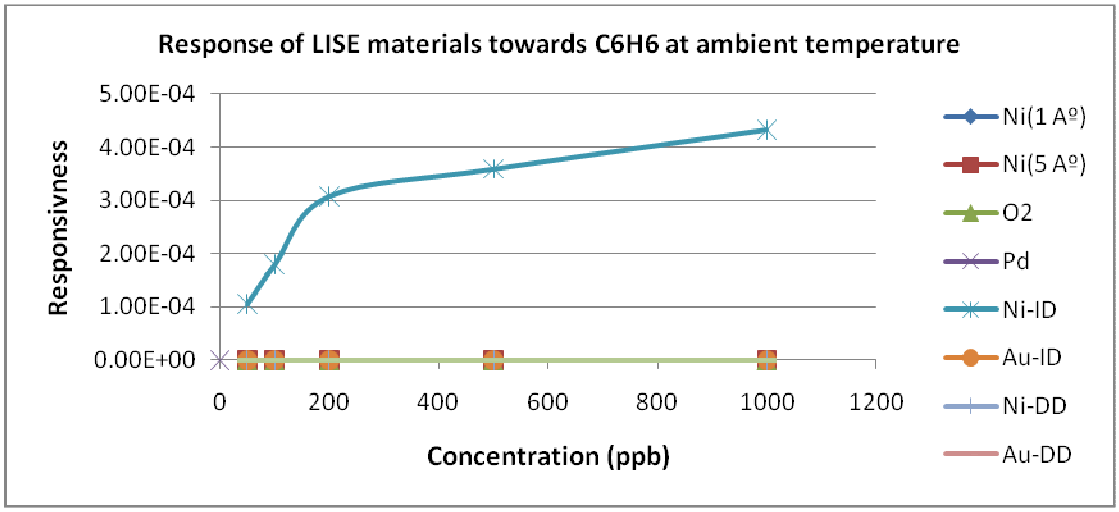

ISBN:978-84-694-0326-6/DL:T-207-2011

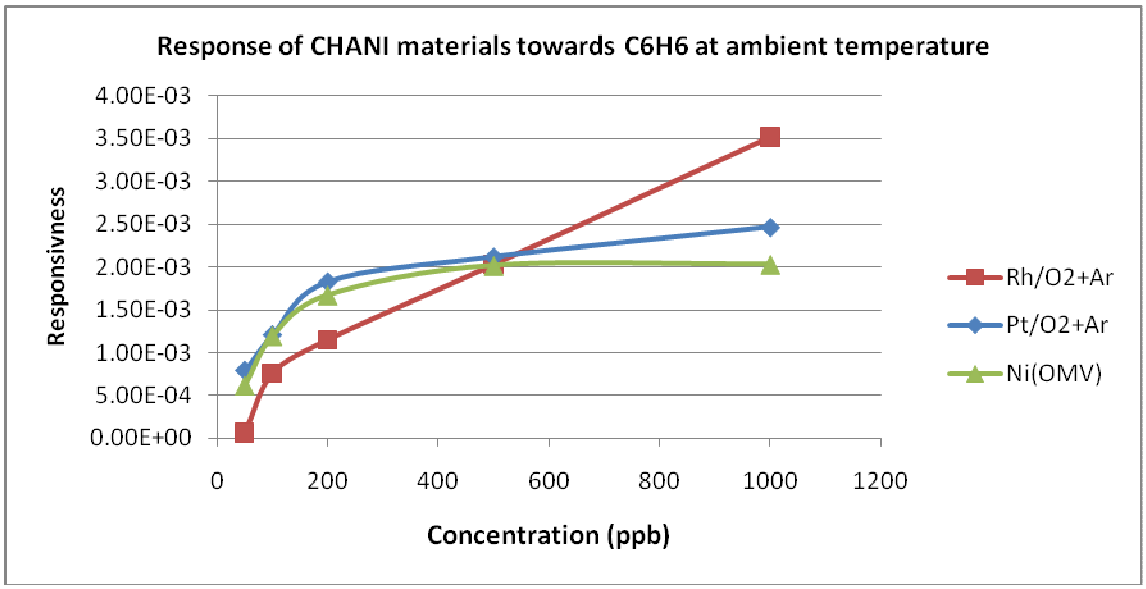

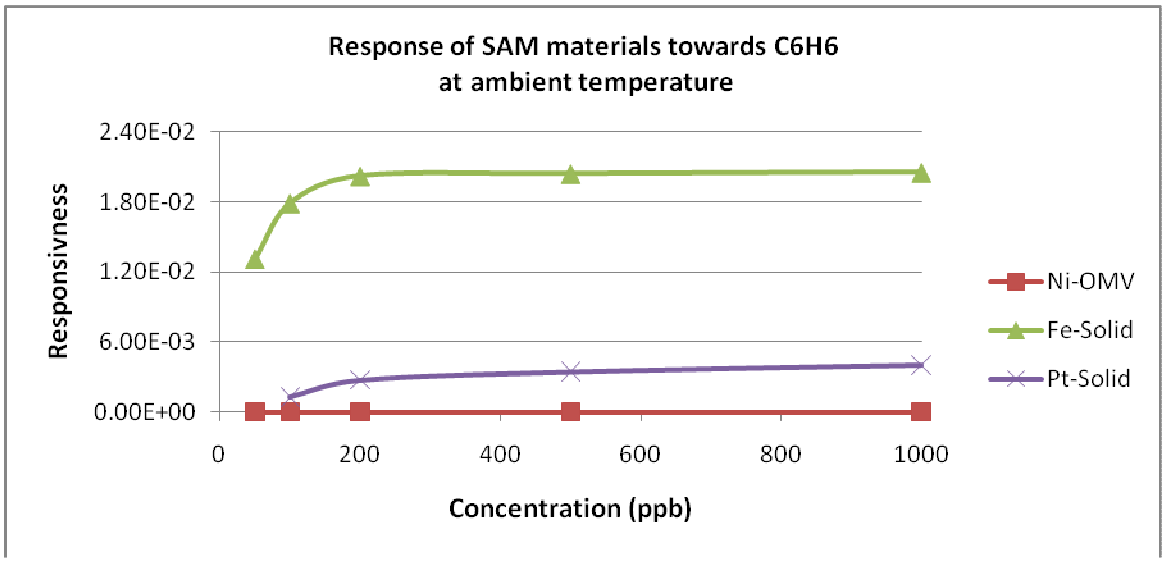

- At 150 ºC

No response of LISE materials.

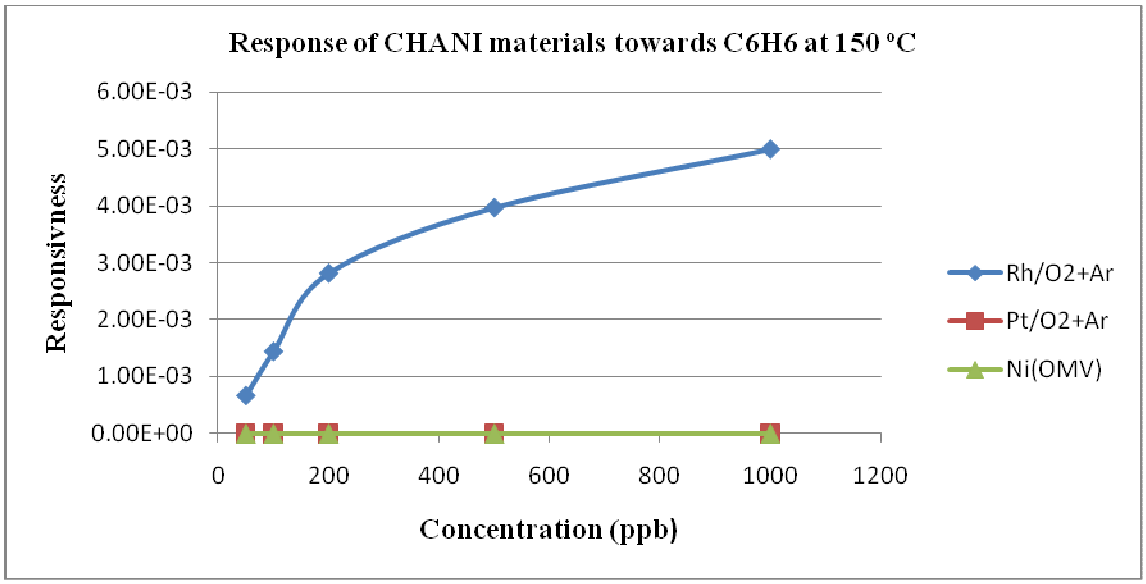

ISBN:978-84-694-0326-6/DL:T-207-2011

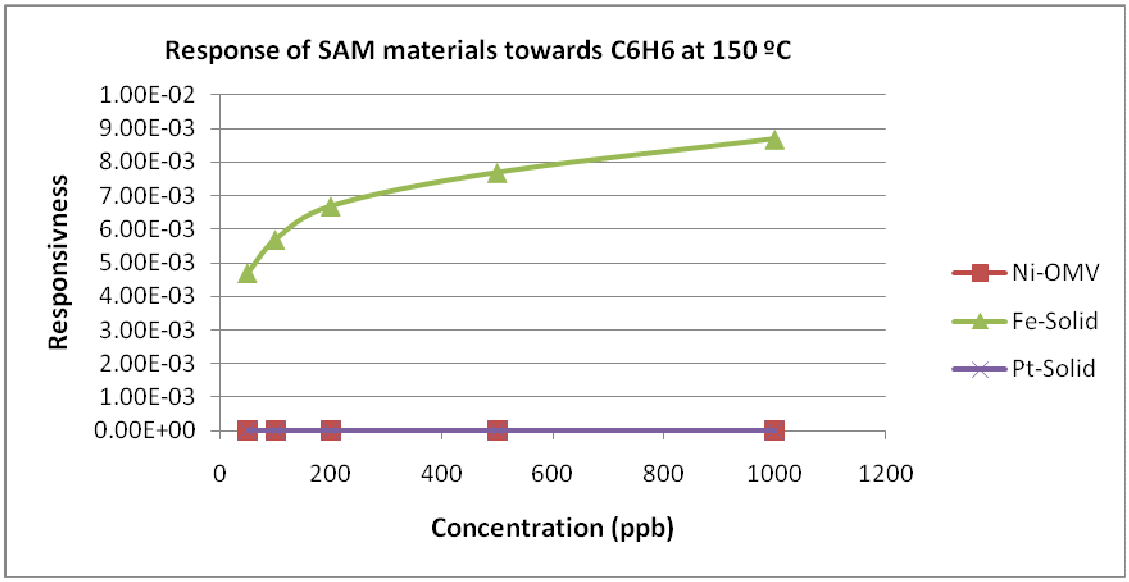

ISBN:978-84-694-0326-6/DL:T-207-2011

❖ Moisture effect

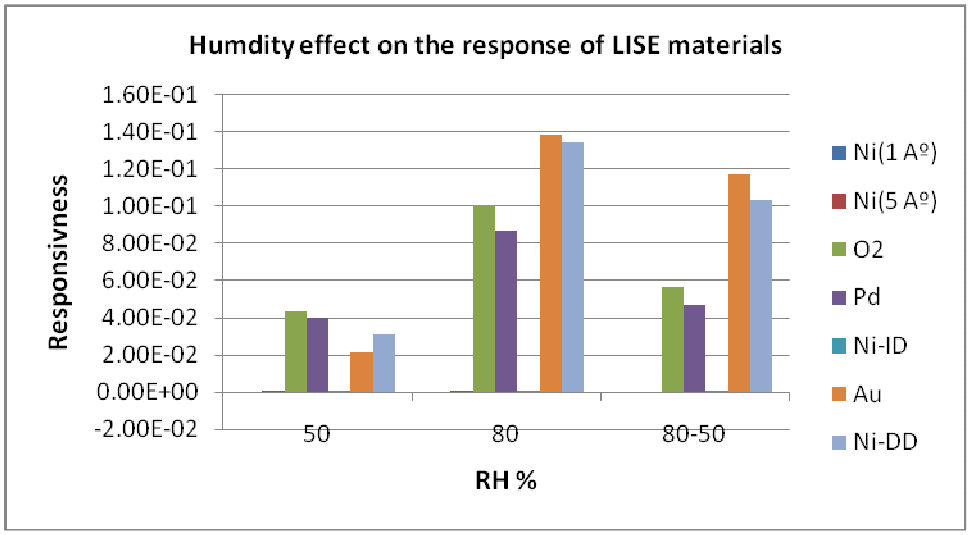

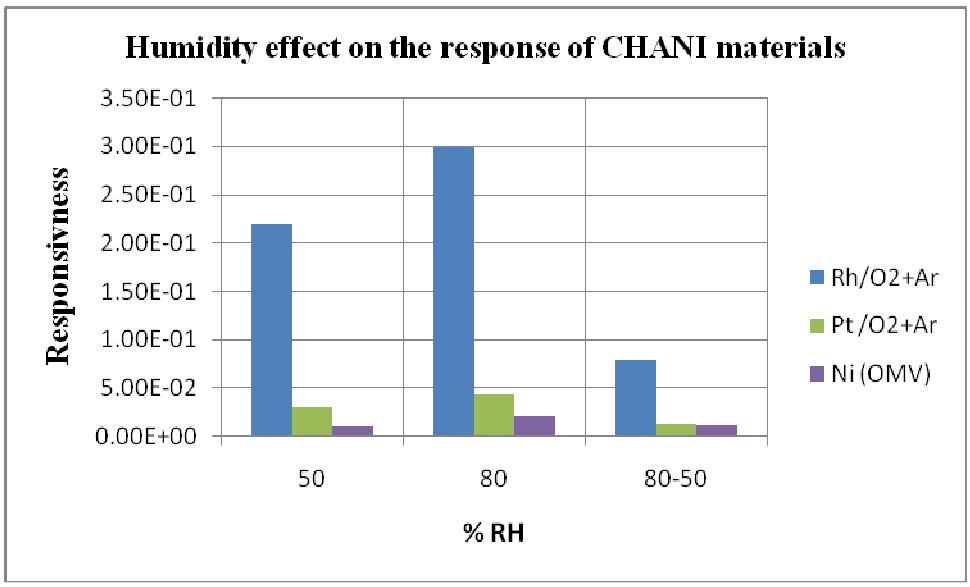

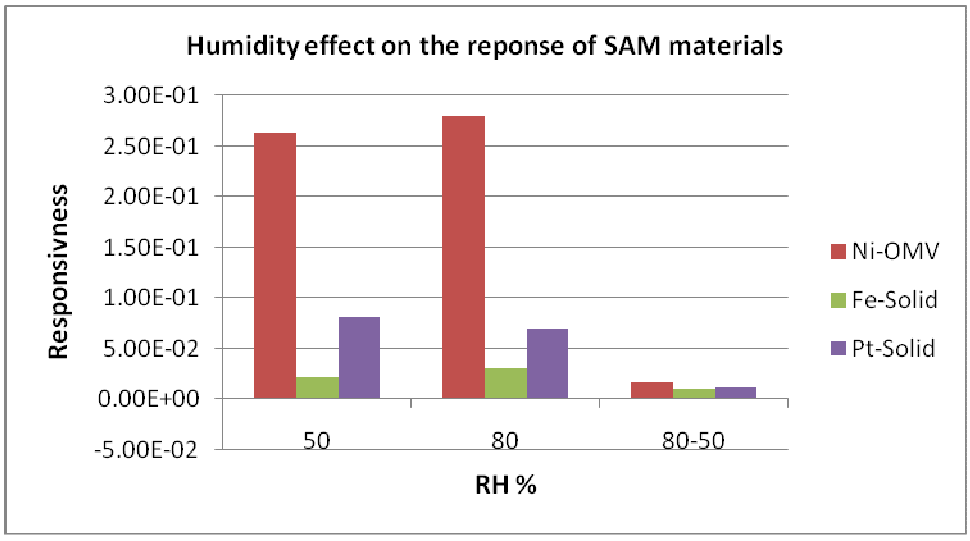

UNIVERSITAT ROVIRA I VIRGILI
DESIGN, FABRICATION AND CHARACTERISATION OF GAS SENSORS BASED ON NANOHYBRID MATERIALS
Radouane Leghrib
ISBN:978-84-694-0326-6/DL:T-207-2011

ANNEX III:

RESULTS OF THE RESPONSE OF CARBON NANOTUBE/METAL OXIDES HYBRID SENSORS TOWARDS GASES

UNIVERSITAT ROVIRA I VIRGILI
DESIGN, FABRICATION AND CHARACTERISATION OF GAS SENSORS BASED ON NANOHYBRID MATERIALS
Radouane Leghrib
ISBN:978-84-694-0326-6/DL:T-207-2011

ISBN:978-84-694-0326-6/DL:T-207-2011

1- *Responsiveness of commercial metal oxide/CNTs composites*

1.1- *Detection of NO_2*

❖ *At room temperature:*

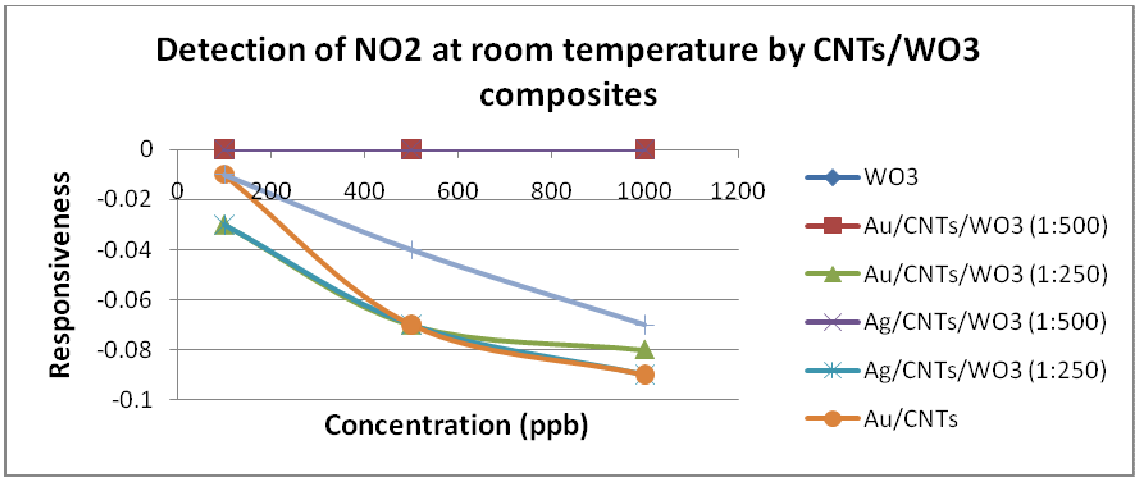

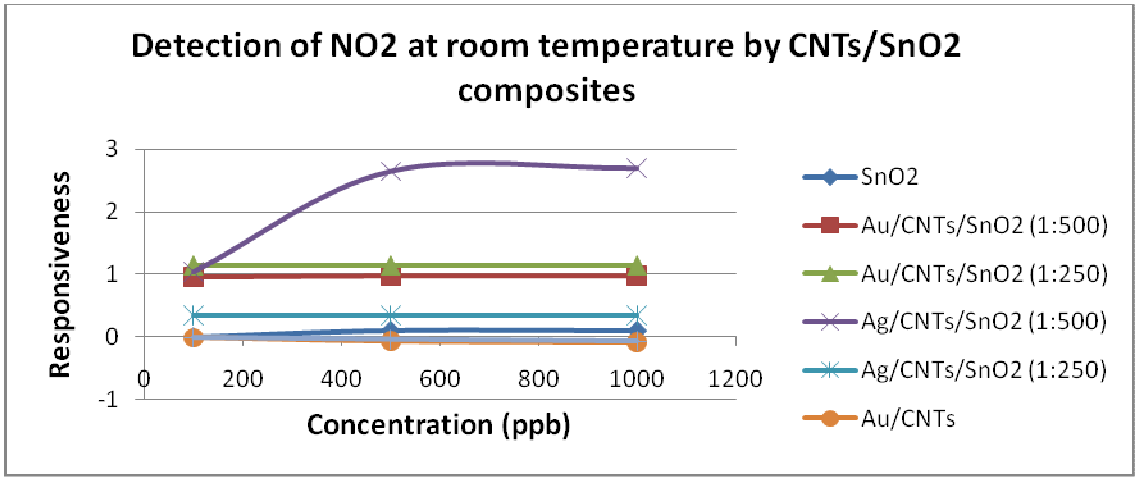

❖ *At 150 ºC:*

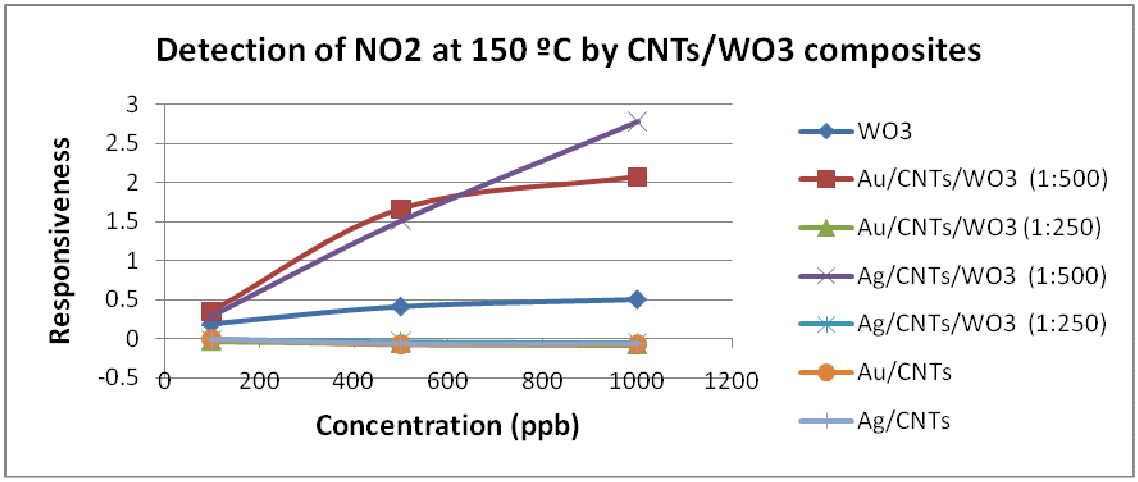

ISBN:978-84-694-0326-6/DL:T-207-2011

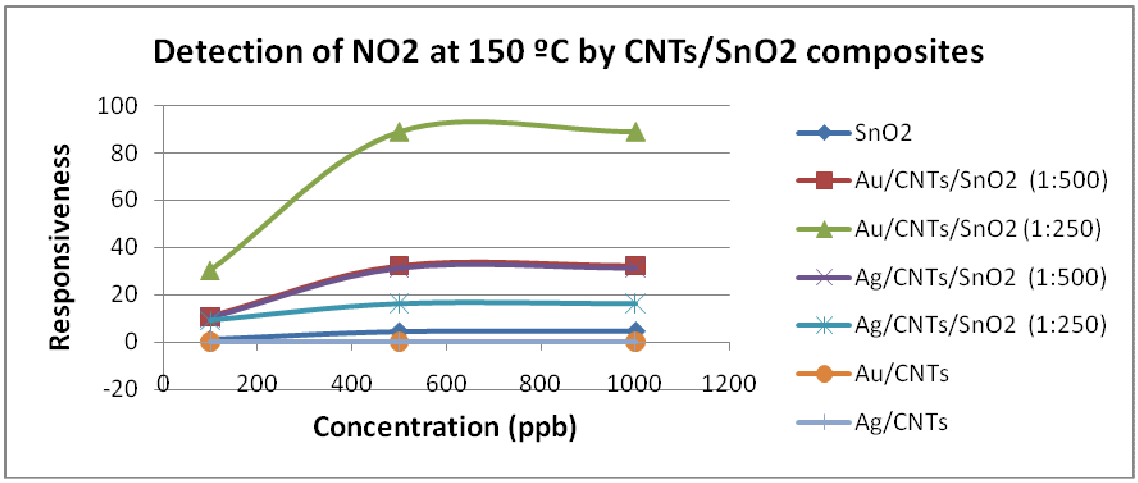

❖ ***At 250 ºC:***

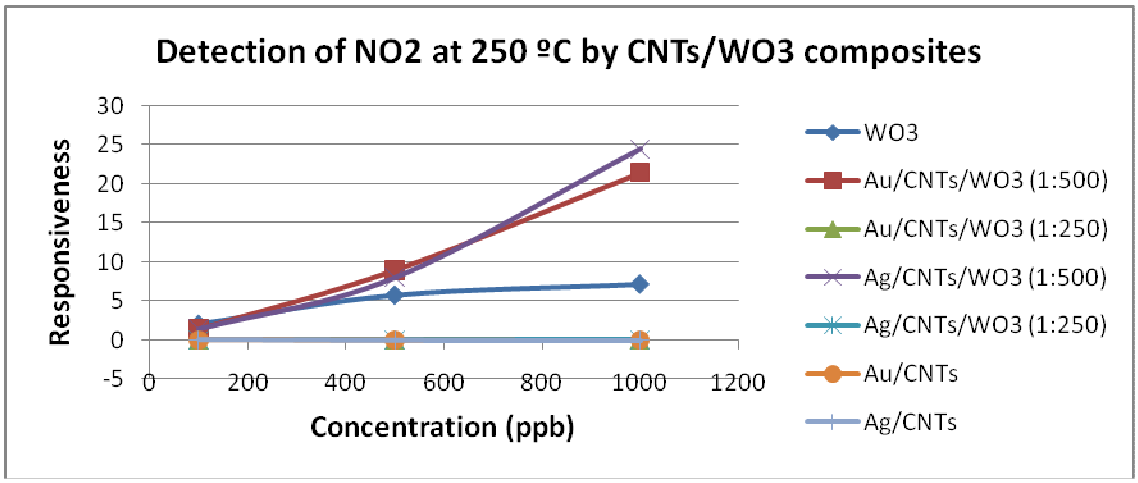

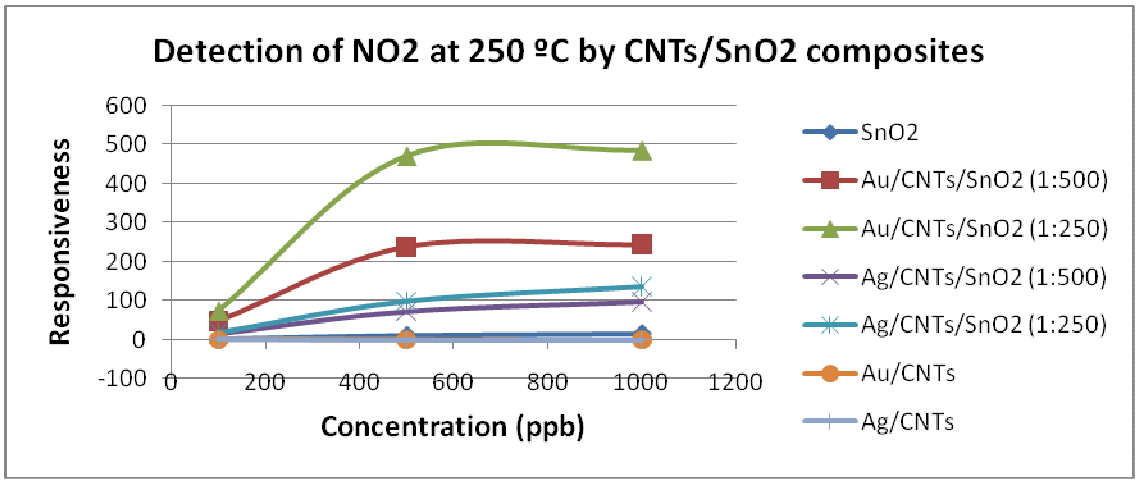

ISBN:978-84-694-0326-6/DL:T-207-2011

1.2- Detection of CO

❖ *At room temperature:*

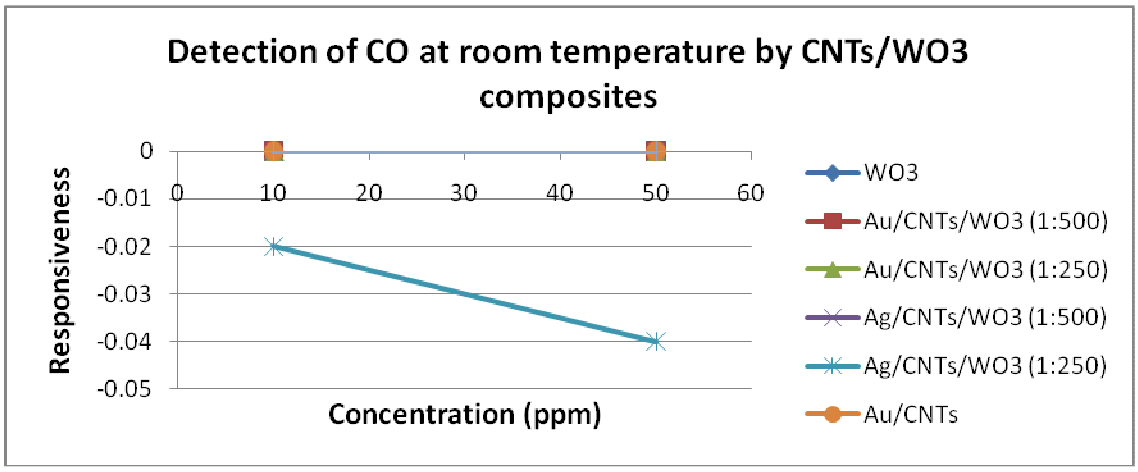

➢ ***No response of CNTs /SnO2 composites towards CO at room temperature***

❖ *At 150 ºC:*

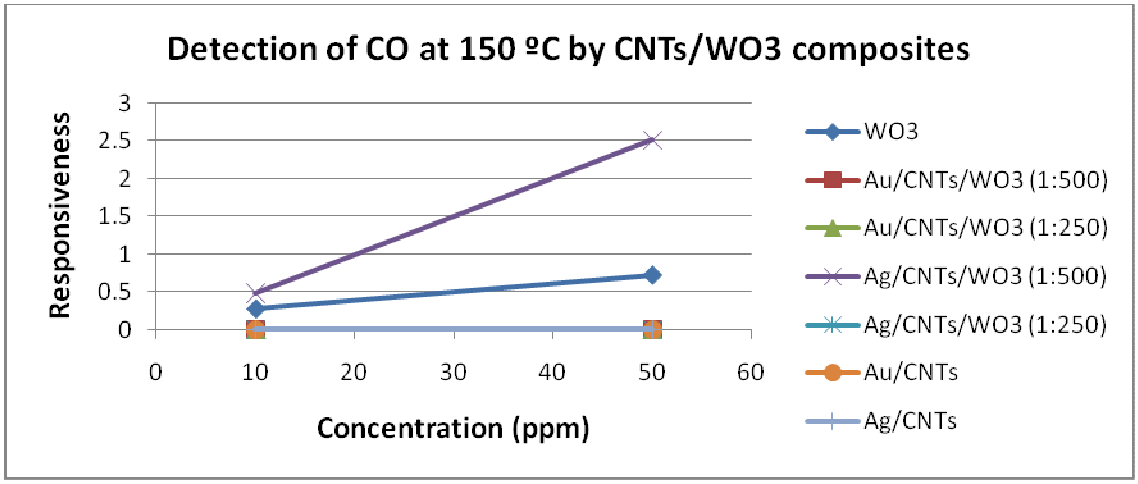

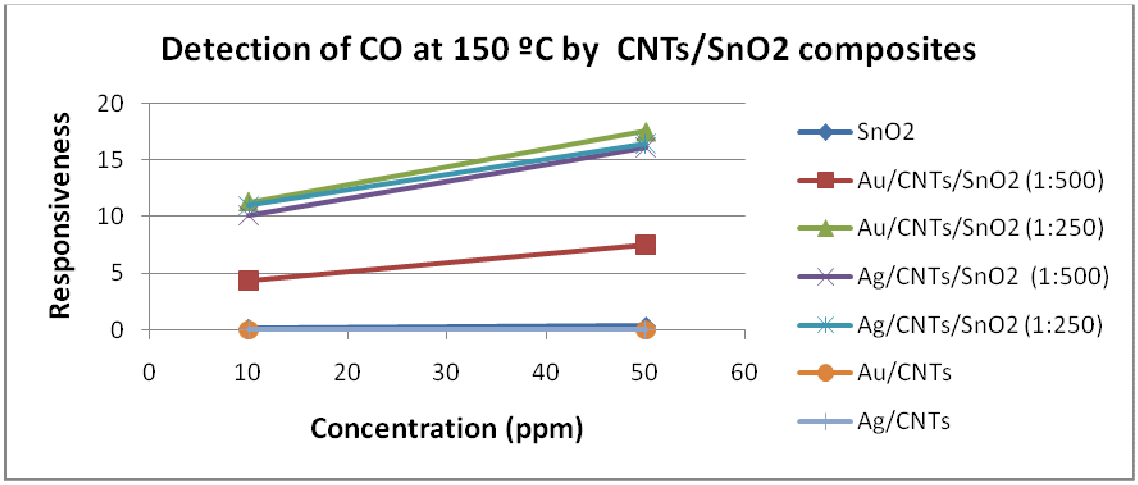

ISBN:978-84-694-0326-6/DL:T-207-2011

❖ *At 250 ºC:*

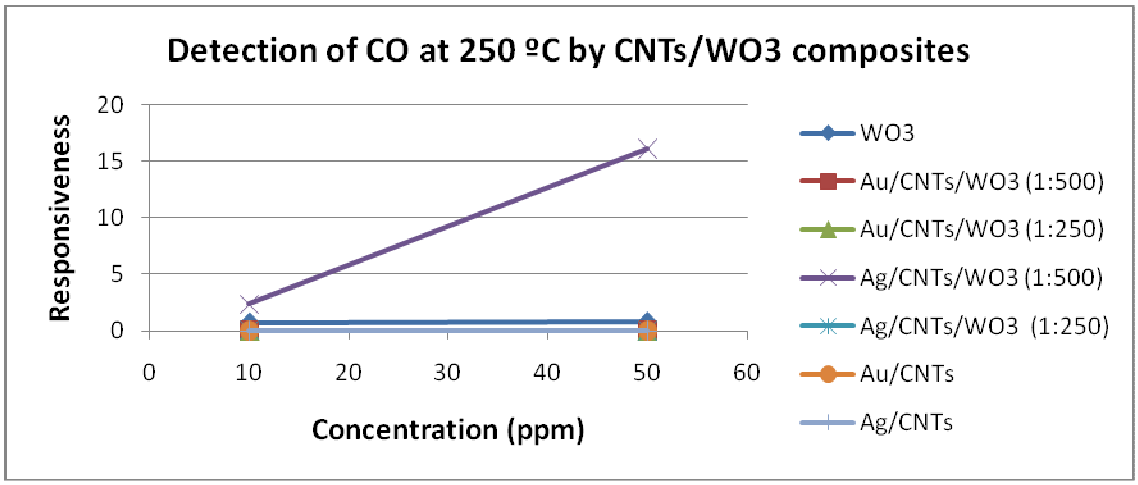

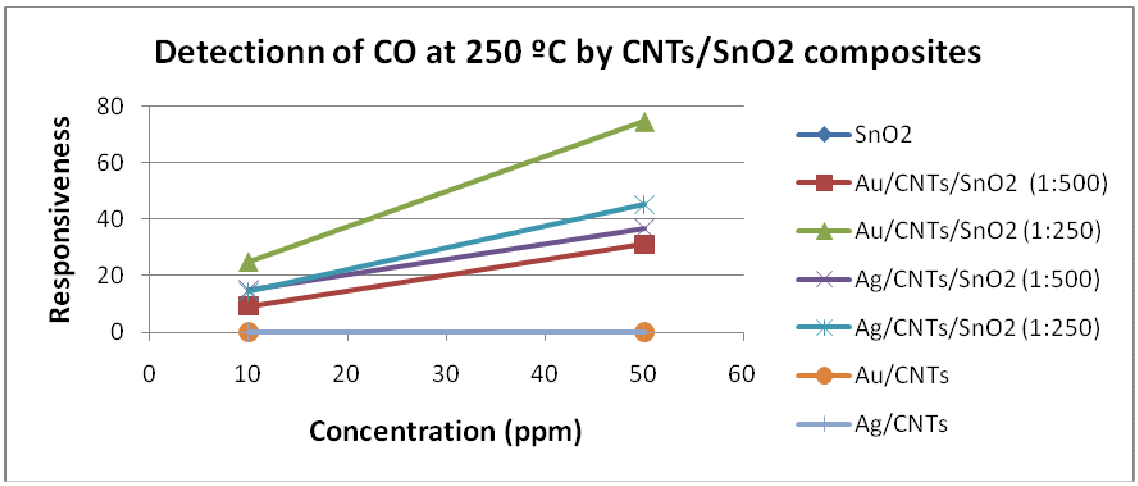

2- Humidity effect on home-synthesized metal oxide/CNTs composites

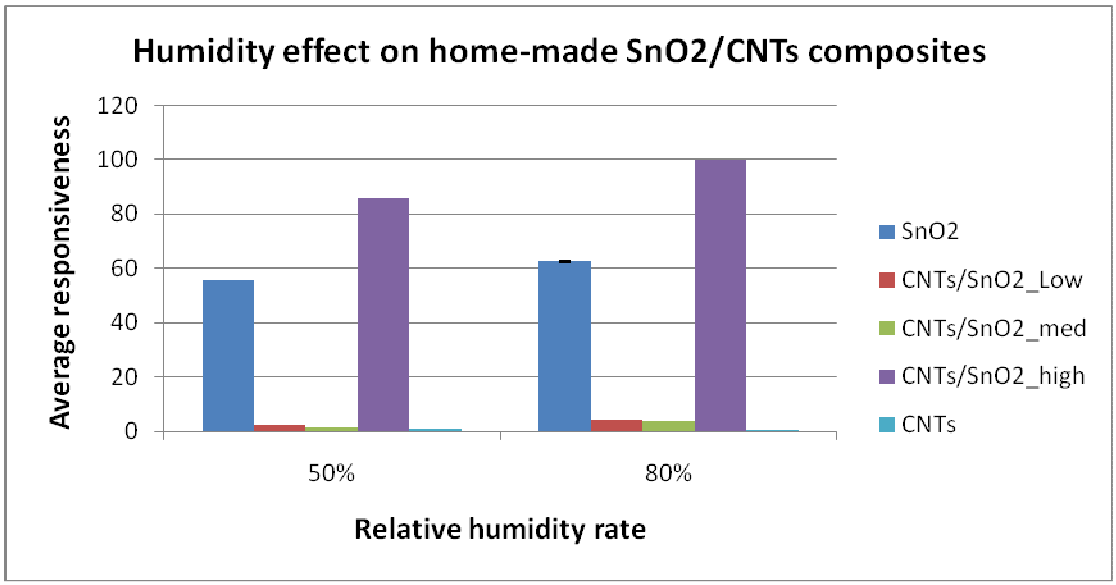

UNIVERSITAT ROVIRA I VIRGILI
DESIGN, FABRICATION AND CHARACTERISATION OF GAS SENSORS BASED ON NANOHYBRID MATERIALS
Radouane Leghrib
ISBN:978-84-694-0326-6/DL:T-207-2011

3- *Responsivenss of pristine CNTs, N- and B-doped CNTs*

3.1-Detection of NO_2

❖ *At room temperature*

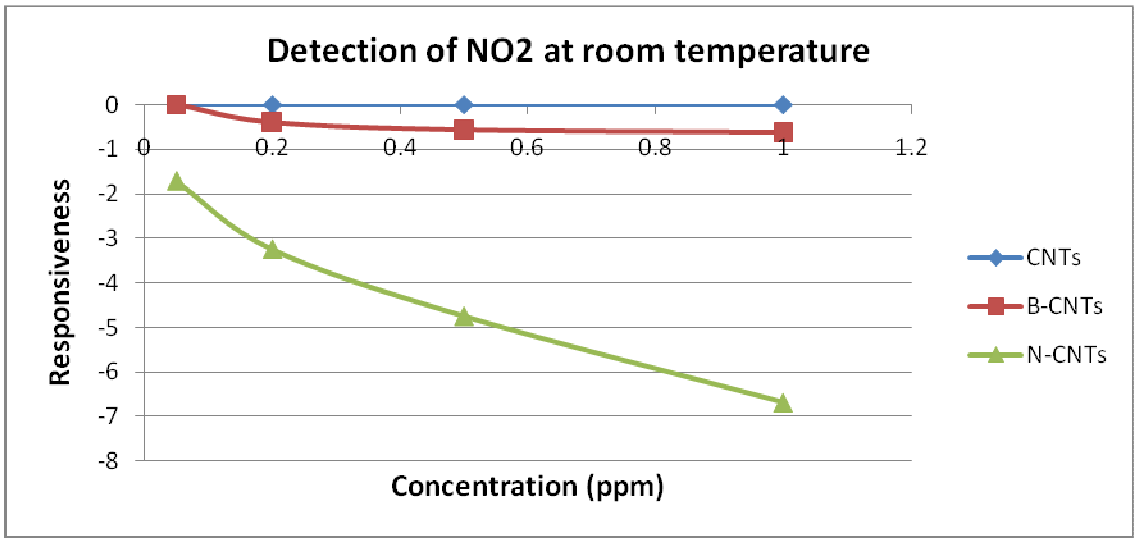

❖ *At 150 ºC*

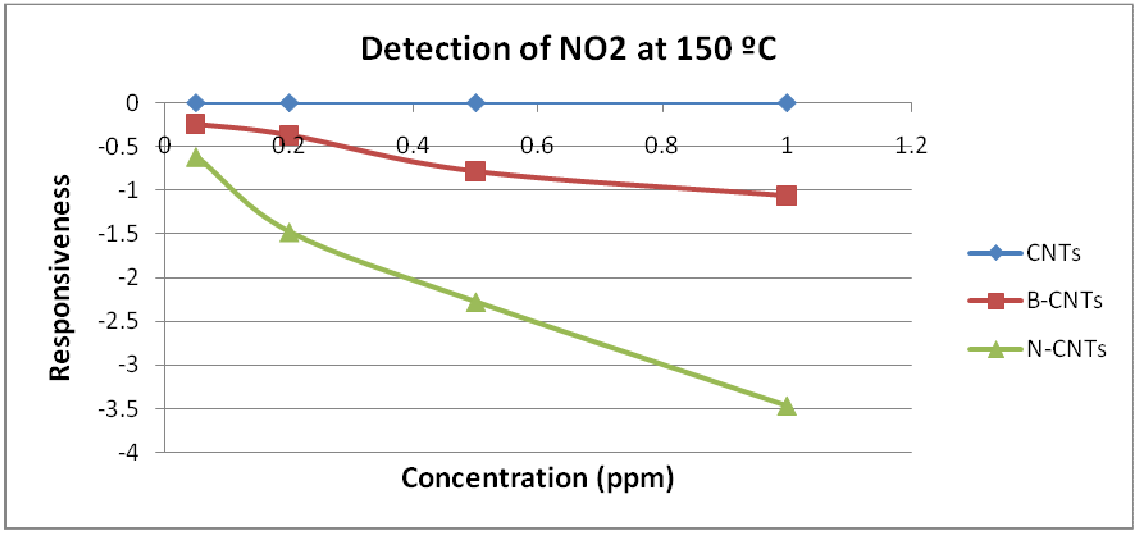

ISBN:978-84-694-0326-6/DL:T-207-2011

3.2- Detection of CO

❖ *At room temperature*

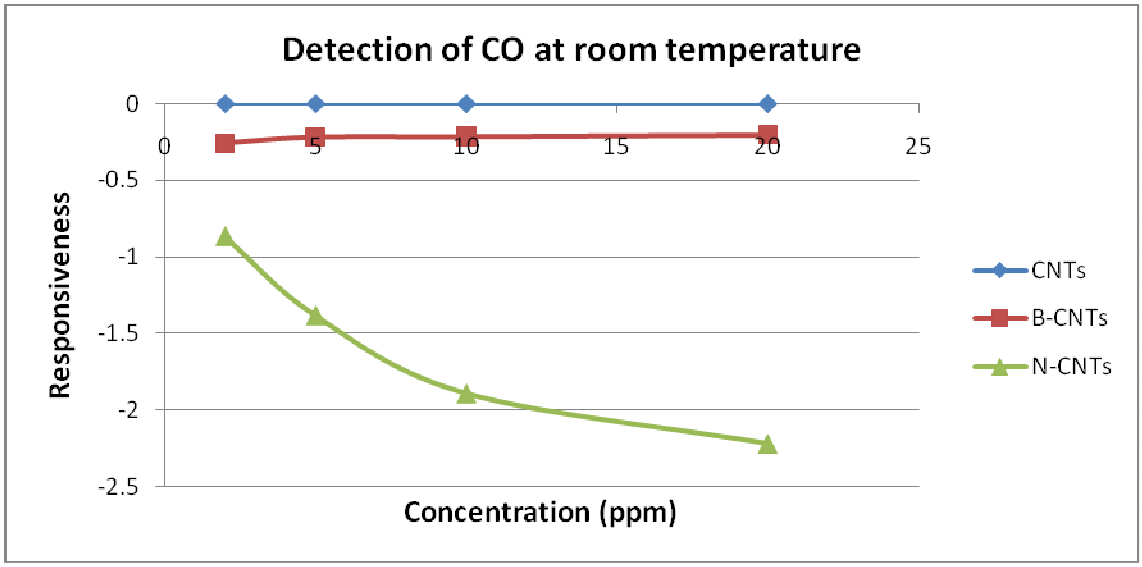

❖ *At 150 ºC*

➢ ***No response of towards CO***

3.3- Detection of C_2H_4

❖ *At room temperature*

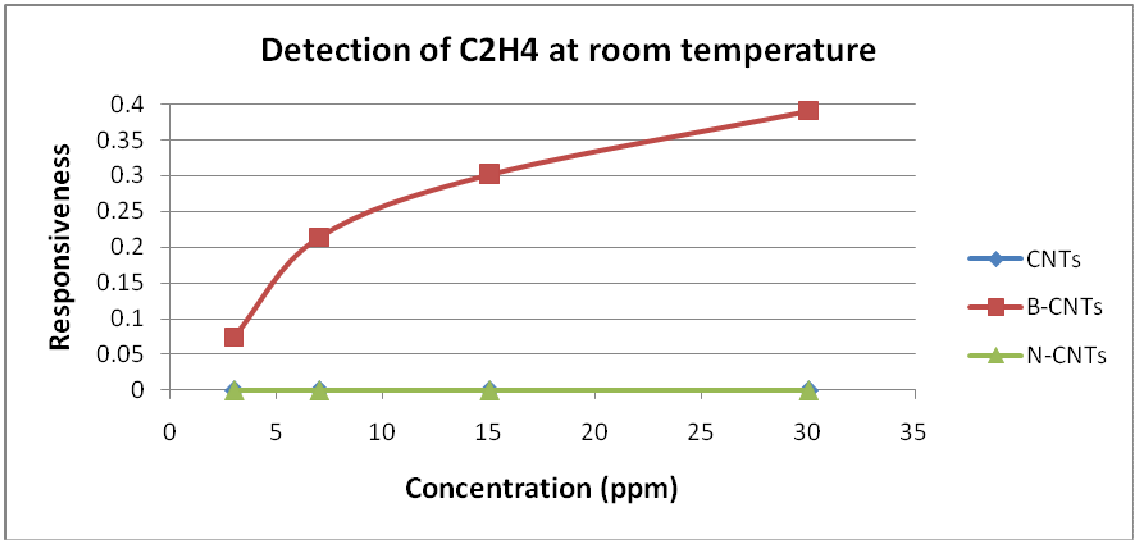

ISBN:978-84-694-0326-6/DL:T-207-2011

❖ *At 150 ºC*

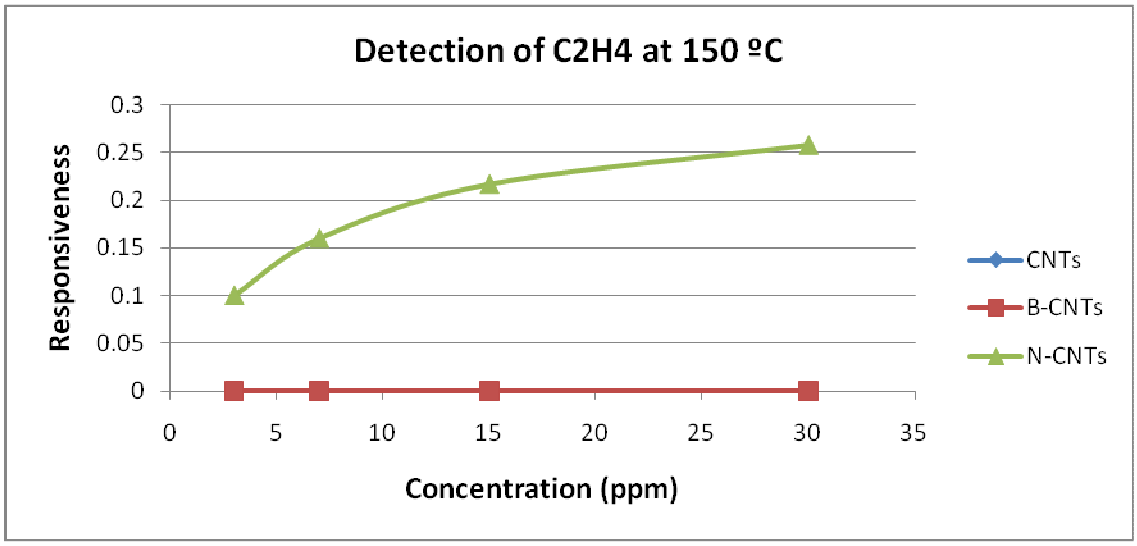

4. Humidity effect

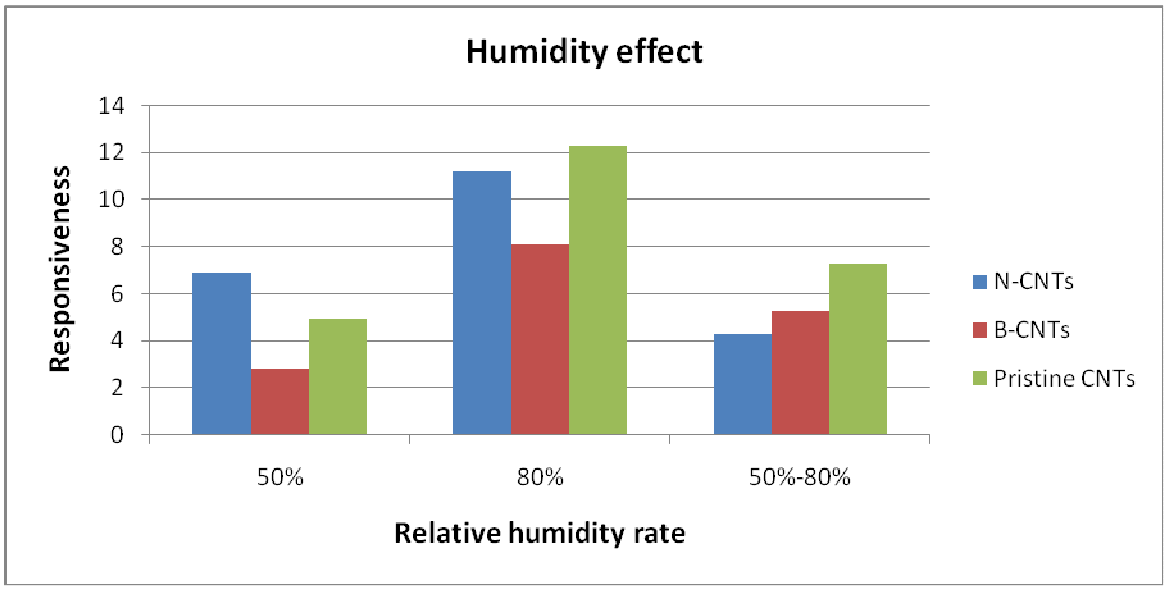

UNIVERSITAT ROVIRA I VIRGILI
DESIGN, FABRICATION AND CHARACTERISATION OF GAS SENSORS BASED ON NANOHYBRID MATERIALS
Radouane Leghrib
ISBN:978-84-694-0326-6/DL:T-207-2011

UNIVERSITAT ROVIRA I VIRGILI
DESIGN, FABRICATION AND CHARACTERISATION OF GAS SENSORS BASED ON NANOHYBRID MATERIALS
Radouane Leghrib
ISBN:978-84-694-0326-6/DL:T-207-2011

ANNEX IV:

DETAILS ABOUT PINCIPAL COMPONENT ANALYSIS (PCA)

UNIVERSITAT ROVIRA I VIRGILI
DESIGN, FABRICATION AND CHARACTERISATION OF GAS SENSORS BASED ON NANOHYBRID MATERIALS
Radouane Leghrib
ISBN:978-84-694-0326-6/DL:T-207-2011

ISBN:978-84-694-0326-6/DL:T-207-2011

Basic concepts about Principal Component Analysis (PCA)

Considering the high number of sensor responses gathered during the measurements (i.e., different hybrid materials, different sensing temperatures, different gases, and experiment repetitions) a statistical analysis tool was employed to determine which sensors were performing better and which nanohybrid materials should be used for selectively detect benzene. Principal component analysis method was used as the statistical analysis tool. In fact, by comparing the results of several gases, it is possible to determine which sensors will respond in which way (eg. Large or small, positive or negative, reproducible or not, etc). By such a way, when the sensors responses to an unknown subject are compared with the smell prints of several known substances, the unknown subject can be identified by matching its pattern to one of the known substances in a final data set (made from the first calibration).

The raw data set contains the responses from all the sensors. Pattern recognition algorithms are very powerful tools to deal with a large set of data. For example, the principal component analysis (PCA) was applied to the data set that was collected from this carbon nanotube based sensors. The PCA is to express the main information in the variables $X = \{x^k, k = 1,2, \ldots ,K\}$ by a lower number of variables $T=\{t_1, t_2,\ldots,t_A\}$, (A< k), the so-called principal components of X [1, 2]. . The first principal component accounts for as much of the variability in the data as possible, and each succeeding component accounts for as much of the remaining variability as possible. This method was selected for the following reasons [3]:

- It is an unsupervised method; indeed, the raw data is introduced and plotted without any external intervention of the user.
- It uses response variance to cluster data.
- Loadings (eigenvectors of the covariance data matrix) give information about sensor correlation and sensor reproducibility.
- Scores (data projected onto the space defined by PCs) show data clustering.

In our case, PCA was performed in two steps:

- ✓ In the first step PCA helps in the selection of the most adequate sensors for the selective detection of each gas separately.
- ✓ In the second step PCA helps studying the selective detection of benzene in dry or humid ambient employing the few sensors selected.

ISBN:978-84-694-0326-6/DL:T-207-2011

For performing the principal component analysis or building the linear discriminant, the partial least squares or multilayer perceptron models, standard routines from MATLAB were used. This annex groups the scripts used.

AIV.1 Principal component analysis

Prior to perform a PCA data were mean-centered. This is usually employed when sensors of the same nature are being used. It helps removing non informative offsets from sensor signals. The script employed in MATLAB was as follows:

MNCN Mean center scales matrix to mean zero: I/O format is:

[mcx,mx] = mncn(x)

Mean centers matrix x, returning a matrix with mean zero columns (mcx) and the vector of means (mx) used in the scaling.

The script employed to perform PCA was as follows:

PCA Principal components analysis The I/O format is:

[scores,loads,ssq,res,q,tsq] = pca(data,plots,scl,lvs)

It is assumed that samples are rows and variables are columns. The inputs are the input matrix (data), an optional variable (plots) that controls the graphs produced (if set to 0 no graphs are produced), an optional vector (scl) for plotting scores against and an optional variable (lv) which specifies the number of principal components to use in the model and which suppresses the prompt for number of PCs. The outputs are the scores (scores), loadings (loads), variance info (ssq), residuals (res), calculated q limit (q), and t^2 limit (tsq).

The results of the PCA are shown by plotting either the *scores* or the *loadings*. There are specific MALAB function for doing so.

PLTSCRS Plots scores from PCA

This function may be used to make 2-D and 3-D plots of scores vectors against each other. The inputs to the function are the matrix of scores vectors (scores) where column represents a scores vector from PCA and an optional variable of labels (labels) which describe the original data samples.

ISBN:978-84-694-0326-6/DL:T-207-2011

PLTLOADS Plots loadings from PCA

This function may be used to make 2-D and 3-D plots of loadings vectors against each other. The inputs to the function are the matrix of loadings vectors (loads) where each column represents a loadings vector from PCA and an optional variable of labels (labels) which describe the original data variables.

AIV.2 Linear discriminant analysis

Linear discriminant analysis is performed by using a one-way multidimensional analysis of variance. The script employed in MATLAB is as follows:

MANOVA1 One-way multivariate analysis of variance (MANOVA).

D = MANOVA1(X,GROUP,ALPHA) performs a one-way MANOVA for comparing the mean vectors of two or more groups of multivariate data.

X is a matrix with each row representing a multivariate observation, and each column representing a variable.

GROUP is a vector of the same length as X, or a string array or cell array of strings with the same number of rows as X. X values are in the same group if they correspond to the same value of GROUP.

ALPHA is the scalar significance level and is 0.05 by default.

D is an estimate of the dimension of the group means. It is the smallest dimension such that a test of the hypothesis that the means lie on a space of that dimension is not rejected.

- If D=0, for example, we cannot reject the hypothesis that the means are the same.
- If D=1, we reject the hypothesis that the means are the same but we cannot reject the hypothesis that they lie on a line.

[D,P] = MANOVA1(...) returns P, a vector of p-values for testing the null hypothesis that the mean vectors of the groups lie on various dimensions. P(1) is the p-value for a test of dimension 0, p(2) for dimension 1, etc.

ISBN:978-84-694-0326-6/DL:T-207-2011

[D,P,STATS] = MANOVA1(...) returns a STATS structure with the following fields:

W within-group sum of squares and cross-products

B between-group sum of squares and cross-products

T total sum of squares and cross-products

dfW degrees of freedom for W

dfB degrees of freedom for B

dfT degrees of freedom for T

lambda value of Wilk's lambda (the test statistic)

chisq transformation of lambda to a chi-square distribution

chisqdf degrees of freedom for chisq

eigenval eigenvalues of (W^-1)*B

eigenvec eigenvectors of (W^-1)*B;

These are the coefficients for canonical variables, and they are scaled so the within-group variance of C is 1

canon canonical variables, equal to XC*eigenvec, where XC is X with columns centered by subtracting their means

mdist Mahalanobis distance from each point to its group mean

gmdist Mahalanobis distances between each pair of group means

The canonical variables C have the property that C(:,1) is the linear combination of the X columns that has the maximum separation between groups, C(:,2) has the maximum separation subject to it being orthogonal to C(:,1), and so on.

The canonical variables can be thought of as the *scores* of a PCA analysis, Therefore, they represent data points in the new space of discriminant factors. To visualize the results of an LDA, the gscatter function is employed to represent canonical variables onto the most representative discriminant factors. The matlab script for this function is as follows:

GSCATTER Scatter plot with grouping variable

GSCATTER(X,Y,G) creates a scatter plot of the vectors X and grouped by G. Points with the same value of G are shown with the same color and marker. G is a grouping

ISBN:978-84-694-0326-6/DL:T-207-2011

variable defined as a vector, a cell array of strings, or a string matrix, and it must have the same number of rows as X and Y.

AIV.3 Partial least squares

Partial least squares calibration models were used to build predictive quantitative models for benzene. The objective was to quantify benzene employing the optimal sensor array in the presence of other interfering species or humidity.

To assess the performance of PLS in this task it is not enough to train the model employing all the measurements available, but it is necessary to employ a cross-validation strategy in which the database is split in training and testing data sets. In this thesis a multiple-fold cross-validation approach was employed, which consisted in selecting continuous blocks of measurements that were left out for validation and employing the remaining ones for testing. The results shown in the thesis are always validation results. The MATLAB script employed to implement this strategy is as follows:

PLSCVBLK Cross validation for PLS using contiguous data blocks
I/O format is:

[press,cumpress,minlv,b] = plscvblk(x,y,split,lv,noninter);

Any input for noninter will suppress the prompt

Inputs are the matrix of predictor variables (x), matrix of predicted variables (y), number of divisions of the data (split), maximum number of latent variables to calculate (lv) and an optional variable (noninter) which can be used to suppress the user override prompt to select optimum numbers of latent variables. Outputs are the prediction residual error sum of squares for each test set (press), cumulative PRESS (cumpress), number of latent variables at minimum PRESS (minlv), and the final regression vector (b) at minimum PRESS.

This cross validation routine forms the test sets out of contiguous blocks of data and is the best choice when time series data are being modelled. See PLSCV, PLSCV1 and PLSCVRND for other methods of forming the cross validation test sets.

ISBN:978-84-694-0326-6/DL:T-207-2011

In our specific case the x matrix was the sensor response matrix and the y matrix was the corresponding benzene concentrations.

Data were mean-centered prior to building the PLS models and this was true both for the sensor response data and the benzene concentrations. After the PLS model is employed for estimating benzene concentrations, the result is in fact a column of predicted benzene concentrations that are mean-centered. There fore it is necessary to rescale those predictions before comparison with actual benzene concentrations. This is done by employing the script:

RESCALE Rescales matrix

Rescales a previously mean centered matrix (y) using the means (my) vectors specified. I/O format is:

```
ry = rescale(y,my);
```

To assess the performance of the PLS predictive models, estimated versus real benzene concentrations are plotted and the liner fit between estimates and real concentrations is shown (slope and intercept). In addition, the correlation coefficient between real and estimated benzene concentrations is also shown.

AIV.4 Multilayer perceptron models

Unlike PCA, LDA or PLS, the MLP is a non-linear algorithm that is known to perform well both to classify and quantify data from sensor arrays. In this thesis an MLP was trained ad validated for estimating benzene concentration in the presence of interfering species such as H_2S or humidity. This strategy was envisaged because the performance of PLS models was poor when humidity changed. The MLP had as inputs the responses of the gas sensor array plus an input with humidity level information. This was done for the algorithm to learn compensate humidity effects during the training phase.

In this case a leave-one-out cross-validation strategy was employed. It consists of, given an *n* measurement database, training the MLP *n* times using *n*-1 data vectors and validating with the vector left out. The performance of the MLP is judged on the basis of the performance for predicting benzene concentration over the *n* vectors left out. The MATLAB script employed for ding so was as follows:

ISBN:978-84-694-0326-6/DL:T-207-2011

```
% Leave one out process
% A matrix called 'P' with the data and a matrix called 'T' with
% the target outputs and 'R' with minmax of P are to be found in the workspace.
A=[];
B=[];
Pl=[];
Tl=[];
Num_max=60; (number of measurements available)
i=5; (number of hidden neurons in the MLP, this number can be changed
remain=Num_max
for j=1:Num_max
        l=1;
        for k=1:Num_max
            if k==j
                tester=P(:,k);
                targ=T(:,k); (this corresponds to the vector left out)
            else
                Pl(:,l)=P(:,k);
                Tl(:,l)=T(:,k); (this is the training set, i.e., all vectors but
the one left out)
                l=l+1;
            end;
        end;
    net = newff(R,[i 1],{'tansig' 'purelin'}); a new MLP is initialised with i neurons
in the hidden layer and 1 neuron as output (benzene concentration has to be estimated,
tansing and purelin are continuously differentiable transfer functions for the hidden and
output layer neurons, respectively)
  net.trainParam.epochs = 600;
    net = train(net,Pl,Tl); (The MLP is trained using the data in the training set.)
    A(:,j)=sim(net, tester); (The trained MLP is used to estimate benzene
concentration for the vector that had been left out)
  B(:,j)=targ;
  remain=Num_max-j
```

ISBN:978-84-694-0326-6/DL:T-207-2011

end;

The process is iterated Num-max times (the total number of measurements within the sensor response database).

Once more data were mean-centered prior to perform the training and validation of the MLP. The comparison between predicted and real benzene concentrations was performed identically as for the PLS models.

ISBN:978-84-694-0326-6/DL:T-207-2011

References

[1] H. Martens, T. Naes, Multivariate Calibration, John Wiley & Sons, Chichester, 1998.
[2] Y. Lu, C. Partridge, M. Meyyappan and J. Li , A carbon nanotube sensor array for sensitive gas discrimination using principal component analysis, Journal of Electroanalytical Chemistry 593, 105–110 (2006)
[3] E. Westerlund, R. Andersson, M. Hamalainen and P. Aman, Principal Component Analysis - an Efficient Tool for Selection of Wheat Samples with Wide Variation in Properties, Journal of Cereal Science 14, 95-104 (1991)